CONF-891132-Summs.
(DE89016837)
Distribution Category UC-212

CONF-891132--Summs.

DE89 016837

Extended Abstracts: Ninth Battery and Electrochemical Contractors' Conference

November 12–16, 1989
Alexandria, VA

Sponsored by:
U.S. Department of Energy
Office of Energy Storage and Distribution
Office of Transportation Systems
Washington, D.C. 20585

and

Electric Power Research Institute
Generation and Storage Division
Customer Service Division/Transportation
Palo Alto, California 94303

Published:
November 1989

Prepared by:
Synergic Communication Services, Inc.
Columbus, Ohio 43212

and

Battelle/Pacific Northwest Laboratory
Richland, Washington 99352
Under Contract No. DEAC06-76RL01830

Prepared for
U.S. Department of Energy
Assistant Secretary for
Conservation and Renewable Energy
Office of Energy Storage and Distribution
Washington, D.C. 20585

TABLE OF CONTENTS

FOREWORD

This document contains the extended abstracts for presentations scheduled for the Ninth Battery and Electrochemical Contractors' Conference, highlighting research supported by the U.S. Department of Energy and the Electric Power Research Institute. It is intended to be a technical overview for engineers and scientists in government, industry, and academia who are interested in learning more about electrochemical energy storage.

The abstracts are grouped according to the following technical sessions:

- Introductory Session
- Sodium/Sulfur Battery Development
- Planning, Analysis, and Technology Transfer
- Fuel Cells
- Zinc/Bromine Battery Development
- Aqueous Battery Development
- Non-Aqueous Batteries
- Battery Testing and Evaluation
- Metal/Air Batteries

INTRODUCTORY SESSION

CHAIRPERSON:

James Quinn
U.S. Department of Energy

OVERVIEW OF EPRI - ELECTRIC TRANSPORTATION PROGRAM

Larry O'Connell and Robert Swaroop
Electric Power Research Institute
Palo Alto, CA 94303

Environmental concerns represent significant challenges for our nation in the coming decade. This is especially true for the metropolitan areas, such as Los Angles and New York. Air pollution has long been a major issue for our large populated cities. The transportation system is a large contribution to this pollution. Clean fuel vehicles can make an important contribution to urban air quality improvement.

The Electric Power Research Institute (EPRI), formed the Electric Transportation Program in 1979. The program objective are two fold: one, to accelerate commercial introduction of electric vehicles (EVs) and two, to explore future applications for electricity to our transportation systems. To support these goals, the program conducts R&D in three areas:

- Vehicle System Development
- Battery Systems Development
- Advanced Transportation Systems Development

Vehicle Systems Development

The Electric Transportation Program's work in vehicle systems focuses on the development, evaluation and introduction of near term electric fleet vans. It also includes testing of independently developed prototype EVs and powertrains. Presently EPRI, with the support from Southern California Edison (SCE), DOE and other organizations, is sponsoring the development of two near term electric vans -- G-Van and TEVan. The G-Van is a product of cooperative development efforts between Magna Internationals Inc., Chloride Ltd. (CEVS) and General Motors. Based on the full size GMC Vandura/ Rally, the G-Van as a cargo has a payload of nearly one ton, with a large cargo space (see figure 1). It is also being developed as a passenger wagon. The van uses Chloride's powertrain and tubular lead-acid battery. These were developed for the G-Van's predecessor, the very reliable G.M. Griffon. The G-Van has a range of 60 miles between overnight charges and this range could be extended if midday charing is applied. In 1989, twenty-five G-Vans will be built for various utilities. Another eight are being produced for Federal Motor Vehicle Safety Standards and Industrial Standards testing.

The TEVan is being developed by Pentastar Electronices, a subsidiary of Chrysler Corporation, under contract with EPRI. The van is half-ton payload cargo vehicle based on the popular Chyrsler mini vans the Dodge Caravan and the Plymouth Voyager (see figure 2). It also comes as a passenger wagon. The TEVan propulsion system includes a high performance nickel-iron battery, an advanced electronic controller with an integrated battery charger and a two speed electronically shifted automatic transmission. It has a battery management system including automatic watering. Presently four TEVans are being built for track and performance testing.

Battery Systems Development

The Electric Transportation Program is actively promoting the development and testing of near term and advanced EV battery systems. The objective is to develop batteries. with the performance, life and cost necessary for broad-based EV market acceptance.

Near-Term: Lead Acid Battery:

During the past five years EPRI has evaluated tubular lead-acid batteries, model EVST and 3ET205 manufactured by Chloride Ltd. of England among others. The high energy model, 3ET205, used in the G-Van has a specific energy of 34 wh/kg and an effective life of two to three years or 25,000 to 30, 000 miles.

Improved Near Term: Nickel-Iron Battery

Batteries developed by Eagle-Picher with DOE funding are now being evaluated by EPRI for in-vehicle performance tests. An NIF270 model battery was evaluated in a Volkswagen bus for five years. It had accumulated 46,700 mile (650 + cycle) and it was decommissioned due to carbonate poisoning and swelling in the electrodes. One half of the pack is still being continued for static performance tests. The new model NIF220 battery packs are now being evaluated for in-vehicle performance at Electric Vehicle Test Facility (EVTF), in Chattanooga. A number of NIF220 modules are also being evaluated at Argonne National Laboratory for cycle-life and performance characterization. This battery has a specific energy of 50-55 wh/kg. A NIF200 model battery is being manufactured and will be evaluated for optimum cycle-life performance.

EPRI, Eagle-Picher, Southern California Edison and two other as yet uncommitted organizations are in the process of establishing a joint venture to manufacturer nickel-iron battery for EVs. The battery is scheduled for production at pilot levels (500 - 1,000 batts per year) mid 1991. This pilot plant will serve as precursor for establishing a large scale NIF200 series production facility.

Advanced Batteries:

EPRI and DOE support a lithium-iron sulfide battery development project. The battery has an expected energy level of 90 wh/kg. Argonne National Laboratory developed this battery and EPRI/DOE is presently in the process of selecting an industrial contractor to develop and manufacture a proof-of-concept battery.

The sodium-sulfur battery, developed by ABB and CSPL, is another advanced battery suitable for EVs. There are plans to evaluate these batteries for in-vehicle performance, as soon as the cycle-life of a full-scale battery is proven to be more than 400 cycles.

Advanced Transportation Systems

Various advanced transportation system concepts are being evaluated. They could provide for increased utilization of electricity in transportation, while at the sametime relieving the growing problem of urban traffic congestion and poor air quality. Bechtel, under EPRI contract, is completing an assessment of advanced transportation concepts. One of the most promising concepts they have been studying with is roadway electrification. If the development of such a system is successful, commercial use of the technology may be possible early in the next century. Such a system would allow long range EVs by transfering energy inductively from the road to the vehicle.

Figure 1: Electri G-Van

Figure 2: Chrysler TEVan

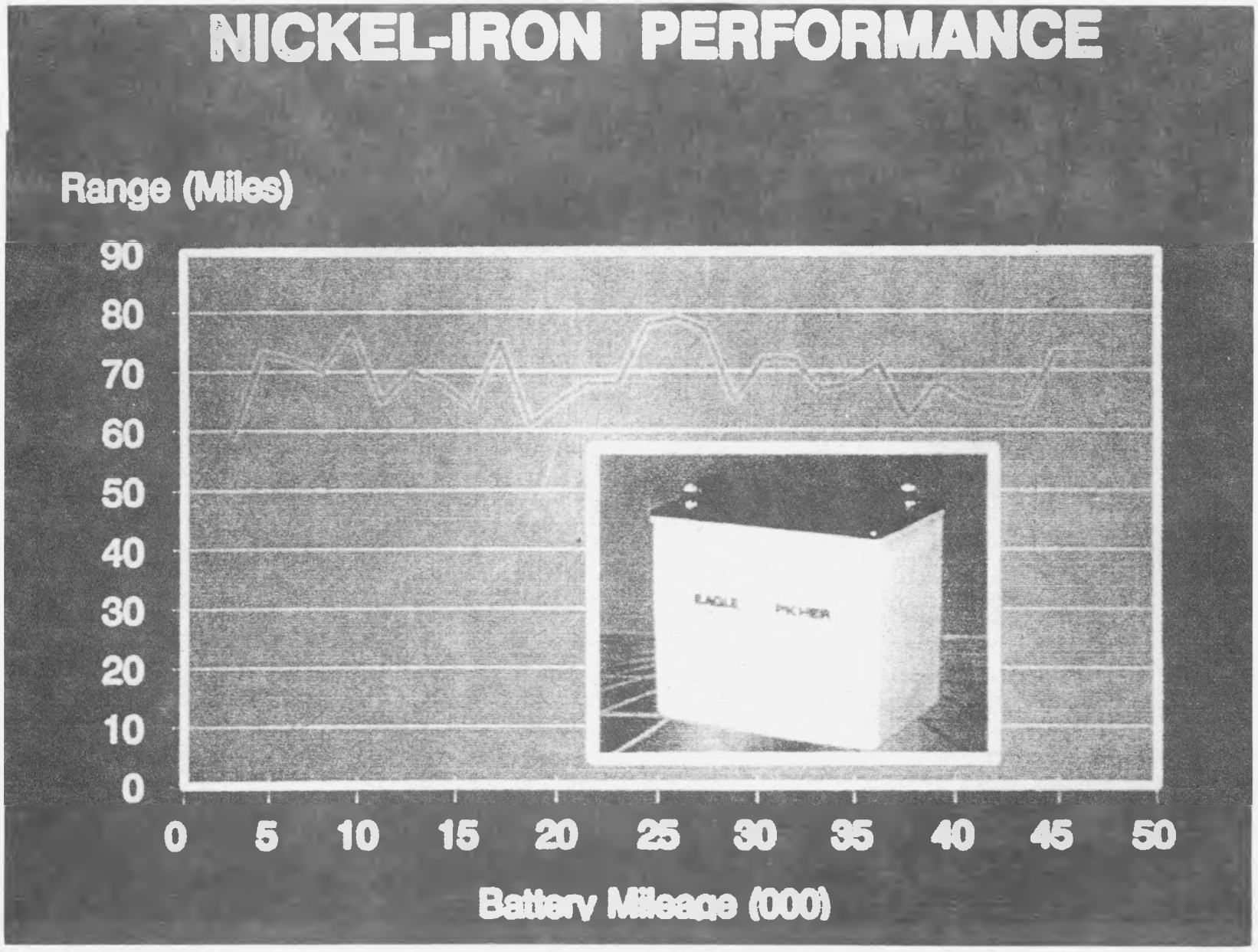

Figure 3: NiF270 Battery Performance

OVERVIEW OF THE DOE ELECTRIC VEHICLE PROGRAM

Paul J. Brown
U.S. Department of Energy

This is an exciting and challenging time for the Department of Energy's electric and hybrid vehicle program. President Bush has forwarded his Clean Air Program to the Congress that contains major initiatives for alternative fueled vehicles including electricity as one of the alternative fuels. By direction of the President, the Secretary of Energy has initiated the development of a National Energy Strategy--an action plan essential to providing this Nation with adequate supplies of competitively priced, clean energy. On both of these critical National issues of reducing urban air pollution and reducing our dependence on imported petroleum, electric and hybrid vehicles present an attractive alternative to conventional petroleum-based vehicles.

In the Department's program, a Dual-Shaft Electric Propulsion (DSEP) system has been developed by the Eaton Corporation with Eagle-Picher Industries supplying an advanced nickel-iron battery subsystem. The powertrain and battery have been integrated into the Chrysler T-115 Minivan by ASC. The range of this vehicle with nickel-iron batteries in urban driving will be on the order of 120 miles. Another advanced electric minivan is being developed for the Department of Energy by the Ford Motor Company. The Ford design includes a new interior permanent magnet motor and an advanced sodium sulfur battery that is being developed by Asea Brown Boveri in a joint venture with Magna International of Canada. In a separate contract with DOE a sodium sulfur battery is being developed by Chloride Silent Power. The zinc-bromine battery continues to be developed by Johnson Controls. JCI is perfecting infra-red vibration welding techniques to reduce the electrode leakage problem and increase the reliability and performance of this battery couple. A competitive procurement jointly funded by EPRI and DOE is in process for lithium-metal sulfide battery development. First generation full size iron-air battery cells are being developed by the Westinghouse R&D Center. The program is emphasizing the development of bifunctional air electrodes. Johnson Controls is continuing to develop an advanced lead acid battery based on the forced flow of electrolyte around the electrodes concept. The development of the new porous electrodes is demonstrating a dramatic increase in the utilization of the lead and lead dioxide materials. Beta Power, Inc. of Salt Lake City, Utah has been issued a contract to conduct a conceptual study of high-performance sodium-metal chloride battery technology. This battery has a number of potential attractive features: it is inherently safe, maintenance free, and has the potential of being relatively low cost. In addition to the completed nickel iron battery subsystem for the DSEP program, the Department is also providing the nickel-iron battery subsystem for the Chrysler TEVan program in cooperation with EPRI. In a separate three year contract with the Department, Eagle Picher is developing new fiber technology for the nickel electrode. A five-cell fiber-plate module has achieved over 800 cycles on testing at ANL. Recent experimental fiber electrodes with increased active material loading have been fabricated into full size modules for testing at Argonne.

The Department of Energy, Department of Transportation and the South Coast Air Quality Management Distric are cofunding a multi-year program for the development of a fuel cell/battery hybrid system utilizing a phosphoric acid fuel cell and battery to power a small urban bus through an electric motor drivetrain. The team of Booz, Allen and Hamilton, Chrysler, and Engelhard/Fuji have fabricated a half-scale propulsion system consisting of a 25 kW fuel cell system, 30 kW battery, high-speed D.C. motor and interface controls for laboratory testing. The team of ERC, Los Alamos, and Bus Manufacturing are completing a half-scale propulsion system consisting of a 32 kW fuel cell and reformer, 25 kW battery and interface controls.

At the Idaho National Engineering Laboratory (INEL) we are able to subject batteries to the actual electrical loads of high-technology EVs on a dynamometer and in test bed vehicles; test auxiliary systems such as battery chargers, state-of-charge indicators and battery monitoring systems; and test advanced batteries loading them with driving cycle power profiles in controlled laboratory environments over a range of operating temperatures from -20 degrees C to +80 degrees C. At INEL dyamometer testing of the Ford ETX-I passenger car confirmed the prediction and measured powertrain performance and identified auxiliary and vehicle related losses. The first Eaton TB1 test vehicle of the DSEP program was tested on the INEL dynamometer. The tubular plate lead-acid battery for ETX-I, the nickel-iron battery system for DSEP, gel-cell batteries by Johnson Controls and other batteries not in the DOE program have been tested on the dynamometer and the special battery test laboratory at INEL. This independent controlled testing is providing insights into the areas requiring further development for these new battery technologies.

STRATEGIC BENEFITS OF ENERGY STORAGE: IMPLICATIONS FOR UTILITY RD&D AND APPLICATIONS

Dr. Robert B. Schainker
Electric Power Research Institute

Electric utilities currently face two major issues that directly affect business and R&D strategy: industry deregulation and increasing environmental concerns. In response to these trends, the utility industry is undergoing significant changes in terms of their organizational structure, business orientation, market strategy, financial valuation, and environmental policies. These evolutionary changes in electric utility strategies can be characterized by the three time periods shown in Exhibit 1. Deregulation in other industries have typically resulted in new opportunities, as well as the erosion of traditional business boundaries, a re-arrangement of the traditional organizations and roles between suppliers, intermediaries and end-users, and increased competition from independent (power) producers and users. Such radical major changes require timely business strategy redefinition, not only in terms of physical territories but also in terms of the overall business goals, such as by shifting emphasis from power generation to power distribution for utilities or to a fully-integrated energy company.

In a deregulated environment, unlike the current utility industry, a least-cost approach to planning is insufficient to maintain competitiveness. Instead, a more synergistic and integrated approach to business planning has to be taken, incorporating market feedback and making adjustments accordingly in a timely fashion, including a basic understanding of the mechanics of free market competition. The need for an increased sensitivity to *market-derived* system requirements dictates that utilities must continually evaluate their relative market position and consider all business and technological options available in order to remain competitive. Mergers, acquisition, joint ventures, and hub-and-spoke structures may the best tactical and/or strategic decisions, however, their potential ability to produce the desired results will require the availability and proper implementation of suitable technology options. Whether or not the strategic plans can be implemented may ultimately depend upon whether they are technologically feasible. Consequently, technological innovations and their *associated RD&D* to bring new technologies from concept to commercial reality must be considered and integrated into the overall utility strategic plans. As a result, technological innovations, such as advanced storage batteries and superconductivity will play a significant role in the future conduct of business in the electric utility industry.

In addition to deregulation trends, the utility industry must respond to an increasingly environmentally-sensitive environment to such extent that environmental considerations, while providing new opportunities, may well become the primary factor driving technology choices in the future. With the current renewed emphasis placed upon air quality improvements, the utility industry needs to re-evaluate plant emission controls and ways to meet the more stringent requirements that may result from commensurate new environmental legislation. The industry has several options to meet these new criteria: improved effluent control technologies, combustion modifications, and/or incorporation of alternative clean technologies into the generation mix. The proposed legislation, such as recently delineated by President Bush, will probably permit a free-market approach, by allowing credits from plants with excess reductions for off-setting or trading with other plants in a given area. Consequently, the overall approach will most likely be a *mix* of these alternative options that will

satisfy the environmental criteria at the lowest possible costs.

In view of these trends, new technologies must be developed (and demonstrated) that allow electric utilities to adapt quickly to changing business, regulatory, and environmental conditions. In this regard, storage technologies provide strategic roles that directly address both regulatory and environmental trends. These roles include the potential benefits of storage in facilitating power transfers and hub-and-spoke systems within a framework of changing contractual arrangements and market structure, as the industry moves towards deregulation, and the value added by storage in the context of storage analogies to money and the commodities futures market. These strategic benefits are summarized in Exhibit 2.

In addition, storage technologies inherently have the potential to abate the overall emissions and, therefore, improve the air quality, especially in the vicinity of designated non-attainment population centers. These environmental benefits include direct air quality improvements and the relative cost-effectiveness of incorporating storage plants as part of an overall emissions control strategy. They also include the indirect environmental benefits of storage in complementing coal-fired base-load plants in response to increasing environmental restrictions in major non-attainment load centers. These environmental benefits also include the potential for storage technologies to facilitate free-market trading of credits for excess reductions in emissions, which the utility can use to offset higher-than-standard emissions from fossil-fueled plants, or to sell these credits to other non-attaining utilities. Storage technologies can also facilitate the integration and supply management of dispersed power sources and can potentially be deployed by PURPA contractors in order to comply with applicable requirements of air quality management plans.

Based upon the above market conditions and existing technologies, the energy storage RD&D strategy is thus specified. (Exhibit 3). RD&D must be directed at technologies that will enhance the market value of utilities, as well as help utilities comply with environmental (air quality) standards. New analytical methods and tools that directly reflect strategic benefits under changing business and regulatory conditions must be developed. Storage technologies, in general, readily meet these specifications and thus will play an increasingly significant strategic role in utility systems. Previous studies have identified the *operational* and *dynamic* benefits of storage. A recent assessment of the strategic and *financial* bottom-line benefits of storage found, that under deregulation, storage plants increased the value of the utility up to 40% as a result of reducing operating (fossil fuel) costs uncertainties.

The market-driven considerations and associated potential strategic benefits of storage establish the increasing importance of energy storage as the industry moves towards deregulation, while at the same time providing an alternative in meeting the increasingly stringent environmental constraints. The strategic edge provided by storage in power negotiations, combined with its potential to reduce vulnerability to oil and gas prices and increasing environmental requirements, provide additional incentives for increased consideration of the various storage technology options within the generation portfolio of the utility industry.

Given the many potential benefits of energy storage, it is not really a question of whether utilities need storage, but how much and when. Given these operational and strategic benefits of energy storage, EPRI has implemented a RD&D program plan that fully reflects and addresses these market derived considerations. (Exhibit 4). The associated energy storage system development and deployment schedule is shown in Exhibit 5.

EVOLUTION OF ELECTRIC UTILITY STRATEGIES

	1930s-1970s	1970s-1980s	1980s-
STRUCTURAL	Franchise Monopolies	Profit Centers	Functional Organizations - Gencos - Transcos - Discos
ORIENTATION	Internal Focus	Efficiency	Competition
MARKET STRATEGY	Meet Load ("high entry barriers")	Control Costs (reduced entry barriers)	Market Share (competition); Growth (mergers, etc.)
FINANCIAL	Minimum Revenues ("cost plus"); Regulated ROE ("low risk")	Competitive Prices (lower costs)	Maximize Corporate Value ("bottom-line")
ENVIRONMENT	Few constraints	Increased Requirements	Severe Restrictions

POTENTIAL STRATEGIC BENEFITS OF STORAGE

- DYNAMIC BENEFITS
- REDUCE (FUEL) OPERATING RISK AND ENHANCE MARKET VALUE
- REDUCE CAPITAL RISKS (MODULARITY)
- FACILITATE HUB-AND-SPOKE SYSTEM
- FACILITATE POWER TRANSFERS
- ENVIRONMENTAL BENEFITS
- SERVE AS MEDIUM OF EXCHANGE (MONEY)
- FACILITATE FUTURES/OPTIONS MARKET

MARKET-DERIVED R&D SPECIFICATIONS

- TECHNOLOGIES MUST
  - ENHANCE MARKET VALUE OF THE UTILITY TO STOCKHOLDERS
    - Equivalent or better cost, performance
    - Low capital, operating, and financial risk
    - Facilitate power purchases and trading
    - Modular configuration
  - HAVE SIGNIFICANTLY REDUCED NET ENVIRONMENTAL IMPACT
- ANALYTICAL TOOLS MUST CAPTURE STRATEGIC (AND ENVIRONMENTAL) BENEFITS

ENERGY STORAGE PROGRAM: OBJECTIVES

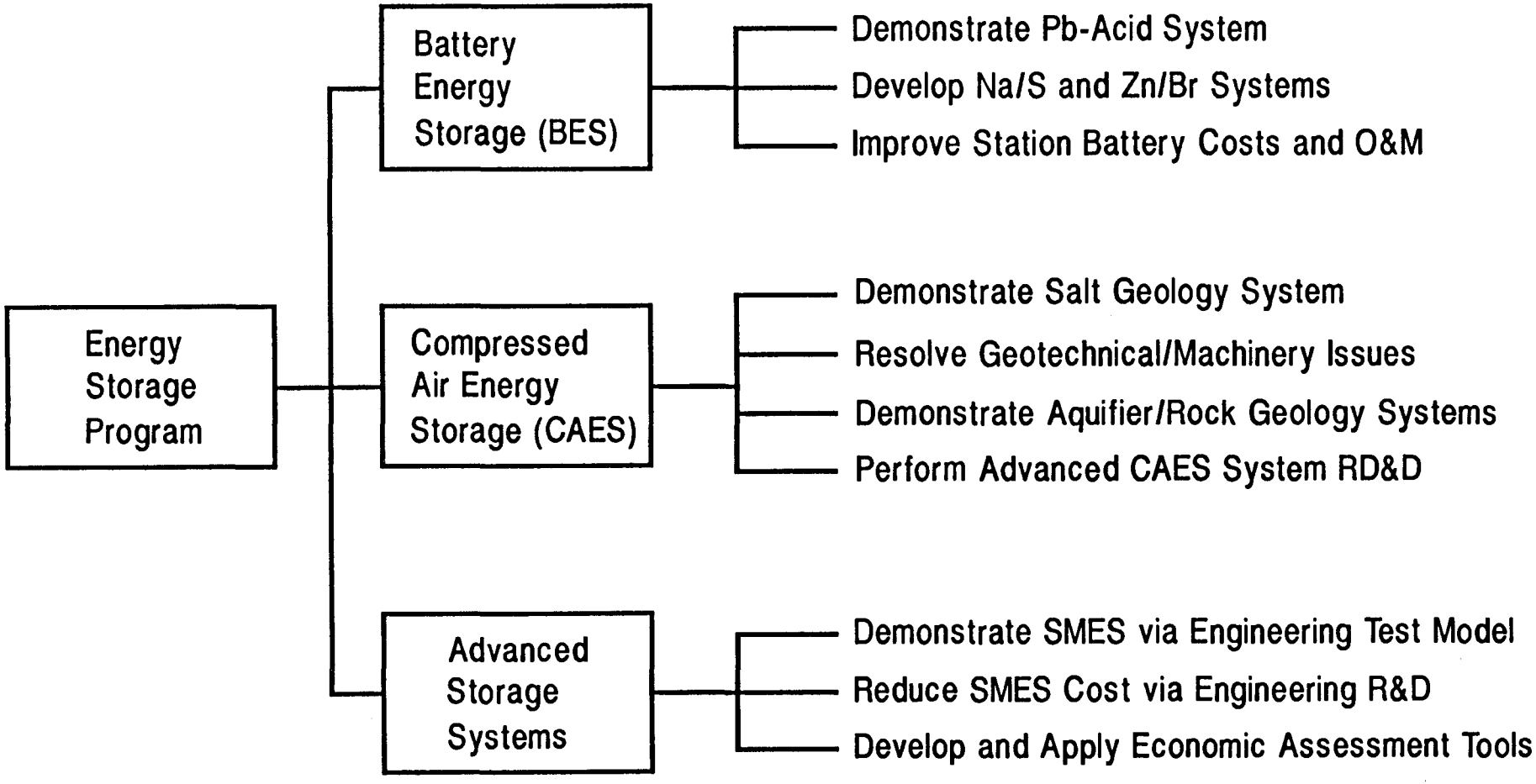

TIME PERSPECTIVE ON ENERGY STORAGE SYSTEMS*

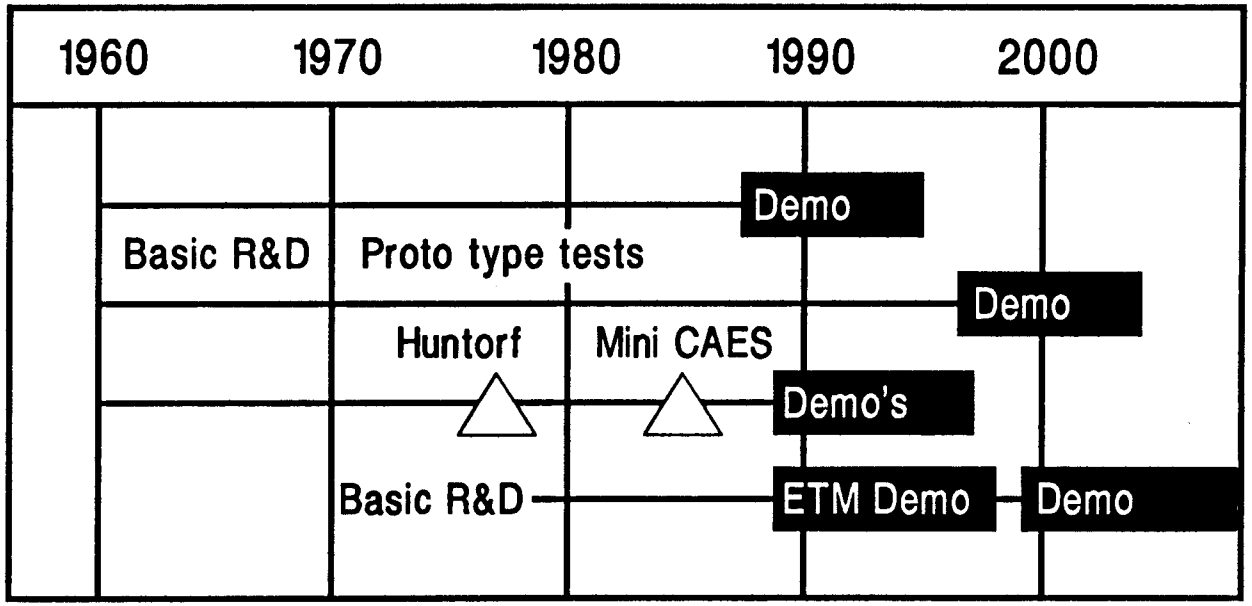

*As of January 1988, EPRI is in the demonstration phase for three attractive storage options

TECHNOLOGY BASE RESEARCH PROJECT OVERVIEW

Frank R. McLarnon, Kim Kinoshita and Elton J. Cairns
Applied Science Division
Lawrence Berkeley Laboratory
Berkeley, California 94720

The Technology Base Research (TBR) Project and the Exploratory Technology Development and Testing (ETD) Project have a common goal to develop advanced rechargeable batteries and fuel cells for applications such as electric vehicles and load leveling. The role of the TBR Project is to perform supporting research for the advanced battery systems under development by the ETD Project, and to evaluate new systems with potentially superior performance, durability and/or cost characteristics. The specific goal of the TBR Project is to identify the most promising electrochemical technologies and transfer them to industry and/or the ETD Project for further development and scale-up. The TBR Project is divided into three major project elements: Exploratory Research, Applied Science Research, and Air Systems Research. Recent research accomplishments are described in an annual report (1), and a summary is provided below.

EXPLORATORY RESEARCH

The objectives of this project element are to evaluate and initiate development of new electrochemical couples with the potential to meet or exceed advanced battery performance goals. Argonne National Laboratory (ANL) is conducting research on molten-salt cells based on Li-alloy negative electrodes and metal disulfide positive electrodes. These cells exhibit very high performance, ease of manufacture, and freeze-thaw capability. A major advancement during the past year is ANL's achievement of stable performance for over 280 charge/discharge cycles with a flooded-electrolyte, upper-plateau Li/FeS_2 cell that was subjected to overcharge.

APPLIED SCIENCE RESEARCH

The objectives of this project element are to provide and establish scientific and engineering principles applicable to batteries and electrochemical systems; and to identify, characterize and improve materials and components for use in these systems.

Alkaline Cells often use Zn as the negative electrode, and efforts are underway to identify electrode and electrolyte compositions that will improve the cycle-life performance of the Zn electrode, and to determine the operating conditions that lead to unwanted Zn dendrite formation. During the past year, LBL completed the development of the first two-dimensional mathematical model of the porous Zn/ZnO electrode, and the predicted results agreed with experimental measurements using microelectrodes in model Zn/NiOOH cells. LBL has also employed *in situ* videomicroscopy to observe the deposition of Zn in flowing alkaline electrolytes.

Zinc/Halogen Cell performance is limited by the tendency of the electrodeposited Zn to assume unwanted shapes, and efforts are aimed at understanding the complex phenomena that control the Zn electrode morphology. Illinois Institute of Technology (IIT) has observed that the grain size of the Zn deposit obtained in acidic $ZnBr_2$ electrolytes by pulse reverse voltage was considerably smaller than that obtained at constant voltage. Brookhaven National Laboratory (BNL) has observed that electromigration in $ZnBr_2$ electrolyte is enhanced when the electrolyte contains quaternary ammonium complexes.

Improved Components for *Alkali/Sulfur Cells* cells are under investigation. Preliminary results obtained at LBL indicate that the addition of 0.2 wt% oxides of Ge, Nb, Mg or Zn all improved the total conductivity of β"-Al_2O_3 by lowering the grain-boundary resistance. Investigations at LBL of novel, low-temperature (120-150°C) secondary cells that contain a liquid Na negative, β"-Al_2O_3 electrolyte, and organosulfur positives, showed that fluorinated organosulfur compounds in such cells yielded open-circuit voltages between 2.4-3.0 V, depending on the degree of fluorination. The Massachusetts Institute of Technology has observed that the addition of CaO to lithium borate glasses improves their stability to high-activity Li environments but results in a lower ionic conductivity. The MIT work has been completed.

Sodium/Metal Chloride Cells offer a number of advantages over Na/S cells. Argonne National Laboratory is evaluating novel metal-chloride electrode designs that will lead to improved cell performance. Stanford University is exploring the development of alternative electrodes and electrolytes for these cells, and their studies suggest that a number of Na alloys offer interesting possibilities as negative electrodes in cells without the solid electrolyte.

Corrosion Processes in high-specific-energy cells are under investigation, and the aim is to develop low-cost container and current-collector materials Tests at IIT of Mo-, Mo_2C- and TiN-coated samples in Na_2S_x melts at 330°C showed corrosion resistance similar to that of solid Mo. Johns Hopkins University has observed that Fe passivates in 0.5 M $LiClO_4$/propylene carbonate (PC) containing >500 ppm H_2O because of the presence of an oxide film.

Components for *Ambient-Temperature Nonaqueous Cells*, particularly metal/electrolyte combinations that improve the rechargeability of these cells, are under investigation. Case Western Reserve University (CWRU) has used high-resolution electron energy loss spectroscopy to detect the presence of carbonate-like species coordinated to K that was exposed to CO_2. This finding suggests that CO_2 undergoes partial polymerization on the K surface. Jackson State University has observed, by *in situ* Raman spectroscopy of 1000-Å thick layers of Li on Ag, that surface products such as Li_2CO_3 and lithium alkyl carbonate may form in PC. The University of Minnesota has observed that Na/V_6O_{13} cells with poly(ethylene oxide) (PEO) polymer electrolyte showed stability and rechargeability up to 11 cycles, and the Na anode showed no evidence of irreversibility. The University of Minnesota work has been completed. Studies as the University of Pennsylvania indicate that cations with mixed valency in the PEO electrolytes provide a redox couple that may be promising electrode materials in solid-state batteries.

Cross-Cutting Research is carried out to address fundamental problems in electrocatalysis and current-density distribution, solutions of which will lead to improved electrode structures and performance in batteries and fuel cells. LBL developed a mathematical model of the Na/$FeCl_2$ battery that predicts the cell voltage as a function of the depth of discharge, and has been useful in showing porosity and volume fraction profiles and how they can affect cycle life. LBL is employing a number of sophisticated techniques for *in situ* studies of the electrode/electrolyte interface during anodic film formation. Light-scattering measurements and scanning tunneling microscopy have confirmed earlier conclusions from ellipsometer observations that metal oxide crystallites undergo redistribution during film formation. LBL has also demonstrated the versatility of Photothermal Deflection Spectroscopy for investigation of electrochemical interfaces, using a number of electrodes types.

Early results with Pt_3Sn (100) surfaces at LBL suggest that methanol electrooxidation is catalyzed by the redox process of Sn that occurs at high anodic potentials. The effect of rising gas bubbles on mass transfer at vertical electrodes was also investigated at LBL. Rising bubbles in the boundary layer were found to enhance the limiting current for Fe^{3+} reduction, but this enhancement was localized to a region corresponding to ~5 times the bubble diameter.

AIR SYSTEMS RESEARCH

The objectives of this project element are to identify improved materials for air electrodes, and to develop metal/air and fuel-cell technology for transportation applications.

Metal/Air Cell research projects address bifunctional air electrodes that are needed for electrically rechargeable metal/air cells, and novel alkaline Zn electrode structures that could be used in either electrically recharged or mechanically recharged cell configurations. LBL has developed a quantitative method for determining the number of oxygenated carbon atoms in carbon black samples. The corrosion rate of these carbon blacks in alkaline electrolytes could be correlated to the concentration of oxygenated species. CWRU has concluded from extended X-ray absorption fine structure studies of heat-treated cobalt tetramethoxyphenyl porphyrin that a significant amount of Co is retained in the N_4 centers, in agreement with studies at BNL.

LBL has developed a new design for a Zn/air cell that contains a particulate Zn electrode. This cell differs from previous designs in that it does not require an external pump to circulate electrolyte. Instead, recirculation is achieved by natural convection. Preliminary discharge tests indicate that its performance is comparable to the Zn/air cell with a reticulated Zn electrode. Metal Air Technology Systems International has recently initiated a program to extend the LBL-developed concept of using a reticulated structure as a substrate for Zn deposition in secondary Zn/air cells. Preliminary results indicate that the entire Zn deposit can be discharged, and that dense, uniform Zn deposits are obtained on charge. Pinnacle Research Institute (PRI) has successfully demonstrated that a slurry Zn powder obtained from dendritic Zn can be discharged in a Zn/air cell. The PRI work has been completed. SRI International has completed an investigation of solution-phase inhibition as an alternative to alloying as a means of reducing the corrosion rate of Al in alkaline media.

Fuel Cell Research, managed by Los Alamos National Laboratory (LANL), includes research in several areas of electrochemistry, theoretical studies, fuel-cell testing, fuel processing, and membrane characterization. LANL has obtained enhanced performance in polymer-electrolyte membrane (PEM) fuel cells with thinner Nafion perfluorinated polymer and at higher air pressure. LANL has also demonstrated that the addition of low amounts of O_2 to the CO-containing reformed H_2 stream produces anode performance that is similar to that obtained with CO-free fuel.

BNL has initiated investigations of underpotential deposited (UPD) Cu on Pt as an electrocatalyst for methanol electrooxidation. X-ray absorption near-edge spectroscopy studies of UPD Cu on supported Pt indicate that the adsorbed Cu has a +1 oxidation state.

NEW DIRECTIONS

As the result of an RFP issued by LBL, a new project was initiated at SRI International to evaluate and develop new, highly-conductive polymer electrolytes for use in solid-state lithium batteries. It is anticipated that an RFP will be issued during FY 1990 to solicit new work on advanced *in situ* characterization techniques, and possibly other topics.

Acknowledgement

This work was supported by the Assistant Secretary for Conservation and Renewable Energy, Office of Energy Storage and Distribution, Energy Storage Division of the U.S. Department of Energy under Contract No. DE-AC03-76SF00098. The support from DOE and the contributions to this project by the participants in the TBR Project are acknowledged.

Reference

1. "Technology Base Research Project for Electrochemical Energy Storage: Annual Report for 1988," Lawrence Berkeley Laboratory Report No. LBL-27037 (1989).

EXPLORATORY BATTERY TECHNOLOGY DEVELOPMENT AND TESTING PROJECT OVERVIEW

Ronald B. Diegle
Sandia National Laboratories

The Exploratory Battery Technology Development and Testing (ETD) Project, under the lead center direction of Sandia National Laboratories, is supported by the U.S. Department of Energy's Office of Energy Storage and Distribution. This project is operated in conjunction with the Technology Base Research (TBR) Project, under the lead center direction of Lawrence Berkeley Laboratory. Together, the two projects seek to establish the scientific feasibility of electrochemical energy storage systems and to conduct the initial engineering development for systems judged suitable for mobile and stationary applications. Sandia is also responsible for technical management of the Electric Vehicle Advanced Battery Systems (EV-ABS) Development Project, which is supported by the U.S. Department of Energy's Office of Transportation Systems.

The ETD Project assumes responsibility for engineering development of those electrochemical systems whose feasibility has been demonstrated either by the TBR Project or by other technically sound investigations. The end use of the battery technologies include electric hybrid vehicles (EV-ABS Project), utility load-leveling, dispersed energy storage, photovoltaic systems, and wind-based electric generating systems. Sandia has divided the Project's activities into three elements. The Battery Technology Development Element encompasses core technology development and engineering of advanced battery systems. These activities are predominantly performed by private industry under contract to Sandia. Battery technologies currently under development are the sodium/sulfur, zinc/bromine, nickel/hydrogen, and aluminum/air systems. The Battery Technology Evaluation Element seeks to characterize the performance of developmental units; the resulting data are used to help guide the work of developers. Actual testing and analysis of the batteries or components are performed either at Sandia or, with monitoring by Sandia, at Argonne National Laboratory (ANL). The Battery Technology Improvement Element involves in-house scientific investigations aimed at solving specific problems encountered in the development process.

Technology development highlights for the past two years include the following: Chloride Silent Power, Ltd. (CSPL), has nearly completed the fourth year of a four-year sodium/sulfur core technology contract (to be extended one year) with major progress in production reliability, capability, safety, and testing of both PB and XPB cells. System level studies have been performed to define battery level requirements. CSPL has completed a three-year contract (also to be extended one year) for development of a proof-of-concept sodium/sulfur electric vehicle battery for integration into the DOE/Ford ETX-II Electric Van Program. A one-third size intermediate battery recently met all performance expectations during evaluation at ANL. A 200-cell XPB module has been designed and fabricated and will be evaluated at CSPL.

Energy Research Corporation (ERC) has nearly completed the fourth year of a four-year zinc/bromine core technology development program with advancements having been made in: redesign and enlargement of flow frames; qualification of a stable electrode material; scale up to 52 cell stacks; design and development of system-level components; and design of a 36-kWh proof-of-concept battery system. Johnson

Controls, Inc. (JCI), has completed the third year of a three-year contract to develop a proof-of-concept zinc/bromine electric vehicle battery, and it resulted in a new flow frame and new stack sealing technique that are currently under evaluation. In addition, JCI concluded the evaluation of a prototype 20-kWh zinc/bromine stationary energy storage battery in their Keefe Avenue Load Management Facility.

They completed three years of a contract for advancement of nickel/hydrogen technology, which produced significant progress in reducing the cost of this technology; in addition, a 7-kWh battery was delivered to Sandia for testing with a photovoltaic array. Eltech Research Corporation has completed over two years of a 30-month contract for the engineering development of an aluminum/air battery for electric vehicles. The first ten-cell stack was operated successfully, and a chemical engineering systems study has been performed.

Evaluation of deliverables from the several technology development programs has continued over the past two years. Testing was performed at ANL primarily on CSPL sodium/sulfur cells, modules, and a one-third size battery mentioned above. At Sandia, testing was performed on sodium/sulfur cells from four developers: CSPL, Ford Aerospace, Ceramatec, and Powerplex. Evaluation of zinc/bromine deliverables included two ERC 5-cell stacks, one ERC 30-cell stack, and two 8-cell stacks from JCI. Testing of a 7-kWh nickel/hydrogen JCI battery has shown that it operates reliably in a photovoltaic array/battery system without a voltage controller, without the need for active thermal management, and with prioritized load shedding. Cycle testing of other nickel/hydrogen cells is confirming JCI's baseline technology. Evaluation of a single aluminum/air cell was initiated, and over 273 hours of operation were successfully completed. A simple solids removal option was identified, and improvements for the anode recharge procedure were recommended.

Current activities in the Technology Improvement Element support the sodium/sulfur and zinc/bromine technologies. Over the past two years, Sandia's in-house investigations have resulted in a number of significant accomplishments, including: 1) refinement of a mathematical model describing stress during freeze/thaw cycling of sodium/sulfur cells is nearly completed, and model validation is expected by the end of CY89; 2) improved techniques have been developed for electroplating chromium onto sodium/sulfur cell containers for corrosion control; 3) promising latent heat-of-fusion salts have been identified for thermal management in sodium/sulfur electric vehicle batteries; 4) chemical treatments for microporous separators for zinc/bromine cells have been developed that substantially reduce bromine permeation with only a modest increase in ionic resistivity; 5) studies of polyvinychloride (PVC), used in zinc/bromine flow frames, have identified a degradation mechanism and indicate an alternate polymer that may better resist chemical degradation.

This work is supported by DOE Contract #DE-AC04-76-DP00789.

EXPLORATORY BATTERY TECHNOLOGY DEVELOPMENT AND TESTING PROJECT CONTRACTS

TECHNOLOGY	DEVELOPER	APPLICATION	PROGRAM VALUE	DOE SHARE	START	END
OESD:						
Na/S	CSPL[1]	SES	$ 8.9M	$ 5.9M	10/85	9/90
Zn/Br	ERC[2]	SES	$ 5.1M	$ 4.7M	10/85	12/89
Zn/Br	JCI[3]	SES	$ 59K	$ 50K	2/87	5/89
Ni/H_2	JCI[3]	RE	$ 380K	$ 310K	9/86	3/90
Al/Air	Eltech[4]	EV	$2.48M	$1.93M	8/87	3/90
OTS:						
Na/S	CSPL[1]	EV	$2.20M	$ 2.0M	9/86	9/90
Zn/Br	JCI[3]	EV	$2.70M	$ 2.3M	12/86	12/89

[1] Chloride Silent Power, Ltd.
[2] Energy Research Corporation
[3] Johnson Controls, Inc.
[4] Eltech Research Corporation

BUE1

Technology Development Highlights: Sodium/Sulfur

- Good progress in core technology:
  - ETX-II one-third battery has met performance expectations
  - Pilot production facility approved by Chloride Group
  - Qualification of XPB cell is under way
- XPB cell development proceeding well:
  - Production rate increase
  - Parametric cell and module evaluations
  - Freeze/thaw and safety qualifications
  - 200-cell SES module fabricated
- Increased cell production rate facilitates statistical testing
- Successful design changes implemented to improve safety and reliability
- System level studies performed to define battery requirements

Technology Development Highlights: Zinc/Bromine

Energy Research Corporation:

- **Enlarged (1500 cm^2) flow frames have been fabricated and are undergoing evaluation**
- **Design and development of system-level components for proof-of-concept SES battery are nearly complete**
- **Stable bipolar electrode material (Kynar) qualified for use**
- **Stacks scaled up to 52 cells with 1500 cm^2 electrodes**
- **Design of a 36-kWh proof-of-concept battery completed**

Johnson Controls Inc:

- **Z-20LL battery exhibited 60 - 64% efficiency and exceeded 180 cycles**
- **New flow frame and stack sealing technique developed**

Technology Development Highlights: Nickel/Hydrogen

- **Significant progress made in cost reduction:**
  - **Platinum catalyst loading reduced**
  - **Lower cost catalyst identified**
  - **Replacement developed for hydrophobic film on negative electrode**
  - **Progress made in developing 0.090-inch thick positive electrode**
- **Solar tests exhibit continued success**
- **Field deployable pressure vessel designed**
- **Thermal model developed to aid in battery design**

Technology Development Highlights: Aluminum/Air

- **Feasibility of single cell (B-300) design proven**
- **First 10-cell stack successfully operated**
- **Chemical engineering systems study completed**
- **Anode improvement task initiated**

SODIUM/SULFUR BATTERY DEVELOPMENT

CHAIRPERSON:

Jeff Braithwaite
Sandia National Laboratories

SODIUM SULFUR CORE TECHNOLOGY DEVELOPMENT

M McNAMEE, F M STACKPOOL

CHLORIDE SILENT POWER LIMITED, RUNCORN, ENGLAND

Chloride Silent Power Limited has been developing sodium sulfur batteries which utilise the relatively small PB cell concept. The PB cell[1] has a capacity of 10 Ah and is part of a family of cells under development with capacities of up to 40 Ah. CSPL has been partly funded by the U.S. Department of Energy, since 1985. The objective of the DoE program is to develop generic core technology applicable to both electric vehicle and utility load levelling applications.

Since the last contractors' conference in November 1987 considerable progress has been made. After road testing of the MkIIA PB cell in a Bedford CF Electric van, substantial cell design changes were introduced to meet the additional demands which the road testing had highlighted. These newer designs, which had been developed under the DoE sponsored contract, were relatively mature by the time the production change over was effected in January 1988. Since that time, further developments have improved cell performance, safety, break-in and freeze thaw survivability to the highest levels achieved to date. The latest cell design, designated the Mk 3SF cell, is to be employed in the construction of the ETX-II battery of the parallel, DoE sponsored, Electric Vehicle Battery Design and Engineering Program. The 30 Ah extended PB cell (XPB) has also been progressed and at the time of writing had been tested for 200 electrical cycles in a small module.

CYCLE PERFORMANCE

The capacity and resistance of the Mk3SF PB cells over 1000 cycles are shown in Figure 1. The average capacity of these cells at 950 cycles was 84% of theoretical; the average resistance at 950 cycles was 32.1 m.ohm. Changes to manufacturing methods also enabled rapid cell break-in to be achieved with this design. Figure 2 shows a group of cells attaining target resistance on the first electrical cycle. Consistency of performance of production output is also important. Cells are routinely taken from CSPL's production line and electrically tested for Quality Control purposes. Figure 3 shows the resistance of 30 such cells, and indicates the consistency of performance which is being demonstrated.

CELL RELIABILITY

The statistics of cell reliability can be expressed in a variety of ways, reflecting the requirements of their usage in batteries. Infant mortality (defined as warm-up failures and failures within the first 50 cycles) has been reduced to such an extent that no failures were recorded in 2400 warm-up attempts. In cells made by optimised processing routes, the failure rate at 500 cycles was 0.0076%. Out of 132 cells tested in banks and as single cells, only 5 failures occurred in 66,000 cell cycles, too few for meaningful Weibull statistics to be computed. The majority of cells in this group had exceeded 500 cycles at the time of writing.

Figure 4 shows the progression of the data base of PB cells exceeding 500 cycles during recent years. The cells have been tested in small batteries, as single cells and as 4-cell strings.

CELL FREEZE THAW

The ability of a sodium sulfur battery to withstand periodic cool down without detriment to performance is an important requirement of the system. The maximum likelihood estimate of the Weibull characteristic for the current PB cell is in excess of 400 freeze thaw cycles with an associated modulus of 2.8. Groups of PB cells have withstood more than 640 freeze thaw cycles. Using statistics such as these, it is predicted that a 3300 cell battery would survive 50 freeze thaw cycles at the top of charge with a loss of 1.3% of cells. This is very close to commercial requirements. Further testing has shown that cells subjected to freeze thaw in the discharged state are less able to withstand the thermal cycling. However, changes in the ceramic to metal sealing process are anticipated to give further improvements, as this component has been found to be the predominant source of the failures.

CELL SAFETY

A major objective of the development work conducted during 1988 and 1989 was the improvement of cell behaviour during cell failure under both normal and abuse conditions. The incorporation of new designs of safety features in the cell had a multi-fold effect. Both the cell resistance and recharge performance were enhanced at the same time as improving cell safety. A total of 117 Mk3SF cells were failed by electrical overvoltage in 24 cell, close packed modules. The data resulting from this testing are shown in Figure 5. Tmax is the maximum temperature attained during the safety test and the period afterwards when current reversal is applied.

Abuse testing was also conducted in which both rapid quenching by immersion in water and destructive side impact were employed. The details have been reported by Stackpool[2]. The effect of rapid water quench testing is illustrated in Figure 6. In this test, the cell was removed from the test bath at 350 C and quenched in a container of cold water. The cell was then reheated to operating temperature, electrically cycled and then quenched again. The graph shows the second quench. No change was observed in the electrical performance.

SMALL BATTERY PERFORMANCE

More than 30 small batteries have been tested by CSPL since the programs of work on the PB cell commenced. These tests have been funded from a variety of sources. A 120 PB cell bank of 30 parallel, 4-cell strings has become CSPL's standard size of test unit. These units are a sub-section of a typical EV Battery and are made to a standard design. Three 120 cell banks have exceeded 500 cycles without any maintenance being required. More detail of bank testing is reported by Mangan (these proceedings).

A 16 cell module of XPB cells was tested for 200 cycles to provide baseline data for airflow calculations on a larger XPB module intended to simulate full size battery designs. This module was operated successfully and provided important data on the effect of moving air upon temperature distribution and homogeneity within the module. The capacity of the module is shown in Figure 7.

SUMMARY

The status of the Mk3SF cell is summarised in Table 1. A practical demonstration of the progress that has been made is embodied in the testing conducted by DeLuca[3] et al, at Argonne National Laboratories. The intermediate deliverable of the parallel EV Battery Design and Engineering Program was tested at ANL for more than 200 cycles and details of this testing are to be provided in these proceedings. Despite some manufacturing problems, which have since been eliminated, the battery performed to the pre-test predictions. A prediction of 500 cycles is being made for the prototype ETX-II battery, based upon current experience.

TABLE 1

Mk3 SF Cell - Performance Summary

- Lowest group average resistance yet tested.
- Capacity at 950 cycles is 84% of theoretical.
- Demonstrated freeze thaw >500 thermal cycles.
- Zero infant mortality in 2400 warm-ups.
- Benign failure characteristics demonstrated.
- Stable in-cycle charge and discharge performance.
- Rapid break-in to target performance figures.

REFERENCES

1. Bindin P J and Molyneux J, Small Battery Performance, Proc DoE/EPRI Beta Battery Workshop, EPRI AP-6012-JR Oct 1988, Toronto, June 1988.

2. Stackpool F M, Advances in Sodium Sulfur Cell Safety, 176th Meeting of Electrochemical Society. Oct 1989, Hollywood, Florida.

3. DeLuca W H, Kulaga J E, Hogrefe R L, Tummillo AF and Webster C E., Argonne National Laboratories, Evaluation of Advanced Battery Technologies for Electric Vehicle Applications. SAE Technical Paper Series 890820, International Congress and Exposition, Detroit, Michigan, Feb 1989.

ACKNOWLEDGEMENTS

The authors wish to thank their colleagues for their contributions to the preparation of this paper. This work is supported by the US Department of Energy, Office of Energy Storage and Distribution under Sandia Contract 48-8837

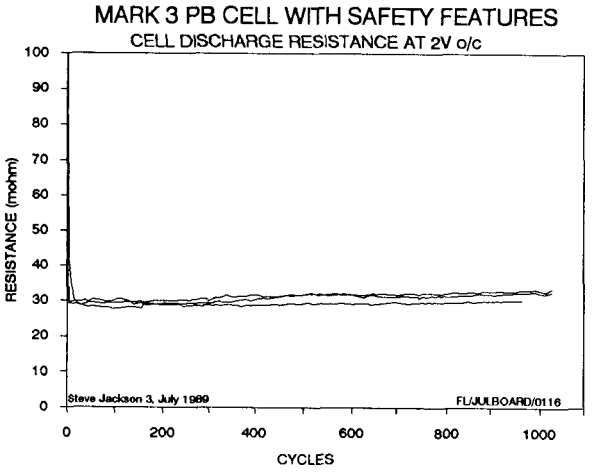

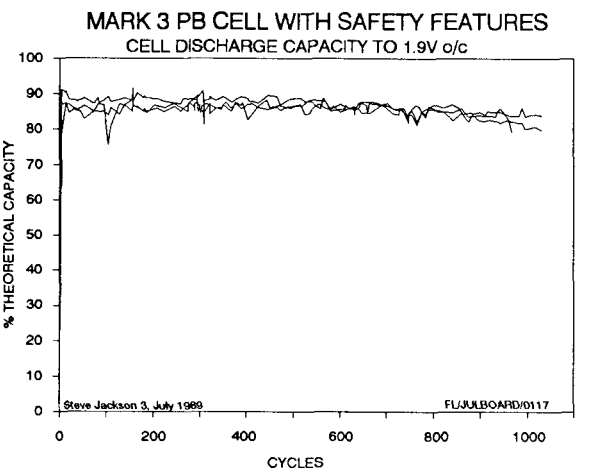

FIGURE 1

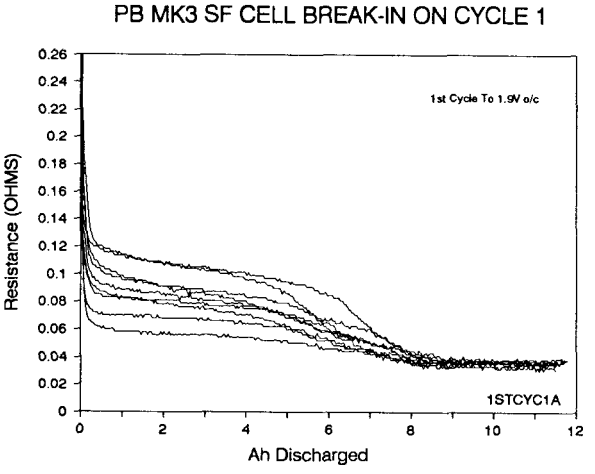

FIGURE 2

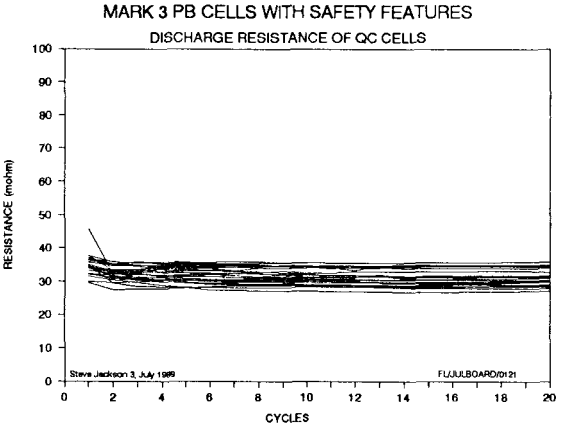

FIGURE 3

CNTRC891

CHLORIDE
SILENT POWER LTD

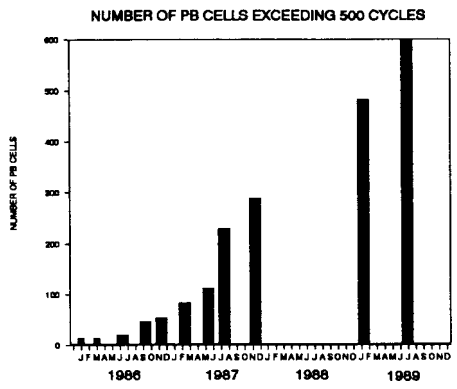

FIGURE 4

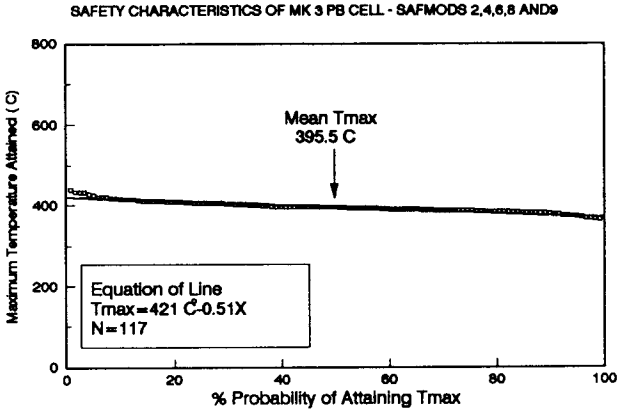

FIGURE 5

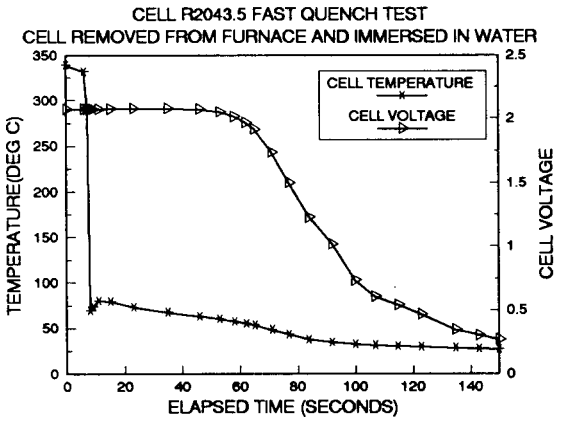

FIGURE 6

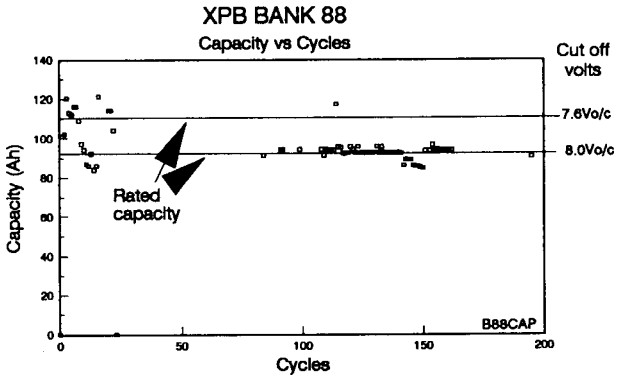

FIGURE 7

CNTRC892

CHLORIDE
SILENT POWER LTD

SODIUM/SULFUR BATTERY COMMERCIALIZATION

William Auxer
Beta Power, Inc.
940 West Valley Road, Wayne, PA

Background. The Electric Power Research Institute (EPRI) contracted with Chloride Silent Power Ltd. in 1986 to develop a plan for the commercialization of sodium sulfur utility energy storage (UES) batteries. One of the primary tasks comprising the study involved the design and costing of a 100 MWh load leveling (LL) battery plant. This study was completed at the end of 1987, and the major results were presented at the Eighth Battery and Electrochemical Contractors' Conference.

The study identified several design related issues that remain to be resolved before the viability of the technology can be demonstrated for the UES application. One of these issues is the development of a device which dictates the mode of cell failure. Such a device may be necessary in order for the sodium sulfur UES battery to achieve battery module life times that allow it to be competitive with alternative energy storage systems and gas turbine peaking plants.

Battery Design. An artist's rendition of the 100 MWh LL battery is presented in Figure 1. It is comprised of three, 10 MW unit batteries connected in series. Each unit battery has 32, 62 volt nominal modules which are then connected in series to form a 2000 volt string; two such strings are connected in parallel to make-up the unit battery. The design requirements for the 100 MWh battery are summarized in Table 1.

Sodium sulfur is a high temperature battery system, and thermal management of the UES battery is therefore a major design driver from the standpoint of capital cost, operating cost, battery performance and safety. The approach presently being pursued for the 100 MWh LL battery is to cluster four, 625 kWh modules with each 4-unit cluster having its own self-contained thermal management system (TMS). This is accomplished by employing a closed loop air circulation system and flowing air directly across the individual cells to either cool the cells during discharge of the battery or to heat the cells during extended periods of non-operation or during the initial warm-up of the battery. An artist's drawing of the 4-module TMS unit is presented in Figure 2.

The sodium sulfur cell proposed for the UES battery application is a high capacity version of CSPL's XPB cell. At a 3 1/3 hour discharge rate, this cell, designated the XPB_{HC}, has a capacity of 88 Wh when discharged to 1.76 volts open circuit; the deliverable capacity of the XPB_{HC} cell is 27% higher than the XPB cell, requiring an increase in cell diameter of only 3 mm with no change in cell height. The overall impact on the number of cells comprising the LL battery is significant as a result of utilizing this higher capacity cell; the number of cells is reduced from 1.8 million to 1.15 million.

Maintenance Considerations. Individual replacement of failed cells is not considered to be a cost effective approach for maintaining the XPB_{HC} cell LL battery. For this battery, the maintenance approach which offers the lowest annualized cost of electricity is to replace all the modules comprising a string in the unit battery. The first string replacement is required approximately ten years after plant start-up; subsequent maintenance is performed every 2½ years. In total, nine string replacements are made, or the battery capacity is replaced 1½ times throughout its life. The capacity variation of the LL battery during its 30 year life is shown in Figure 3.

Selling Price. The costs to manufacture the 4-unit TMS and to construct the LL battery plant were estimated based upon the conceptual design developed during the commercialization planning study. The selling price of the battery plant, excluding the power

conversion system, is less than $100/kWh. The battery modules, which comprise approximately 70% of this cost, are the most significant cost element; the thermal management system, which includes building insulation as well as the closed loop air conditioning system, is the second highest cost element, comprising approximately 12% of the total selling price.

Though these costs were based upon a preliminary design, areas to further reduce costs have been identified. These include lower cost manufacturing methods to fabricate cell components and to assemble the cell and the elimination of the need for the cell failure device and for active thermal management. The other elements comprising the battery balance of plant may be understated due to the preliminary state of the design; however, given the areas identified for cost reduction, the selling price for the energy related components is envisioned to remain in the range of $90/kWh or lower.

Cell Failure Device Development. Two cell networking arrangements can be considered for the LL battery; one is a long series string arrangement, and the other is a bank comprised of many single cells networked in parallel (complete parallel array). The former approach requires that a device be placed in parallel with the cell which will bypass current around the failed cell. The latter approach requires a device to be placed in series with the cell which will open circuit upon failure of the cell. Therefore, devices which satisfy both cell networking arrangements are being developed.

Analytical studies investigating battery reliability are being performed to support the device development activities. One such study was the prediction of battery capacity degradation for alternative cell networking configurations for the LL battery design developed during the commercialization planning study. The two networking configurations proposed for the LL battery were investigated as well as the 4-cell string approach which is presently being employed by CSPL in their electric vehicle battery. The 4-cell string approach does not require a failure device; however, a limitation of this approach is that the capacity of all four cells in the string is lost when only one of the cells fails. The results of the analysis are presented in Figure 4 in terms of the Weibull durability characteristics which are necessary for the module to achieve a ten year life; the durability characteristics are characteristic life (α) and shape factor (β).

The conclusions from this battery capacity degradation study are as follows:

- The cell must have a shape factor > 2 irrespective of the networking configuration.
- For shape factors > 5, α is relatively insensitive to β. Furthermore, the battery design is indifferent to the cell networking configuration.
- Over the range of shape factors from 2 to 4, the complete parallel array requires a slightly lower durability for the cell as compared to the long series string configuration; however, both arrangements can achieve a ten year module life with a significantly lower cell durability as compared to the 4-cell string approach.

The most significant finding is that the incorporation of a failure device with the cell is not an absolute requirement for the LL battery. If a shape factor in the range of 4 to 6 can be achieved with mass production manufacturing methods and with reasonable quality control costs, the 4-cell string networking approach is viable, requiring a characteristic life in the range of 4000 cycles.

UES Battery Qualification. Qualification of the sodium sulfur cell technology for the UES application is being performed in conjunction with the DoE/Sandia National Laboratories *Sodium Sulfur Battery Development* Program. A 16-cell XPB module was built in 1988

and testing is continuing at CSPL. The purpose of this module build and testing was to confirm the thermal management approach being proposed for the UES battery. Results have verified the acceptability of the direct air flow TMS approach in regards to meeting the temperature uniformity and temperature rise requirements. Consequently, a 200 cell, 12 kWh battery representative of a LL battery tray will be built during the 4th quarter of 1989 and tested in 1990.

Acknowledgement. The work discussed is being supported by the Electric Power Research Institute under Contract RP2123-4 and by the US Department of Energy and the Sandia National Laboratories under Contract 48-8837.

Table 1

100 MWh Sodium Sulfur LL Battery Requirements

1.	Battery Plant		
	a.	Nominal Capacity:	100 MWh
	b.	Installed Capacity:	110 MWh
	c.	Nominal Voltage:	2000 volts
	d.	AC Power Rating:	13.8 kV, ± 5%
	e.	Duty Cycle:	3.33 hr constant power discharge 7 hr constant power charge
	f.	Operating Period:	5 days/week; 50 weeks/year
	g.	Life:	30 years
2.	Battery String		
	a.	Nominal Capacity:	18.33 MWh
	b.	Nominal Voltage:	2000 volts
	c.	Configuration:	32 modules connected in series
	d.	Current, maximum:	3600 amps
3.	Module		
	a.	Nominal Capacity:	625 kWh
	b.	Nominal Arrangement:	62 volts
	c.	Cell Arrangement:	to be specified
	d.	Life:	10 years

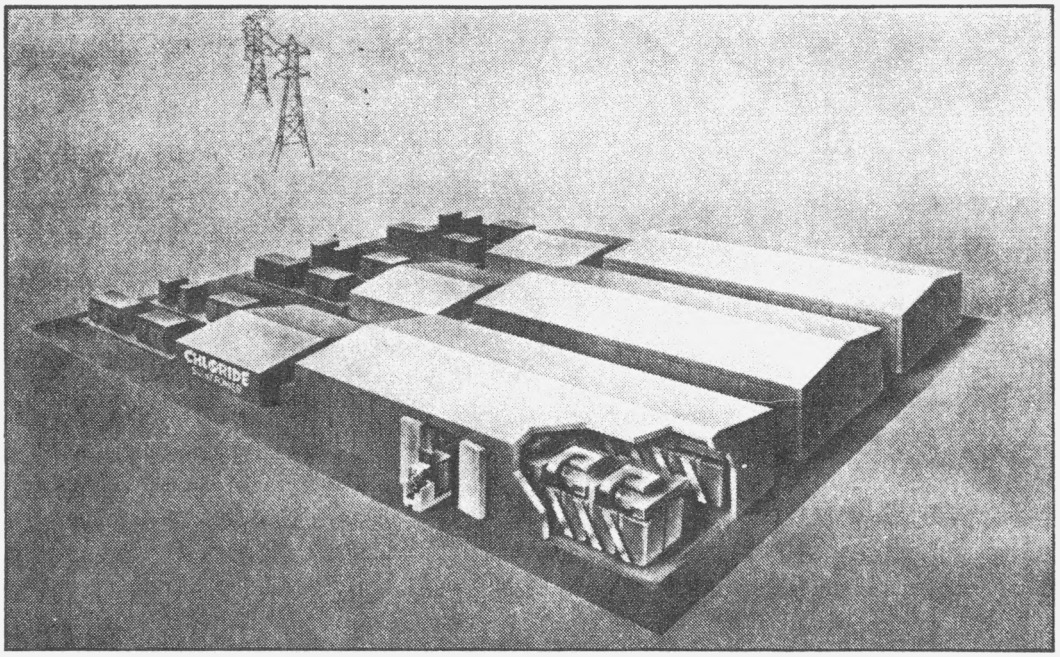

Figure 1. An Artist's Concept of the 100 MWh Sodium Sulfur Load Leveling Battery

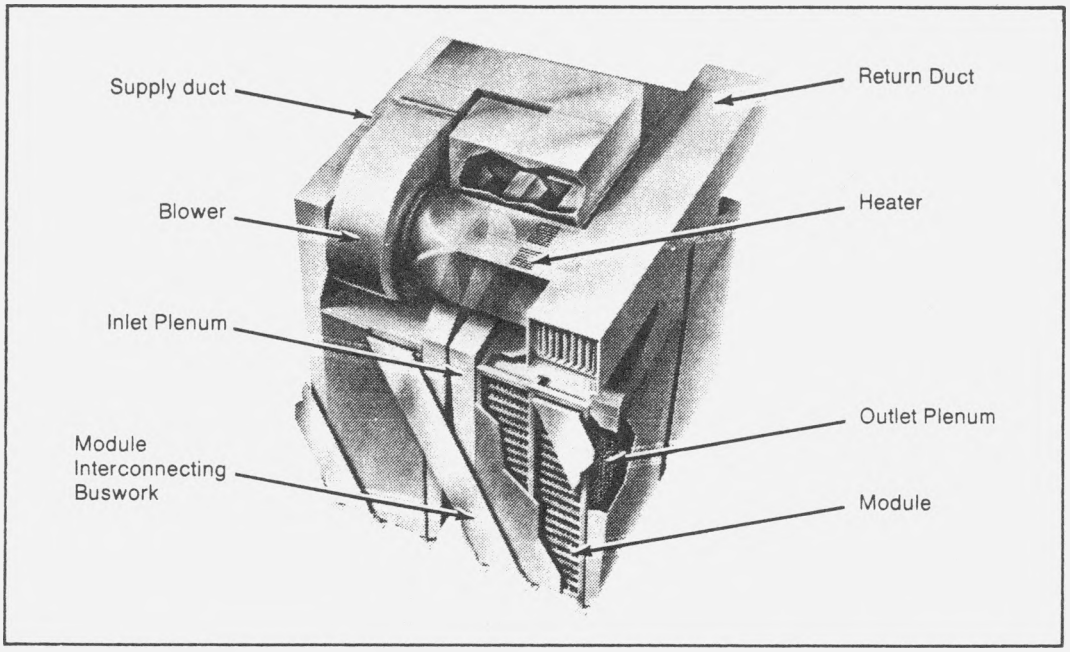

Figure 2. An Artist's Concept of the 4-Module Unit Thermal Management System

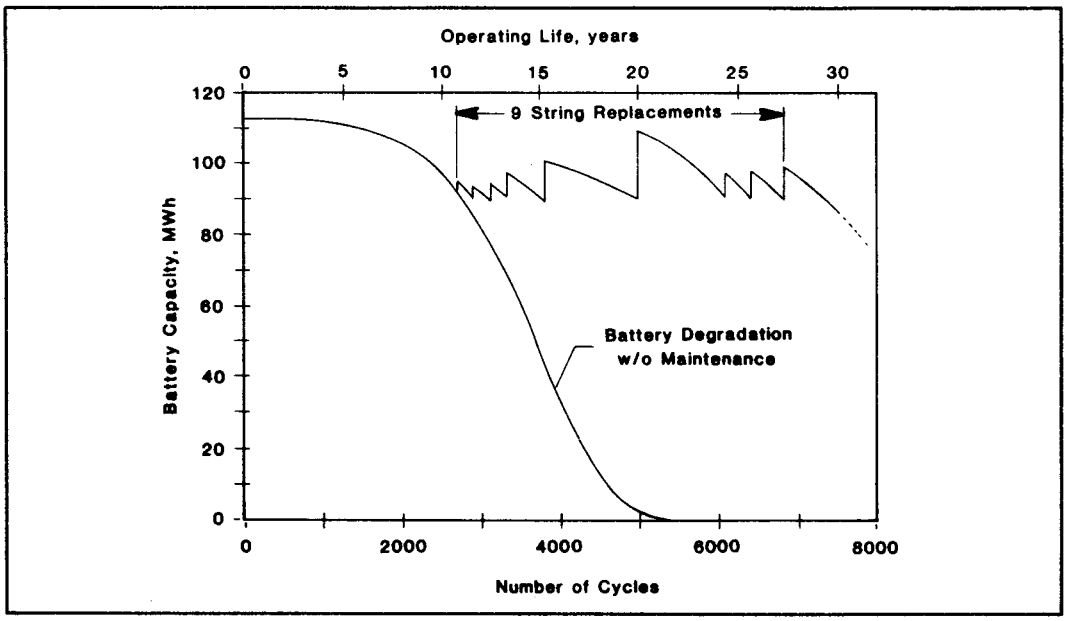

Figure 3. Capacity Degradation and Maintenance Schedule for the 100 MWh Load Leveling Battery

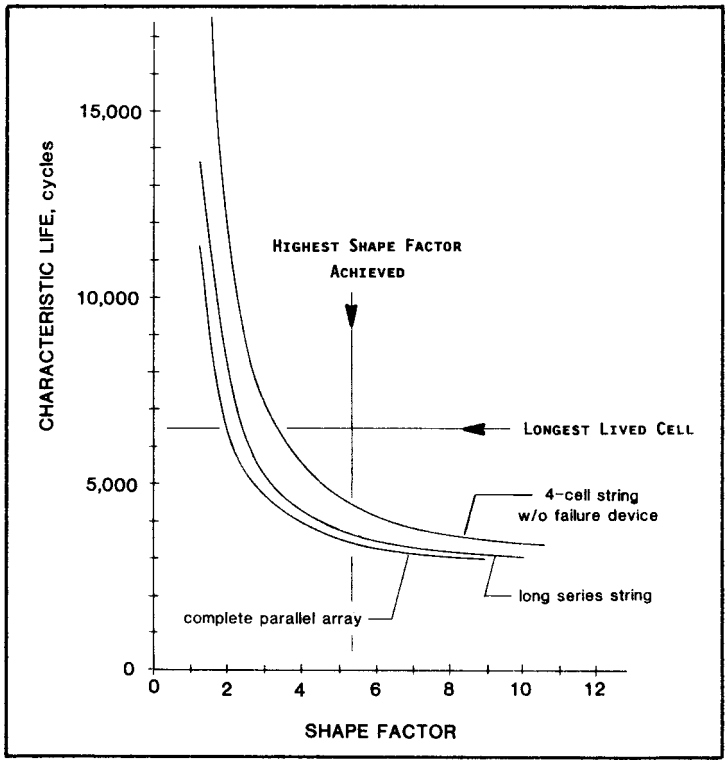

Figure 4. Minimum Cell Durability Requirements to Achieve Ten Year Module Life

SODIUM SULFUR EV BATTERY SYSTEM DEVELOPMENT

M F Mangan, J Molyneux, P G Brocklehurst
Chloride Silent Power Limited

INTRODUCTION

This program is for the development of a sodium sulfur battery system suitable for testing in the Ford ETX-II experimental electric vehicle. The program was initiated in September 1986 and is programed to deliver a battery in late 1989. Substantial development has taken place since the last review, in December 1987 and CSPL is confident that the deliverable battery will meet the required specifications in all respects but weight.

ELECTRICAL DESIGN

The battery is composed of 2880 PB Mark 3 SF Cells, each of which has a capacity of 10 Ah.[1] These cells, arranged 96 in series by 30 in parallel, are subdivided into 8 volt banks to give a terminal voltage of approximately 200 volts with a capacity of 300 Ah.

MECHANICAL DESIGN

The cells are supported in a fully insulating matrix, in banks of 120 cells. Each bank contains 30, 4 cell series strings giving each bank a voltage of 8 volts and a capacity of 300 Ah. The positive and negative paralleling connections are made using mild steel plates and, at this stage of the program, weight reduction of this structure has not been a priority. Each bank weighs approximately 18.5 kg and is connected to its neighbour via steel strips. All connections within the battery are welded and the bank design incorporating the small cell, gives a structure which is mechanically robust and which is electrically able to withstand the effects of individual end-of-life cell failure. The bank design is such that maintenance is not required. Shock tests carried out as part of the qualification procedure for transportation have demonstrated the ability of cells to withstand shocks in excess of 150 g, when cold, in both horizontal and vertical orientations. Limited shock testing has been carried out on hot cells though liquid filled dummy cells have been tested at ambient temperature without leakage.

THERMAL DESIGN

Following early experiments with lidded thermal enclosures CSPL now concentrates on the design of fully sealed batteries. The double skin stainless steel enclosures have an evacuated mineral insulation between the skins and a thermal loss of 325 watts is forecast for the completed battery. Terminal and instrumentation losses will account for a further 75 watts. A number of cooling system principles have been investigated, including switching heat pipes, thermal shunts, evaporative cooling and air cooling. CSPL has adopted air cooling using sealed plenum chambers above and below the battery so that, in the event of catastrophic failure within the battery, the failure site is not fed with forced air.

It had been thought during the early stages of the program that active cooling would not be required and provision of active cooling has increased both the system weight and the system volume above those originally forecast by CSPL. Volume remains within specification but the weight, at 750 kg, is 200 kg above the target. Much of this deficiency could be recovered in subsequent designs by eliminating the

air cooling, reduction in the weight of the bank plate materials and, since the battery as designed has a higher capacity than the specification, reduction in the number of cells.

ELECTRONIC SYSTEM DESIGN

The battery is protected against overcharge and overdischarge at the bank level and bank voltages are monitored using commercially available equipment. This approach has allowed development of the battery protection algorithms to proceed in parallel with hardware development. Bank by-pass during charging is used to ensure that, as the battery ages and individual cells start to fail, the banks are all brought to top of charge at the same time. A working by-pass arrangement has been successfully demonstrated at CSPL.

Batteries have been successfully charged using 3 phase rectified supplies with minimal smoothing, showing no loss of capacity and no significant change in the thermal performance. Trials at CSPL have not identified any long term effects associated with the use of the simple charger and the deliverable battery will be provided with a charger of this type. The charger supplies constant current until the battery is fully charged, whereupon it is disconnected. If bank by-pass is required, this takes place at a reduced current for a period of up to one hour.

CSPL TESTING Program

Test have been carried out at the bank level and also at the small battery level. The small batteries use the same bank configuration as that adopted for the deliverable battery, connecting 7 banks in series to give a voltage of 56 volts. These batteries are tested in their own evacuated thermal enclosure. A measure of the string resistance consistency and the effect of cycling on string resistance is shown in Figure 1. Capacity and resistance as a function of age for a typical test bank are shown in Figure 2 and the overall trend downwards in bank resistance is shown in Figure 3. CSPL has also carried out some high current discharge testing appropriate to intensive EV operation. Tests conducted at the one hour rate on a 7 bank battery have confirmed that the battery will sustain this one hour discharge rate for 36 minutes before the test is terminated on temperature and that, during this period, the voltage profile remains extremely flat. The results are shown in Figure 4.

BATTERY COMMISSIONING CYCLE

The electrical and thermal commissioning occur at the same time. Test batteries are located in an oven and, over a period of 36 hours, the internal temperature is increased to 350^{o}C while the external temperature is increased more quickly but held at 175^{o}C. The insulation is evacuated during the whole of the commissioning cycle. The battery is given three electrical cycles starting with a relatively gentle discharge and recharge cycle. Typical bank performance during this first cycle is shown in Figure 5. At the end of the 3rd cycle, the battery resistance is within 10% of its final minimum resistance. In over 3000 cells of the frozen design to be adopted for the ETX-II battery deliverable, there have been no cell failures whatsoever during this commissioning cycle. In addition, in some 1700 cells which have subsequently been reheated, there have also been no cell failures. The remaining cells have not yet been re-heated. CSPL therefore has a high degree of confidence that the battery can be fully evaluated before despatch and that, on re-warming, it will perform as expected.

INTERMEDIATE DELIVERABLE BATTERY TESTING

The final deliverable battery is divided into 3 very similar sections as shown in Figure 6. As part of the testing program, a battery section, $^1/_3$ of the final deliverable, was fully assembled for evaluation at the Argonne National Laboratory. The performance of this battery is reported elsewhere[2] but in all respects, it met or exceeded the electrical and thermal performance specification appropriate to its size. The battery delivered in excess of 300 Ah, sustained the hill climbing power for over 1 hour and exceeded 200 mixed charge/discharge cycles, over half of which were to full depth of discharge, before the battery capacity fell to 80% of nominal.

SUMMARY

All the major design features for the deliverable battery have been finalised and a complete series of tests at CSPL and the Argonne National Laboratory has confirmed the effectiveness of the design solutions. More work is required to reduce battery system weight and CSPL believes that weight reduction can be readily achieved. Many of the design features in this battery have already been superseded in the laboratory by better designs which have not yet been formally qualified.

ACKNOWLEDGEMENTS

This work is supported by the DoE under contract No DE-AC04-88AL54303 and the technical program is managed by the Sandia National Laboratories. The support of both organisations is gratefully acknowledged. The authors also wish to thank their many colleagues who support the work and have contributed greatly to its success.

REFERENCES

1. M McNamee et al., Sodium Sulfur Core Technology Development, Ninth Battery and Electrochemical Contractors' Conference, November 13-17, 1989

2. J Freese and W de Luca, Sodium Sulfur Core Technology Development, Ninth Battery and Electrochemical Contractors' Conference, November 13-17, 1989

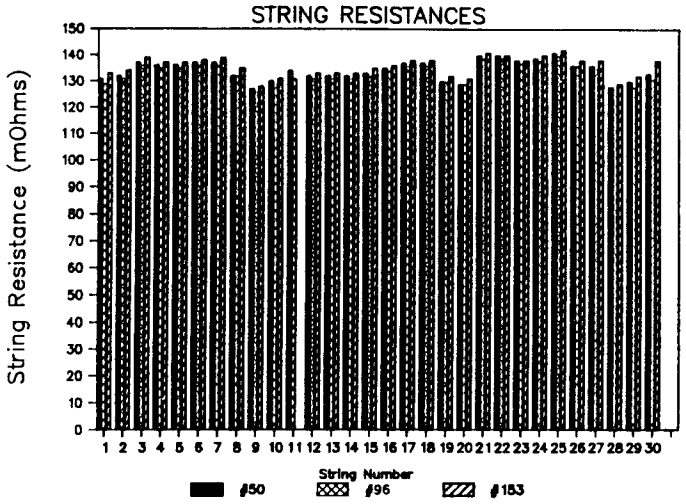

Figure 1. Variation of String Resistance in a Typical Bank

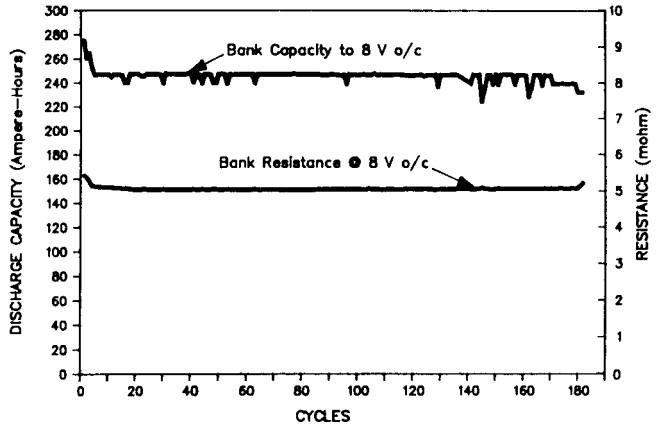

Figure 2. Bank Capacity and Resistance as a Function of Age

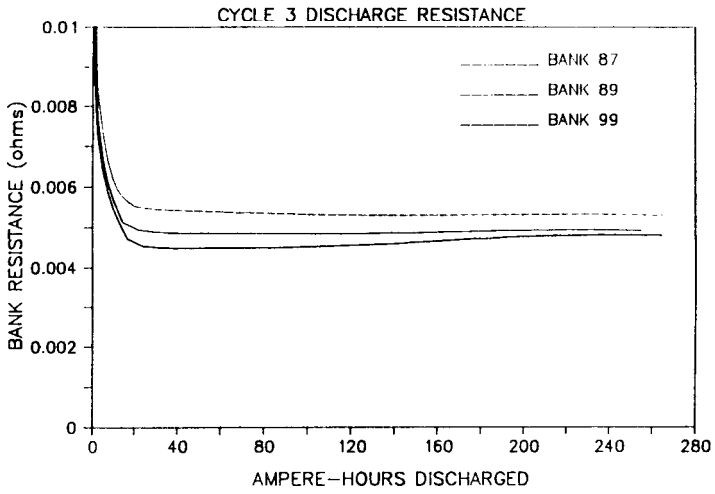

Figure 3. Bank Resistance Trends

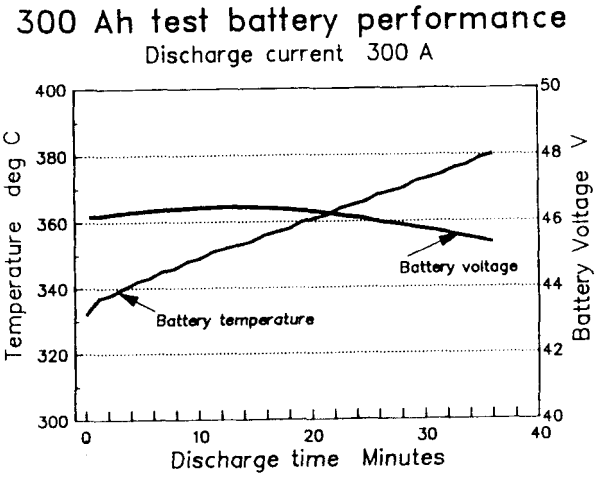

Figure 4. High Current Battery Performance

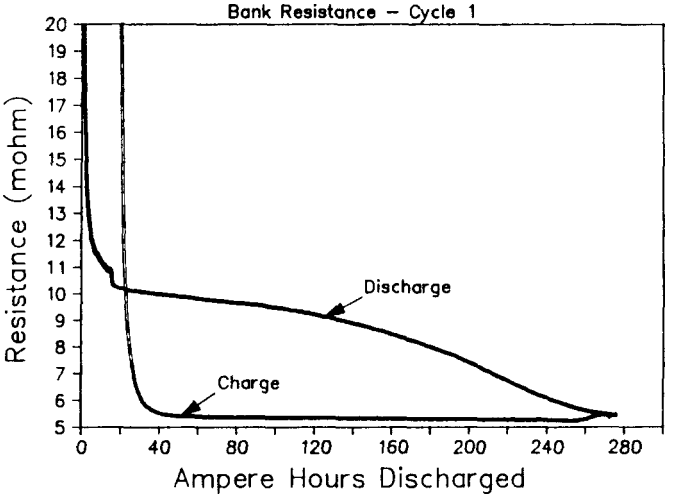

Figure 5. Commissioning Cycle Bank Resistance

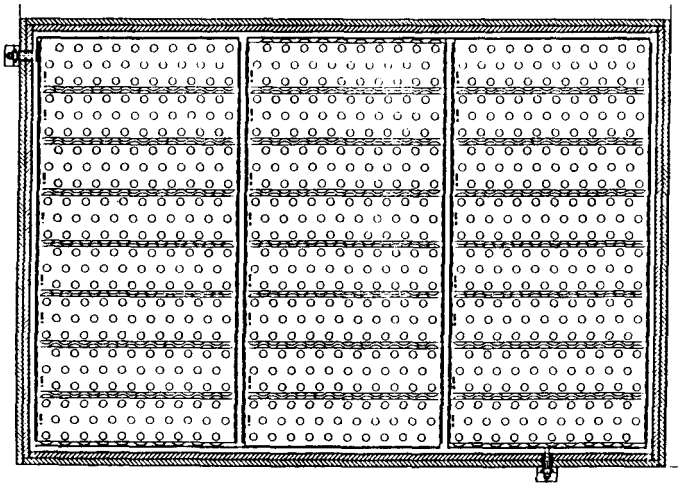

Figure 6. Bank Layout in ETX-II Battery

NaS BATTERIES FOR ELECTRIC VEHICLES

Wilfried Fischer
Powerplex Technologies Inc.

The development of a commercially viable battery for electric vehicles requires extensive testing and evaluation outside of the laboratory, in real world operating conditions. In turn, an electric vehicle battery must be demonstrated inherently safe, and compatible with an appropriate motor/controller system. Battery geometry is also an important criteria for eventual integration in various vehicle platforms. Finally, the battery system must be commercially viable from a manufacturing cost perspective.

Asea Brown Boveri (ABB) and Powerplex Technologies Inc. through their joint NaS battery development program have undertaken extensive testing of hundreds of full size prototype B-11 type NaS batteries in both stationary and on-road test conditions. Accordingly, hundreds of thousands of kilometers and thousands of charge/discharge cycles have been logged on prototype NaS batteries, providing invaluable information for further development. Prototype NaS batteries have also undergone extensive safety and durability tests, including vibration, crash, crush, fire and water emersion experiments. As a result, ABB/Powerplex NaS batteries are now certified by TUV for operation on all public roadways in West Germany.

Motor/controller systems have also been developed by ABB specifically for NaS batteries. These motor/controllers incorporate features such as on-board charging, and are compatible with a variety of vehicle applications.

Based on the numerous full size battery tests to date and utilizing the same basic NaS cell design, ABB and Powerplex have developed a next generation battery for commercial introduction in the early to mid 1990s. These batteries are inherently less expensive to manufacture than the B-11 battery design and are dimensionally compatible with a variety of vehicle platforms. Prototype batteries of this design are currently in production and under test in a variety of stationary and on-road evaluation programs.

Acknowledgement:

This research is sponsored by Energy, Mines and Resources (IERD) Canada and The National Research Council of Canada.

PROPERTIES AND MORPHOLOGY OF DOPED POLYCRYSTALLINE BETA"-ALUMINA ELECTROLYTES

Steven J. Visco, Meilin Liu, Patricia Kimes, and Lutgard C. De Jonghe

Materials and Chemical Sciences Division
LAWRENCE BERKELEY LABORATORY
1 Cyclotron Rd.
Berkeley, CA 94720

1. EXPERIMENTAL

β''-alumina specimens were fabricated from commercial β''-alumina powders* of nominal composition 90.40 wt% Al_2O_3, 8.85 wt% Na_2O, and 0.75 wt% Li_2O. A series of 100 gram samples of the commercial β''-alumina powder were mixed with 0.2 wt% of one of the oxides of germanium (GeO_2), magnesium (MgO), niobium (Nb_2O_5), or zinc (ZnO). The samples were subsequently ball-milled in acetone with 2 mm ZrO_2 balls, air dried, and filtered through 100 mesh sieves. The homogeneous powders were then cold uniaxially pressed at low pressure into disks of approximately 1 cm diameter by 0.5 cm thickness. The green bodies were finally hot-pressed two pellets at a time with one pellet composed of pure β''-alumina and the second pellet containing the impurity oxide. The green pellets were surrounded by boron nitride powder and were separated by tantalum sheets. The hot-press furnace was brought to sintering temperature at a heating rate of 29^o per minute, and the samples were densified at a temperature of 1450^oC and a pressure of 5815 PSIA for a total of 30 minutes; the resulting ceramics all had relative densities in excess of 96% of theoretical density. The faces of the hot-pressed ceramic electrolytes were then polished to a mirror finish with successively finer grades of alumina powder and diamond paste. Blocking gold electrodes were subsequently sputtered onto both faces of the polished polycrystalline samples prior to analysis by ac impedance spectroscopy. Ionic conductivity measurements were performed in the frequency range of 1 Hz to 1 MHz under an argon atmosphere in a quartz furnace, from ambient to 350^oC. After analysis by ac impedance, the ceramic electrolytes were notched and fractured for microstructural analysis by optical and scanning electron microscopy.

2. RESULTS AND DISCUSSION

The impedance spectrum of the doped and undoped β''-alumina disks displayed impedance/admittance spectra characteristic of polycrystalline β'' (Figs. 2,3) The equivalent circuit for the ceramic electrolytes can be described as shown in Fig. 1 where the ionic current path involves the series resistance of bulk (intergranular) transport and grain boundary (intergranular) transport.

The admittance spectra of the GeO_2-doped electrolyte typifies the spectra of the doped and undoped samples; the spectra over a range of temperatures is shown in Figs. 2 and 3. As can be seen from the experimental data, the low frequency arc attributed to the grain boundary resistivity is dominant at low temperatures, and decreases in magnitude with increasing temperature, until at temperatures above approximately 130 to 180^oC the grain boundary resistance has diminished to the extent as to be unresolvable from the bulk resistance.

---

* Ceramatech, Inc., 2425 South 900 West, Salt Lake City, Utah 84119

Arrhenius plots of the total ionic conductivity for the β''-alumina ceramics are shown in Fig. 4. As can be seen from the graph, the total conductivity of all the doped samples was increased over the entire temperature range relative to the undoped β''-alumina samples. Further, the increase in the total conductivity was larger at lower temperatures where grain boundary effects are most important; in fact the conductivities appear to merge at higher temperatures where intergranular transport should be the dominant current path. As can be seen from table 1, the lowest resistivities over the entire temperature range were obtained for the ZnO-doped β''-alumina polycrystals (MgO-doped electrolytes were slightly less resistive at 170°C).

Since the Arrhenius plots of the conductivity data tend to converge at high temperatures, it would seem that the dopant effect is manifested in the grain boundary resistance. This is also likely in that the low concentrations of dopant cations are unlikely to cause appreciable changes in the bulk conductivity of the electrolytes. The observed trends in the conductivity are consistent with lowering of the grain boundary resistance, but this may be due either to lowering of the activation energy for intragranular transport, or through morphological changes which reduce the number of grain boundaries which the mobile sodium ions encounter on transport through the polycrystals. In fact it appears likely that the latter is true, since SEM investigations imply increased grain size upon addition of the dopant metal cations. Further, since the activation energy for grain boundary conduction was essentially unchanged, it is likely that the increase in conductivity is due to the increased grain size of the doped ceramics. However, since the microstructure of the doped electrolytes was not a constant, it is difficult to determine whether the effect is due to grain boundary resistivity changes or beneficial morphological effects. As can be seen from table 1 and Fig. 4, the largest observed changes were for MgO and ZnO additives, which have also been used as stabilizers for the β''-alumina structure (both cations can enter the spinel blocks).

Table 1.

	TOTAL RESISTIVITIES OF DOPED/UNDOPED SAMPLES (Ωcm)				
TEMP (°C)	Pure β''	ZnO	MgO	Nb_2O_5	GeO_2
290	6.17	3.64	4.23	5.02	5.47
170	16.1	7.7	6.55	9.92	10.63

3. CONCLUSIONS

The addition of low concentrations of metal oxides (Zn, Mg, Nb, and Ge) to β''-alumina powders results in lowered resistivity values over the temperature range of 70 to 350°C. SEM studies of the fractured electrolytes indicated that in each case the grain size of the hot-pressed samples was increased (relative to undoped samples) as a result of the addition of the impurity metal oxide. It is unclear whether the enhanced conductivity is due to increased grain size or reduced grain boundary resistivity (or both). The observed increase in total ionic conductivity, particularly over the temperature range of 100 to 250°C, may prove useful in boosting the energy and power densities of β''-alumina-based intermediate temperature cells, such as the Zebra or Na/RSSR cells.

4. ACKNOWLEDGEMENT

This work was supported by the Assistant Secretary of Conservation and Renewable Energy, Office of Energy Storage and Distribution of the U.S. Department of Energy under Contract No. DE-AC03-76SF00098.

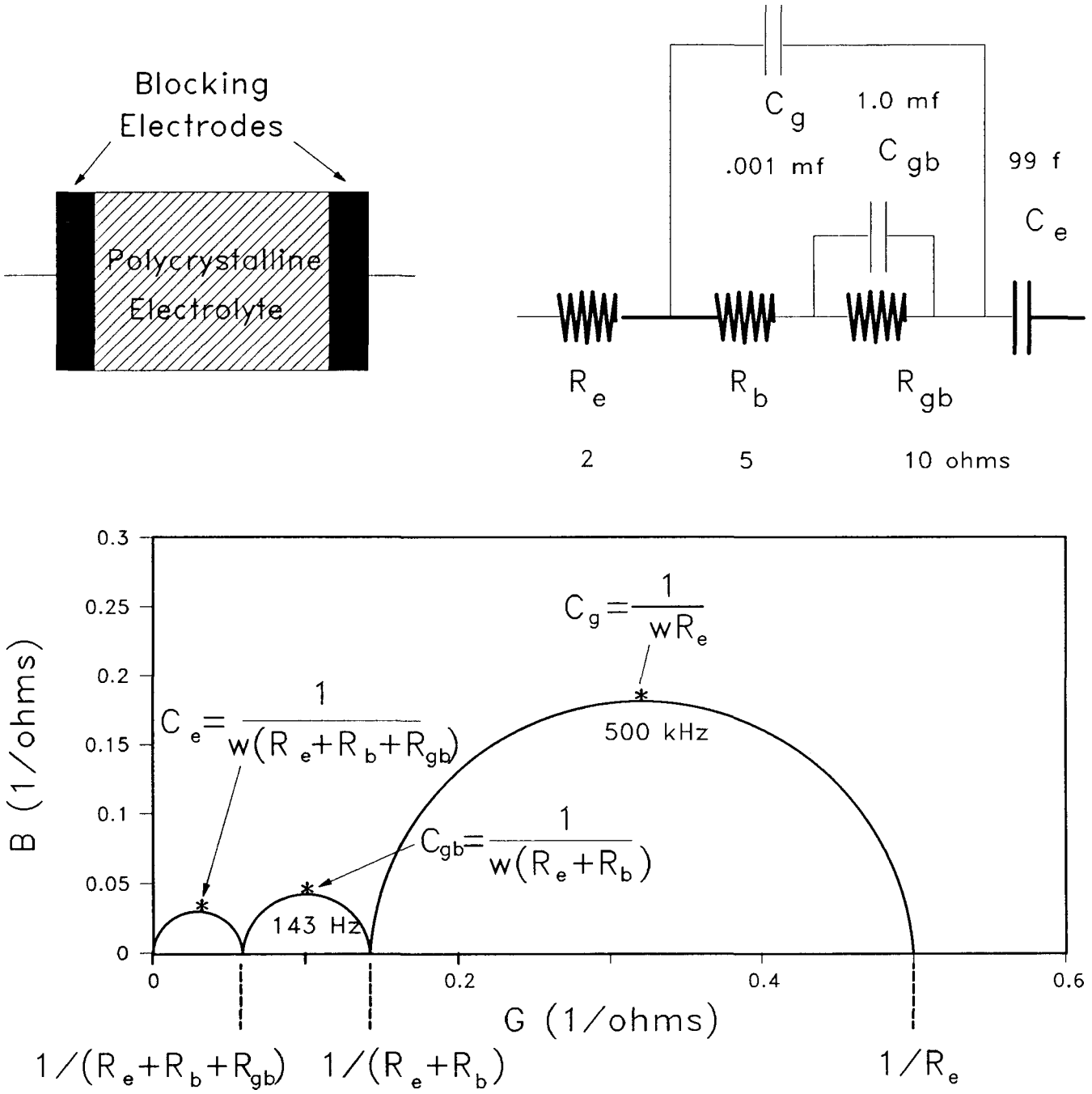

Fig. 1 Equivalent circuit for polycrystalline β''-alumina electrolytes

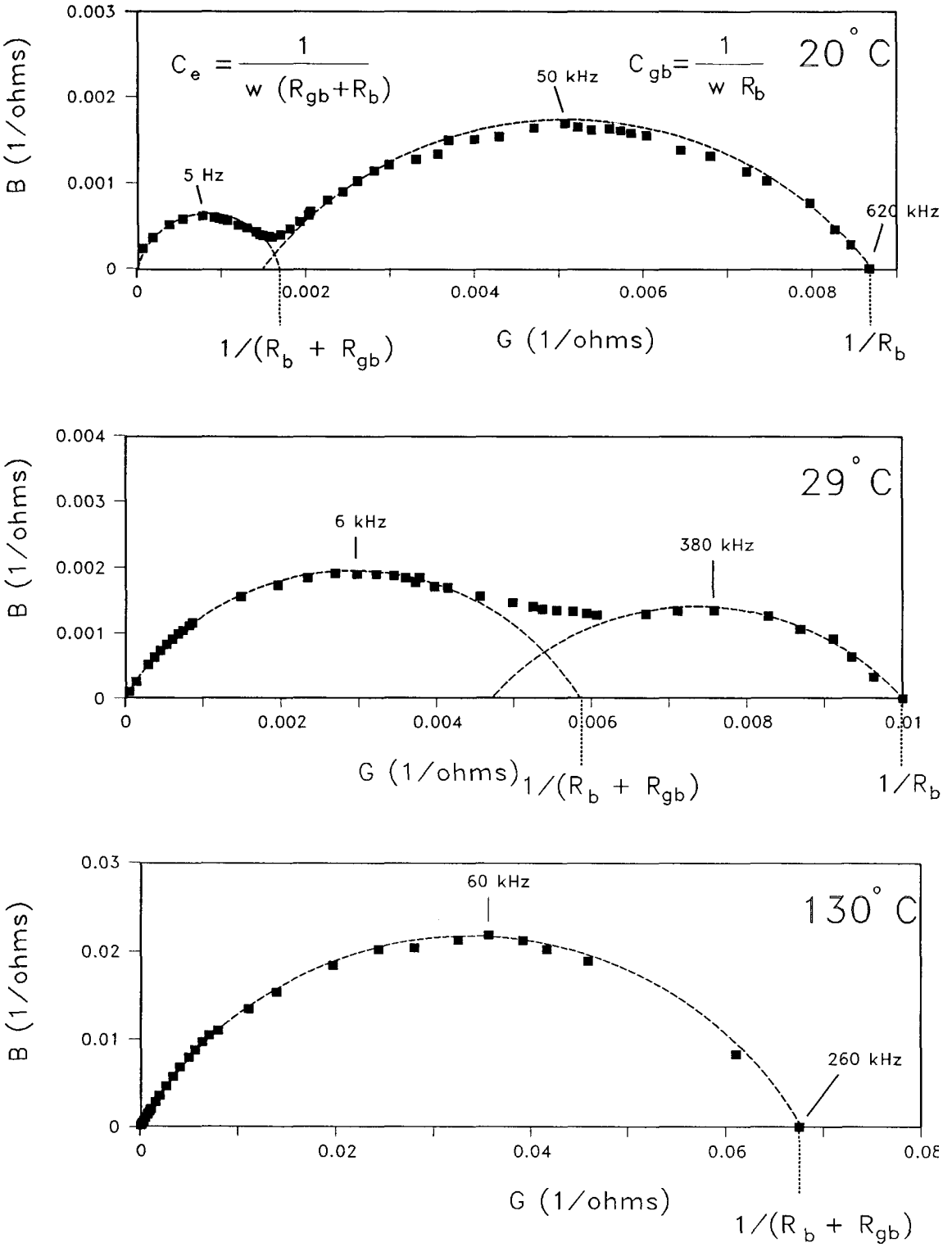

Fig. 2 Complex admittance plot for β''-alumina electrolytes doped with 0.2 wt% GeO_2 as a function of temperature

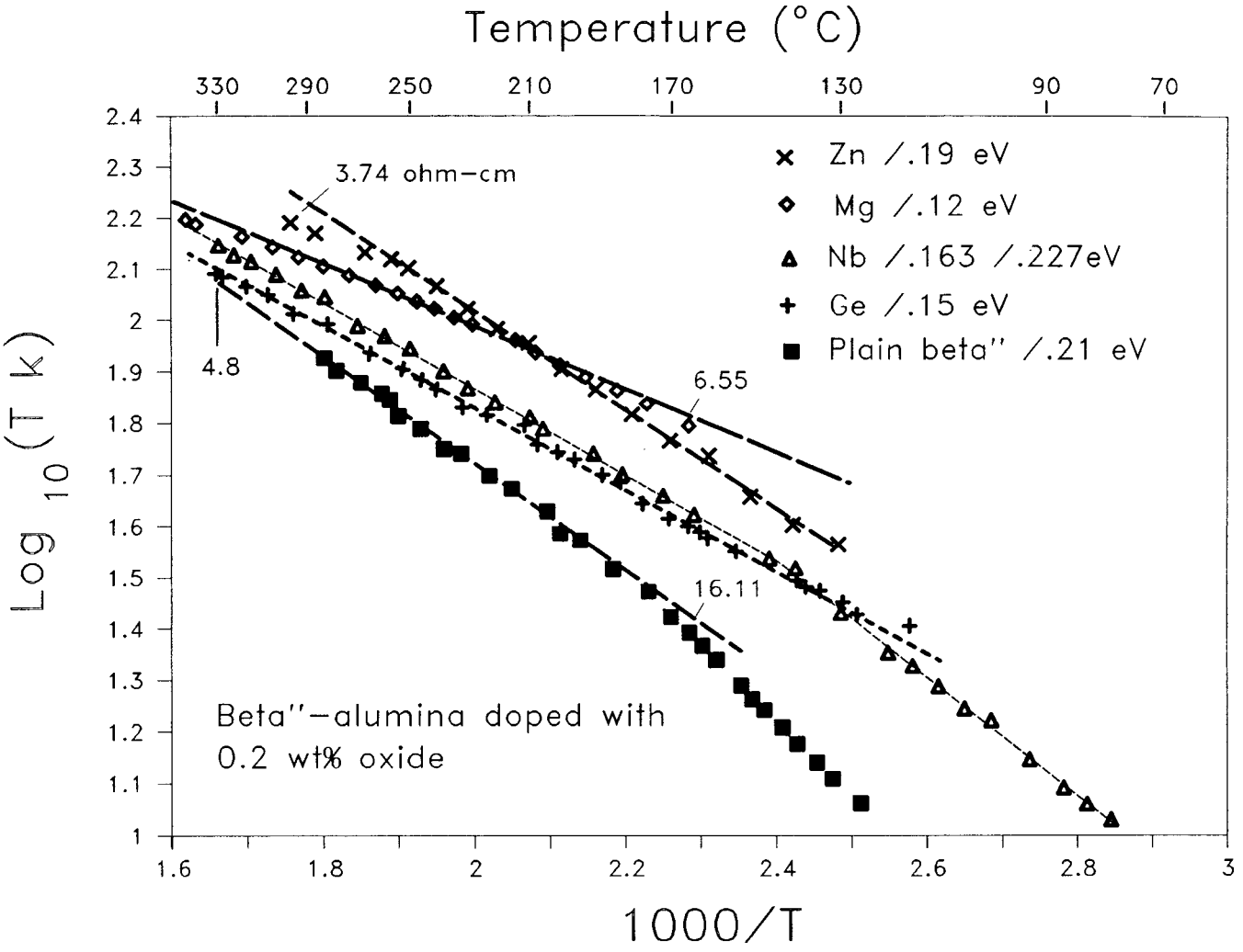

Fig. 4 Arrhenius plots of total conductivity for polycrystalline β''-alumina electrolytes with and without impurity oxides

SODIUM/SULFUR STUDIES AT SNL

Jeffrey W. Braithwaite
Sandia National Laboratories

Sandia National Laboratories (SNL) provides the technical management for DOE-sponsored advanced-battery development programs. A part of Sandia's responsibility is to study specific problems that are encountered during the development process. The number and size of these studies are limited to ensure that the funding emphasis is given to the contracted engineering development of promising battery technologies.

Five sodium/sulfur-related tasks are currently being performed at Sandia. The activity for each is closely coordinated with the prime DOE contractor, Chloride Silent Power, Ltd. (CSPL). These tasks include:

- Beta"-Alumina Electrolyte Degradation
- Component Stress during Freeze/Thaw Cycling
- Improved Chromium Plating Techniques
- Materials for Passive Thermal Management Systems
- Design of Thermal Cutoff Fuses

The first four tasks involve more fundamental aspects of the sodium/sulfur development program. The product from the final task will be part of an upcoming development contract, the engineering of large battery modules. Brief descriptions of each task along with selected results are given in the following sections.

Beta"-Alumina Electrolyte Degradation: The long-term failure of the beta"-alumina electrolyte remains an area of concern and the goal of this ongoing task is to identify failure mechanisms. Post-mortem analyses have shown that, in general, electrolyte failure can now be traced to identifiable external factors, such as contamination or a problem during production of a particular component. The conclusion has been reached that only limited information can be gained from detailed analyses of electrolytes taken from failed cells. Therefore, a specific mechanism of electrolyte degradation is now being studied that is related to a probable contamination effect: stress-assisted electrolytic degradation. Three specific subtasks are being pursued: (1) the identification of possible mechanisms--occurring during processing of the ceramic, cell assembly or cell operation--that can result in undesirable surface layers, (2) the measurement of crack growth rates within these layers, and 3) an evaluation of the potential for sub-critical crack growth within the electrolyte.

Component Stress during Freeze/Thaw Cycling: Sodium/sulfur batteries will be subjected to numerous freeze/thaw (F/T) cycles during their lifetime. Most developers, including CSPL, feel that improvement in F/T durability will be needed when and if cost issues force larger cell sizes to again be considered. The purpose of this task is to provide developers with an analytical tool and the necessary knowledge to improve the long-term F/T durability of cells.

Recent activity has successfully concentrated on developing an understanding of the stress-producing processes and a validated thermomechanical model for a normally operating cell. To demonstrate the progress, a typical mechanical strain response measured during the freezing of a Sandia lab cell is shown in Figure 1. A correlation of the measured values and those calculated using the model are shown in Figure 2. Figure 2 shows only the hoop stress; the axial strain correlation is almost exact. The validated model represents a very significant accomplishment in

that a methodology is now available for two needed future studies: (1) identification and analysis of potential F/T failure mechanisms, and (2) optimization of cell design to reduce F/T-induced stress.

Improved Chromium Platings: In this task, techniques are being developed to electroplate high-quality chromium-layers onto carbon and stainless steels and to identify methods to use these techniques to effectively plate closed-end CSPL cell containers. Three studies are being performed that involve: (1) the modification, with vanadium pentoxide (V_2O_5), of a commercial electrolyte that is used to produce crack-free deposits; (2) the investigation of the feasibility for producing and utilizing a highly cracked deposit; and (3) the development of pulse and pulse-reverse plating techniques as a method to increase efficiency and reduce the stress in crack-free deposits.

The modified techniques have been used to plate CSPL cell containers and corrosion coupons. The performance of these platings is being evaluated using both corrosion and in-cell exposures. A result from an evaluation of a crack-free deposit is shown in Figure 3. In this test, a chromium deposit was exposed to Na_2S_4 for two weeks at 400°C (upper) and remained relatively unaffected. Severe corrosion of the unprotected stainless-steel vessel used to contain the Na_2S_4 is evident in the lower photograph. The behavior of these platings in an operating cell is being determined.

Materials for Passive Thermal Management Systems: The use of a thermal management system (TMS) may be required in sodium/sulfur EV batteries. One of the preferred TMS concepts is a passive technology that utilizes the latent heat-of-fusion of a material contained within the battery enclosure to limit temperature increases during discharge. The objective of this task is to identify suitable latent-heat-storage (LHS) materials and characterize their performance in a TMS environment. Selection criteria for the LHS materials included melting temperature, heat-of-fusion, density, corrosivity, stability, safety, and cost. Two candidate materials have been identified and characterized. The first is a binary eutectic salt containing LiCl and KCl (m.p. = 356°C, ΔH_f = 55 cal./gm.) and the second is a ternary eutectic salt containing K_2CO_3, Li_2CO_3, and LiOH (m.p. = 370°C, ΔH_f = 100 cal./gm.). Because each of these materials has advantages and disadvantages over the other, the final selection will depend on the actual TMS design.

Development of Thermal Cutoff Fuses: A fuse that opens if the internal battery temperature exceeds a desired value may have to be included in all high-energy battery systems. The function of such a device in a sodium/sulfur battery is to prevent internal short circuits in the worst-case situation when major cell failures occur. This task is being performed to develop an inexpensive thermal fuse. The initial activities consisted of selecting suitable fusible materials (based on melting point, fabrication capability, conductivity, cost), identifying techniques for making reliable connections, and experimentally characterizing their performance. After a comprehensive screening of candidate metals, zinc (m.p. = 420°C) was selected. Its oxidation, electrical, and mechanical properties were determined. Several conceptual fuse designs have been formulated, fabricated and tested. One of these is shown schematically in Figure 4. The container is used to protect the zinc from oxidation and to contain the molten zinc if the fuse activates. Other concepts include protecting the zinc with a coating such as sol-gel. The performance to date is promising, however, aging characteristics remain an unknown and are being studied.

This work is supported by DOE Contract #DE-AC04-76-DP00789.

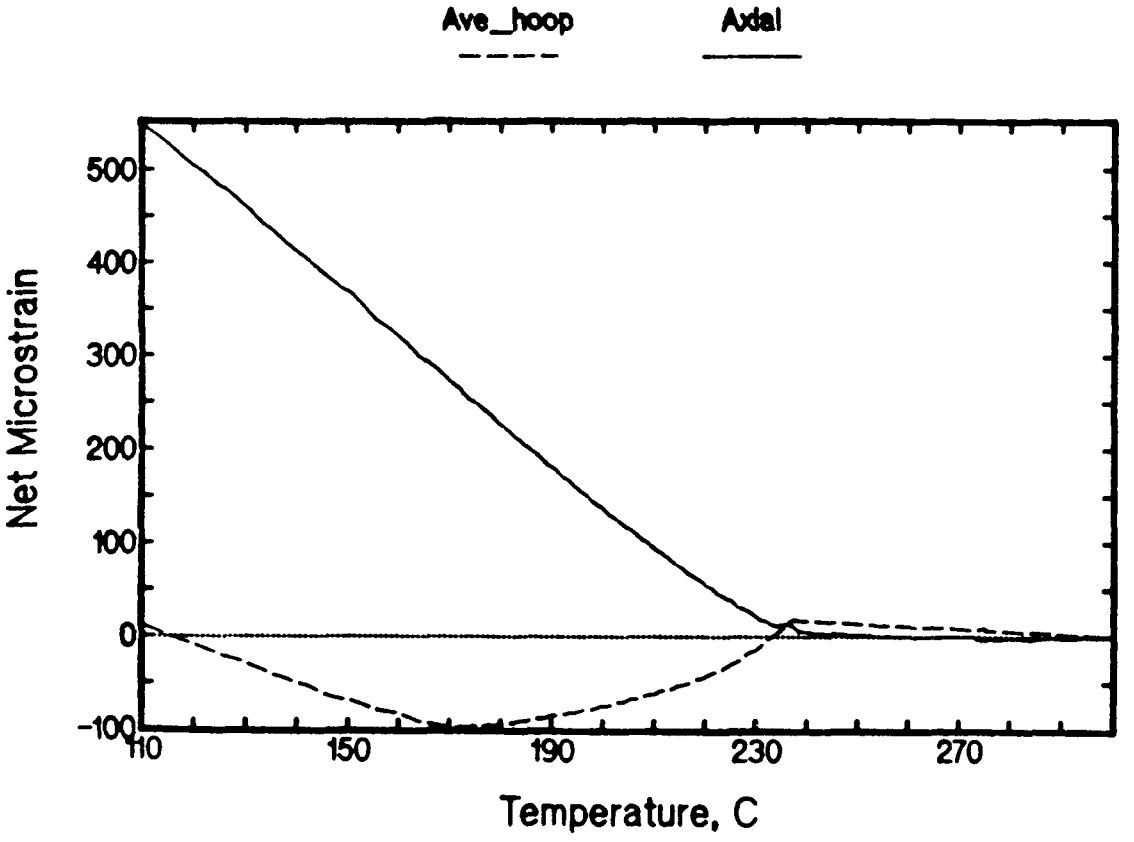

Figure 1. Measured mechanical strain on the stainless steel container as a function of temperature during the freeze cycle of a discharged SNL lab cell (OCV = 1.9 v.).

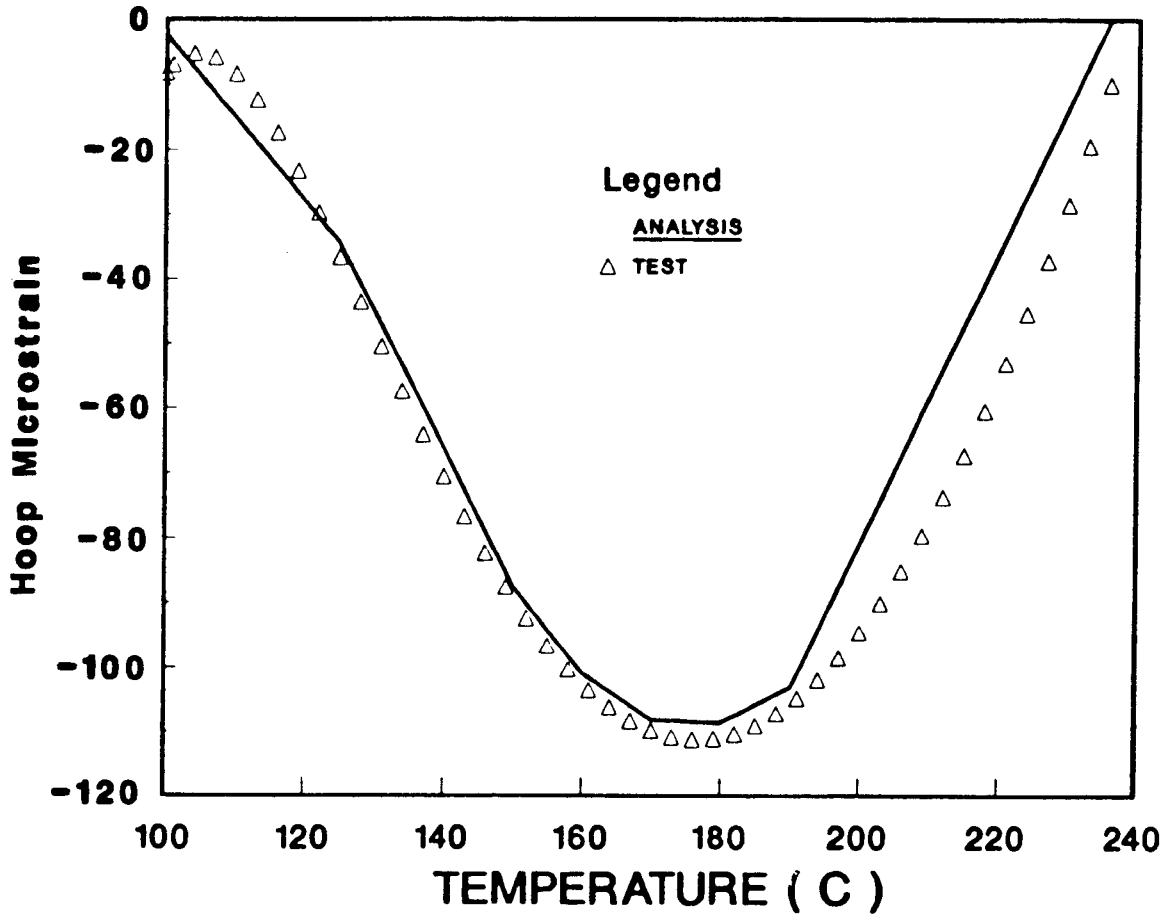

Figure 2. Comparison of calculated and measured hoop strain from the freezing of a SNL lab cell. The calculations utilized a thermomechanical model and the measurements are those shown in Figure 1.

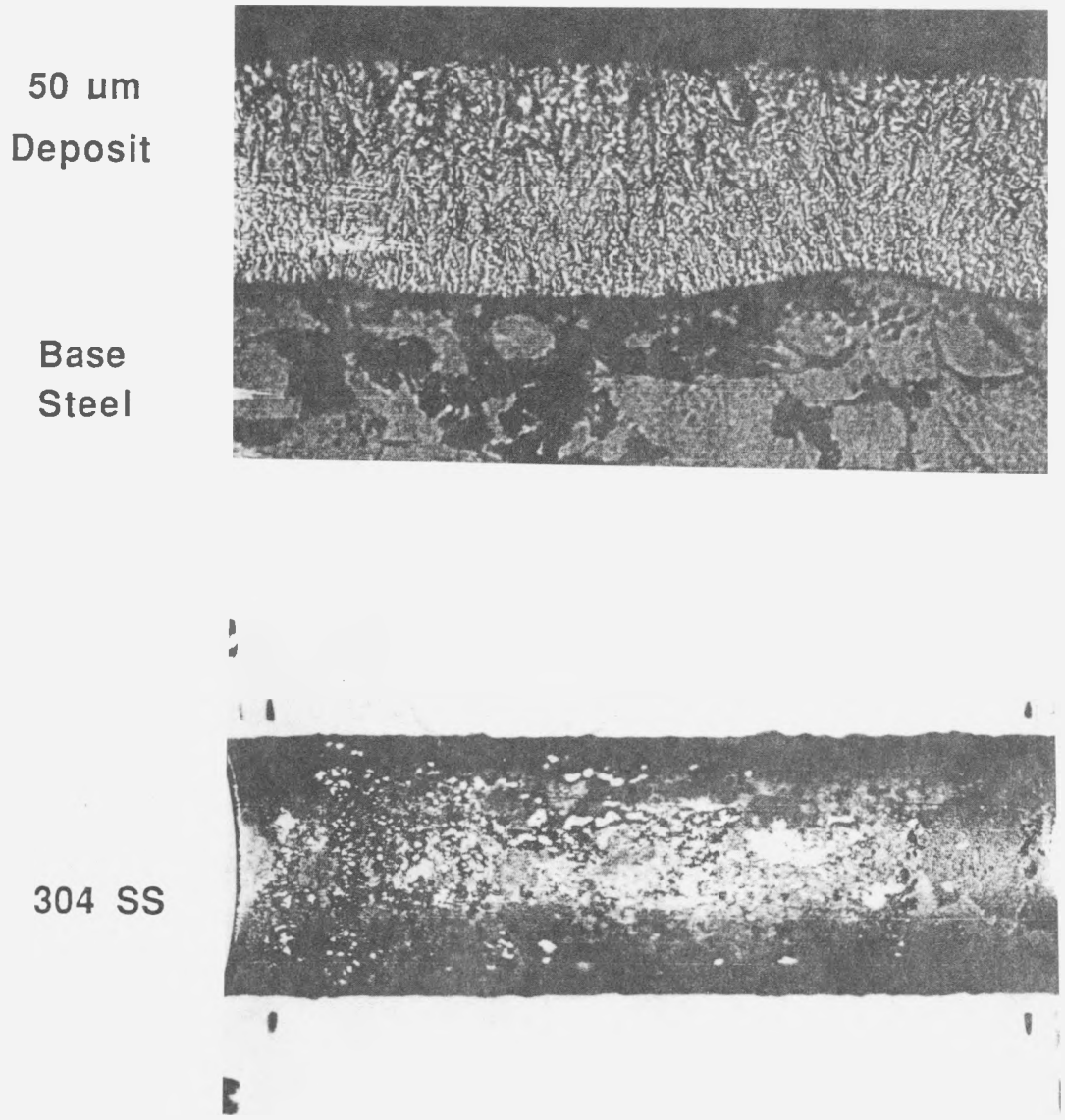

Figure 3. Optical micrographs of the cross-section of a chromium deposit after exposure to Na_2S_4 for two weeks at 400°C (upper) and of the unprotected stainless-steel containment vessel (lower). The crack-free chromium plating was produced using a procedure identified at SNL.

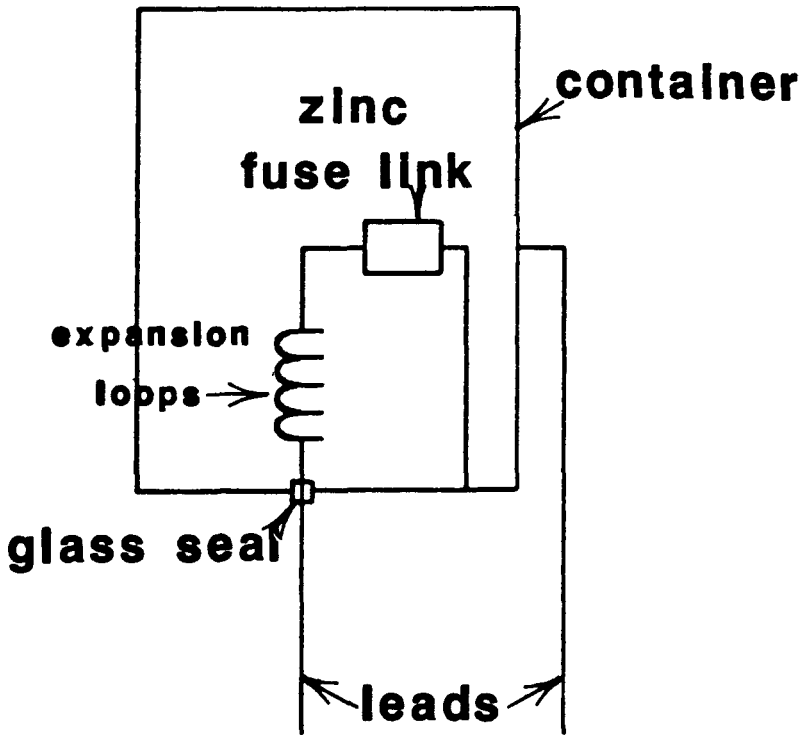

Figure 4. A schematic diagram of a thermal cutoff fuse concept. A stainless steel container and glass to metal seal would be utilized.

SODIUM/SULFUR RESEARCH AT SRI

Michael C.H. McKubre, Stuart I. Smedley, Francis L. Tanzella
SRI International
Menlo Park, CA 94025

and

Robert D. Weaver
Electric Power Research Institute
SRI International (Scientific Fellow)

Two research efforts are directed towards anticipating and understanding potential problems of sodium sulfur cells and their implementation in batteries. Current experiments are directed in four major areas:

1) Corrosion of the polysulfide container; alternate materials and coatings.

2) The causes and consequences of polarization of the sulfur electrode, particularly at high states of charge (overcharge), in the single phase region, and at low states of charge (overdischarge).

3) The effects of impurities on corrosion and sulfur electrode polarization.

4) The development of switches to shunt or isolate failed cells in series or parallel arrays.

In this review we will present data concerning items 2 and 4 only.

Polarization of the Sulfur Electrode:

The Electrochemical impedance of Na/S cells comprises three major elements[1,2]: (1) a series resistance due to migration of Na^+ ions in the β"-alumina electrolyte and in a partially blocking layer at the β"-alumina/polysulfide electrolyte interface, (2) a Faradaic impedance due to the charge transfer reactions between S and $S^=$ on the carbon surface of the porous electrode structure, and (3) a diffusional impedance that originates at the membrane boundary between sodium ions in the β"-alumina solid electrolyte and sodium and polysulfide ions in the polysulfide liquid electrolyte.

The three impedance elements are indicated in Figure 1 in data obtained for a typical Na/S cell equilibrated in the single phase region. In the two phase region the large diffusional tail, indicated by a straight line of slope 45° in the complex plane plot, is not

observed. At high and low states of charge, additional polarization is observed as each of the impedance elements increase in magnitude.

Figure 2 shows the effect on each of the impedance components of discharging at 0.5A, to a state of discharge where a second phase (presumed to be solid Na_2S_2) precipitates in the polysulfide electrolyte. The Faradaic impedance, R_f, abruptly increases on application of a discharge current, then increases linearly with coulombs of overdischarge. The ionic, R_i, and diffusional, R_d, resistance terms increase in proportion to the square of the charge passed. The diffusional term, however, increases more rapidly, and becomes the predominant cause of polarization in the overdischarge region.

These observations have been incorporated into a mathematical model to explain the origins of polarization at low states of charge, with the intention of increasing the discharge energy of sodium/sulfur cells.

Reliability Considerations of Batteries

A statistical analysis has been made[3] of the performance characteristics of series/parallel arrays of Na/S Cells, to explore the need for switches in battery networks of size suitable for load-leveling applications. The need for a switching action in the load-leveling and electric vehicle arrays studied has been made clear.[3] Figure 3 indicates that, even with the existence of suitable switches, battery life will be short relative to cell characteristic life, if the battery is made from cells having a low Weibull shape factor.

Work is underway to develop switches in two basic geometries: (1) to switch failed parallel cells out of parallel arrays and (2) to bypass cells in series strings. Development of the simpler, parallel switch is almost complete using a proprietary design. Efforts will be made to assess the reliability and packageability of this switch in future studies.

Acknowledgements

The authors gratefully acknowledge support of this work by Electric Power Research Institute.

References

1) M.C.H. McKubre, S. I. Smedley and F. Tanzella, "The Electrochemical Impedance of the Na/S Cell; Part I, Experiments and Results," (1987), J. Electrochem. Soc. 1989, 136, p. 1962.

2) M.C.H. McKubre, S. I. Smedley and F. Tanzella, "The Electrochemical Impedance of the Na/S Cell; Part II, Interpretation of Results," (1987), J. Electrochem. Soc. 1989, 136, p. 1969.

3) R. D. Weaver, M.C.H. McKubre, P. C. Symons and F. L. Tanzella, "Some Reliability Considerations of Various Battery Networks of Sodium/Sulfur Batteries," Paper No. 899250, *proceedings of the 24th Intersociety Energy Conversion Engineering Conference, Washington, (1989).*

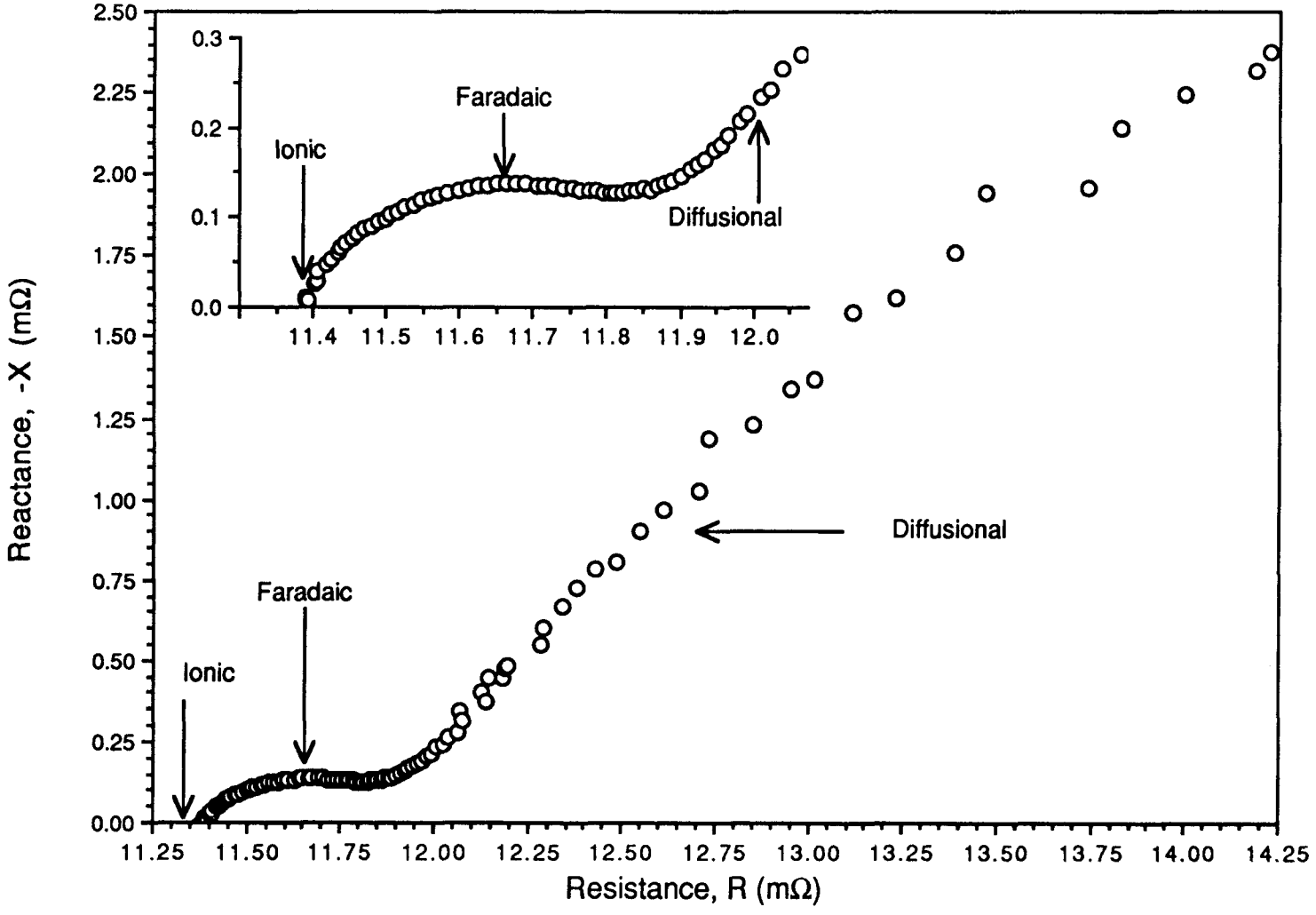

Figure 1 Typical Nyquist Response of a Sodium/Sulfur Cell equilibrated in the Single Phase region

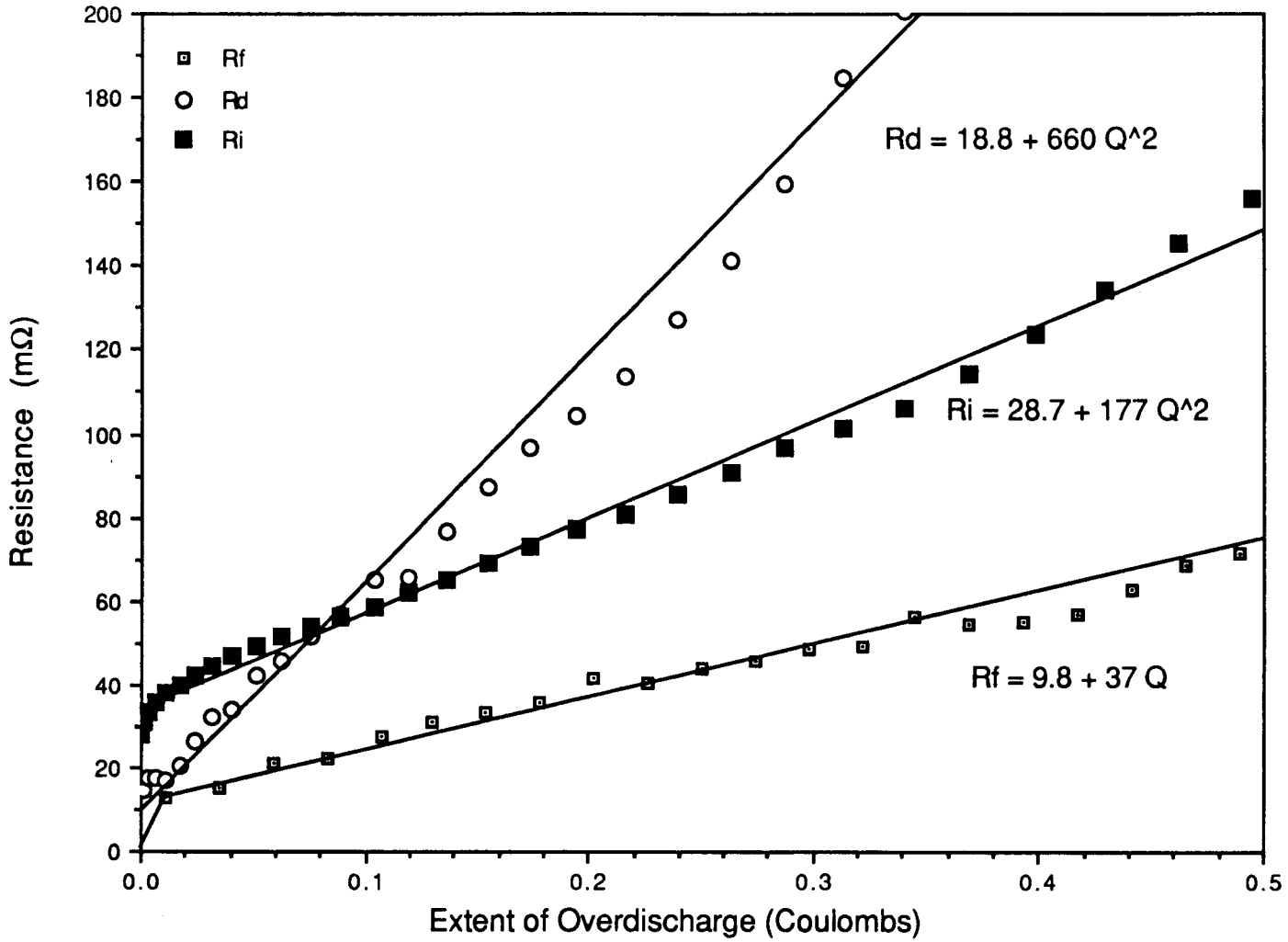

Figure 2 Increase in resistance of a Na/S Cell discharged at -0.5 A below 1.74 V at 350°C

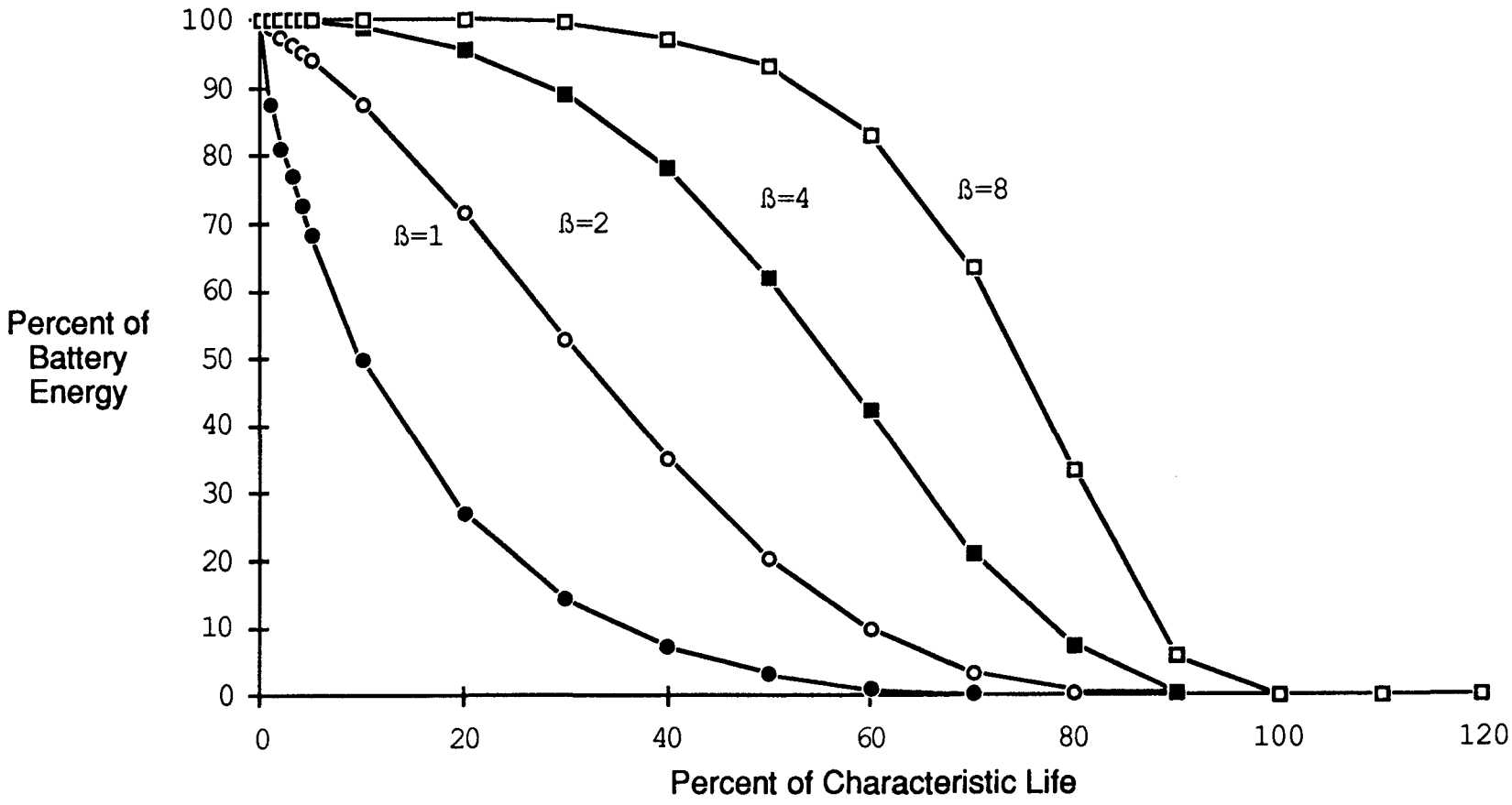

Figure 3. Variation of Available Battery Energy With Time for a Load-Leveling Battery

SODIUM/SULFUR BATTERY TESTING AT ARGONNE NATIONAL LABORATORY

W. H. DeLuca and A. F. Tummillo
Argonne National Laboratory
Chemical Technology Division
Argonne, Illinois

A one-third-size sodium/sulfur (Na/S) battery fabricated by Chloride Silent Power Limited (CSPL) was delivered to ANL for testing in January 1989. The battery, which came with the charger and thermal management system, is rated at 300-Ah, 64-V and contains 960 cells configured into eight series-connected banks. A bank consists of 30 parallel-connected strings, each with 4 series-connected cells. Each cell is hermetically sealed in a chromized steel case and has a rated capacity of 10 Ah. This deliverable is an interim step toward the development of a full-size Na/S battery for the ETX-II vehicle. The latter battery will be three times larger and is scheduled for delivery in September 1989.

The delivered CSPL battery had a measured weight of 309 kg, divided as follows: 126 kg of cells at 131 g/cell, about 100 kg of insulation, ~83 kg and for the enclosure and cell monitoring/interconnections. To determine the power load for constant power (Ragone data) and driving profile discharges, a total electric-vehicle battery weight of 696 kg was projected by CSPL (232 kg for the 1/3 module). This projected module weight limits the peak power demand for the SFUDS simulated driving schedule (79 W/kg) to 18.3 kW, which agrees with the maximum 55-kW demand to be imposed on the full-size Na/S battery in the ETX-II vehicle. The full-size battery weight is also the same as that anticipated for the ETX-II deliverable.

Battery charging is accomplished using the fixed two-step constant-current (CI/CI) charge regime. First, a 30-A charge rate is applied until a bank voltage of 8.7 V is reached, then a reduced charge rate of 10 A is applied until a bank voltage of 8.9 V is obtained. In the latter 10-A charge state, circuitry in the CSPL charger is available to equalize the voltage of the individual banks. The equalizer shunts current around those banks that reach 8.7 V while continuing to charge those banks below 8.7 V. Throughout the ANL tests, the capacity difference between banks has been minimal ($\leq$3 Ah), and the equalizer charger has not been activated. Battery charging has been terminated when any bank voltage of 8.9 V is measured.

CSPL personnel assisted ANL with the heatup and initial testing of the battery in February 1989. The battery was heated at a rate of 5°C/h to an operating temperature of 350°C. Two conditioning cycles were used with low charge and discharge rates because none of the cells had previously been heated to operating temperature. The first cycle had a 270-Ah discharge at a 15-A (20-h) rate followed by a 54-h recharge (5-A rate); the second cycle had a 240-Ah discharge at a 39-A (~8-h) rate and 15-h recharge. Battery end-of-discharge resistance decreased from an initial 229 mΩ on the first cycle (20-h discharge rate) to 46 mΩ on the second cycle (7-h rate). Eventually, a battery resistance of ~44 mΩ was obtained, which exhibited a temperature coefficient of about -0.2 mΩ/°C above 340°C. Preliminary data also showed that all of the cells were operating with uniform capacity, as evidenced by the match in bank voltages at the end of charge

and discharge (within ±0.5%). With life cycling, the individual bank capacities have remained matched to within 1% (3 Ah).

To date, the battery has been operated for about 225 cycles. A capacity history of the constant-current discharges at the 3-h rate to 100% depth of discharge (7.6 V/bank) and to 76% depth of discharge (8.0 V/bank) is given in Fig. 1. A maximum capacity of 306 Ah (18.7 kWh) was achieved at about the 20th cycle. The battery initially exhibited a capacity decline of ~0.03%/cycle, which indicated a projected life of ~600 cycles (to 80% of initial capacity). On the 132nd cycle, however, a cell (or cells) failed in bank No. 4, which resulted in a capacity loss of about 5% (~15 Ah). It appears that the four-cell string(s) containing the failed cell(s) went to a high resistance state (presumably the failed cell short circuits, and the remaining three series-connected cells are overcharged to a high resistance state). The 5% capacity loss is greater than that expected with the failure of a single 10-Ah cell string. The end-of-discharge (EOD) resistance of the affected bank had increased from 5.65 mΩ before the failure to 6.04 mΩ after the failure. The battery EOD resistance increased to 45 mΩ from 42.5 mΩ. The magnitude of this increased resistance indicates that more than one cell string had failed. The battery, however, continued to operate satisfactorily and exhibited the same gradual decline in capacity (~0.03 %/cycle rate) that was present before the cell failures.

Another capacity loss of ~20 Ah, apparently caused by other cell-string failures, occurred between cycles 192 and 198. Following the 215th cycle, another 15-Ah capacity loss decreased module capacity to ~78% of the initial 306 Ah level. These capacity losses were not totally unexpected because CSPL had indicated that a fabrication problem with the cell seals would start to appear at about 200 cycles.

Characterization tests were performed on the CSPL battery in the first 100 cycles. First, constant-power discharges (10 to 50 W/kg) were applied to obtain a Ragone plot of available energy as a function of power discharge rate (Fig. 2). At 50 W/kg, the discharge was terminated by reaching a temperature limit (370°C) instead of the 100% depth-of-discharge (DOD) limit used for the earlier discharges. Then, a partial discharge test was completed, and it was determined that a series of partial discharges (50% DOD) has no effect on the available 100% DOD battery capacity. The standardized hill climb test was also performed. The results showed that the battery maintained a 6-minute hill-climbing capability of 45 W/kg to a discharge level of 88% DOD.

Results of driving profile discharges indicated ranges of 148 miles for the DSEP van on a SFUDS79 driving schedule and 182 miles for the IETV-1 car on an SAE J227aD schedule. During these driving profile discharges, the CSPL thermal management system satisfactorily maintained the battery within an operating temperature range of 330-360°C. After a continuous 1.2-h hill-climbing power discharge of 50 W/kg, an operating temperature limit of 370°C was reached.

The battery has exhibited a high resistance (coup-de-fouet effect) for the first few minutes of discharge after a full recharge. Battery resistance was calculated during a driving profile discharge from variations in module voltage caused by changes in load current. The module resistance vs. DOD is plotted in Fig. 3 for cycles 125 and 190. The plots show that battery resistance increased by ~4% from cycle 125 to 190. The plots also show that the initial resistance is

~15% higher than the minimum value observed at 20% DOD. The resistance increases between 50 and 65% DOD because the cooling system is active and battery temperature is decreasing. At high initial discharge rates, the resistance causes a large temporary drop in module voltage that would limit available power for acceleration, and very high initial battery charge voltages would result with regenerative braking currents. Our discharge termination algorithm was modified to accommodate the large initial voltage drop. In addition, a voltage clamp had to be incorporated into the algorithm to reduce the initial regenerative braking currents and provide a module charge voltage limit during the high resistance state.

Acknowledgment:

This research is sponsored by the Department of Energy, Office of Transportation Systems, Electric and Hybrid Propulsion Division under Contract W-31-109-Eng-38.

CAPACITY HISTORY 960 CELL CSPL Na/S BATTERY

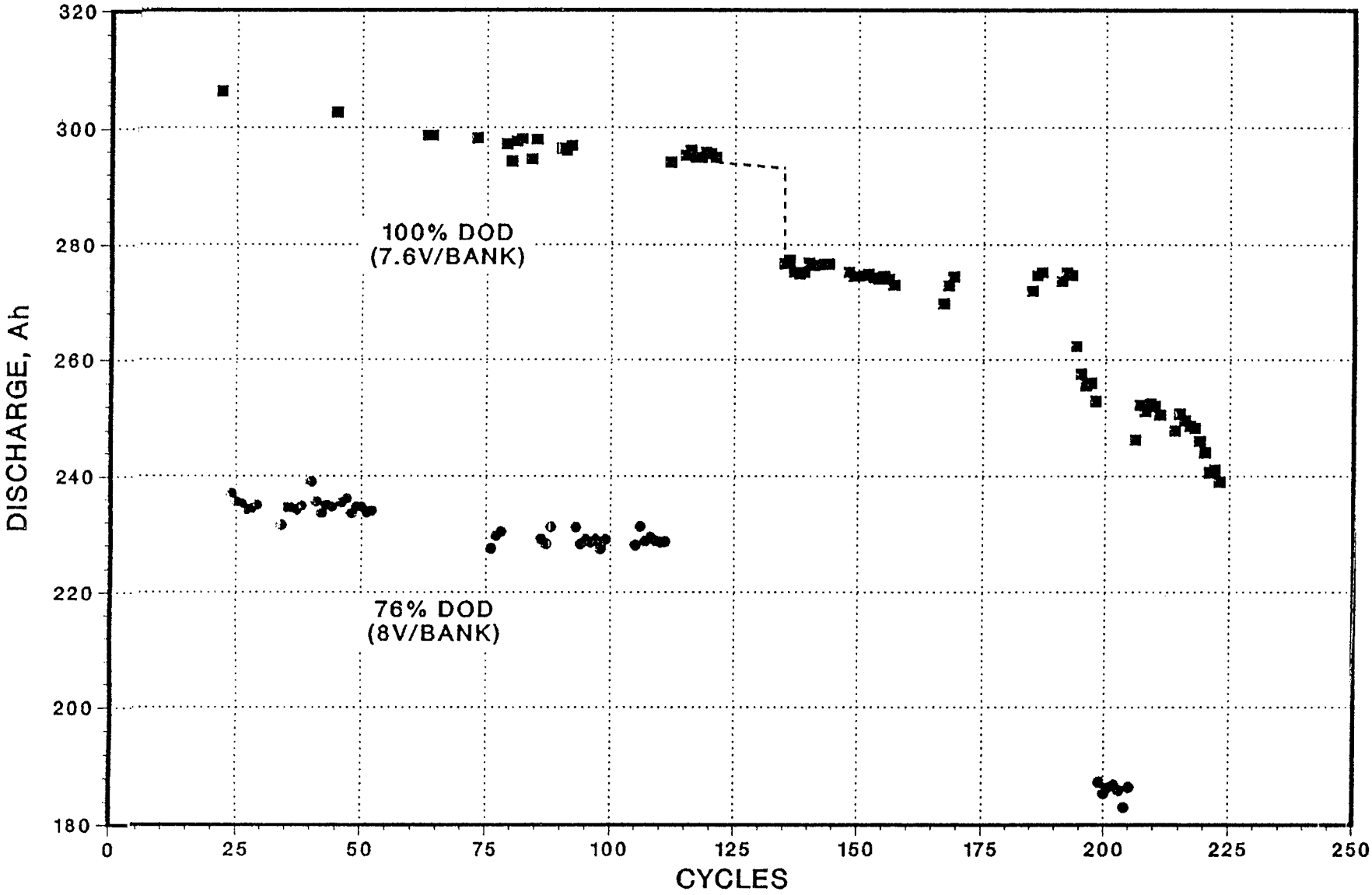

RAGONE PLOT FOR 960-CELL CSPL Na/S BATTERY

PROJECTED 1/3 BATTERY WEIGHT, 232 kg

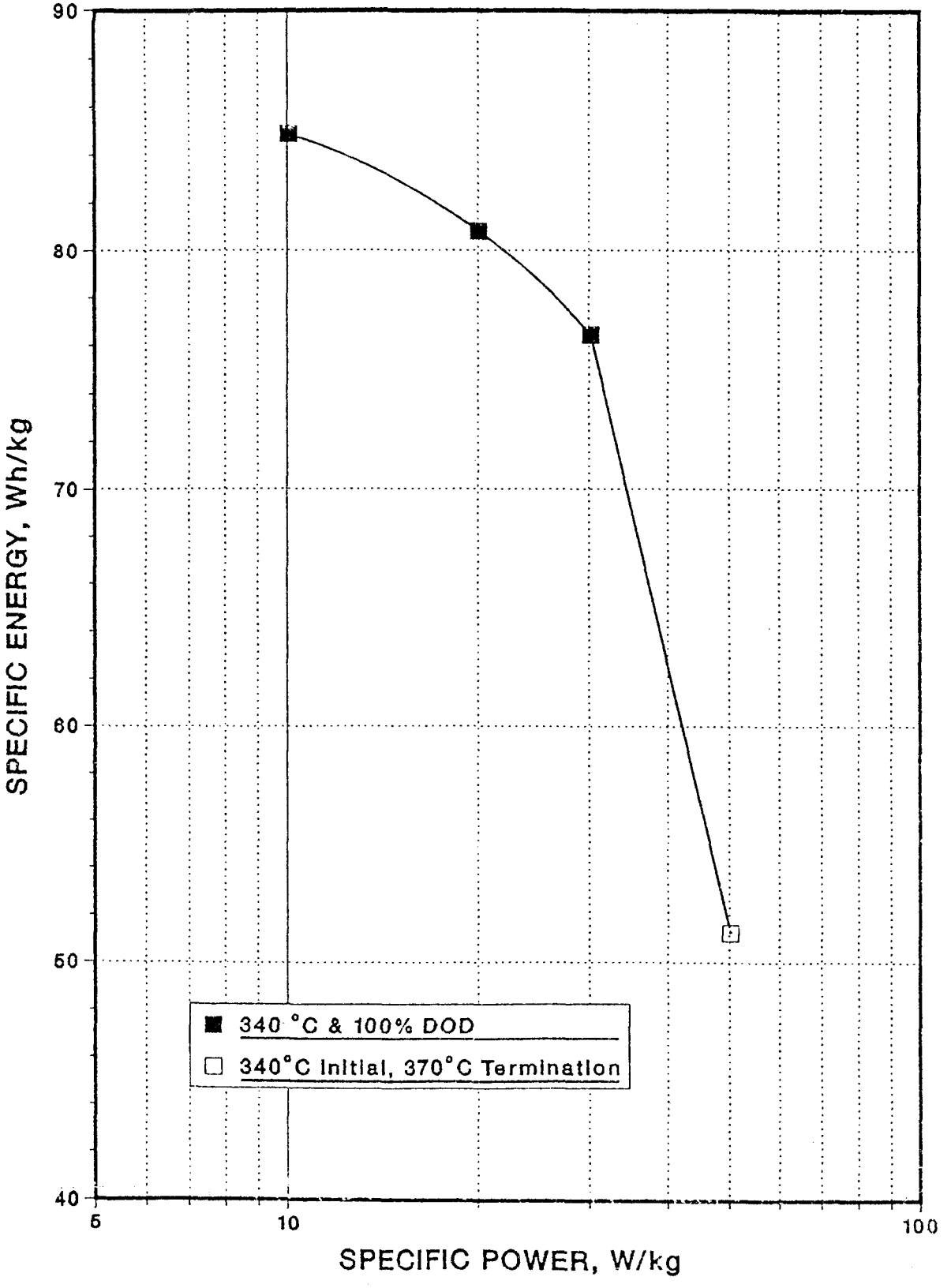

DERIVED RESISTANCE, STDSFUDS
Resistance vs DOD with Life

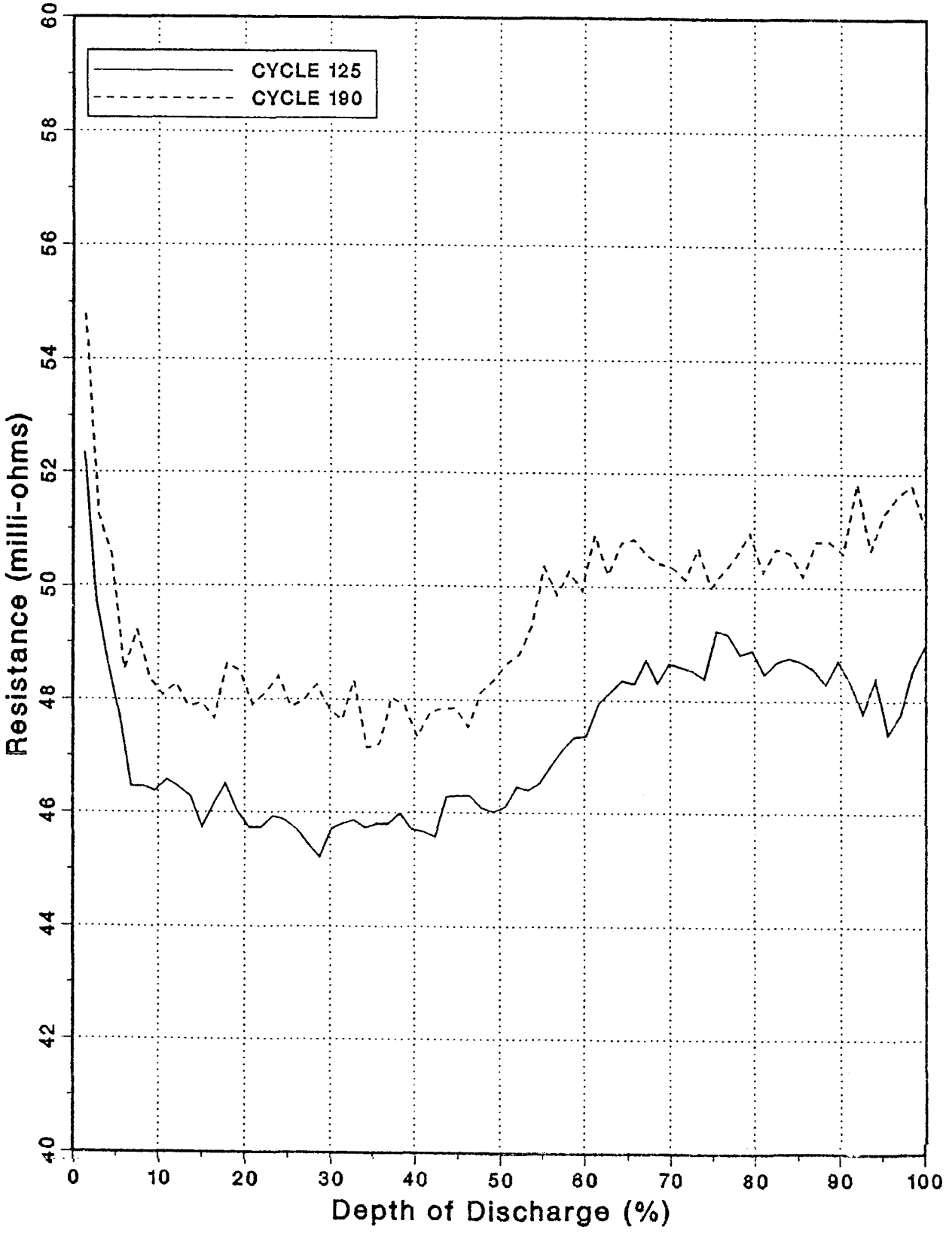

SODIUM/SULFUR EVALUATION AT SNL

J. M. Freese
Sandia National Laboratories

Sandia National Laboratories (SNL) has been involved in evaluation of sodium/sulfur technology for several years. The effort concentrated on the performance of single cells until recently when the evaluation of 4-cell strings was initiated. The majority of the activity during the past two years has focused on cells from Chloride Silent Power, Limited (CSPL). To date, four groups of PB cells and 4-cell strings, which were built with PB cells, have been evaluated. The first group of ten cells delivered to Sandia were on test for approximately one year. The majority of these cells failed due to corrosion problems in the sulfur seal. However, two cells completed over 800 cycles, and one of these cells completed nearly 1600 cycles. Results from this first group of cells were presented at the previous contractors' conference and will not be discussed at this meeting. In addition, seven cells from Powerplex and two cells from Ceramatec have been evaluated. The initial capacity of the Powerplex cells were below their rated values of 38 Ah, and several of these cells failed before achieving 400 cycles. One cell, however, has been cycled over 1000 times. Both Ceramatec cells achieved their rated capacity of 36 Ah and have been cycled over 1000 times. Due to limited abstract space, additional results of tests on these cells will not be discussed at this time.

The second group of cells delivered to SNL consisted of two cells that were assembled under the most favorable conditions at CSPL (#464 & 465). The components for these cells were hand picked and quickly assembled to reduce contamination problems. The only major change in cell construction from the first group was the use of a new, improved seal design (Mark 3). The third group of deliverables consisted of an additional six cells and two 4-cell strings. The only difference between the second and third groups was that group three came from an larger production lot. None of these cells and strings had been cycled, and thus a break-in procedure provided by CSPL was followed before evaluation tests were conducted. Table 1 shows the types of tests performed and the total number of cycles accumulated on the second and third groups of cells and strings.

An observation early in cycle life indicated that all the cells exhibited a charge-acceptance phenomenon when charged at the C/3 rate. At this higher charge rate, there was a decrease in cell capacity. This decrease was also seen, to a lesser extent, at lower charge rates. Because a typical charge rate for an electric vehicle or load-leveling sodium/sulfur battery could be as low as C/8, numerous cycles were run on each cell to determine the extent of the phenomenon. Figure 1 is a typical plot showing the effect that temperature and charge current had on cell capacity. This charge-acceptance phenomenon, however, diminished with cycle life. Other experimenters suggested that an over-discharge cycle on the cells would reduce the charge-acceptance phenomenon. These tests were performed on several cells, but the results were inconclusive. The cause of this charge-acceptance phenomenon is still unclear, however, it may be related to the positive electrode (e.g., lack of electrolyte and graphite fiber wetting, structure inconsistency).

As shown in Table 1, several other types of tests were conducted on these cells. Figure 2 is a plot showing the peak power of a cell at four depths-of-discharge. The low peak power value at full state-of-charge was due to the high resistance that cells experience when fully charged. The measured peak power values at 20% and 50% depth-of-discharge were approximately 170 W/Kg.

A set of parametric tests was performed on a 4-cell string, and the results are shown in Figure 3. These tests were all performed at 340°C, which is a typical projected operating temperature for an electric vehicle. As expected, the capacity of the string diminished with both an increase in discharge and charge rate.

All of the cells experienced at least 300 cycles before being removed from test, and two cells that are on a life cycle test have accumulated over 600 cycles with only a slight loss in capacity. None of the cells and strings from the second and third group have failed, and when charged at the lower rates, their performance is quite good.

The fourth set of deliverables that Sandia received consisted of ten cells and three 4-cell strings. Five of these cells and one 4-cell string had each experienced 47 cycles at CSPL. Testing of these cells at both CSPL and SNL allowed us to compare results such as cell resistance and capacity. The remainder of the cells and strings had not been heated to operating temperature. All of the cells and strings delivered in this shipment had the Mark 3 seal design. In addition, a safety can was inserted between the sodium and beta" alumina electrolyte. Six cells and two 4-cell strings, which consisted of previously tested and unheated cells, were selected from this shipment and placed on test.

Early test results indicate that the cells show the charge-acceptance phenomenon observed on the earlier deliverables. Figure 4 shows the loss in capacity over six consecutive tests at four different charge rates. The first test plotted for each curve represents a baseline cycle that was run at a 3-amp discharge rate to an end-of-discharge open-circuit voltage of 1.9 volts. The charge rate for a baseline cycle was 2 amps to an end-of-charge voltage of 2.4 volts. All of the tests were run under the same discharge conditions, and the only value that changed was the charge rate. The end-of-charge voltage also remained the same (2.4 volts) for all cycles. The temperature was 350°C. These tests will be repeated later in cycle life to confirm if these charge-acceptance effects diminish. Results at CSPL and SNL have indicated that the charge-acceptance effects do indeed diminish with time. In addition to the charge rate issue, three cells appeared to have a higher than normal end-of-discharge cell resistance. These cells are presently being removed from test so that the high resistance behavior can be investigated. The capacity and resistance measurements on the cells and strings that were tested at both CSPL and SNL were in good agreement, with the exception that one cell at SNL experienced an increase in resistance.

This work is supported by DOE Contract #DE-AC04-76-DP00789.

TABLE 1
STATUS OF CSPL CELLS AND STRINGS AS OF 7/25/89
(GROUPS 2 & 3)

CELL OR STRING NO.										TESTS CONDUCTED
464	465	469	470	471	472	475	476	473	474	
X	X	X	X	X	X					Chg. acceptance @ 330 C
X	X	X	X	X	X	X	X	X	X	Chg. acceptance @ 340 C
X	X	X	X	X	X	X	X	X	X	Chg. acceptance @ 350 C
X	X	X	X	X	X				X	Chg. acceptance @ 375 C
		X			X	X	X			Deep-discharge (1.76V)
					X					Over-charge
X	X	X	X	X	X					Cap. vs. dischg. rate
				X					X	Parametric
X		X								SFUDS79
X		X								Peak power
		X	X							Life cycle
457	487	615	710	527	398	569	307	394	374	Number of cycles run
94	99	95	93	93	95	96	99	95	96	% of initial capacity
*	*				*	*	*	*		* Removed from test

473 & 474 - 4-cell strings

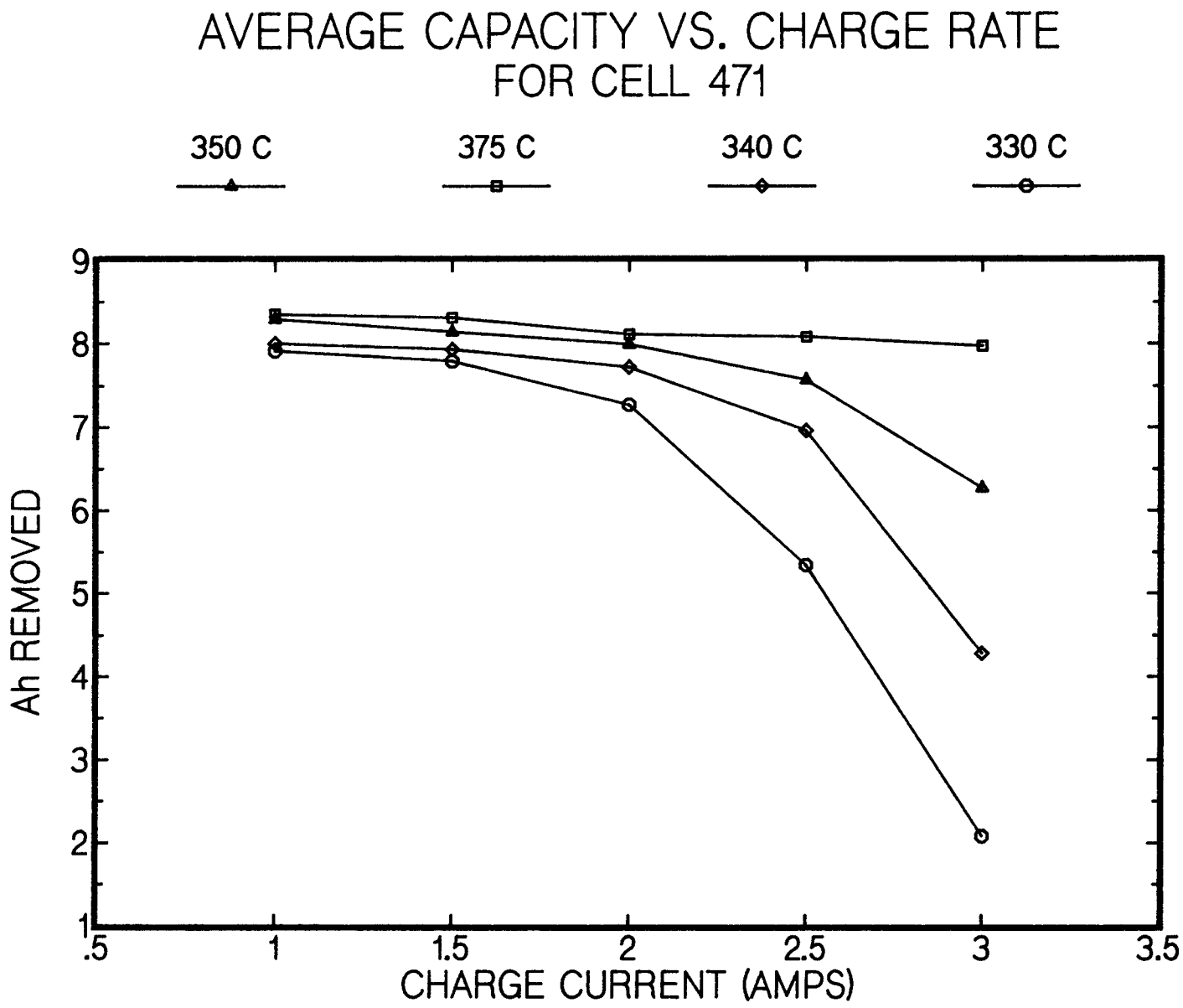
AVERAGE CAPACITY VS. CHARGE RATE
FOR CELL 471
350 C
375 C
340 C
330 C
Ah REMOVED
9
8
7
6
5
4
3
2
1
.5
1
1.5
2
2.5
3
3.5
CHARGE CURRENT (AMPS)

FIGURE 1

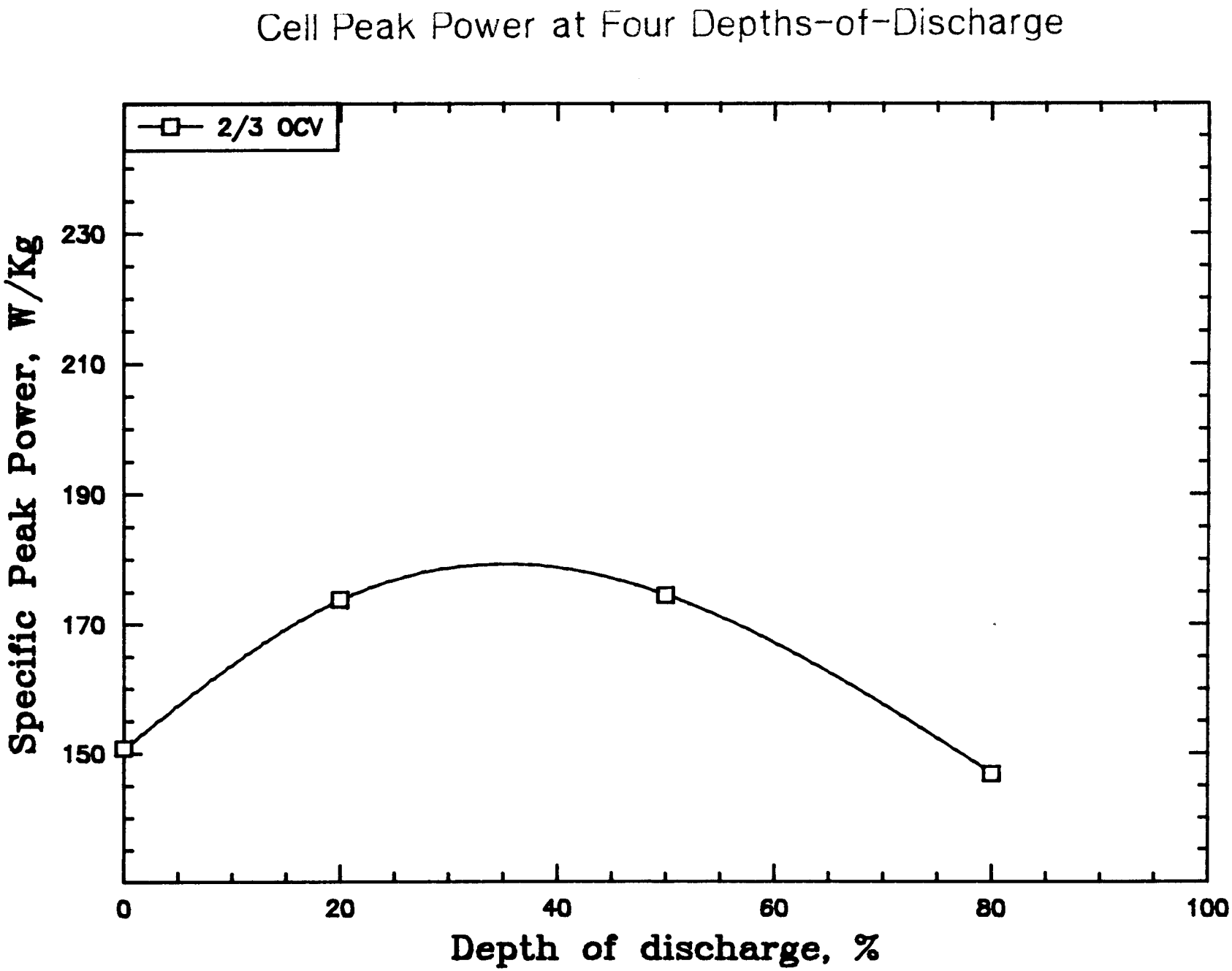
Cell Peak Power at Four Depths-of-Discharge
2/3 OCV
Specific Peak Power, W/Kg
230
210
190
170
150
0
20
40
60
80
100
Depth of discharge, %

FIGURE 2

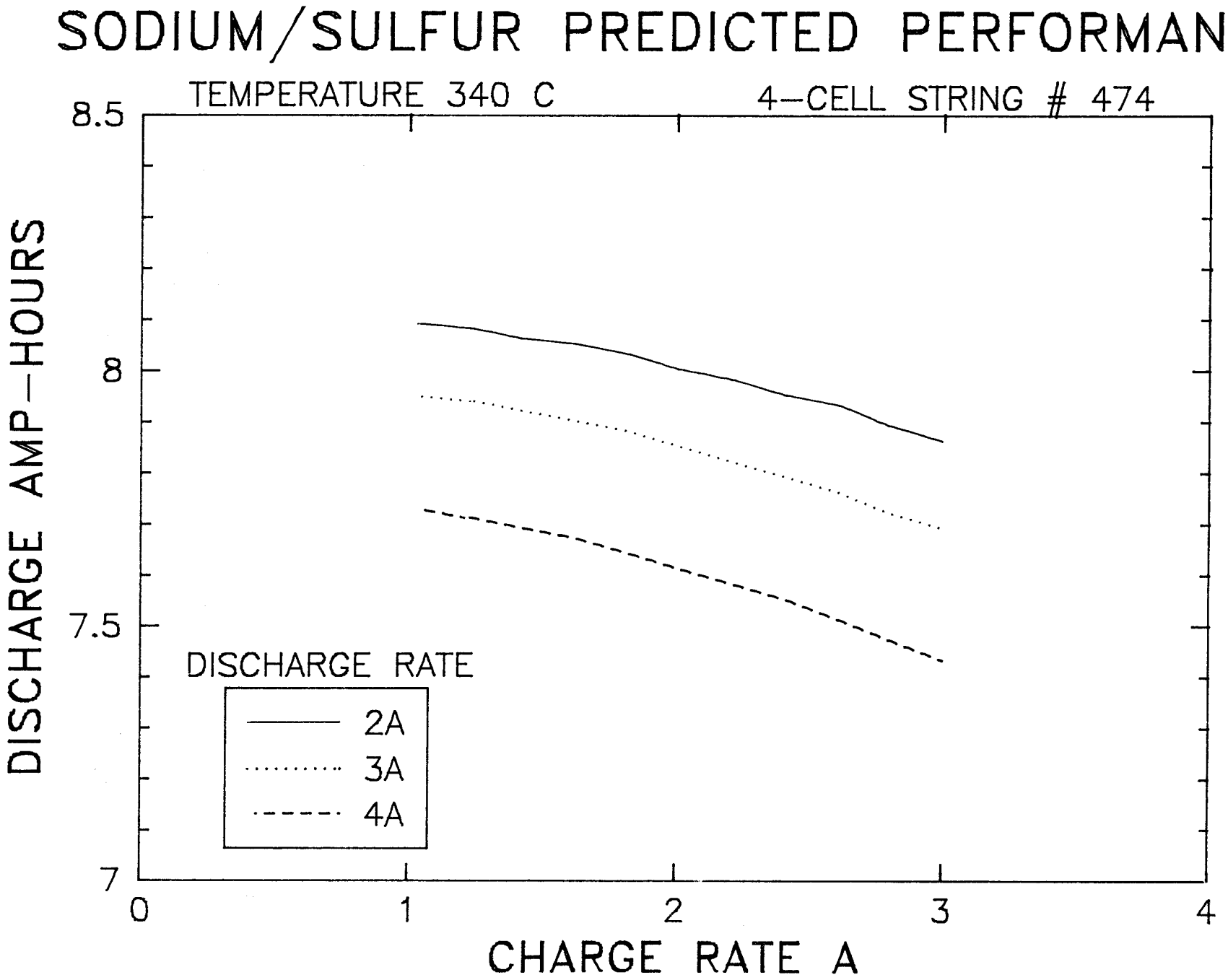
SODIUM/SULFUR PREDICTED PERFORMANCE
TEMPERATURE 340 C
4-CELL STRING # 474
DISCHARGE AMP-HOURS
8.5
8
7.5
7
DISCHARGE RATE
2A
3A
4A
0
1
2
3
4
CHARGE RATE A

FIGURE 3

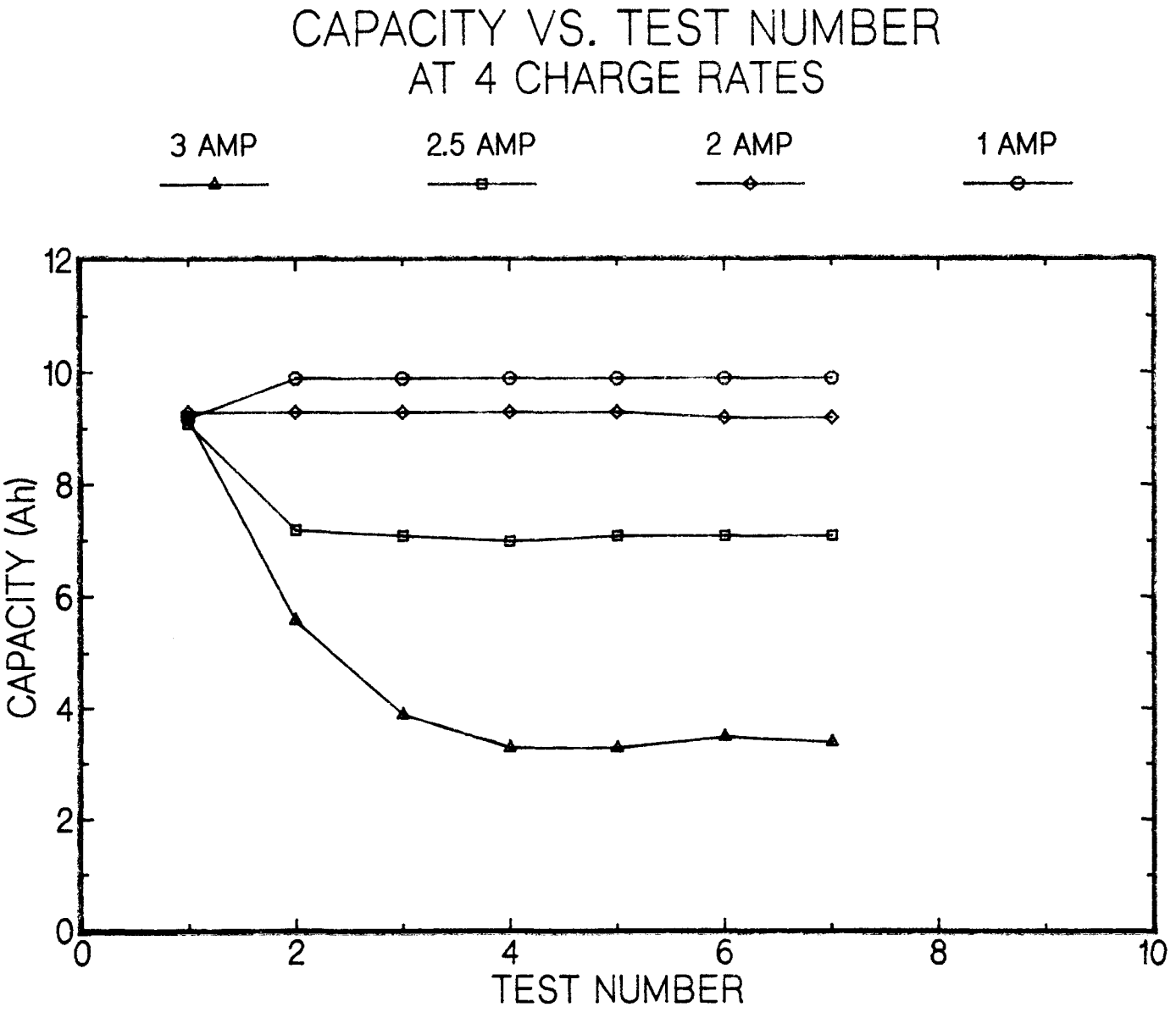
CAPACITY VS. TEST NUMBER
AT 4 CHARGE RATES
3 AMP
2.5 AMP
2 AMP
1 AMP
CAPACITY (Ah)
TEST NUMBER
0
2
4
6
8
10
12

FIGURE 4

SODIUM/SULFUR POST-TEST ANALYSIS AT ANL

John A. Smaga
Argonne National Laboratory

One activity of Argonne's Analysis and Diagnostics Laboratory has been the examination of selected sodium/sulfur cells that were built and tested by Chloride Silent Power Ltd. (CSPL) as part of the Exploratory Battery Technology Development Program at Sandia National Laboratories. The more recent examinations have involved long-lived (>400 cycles) cells of both basic cell designs (PB and XPB). The examined cells can be further differentiated according to the different designs used for the seal assembly and the sodium electrode. The detailed examinations conducted with the specialized facilities maintained at ANL have led to some significant findings stemming from these design variations. Some of the results for case corrosion, electrolyte contamination, and seal degradation are presented, and the effect of the design changes on these conditions is discussed.

All of the examined cells relied on a chromized coating to impart corrosion resistance to the low-carbon steel substrate used as the cell case. The chromizing process produced a duplex layer on both surfaces that consisted of a thin outer layer of chromium and chromium carbides and a thicker layer of iron and chromium. The rate of corrosion through the chromized layer and into the substrate was the same for both PB and XPB cells as is illustrated in Fig. 1, which shows the maximum penetration depth versus cycle life. From these data, the expected lifetime of the chromized cell case is projected to be around 2300 cycles. It should be emphasized, however, that deviations from the fixed set of conditions used to operate these cells can markedly accelerate the rate of corrosion.

Two demonstrated corrosion accelerators are time in the discharged state and thermal cycling. One PB cell, tested as part of a freeze-thaw matrix, spent 20 days on open circuit in the discharged state and accumulated 147 freeze-thaw cycles during a total test period of 62 days. The depth of corrosion was equivalent to 560 cycles or 187 days of continuous electrical cycling. Corrosion by the sodium-polysulfide melt and thermally induced spallation of the resultant scale had combined for a threefold increase in the corrosion rate.

The quality of the chromized coating also influenced the corrosion resistance of the cell case. The early generation of examined XPB cells used a cylindrical extension welded to a standard PB cup to increase the case height. The low-carbon steel used for the extension resulted in an inferior chromized coating for the upper case section. Normally, corrosion was most severe toward the base of the case, but in an XPB cell that accumulated over 1000 cycles, areas of the upper section showed substrate penetration comparable to the penetration found at the base. For two other XPB cells, the diameters of the cylindrical section and the cup were mismatched, creating an interior ledge along the case wall. This irregularity promoted localized breakdown of the coating and attack of the substrate within 450 cycles, more than 320 cycles earlier than expected on the basis of Fig. 1.

None of the examined cells experienced electrolyte failures, but analyses of electrolyte samples identified more subtle forms of degradation. Calcium, a source of increased electrolyte resistance, contaminated the inner surface of the electrolyte in all cells, especially the well-cycled PB cells (>200 cycles). As shown in Fig. 2, the maximum values for calcium contamination showed a nonlinear increase over the first 200 cycles and then reached a plateau value of about 7 at. % Ca.

The incorporation of a new sodium electrode in the XPB cells greatly reduced calcium contamination. The XPB cells used a safety tube and sodium wick to distribute sodium. The change lowered the measured calcium levels in XPB cells to an apparent plateau value of about 2 at. % (Fig. 2). Not surprisingly, the early resistance rise has been found to be much lower for XPB cells. These results suggested that the possible cause of early resistance rise was the buildup of calcium on the electrolyte. Furthermore, the redesigned sodium electrode has resulted in better performance and increased safety.

The presence or absence of corrosion deposits on the outer surface of the electrolyte stemmed from differences in seal design. The Mark IIA seals used for the examined XPB cells contained iron-bearing alloys in the top cap. Corrosion of these alloys produced iron disulfide that ultimately deposited on the electrolyte. The Mark III seals used for the examined PB cells had top caps of chromized steel. Corrosion of these top caps had not yet penetrated the high chromium layer, and no iron disulfide was formed. Corrosion of the cell case is another potential source of corrosion deposits; however, both cell types use a pressed liner along the inner case surface, and it has been largely successful in preventing the migration of corrosion products.

A low-grade reaction was evident for the glass seal used to bond the electrolyte to the alumina cap. This reaction occurred in both PB and XPB cells, although different glass sealants were used. The reaction was restricted to the glass within the sodium compartment, and the depth of the sodium reaction was less than 50 μm beneath the exposed surfaces. Measurements found a substitution of over 20 at. % sodium for silicon and the other elements in the sealants. The large shifts in glass composition were accompanied by increased stress in the transition between the reacted and unreacted glass. The stress was sufficient to cause cracks that ran parallel to the concave meniscus of the exposed glass surface. These spalling-type fractures were relatively benign, since the bulk of the glass seal was unaffected and the fracture did not propagate into the ceramic components.

Thermal cycling induced a more serious fracture in the glass seal of the cell subjected to freeze-thaw testing. The fracture developed in the seal glass between the flat of the alumina cap and the rim of the electrolyte. As shown in Fig. 3, the fracture initiated at the surface exposed to sodium and propagated through the horizontal section of the joint. The fracture developed no branch cracks and made a complete circuit around the seal circumference. Both of these characteristics are typical of thermal shock fractures. In addition, the glass near the fracture showed no discoloration and no significant shifts in composition. Generally, the crack growth was arrested in the glass seal before it could propagate horizontally through the lip of the insulator, but in one section, the fracture deflected upward and continued into the insulator. On the positive side, the 147 thermal cycles that this cell received were insufficient to complete the fracture, and the cell passed nondestructive post-test inspection at CSPL because the ceramic components still maintained a physical barrier between the sodium and the sulfur.

Acknowledgments:

Appreciation is due to Mike Stackpool of CSPL for his help in selecting cells for this study and numerous discussions about the findings.

This work was supported by the U.S. Department of Energy under Contract No. W-31-109-ENG-38.

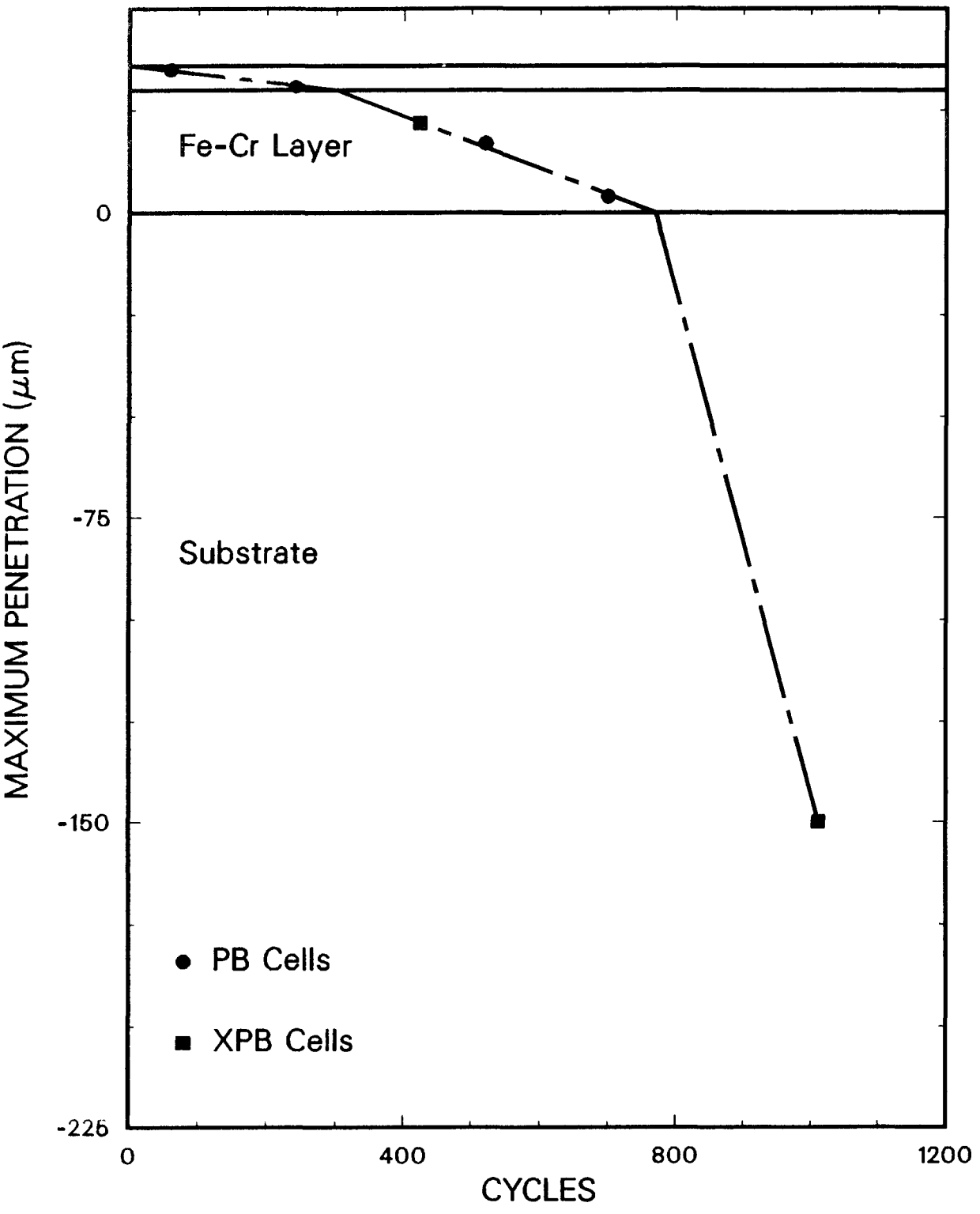

Fig. 1. Corrosion of the Chromized Cases under Standard Testing Conditions.

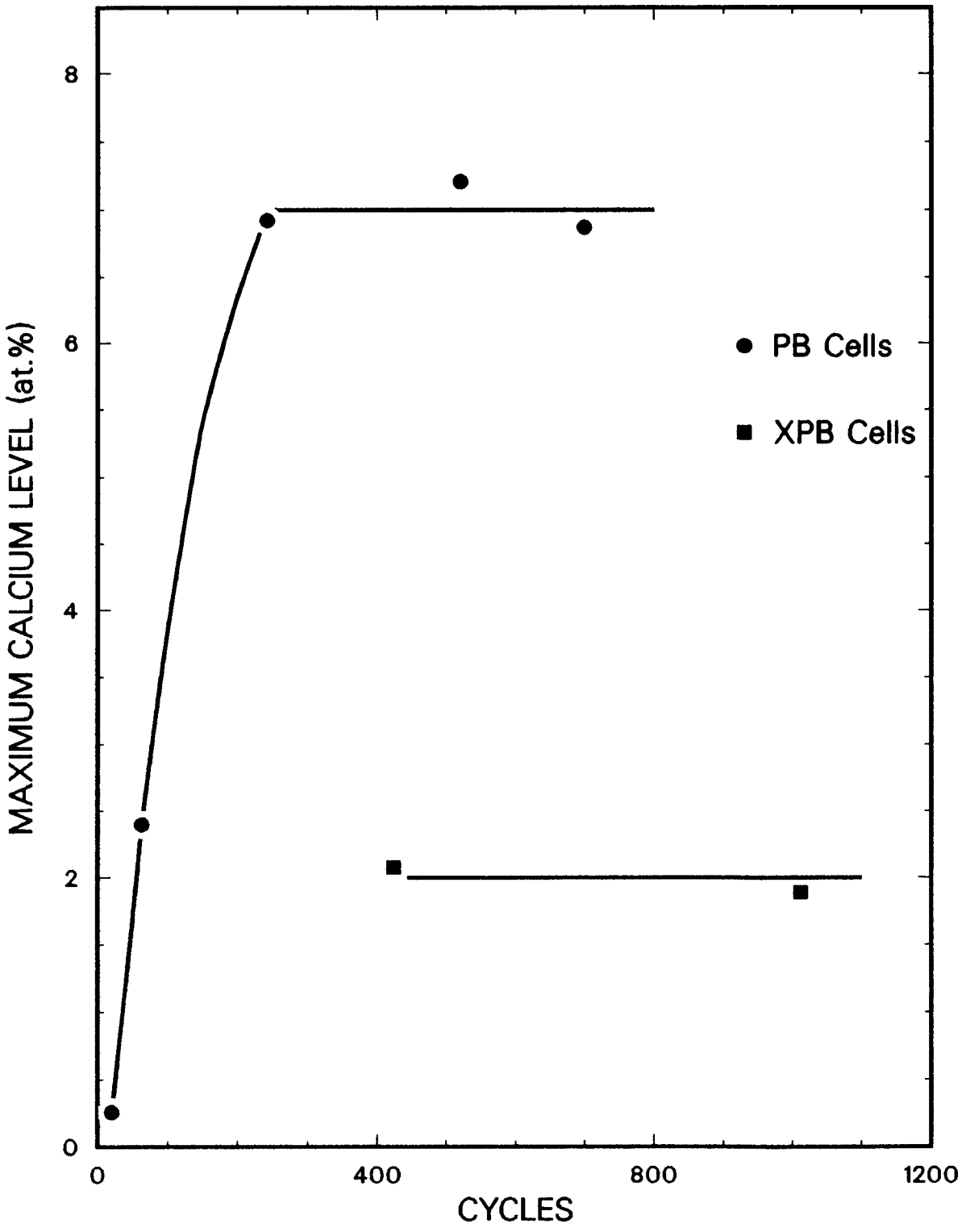

Fig. 2. Calcium Contamination of the Inner Surface of the Electrolytes.

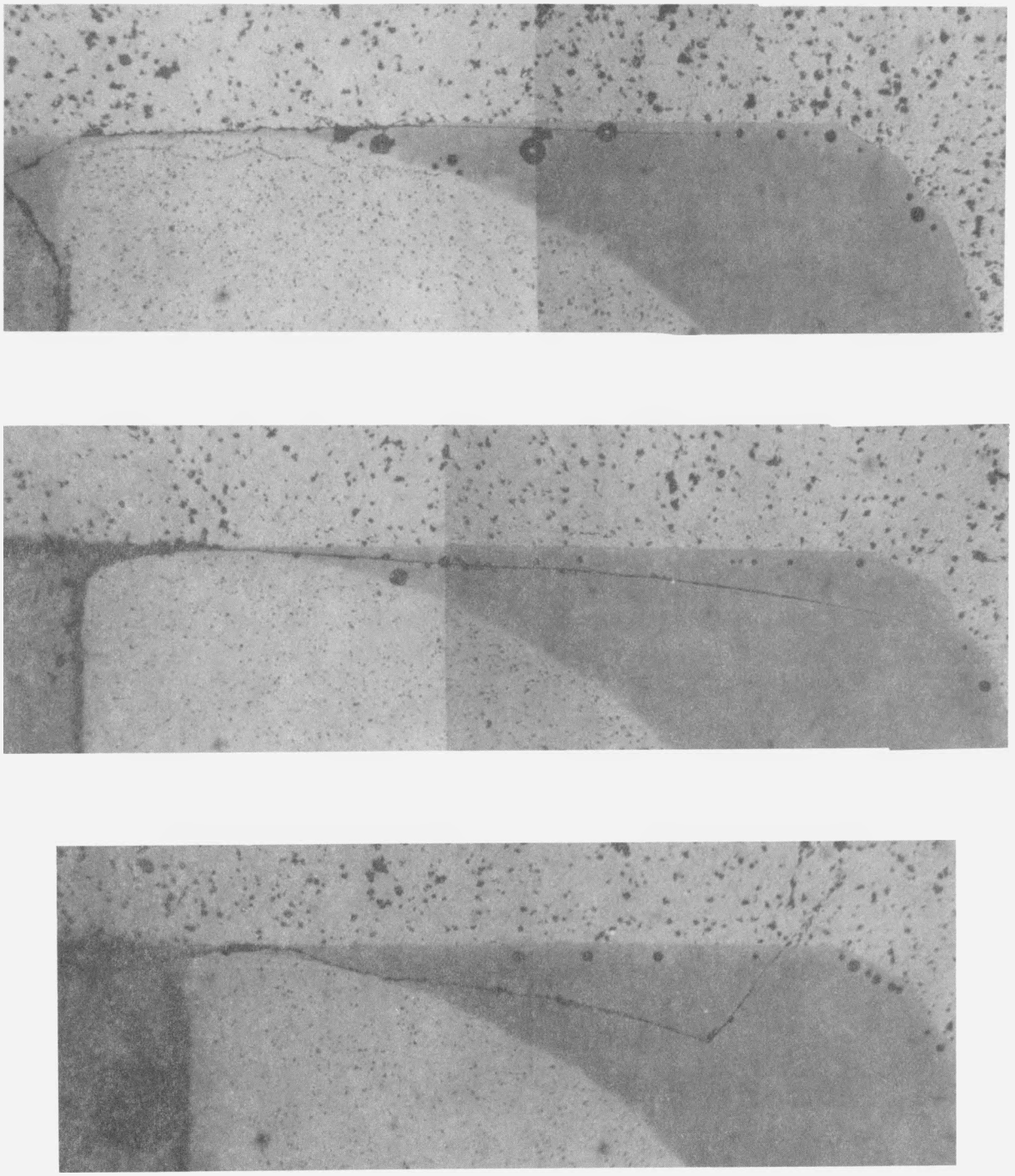

Fig. 3. Seal Fracture Induced by 147 Freeze-Thaw Cycles.

PLANNING, ANALYSIS, AND TECHNOLOGY TRANSFER

CHAIRPERSON:

Linda Fassbender
Pacific Northwest Laboratory

DOE STRATEGIC PLANNING FOR ADVANCED BATTERIES

James E. Quinn
U.S. Department of Energy
Washington, DC 20585

Energy storage systems have long been recognized for their ability to decouple energy supply from energy demand, a feature that offers valuable flexibility in the choice of fuels and energy sources. Batteries are a unique energy storage technology that offer the ability to reserve and retrieve electricity at high efficiency. In performing this function, they provide flexibility for a number of applications where the intermittent nature of supply, the fluctuation in demand, improvement in system efficiency or maintaining power quality under varying conditions are critical factors.

Successful development of advanced battery technologies will help to address potential national energy problems. Load leveling batteries can assist utilities in meeting electric utility capacity constraints expected in the 1990's while improving overall system efficiency. Advanced batteries for utility load leveling can be a cost-effective method to add peak power capacity by substituting low cost energy generated off-peak for high cost energy generated on-peak. For commercial and utility customers, battery load leveling can reduce demand charges and lower energy costs. Batteries for electric vehicles can shift our transportation sector reliance on imported oil towards more abundant domestic sources of energy. Further, environmental emissions from electric vehicles could be better controlled at a central power plant than from the dispersed sources of millions of vehicles. Advanced batteries will broaden the market acceptance of renewable electric technologies by supplying reliable, quality power despite the intermittent nature of renewable energy supply. Batteries are critical to supplying continuous power in stand-alone applications of renewable electric technologies. In addition to these opportunities, developing battery systems for export would enhance U.S. industrial competitiveness and reduce the trade deficit.

The Office of Energy Storage and Distribution (OESD) Battery Development Program performs core technology and engineering development activities for promising advanced batteries. The existing development program, managed in the field by Sandia Laboratories, is a base program, a building block on which battery engineering projects have been designed to accelerate the deployment of advanced batteries in various market applications. At the same time, an applied research program, managed by Lawrence Berkeley Laboratory, is pursued to form a better understanding of electrochemical phenomena, develop new materials and components for batteries, and prove new electrochemical couples and designs in the laboratory.

The operational strategy used for the base development program over the past five years has been to maintain technical options in advanced battery technologies to allow rapid deployment to larger scale development if the national needs arise. This strategy has been implemented to keep several battery technologies under development

at any given time, so that a range of battery options would always be available for the intended applications. The base program is currently investigating sodium/sulfur, zinc/bromine, nickel/hydrogen and aluminum/air battery systems.

OESD has spent the past year investigating potential markets, analyzing advanced battery development efforts in foreign countries and developing strategies to achieve successful technology implementation. With this information an Advanced Battery Storage Multi-Year Plan has been developed to allow DOE management to make informed decisions regarding the future directions and support for battery development.

The Advanced Battery Storage Multi-Year Plan presents the base development program and three strategies that address the need to accelerate battery development. The three strategies target intensive battery engineering activities for load leveling, electric vehicles and renewable energy systems applications. Subsequently, each strategy has two or three project options reflecting a variety of battery systems and/or schedules to be pursued. These projects range from continuation of base program research to fast-track large battery demonstration builds heavily cost-shared with industry.

Funding of one or more project options will supplement, and complement, the present base program and permit the development of advanced battery technologies to meet the energy challenges anticipated in the next decade. Also, the selection of these options will determine whether DOE will provide the leadership for U.S. industry to maintain its role competing in the international race for multi-billion dollar markets.

DOE is now engaged in a major effort to develop a National Energy Strategy (NES) to determine the direction of the U.S. energy economy over the next 40 years. An intensive in-house effort coupled with public hearings, industry participation, and interagency assistance is expected to produce an initial draft strategy by April 1990. This initial strategy will show a comprehensive picture of U.S. energy production and consumption, forecast the energy economy out to the year 2030 under current trends and describe how policy options can alter those trends. Energy policy and program goals and key strategies to meet those goals will be presented. Following a 4-5 month period of public and private sector review and comment and a subsequent refinement of policies and strategies to address comments, a National Energy Strategy (NES) will be presented to the President. This strategy will describe administration energy policies, national energy program and budget priorities, an NES implementation plan, and legislative energy proposals.

As a result of the NES, in the area of battery storage, key decisions will be made on whether to pursue the existing strategy supporting many candidate batteries with long-term potential or to adopt an aggressive battery engineering effort with potential for significant introduction of new technologies before the year 2000.

SUMMARY OF OESD ADVANCED BATTERY STORAGE MULTI-YEAR PLANNING OPTIONS

Base Program	Strategies	Projects/Goals	$
Goal: Continue to support research on all promising battery systems for development in the post-2000 timeframe Investigate fundamental battery systems problems such as: - materials problems - separators - low-cost switching device - cell performance and sizing - cell and module testing ($ 3.6 M)	<u>Load Leveling</u> Develop prototypes of advanced batteries to verify viability for load-leveling in the 1990s to meet projected regional capacity shortfalls.	1) Develop improved lead-acid batteries capable of early penetration of load-leveling market.	$5 M ($1 M/5 yrs.)
		2) Develop improved lead-acid battery <u>and</u> 2 competing advanced batteries with down-selection to one for prototype in **1998**.	$20 M ($4 M/5 yrs.)
		3) Accelerate development of lead-acid battery <u>and</u> 2 advanced batteries leading to down-selection and prototype in **1995**.	$50 M ($10 M/5 yrs.)
	<u>Electric Vehicles</u> Develop advanced electric vehicle advanced battery technologies to mitigate ICE environmental impacts and reduce transportation sector reliance on imported oil.	1) Accelerate sodium/sulfur core technology effort leading to cost competitive high performance batteries.	$4 M ($800 K/5 yrs.)
		2) Expand core technology effort to include other promising high-temperature battery systems.	$10 M ($2 M/5 yrs.)
		3) Expand core technology effort to include ambient temperature battery technologies.	$20 M ($4 M/5 yrs.)
	<u>Renewable Energy Systems</u> Develop prototypes of advanced batteries which broaden utilization and improve performance of renewable energy systems.	1) Improve performance and reduce cost of maintenance-free lead-acid batteries for use with stand-alone photovoltaic and wind systems.	$2.25 M ($750 K/3 yrs.)
		2) Accelerate systems development to reduce cost of reliable long-lived nickel/hydrogen batteries.	$5 M ($1 M/5 yrs.)

STRATEGY FOR ELECTRIC VEHICLE BATTERY AND FUEL CELL TECHNOLOGY R&D

Dr. Pandit G. Patil
Electric and Hybrid Propulsion Division
Office of Transportation Systems
U.S. Department of Energy

The Electric and Hybrid Propulsion Division (EHP) carries out the development of advanced batteries and fuel cells for electric vehicles. A national plan for guiding and focussing the electric vehicle battery R&D has been recently completed. The planning steps and results are briefly described in the first section of this document. Fuel cells are also emerging as a promising electric vehicle power source. The second section of this document presents DOE-EHP's assessment of the perspective and prospects for fuel cells in transportation.

Electric Vehicle Batteries - A National R&D Plan

In 1987 DOE-EHP initiated efforts to establish a national plan for electric vehicle battery R&D. Previously established mission-directed goals for advanced batteries in a light-duty van--denoted IDSEP for "Improved Dual-Shaft Electric Propulsion"--were used as the basis for conducting a comprehensive technical assessment of advanced battery technologies as the first phased of this effort. In the second phase, the assessment results were utilized to establish technical program plans and schedules for the most-promising EV battery technologies. These studies are being used by DOE-EHP to update, refine, and guide its battery R&D program for electric vehicles. Additional factors being considered in this national strategy for EV battery development include: (a) national needs in the areas of petroleum conservation, fuel flexibility, and pollution abatement; (b) continuity of industrial involvement in all phases of R&D; (c) prioritization of battery technologies based on EV market impact, likelihood of successful development, and the extent/urgency of national needs; and (d) coordination with private-sector efforts, in areas of EV technology development, market development, and EV commercialization. The remainder of this section summarizes the EV battery assessment and technical R&D planning studies, which form the basis for DOE's national EV battery development strategy.

EV Battery Assessment

Working through the Idaho National Engineering Laboratory (INEL), DOE-EHP directed a comprehensive technical assessment of viable secondary batteries for the IDSEP light-duty van application. A battery assessment team-comprised of ten battery/EV consultants and the technical program managers representing six national laboratories--conducted a comparative technical assessment of 42 battery design concepts for the IDSEP van. The battery design information was solicited from 60 battery development organizations. The design concepts were evaluated on the basis of a six-criteria scoring system.

Technical R&D Plans

The results of the battery assessment were used as the basis for formulating technical R&D plans for advanced EV batteries. Sealed lead/acid batteries are commercially available. Development of improved electrode technologies, as being conducted by industrial manufacturers, is a product improvement effort being supported by profits from existing sales. Consolidation of the remaining eleven developmental batteries was accomplished by combining batteries of the same technology family: The two lithium/iron sulfide batteries--Li/FeS and Li/FeS2--were combined to form Li/FeSx, while Na/FeCl2 and Na/NiCl2 were combined to form Na/MCl2. A generic EV battery development system was established and used as the format for preparing and presenting the technical R&D plans.

Fuel Cells for Transportation - Perspective and Prospects

Experience over the past fifteen years has alerted the public to our extreme dependence on imported oil. This experience and the concern for good air quality in urban areas, plus the depletion of petroleum supplies, have led to the conclusion that we must inevitably replace the petroleum fueled internal combustion engine (ICE) used in transportation with a more advanced power source.

Electric-powered vehicles have been suggested as a means of decoupling petroleum from the transportation sector and of drastically reducing environmental emissions. However, for many applications user acceptance will only be forthcoming if such a vehicle has the same virtually unlimited range (through rapid replenishment of the fuel) as present ICE vehicles.

Powering a vehicle with batteries alone cannot achieve an acceptable extended range through rapid refueling, but a fuel cell/battery hybrid system, or ultimately a stand alone fuel cell could have that capability. The fuel of choice for such vehicles would be either methanol derived from coal or ethanol obtained from biomass. Both can be converted efficiently and virtually free of emissions to electricity in fuel cell systems, as will be discussed in more detail later.

Recognizing the potential of the fuel cells in transportation, the DOE entered into an initiative with the Department of Transportation to develop an urban bus powered by a phosphoric acid fuel cell/battery hybrid system. The transit bus was selected as the test vehicle since it can easily accommodate the present fuel cell technology, and because higher acquisition costs of fuel cell systems can be amortized over a longer service life than is possible in passenger cars. This program, Research and Development of a Fuel Cell/Battery Powered Bus, was initiated in FY 1987, and is presently in the proof-of-feasiblity stage.

Phosphoric acid fuel cells (PAFC) were chosen because they are the only type of fuel cells that are sufficiently developed to be put on a vehicle in the near term. It was recognized that other types of fuel cells may be more suited for the application but are not yet sufficiently developed.

Previously, the primary motivation for developing fuel cells was their use in manned and unmanned space flight, and potentially in utility power plants. Both applications require an energy conversion device that is efficient, reliable, and that can provide continuous power to an electrical grid. In transportation the power system must not only be efficient and reliable but in addition it must be capable of

-high power density
-rapid start-up
-frequent load changes.

To fit into buses and cars the power density, in terms of weight and volume, must be increased substantially over state-of-the-art PAFC technology. Start-up times must be reduced, and rapid load response between full and stand-by power must be possible. The transportation application, therefore, adds new challenges to the fuel cell development.

Safety in accidents is an issue too. Spillage of hazardous chemicals in a crash would be unacceptable.

An additional challenge is the fact that internal combustion engines are inexpensive by comparison. The cost of a typical engine in automobiles is only about $50/kW. The equivalent cost of fuel cell systems is much higher, although the technology is still in a developmental stage and the margin for improvement is large.

Considering these challenges, along with the potentially enormous pay off of replacing the highly developed but nevertheless antiquated technology of the internal combustion engines (the first combustion engines were built 100 years ago) with a cleaner and more efficient device, it is the objective of the Department of Energy to assess the merits of fuel cells for transportation applications.

HIGH TEMPERATURE BATTERY ASSESSMENT

Rajat K. Sen
R.K. Sen & Associates
3808 Veazey Street N.W.
Washington, D.C. 20016

The sodium/sulfur battery is the most well-known of the high-temperature batteries. It is estimated that approximately $60 to $80 million are being spent annually on the development of the sodium/sulfur battery worldwide. This includes government and corporate investments. The Office of Energy Storage and Distribution (OESD) and the Office of Transportation Systems (OTS) of the U.S. Department of Energy are actively supporting the development of this battery system. Sandia National Laboratory (SNL) is the lead DOE laboratory coordinating the development of the sodium/sulfur battery. The reliability and performance of the sodium/sulfur battery has progressed to the state that pilot scale production of this battery for transportation application is expected to commence in the next few years. Thus over the last twenty years the sodium/sulfur battery has evolved from a laboratory curiosity and has entered into full-scale engineering development. Its anticipated commercial success in the next five to seven years will be a major achievement of a well-coordinated, long-term research and development program.

Three other high-temperature battery systems could make a significant impact on both the stationary energy storage and transportation applications. These are:

1. Lithium/metal monosulfide

2. Lithium/metal disulfide

3. Sodium/metal chloride

These systems are in an earlier stage of research and development than the sodium/sulfur battery and consequently are receiving a much lower level of attention especially in terms of funding. OTS together with the Electric Power Research Institute (EPRI) is supporting research on the lithium/metal monosulfide system and OESD is involved in developing the "technology base" for the "upper plateau" lithium/metal disulfide. Argonne National Laboratory (ANL) is the lead DOE laboratory conducting the research and development in these two systems. The sodium/metal chloride battery, the newest member of this group of high-temperature batteries, is receiving very little DOE support. The main development activity of this battery system is being conducted by a consortium of South African and British companies who appear to have little interest in participating in a program involving DOE support.

This assessment of the high-temperature batteries discussed above was conducted for the Office of Energy Storage and Distribution (OESD) with the objective of evaluating the present status of these battery technologies and to identify for each technology a prioritized list of R&D issues. Finally, the assessment includes recommendations to DOE for a proposed high-temperature

battery research and development program encompassing the four classes of batteries.

In conducting this assessment, it was decided early on that a broad spectrum of technical opinions would be sought. The approach included the preparation of overview documents outlining the status of the three technologies. These overview documents were prepared by Robert Weaver of EPRI (sodium/sulfur battery), Paul Nelson of ANL (lithium/metal mono and disulfide battery), and Rajat Sen of the Pacific Northwest Laboratory (PNL) (sodium/metal chloride battery). A workshop was then convened on August 16-17, 1988 with thirty technical experts in attendance and the three overview documents as the background material. Three working groups were formed; each group considered one battery system, discussed its present status, and produced a list of R&D issues for their system. The working groups were asked to consider each battery on its own merits and not to compare the three systems.

This paper will discuss the specific recommendations and the proposed program plan derived from this assessment. The general conclusions are:

1. The sodium/sulfur battery is approaching the stage where pre-commercial pilot plan production is expected soon. DOE funding of research should be targeted towards applied work to demonstrate cost-effective charge control circuitry, optimum cell size for stationary energy storage applications, and an effective thermal management system. Some research effort must also be directed towards the next generation of sodium/sulfur cells with a much improved sulfur electrode and novel corrosion resistance seals and container materials.

2. The two lithium metal sulfide batteries are in different stages of development. The lithium iron monosulfide battery is approaching engineering development and support for such an effort should continue and must be targeted primarily towards electric vehicle applications. The lithium iron disulfide battery is still in its early research phase and work should continue to establish its technical and economic feasibility prior to its transition to the exploratory engineering development stage.

3. Not much is known about the sodium metal chloride battery apart from the limited amount of information provided by the developers. This assessment recommends that a "technology base" research effort be undertaken to explore the technical issues related to this promising battery.

BATTERIES AND FUEL CELL TECHNOLOGIES CAN MITIGATE AIR QUALITY PROBLEMS

Albert Landgrebe, Frank McLarnon* and Susan Adams**
U.S. Department of Energy
Washington, DC 20585

The recent air quality legislation proposed by President Bush is affirmation of the American public's desire for clean air. Progress has been made in other environmental areas such as cleaning up our waterways and toxic waste dumps, but virtually no improvement has been seen in air quality since enactment of the Clean Air Act in 1970. Although scrubbers and baghouses have been added to electric power plants and catalytic convertors to automobiles, air quality in the summer of 1988 reached an all time low.

The primary air quality issues concerning Americans today include photochemical smog, acid rain and global warming. Ozone is the primary component of photochemical smog, a serious problem in many of the major cities in the United States. Ozone is formed as a by-product of NO_x and hydrocarbon reactions with nascent oxygen and has been related to health problems. Currently, 81 metropolitan areas in the U.S. exceed the Clean Air Act's 0.12 ppm ozone standard. In fact, cities such as Los Angeles and Baltimore have ozone levels over three times the allowable limit. The President's air quality plan is intent on cleaning up the air in all of these cities by 2010 and focusses primarily on vehicle emissions. The plan requires the annual sale of one million clean-fuel cars in the most polluted cities by 1997.

One major air quality problem is acid rain--the increasingly acidic trend due to atmospheric contaminants. Natural rainfall has a pH of approximately 5.5, but the presence of sulfuric acid and to a lesser extent nitric acid in the atmosphere has led to rainfall with an average pH of about 4.4 in the northeastern United States. The primary source of this acid is the emission of NO_x and SO_x from fossil fuel burning. For example, coal often contains high levels of sulphur which forms sulfur oxides when burned. These sulfur and nitrogen oxides undergo a chemical reaction in the atmosphere to form acid. The acid may directly deposit onto a surface such as a building and cause damage or the acid may be washed from the atmosphere by precipitation and form what is commonly called acid rain. Acid rain is detrimental to lakes, aquatic life and forests.

An environmental issue which has been receiving frequent media attention recently is global warming. Global warming is caused by ultraviolet or short length radiation from the sun entering the earth's atmosphere and either being reflected or reaching the earth's surface. The earth then emits infrared or long length radiation in the form of heat back towards space. Before reaching space some of this heat is absorbed by compounds such as CO_2 and H_2O which are naturally occurring in the

atmosphere. Thus, these gases act as an insulating blanket, and this phenomena is referred to as the "greenhouse effect." Increased levels of CO_2 and other greenhouse gases such as NO_x, SO_x and CFCs have enhanced the greenhouse effect and are believed to have increased the average global temperature. CO_2 levels in particular have increased since the beginning of the industrial revolution mainly as a result of anthropogenic activities such as fossil fuel combustion and deforestation. By the middle of the next century, a doubling of the CO_2 concentration in the atmosphere is predicted to occur. If no measures are taken this increase is estimated to raise the average global temperature 2 to 9°F. As a result of this temperature rise, melting of the polar ice caps, rising sea level and increasing precipitation have been theorized by top scientists. These events would have a significant socioeconomic impact on the planet.

The relationship between energy conversion and air quality has received increasing attention during recent years, and there is every reason to expect this trend to continue. Conservation, increased energy efficiency and new technologies will help to mitigate air quality problems associated with energy production. Electrochemical energy conversion and storage technologies, such as advanced storage batteries and fuel cells, will generate, store and deliver an increasing fraction of our electricity during the next century. The quantity of gaseous emissions associated with implementation of these electrochemical technologies can have a profound effect on air quality, to the extent that these technologies penetrate commercial markets. Battery storage technologies for electric vehicles may contribute significantly to improved air quality not through energy savings but rather by fuel switching. Batteries are charged with electricity and then release this stored energy by means of a chemical reaction when the energy is demanded. Because storage batteries are secondary batteries they are capable of being repeatedly charged and discharged. Fuel cells are similar to batteries except that they produce electricity from the chemical reaction of a fuel, and these fuels have very low associated emissions. Fuel cells may be used both for electric vehicles and for power generation.

A simple analysis was performed to compare the emission of air pollutants from contemporary sources and from batteries for electric vehicles and fuel cells for both electric vehicles and power generation. The results indicate that a positive air quality impact will be observed in urban areas suffering from photochemical smog with the adoption of advanced battery and fuel cell technologies. Also, a potentially significant impact may be encountered for acid rain and global warming issues. The conclusions, assumptions, and methodology of this analysis will be detailed at the presentation.

*Lawrence Berkeley Laboratory, Berkeley, CA 94720
**Energetics, Incorporated, Columbia, MD 21045

ELECTRICITY CAPACITY CONSTRAINTS AND THEIR IMPLICATIONS ON BATTERY STORAGE

Jonathan W. Hurwitch
Energetics, Inc.

Energy analysts and forecasters are becoming increasingly concerned about our ability to meet electricity needs in the near future. The projections vary depending upon assumptions made for generation supply, non-utility generation, repowering, demand forecasts, and conservation and load management potential. The Department of Energy, in its March 1987 Energy Security Report, projected a 100 GW (or greater) capacity shortfall by the year 2000 (see Figure 1). Projections from other organizations range from 75 GW to 150 GW depending upon the aforementioned assumptions. Their problem is becoming a concern in the public's eye as attested by recent articles in the *Wall Street Journal* (see Figure 2), *New York Times*, *U.S. News and World Report*, and on national television.

The Department of Energy (DOE) has recognized the consequences to our economy if a shortage of electricity becomes a reality. Our new Secretary of Energy, Admiral James D. Watkins, is committed toward the development of a National Energy Strategy--an action plan essential to providing the nation with adequate supplies of competitively priced, clean energy. A recognized issue to be addressed as part of this strategy is our need for new electricity generating capacity. Technology opportunities to mitigate projected supply constraints will become a critical part of our national energy policy.

DOE's Office of Energy Storage and Distribution is developing several technologies which can impact these supply constraints. Battery storage can provide load-leveling capability and peak power and thus facilitate a variety of demand and supply options. Battery storage can also help maintain power system reliability and quality as the future supply mix becomes more diverse and distributed. In order to assist OESD in its R&D planning and technology transfer function, we have performed a regional analysis of the North American Electric Reliability Council (NERC) data for supply and demand projections. We developed three scenarios representing optimistic, pessimistic, and most likely assumptions regarding these projections. The results of the analysis (Figures 3-5) indicate regions of the country which might expect some electricity reliability problems before the year 2000.

Other issues facing the electric utility will have implications for the adoption of battery storage. Available transmission line capacity and access to transmission lines, concern about the atmospheric impacts of electricity generation, reliability of projected supply from independent power producers, and the overall impact of deregulation causes concern regarding the ability of electric utilities to deliver an adequate supply of reliable electricity. Battery storage can be an important part of a technology strategy to resolve these issues.

The adoption of battery storage by utilities has been limited due to several factors. First, it cannot currently compete on a levelized cost basis with other options to deliver peak power. Second, the dynamic benefits of batteries have not been considered when evaluating the economics of battery storage to a utility. Thirdly, R&D support has declined significantly in the 1980's. Finally, battery manufacturers have not aggressively pressed this emerging utility market.

Interest in battery storage is on the increase because of changes in Federal policy, restructuring of the utility industry, and greater interest by manufacturers. Forces are bringing together organizations to optimize use of limited R&D resources while promoting a high level of industry/government collaboration. This paper will explore these factors and discuss the overall prospects for the market introduction and acceptance of battery storage.

Acknowledgement:

This work is supported by the Department of Energy, Office of Energy Storage and Distribution under Contract DE-AC01-86CE 30844.

Capacity Constraints Expected by Year 2000

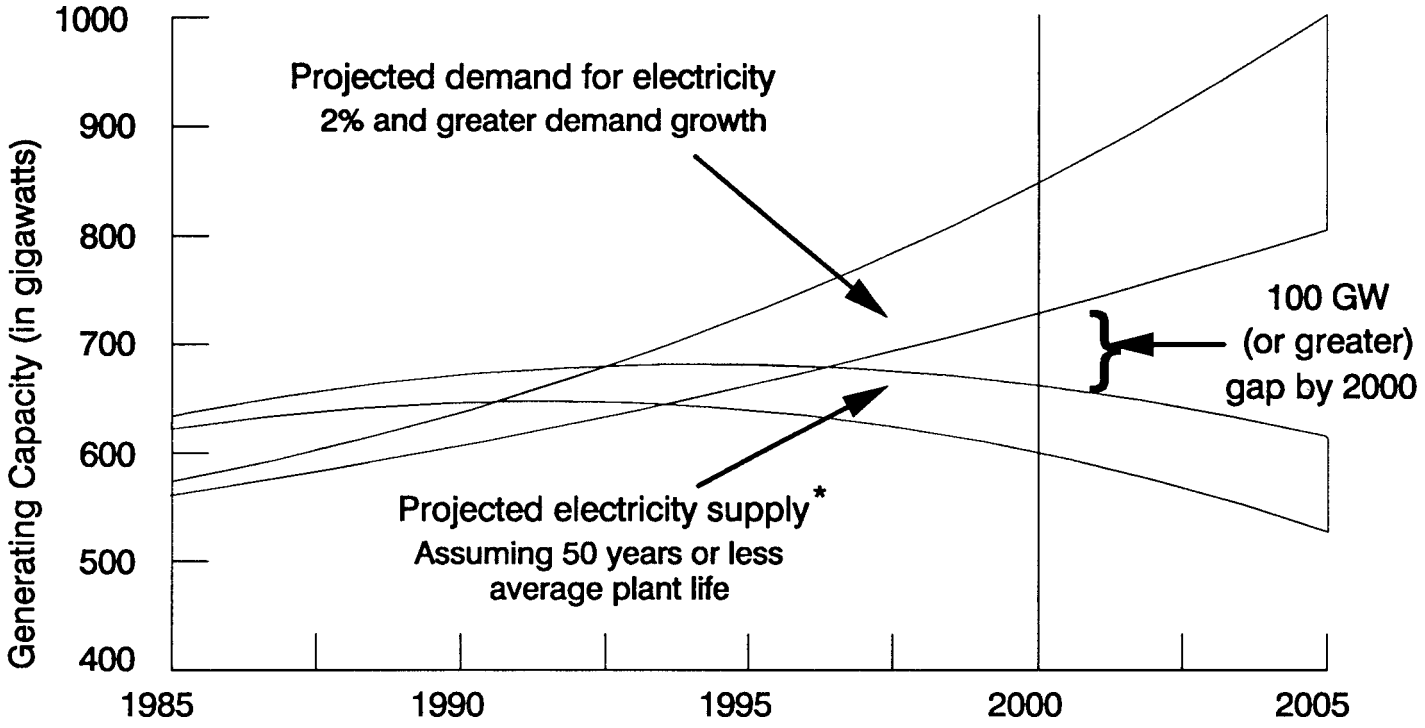

*Existing plants plus plants under construction minus retirements.

Regional Capacity Constraints - Base Case
(<20% Capacity Margins)

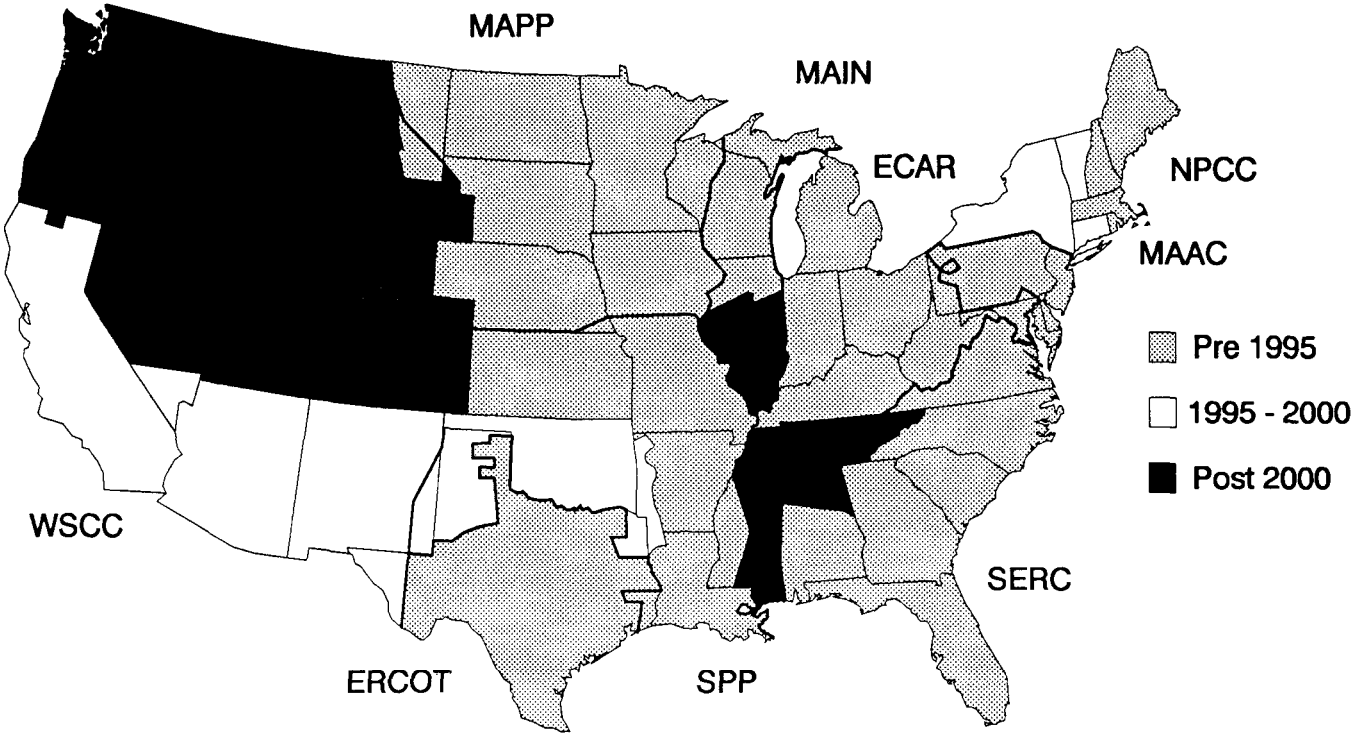

Regional Capacity Constraints - Best Case
(<20% Capacity Margins)

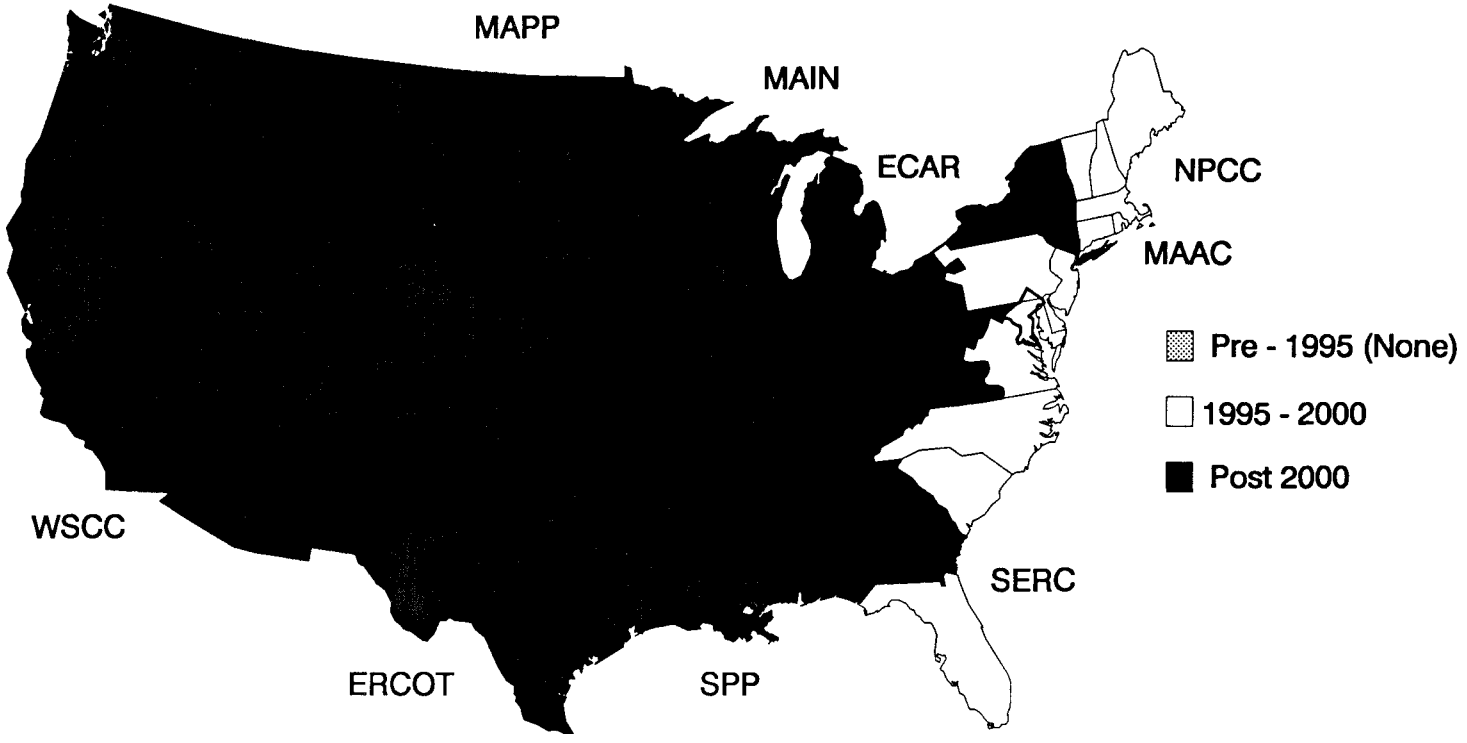

Regional Capacity Constraints - Worst Case
(<20% Capacity Margins)

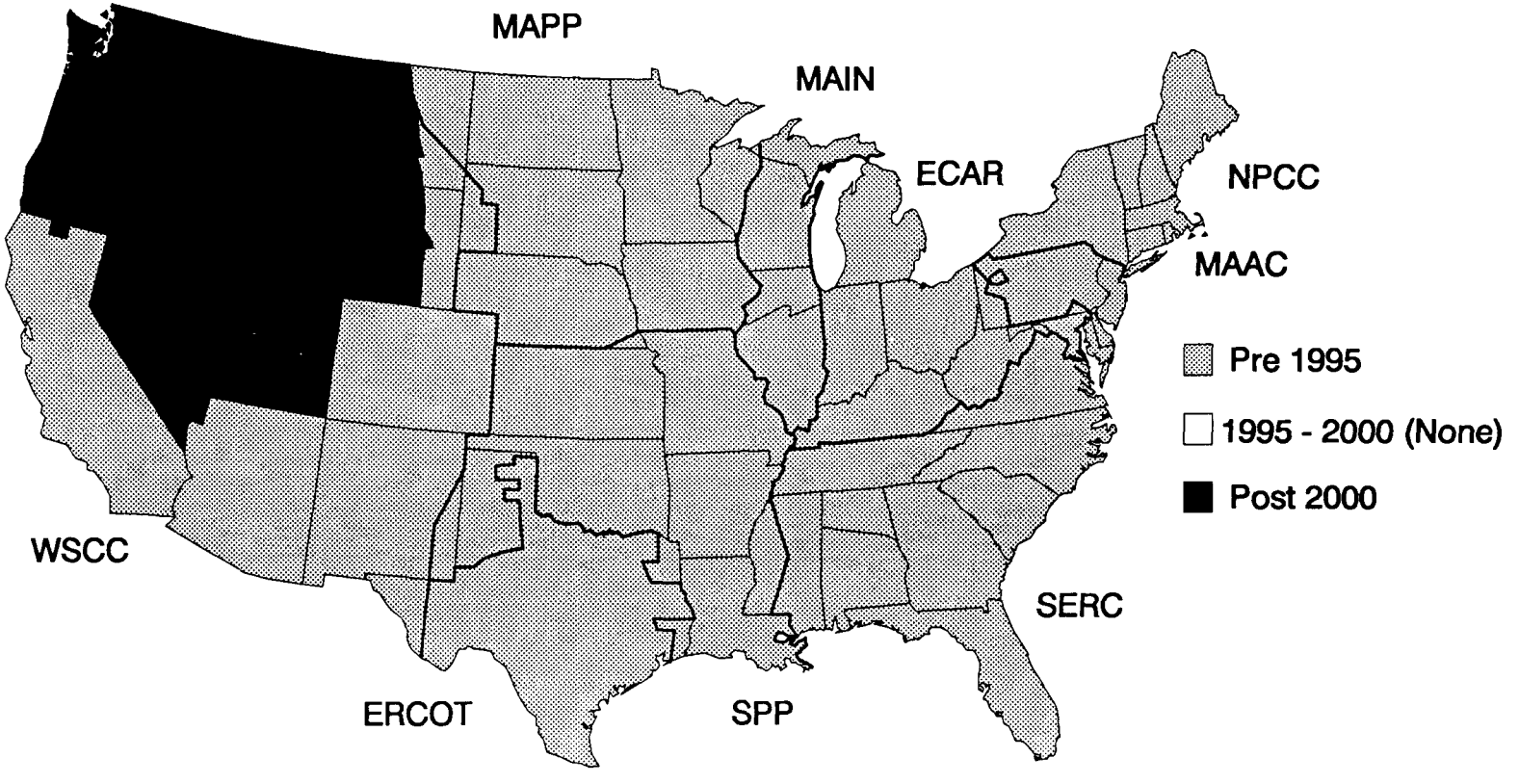

Get Set to Lose Your Cool This Summer

Power Shortages Expected to Hit Much of the U.S.

By Bill Paul
Staff Reporter of The Wall Street Journal

You might want to stock up on candles and ice. There's a chance some dark, unair-conditioned summers may lie ahead.

"Not until the shock waves hit will anyone believe that power shortages are possible," says Leonard J. Kujawa, managing director for utilities at Arthur Andersen & Co., the accounting and consulting firm.

Mr. Kujawa and some other noted utility analysts who've studied the power supply in this country warn that New England, New York's Long Island and possibly the Middle Atlantic states all face brownouts and blackouts this summer. They further contend that by 1992, or maybe sooner, the entire East Coast, much of the Midwest and the Pacific Northwest will be equally hard-pressed to keep the lights burning brightly.

An Annoyed Public

"The public is going to get pretty damn annoyed" over the next several summers when air conditioners and elevators stop running during blackouts and home computers and other electrical equipment get fouled up by voltage reductions, says John Siegel, vice president of the U.S. Council for Energy Awareness, the nuclear-power

Brace for Brownouts

The shaded states are expected to experience brownouts by 1992.

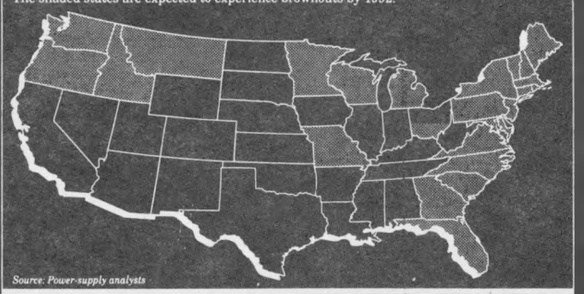

Source: Power-supply analysts

the situation on a utility by utility basis. "It's a localized problem."

Many utility executives, meanwhile, feel they can meet any shortfalls with gas-turbine power plants, which can be put up fairly quickly.

Gas turbines, however, are expensive and that means higher electric bills down the road. One analyst—John Sillin, a utility consultant for Management Analysis Co.—even doubts there's enough turbine-manufacturing capacity in the world to meet what could be huge U.S. demand.

The industry's own assessment is more optimistic. The North American Electric Reliability Council, the industry's forecasting body, generally expects energy capacity to meet demand. Even so, on [illegible]

during a brownout—when power is usually cut around 5%—the reduced energy forces appliances and machines to work harder, causing parts to burn out faster.

Analysts predicting shortages say "rolling" blackouts in rural and suburban areas are a distinct possibility, as utilities are forced to temporarily cut off energy in one place and then another in order to avoid a systemwide blackout. Even with "load-shedding," as such cutoffs are called, it's possible that all of Boston or Providence, R.I., or even all of New England could get blacked out for anywhere from one to 24 hours, the analysts say. Those kinds of total blackouts are "unlikely, but possible," says Marie Corio, president of Applied Economic Research Co., an energy-con-

going to leave them critically short of generating capacity for at least a few years, until alternative generating sources can be brought on line.

"We're going to need the cooperation of our customers, some good weather and a little luck to get through this summer," a Lilco spokesman says.

While New England is this year's focal point, the Pacific Northwest could be next year's. The Pacific Northwest economy is just getting up a full head of steam, says Mr. Siegel of the nuclear-power trade group. At the same time, not much new generating capacity is being planned to meet this added demand, and there are few transmission lines available to transport power in from other regions.

Mr. Sillin at Management Analysis believes that a national electricity crisis is brewing, and along with it the potential for a "severe economic slowdown."

The Boston Chamber of Commerce estimates that for the 12 months ended last August, energy shortages cost businesses in Massachusetts $87 million in lost productivity. Armstrong World Industries Inc., a maker of rubber insulation, says sporadic voltage reductions last year cost its Braintree, Mass., plant about $25,000 to $30,000 in productivity. Power fluctuations changed the temperatures needed to make insulation expand, ruining it the way a souffle collapses when the oven door is opened too early.

Slow Plant Construction

As far as new plant construction goes, utilities have been reluctant to choose the type of non-nuclear power plants they want [illegible]

Wall Street Journal, May 18, 1989

THE LIFE-CYCLE COST NOTEBOOK: AN ENCYCLOPEDIA OF ADVANCED BATTERY AND FUEL CELL COSTS

K. K. Humphreys and D. R. Brown
Pacific Northwest Laboratory(a)

The Life-Cycle Cost (LCC) Notebook represents a fully documented "encyclopedia" of battery, fuel cell, and competing technology cost estimates for load-leveling, stand-alone power system, and electric vehicle applications. The Notebook presents costs estimates at three levels of detail to satisfy the needs of a variety of users. The first level provides summary "bottom line" cost estimates. The second level describes the cost components that make up the bottom line cost estimate for each technology/application combination. The third level is presented at the calculational level with every cost and performance number used traceable to its original source or a stated assumption.

In recent years, PNL has prepared LCC estimates for a number of battery and fuel cell technologies used in load-leveling, stand-alone power system, or electric vehicle applications. In addition, LCCs for gas-fired turbine, mini-compressed air energy storage, pumped hydro energy storage, and internal combustion engine technologies were estimated for comparative purposes. The objectives in preparing the estimates were to determine the relative economics among alternative battery systems and to compare battery system economics with competing energy technologies. Recent work has involved expanding the previous knowledge base to include some new technology/application combinations, updating the knowledge base to include cost information that has recently been disseminated into the public domain, and compiling all this information into the present LCC Notebook.

The estimates prepared and presented in the LCC Notebook were developed from data gathered in a thorough review of the literature, encompassing over 100 different references. Data extracted from these reports were adjusted to a common set of assumptions governing battery module manufacturing, balance-of-plant installation, system size, and price year. However, estimates for materials, equipment, and labor hours found in the literature were not adjusted in this evaluation (i.e., independent cost estimates of these basic data were not developed). Data judged to be unreliable were either not used or given less weight in determining appropriate inputs to the LCC calculations.

Life-cycle costs for the load-leveling application were based on a 100-MWh, 20-MW system. In addition, system sizes of 50-MWh, 10-MW, and 30-MWh, 10-MW were evaluated as sensitivity cases. For the stand-alone power system application, 50-kWh, 10-kW was the basis for the analysis. The electric vehicle analysis was based on vehicles meeting specific mission performance requirements (e.g., acceleration, gradability, and range) for passenger car, light-duty van, and full-performance van applications.

A lifetime cost scenario for each technology was prepared that included the initial capital cost, replacement costs, operating and maintenance (O&M) costs, auxiliary energy costs, costs due to system inefficiencies, the cost of energy stored, and salvage costs or credits. The adjusted capital and O&M cost estimates were used, along with financial data and energy cost data, as inputs to a life-cycle economic model. The model calculated the levelized generation cost or levelized output cost, depending

---

(a) Pacific Northwest Laboratory is operated for the U.S. Department of Energy by Battelle Memorial Institute under Contract DE-AC06-RLO 1830.

upon the technology and end-use application. For the load-leveling application, the sensitivity of life-cycle cost to changes in the discount rate, charging cost of electricity, battery cycle life, battery cell efficiency, and plant life were examined.

The LCC estimates presented in the LCC Notebook require careful interpretation. All are based on the projected costs and characteristics of each technology presuming mass-production of the batteries and reasonable technological improvements in their designs. It is possible that the LCCs could be reduced substantially if major technological breakthroughs occur; however, presuming that such breakthroughs will occur carries considerable uncertainty.

No consideration was given in this analysis to differential benefits that may accrue to alternative technologies. For example, the services (benefits) provided by battery storage to a utility are almost certain to be different than the services provided by a gas-fired turbine, even though both technologies are generally thought of as alternative peaking technologies. Similarly, the potential benefits of electric vehicles (e.g., reduced air pollution) might make them more attractive than the LCC comparison would indicate.

Acknowledgement:

This research was supported by the U.S. Department of Energy's Office of Energy Storage and Distribution.

COMPETITIVE BATTERY PERFORMANCE TARGETS THROUGH PARAMETRIC LIFE-CYCLE COSTS

Joseph S. Badin
Energetics, Incorporated

One of the challenges of managing a battery research and development (R&D) program for the USDOE Office of Energy Storage and Distribution (OESD) is to produce consistent and reliable estimates of technology cost and performance goals. A discounted, levelized life-cycle cost (in $/kWh of retrieved energy) analysis is used to compare commercial and developing technologies on a consistent basis. The application of a parametric life-cycle cost analysis will aid in the following:

- Establishing research goals, by translating improved performance into cost reductions;
- Assessing R&D program performance, as measured by product cost;
- Identifying R&D needs and priorities, by pinpointing high-cost areas; and,
- Comparing investments in battery technologies with investments in other technologies.

The base data for the parametric analysis was obtained from the "Life-Cycle Cost Notebook" produced by Pacific Northwest Laboratory in January 1989. The parametric life-cycle cost analysis not only identifies which cost/performance elements are primary figures of merit, such as battery purchase price or battery life, but what values for these parameters must be achieved in order to be competitive with conventional technologies such as combustion turbines. This approach shows how much the present status of battery technologies needs to be improved, and thereby helps to focus R&D efforts. In addition, secondary considerations such as dynamic operating benefits of battery systems can be readily incorporated into the analysis as a capital credit in the cost analysis.

The parametric life-cycle cost analysis model considers all major cost elements such as initial and replacement capital, salvage, fuel and charging electricity purchases, maintenance, depreciation, and taxes. Depending on the end-user (utility or industrial/commercial sector), appropriate cash flow analyses are conducted. Each method reflects how capital investment decisions are made in these sectors. For regulated utilities, which have a regulated rate of return, the required revenue method was used (consistent with EPRI-TAG). For non-regulated industrial/ commercial users, the internal rate of return cash flow method was used.

Analyses are being completed for several battery systems and for several conventional technologies for utility load-leveling applications, remote stand-alone

systems, and electric vehicles. As an example, the findings for a 100-MWh, 20-MW sodium-sulfur utility load-leveling system are presented. The attached figures show the life-cycle cost impacts of varying battery purchase cost, battery life, round-trip efficiency, and balance of system (BOS) cost. The estimates of life-cycle costs are calculated at varying battery charging costs. The computed life-cycle costs are compared to a competitive technology screening curve, which in this case is a conventional combustion turbine operating at high and low purchased fuel costs and producing 25 million kWh/year (equivalent to 5 hour battery storage capability). The conventional technology curves define the competitive range for the battery system.

The intersection points of the parametric battery curves with the conventional curves indicate target values for each figure of merit. Goals can be targeted when the life-cycle costs of conventional and alternate technologies are equal, and therefore economically competitive. The present status of each figure of merit can be plotted on these curves and the progress in attaining the set goals can be tracked.

The results of the sodium-sulfur battery system base case are interesting. For a 30 year system with 2 periodic replacement batteries, the levelized life-cycle costs with the following charging costs are:

Charging Cost ($/kWh)	Life-Cycle Cost ($/kWh)
0.010	0.135
0.025	0.160
0.050	0.200

The competitive target life-cycle costs of the combustion turbine at the low and high fuel scenarios of $2.2 and $4.5/MBtu, respectively are 0.11 and 0.19 $/kWh.

The comparative parametric results at the life-cycle cost equivalence (intersection) points are summarized below:

Parameter	Base Value	Low Scenario	High Scenario
Batt. Cost ($/kWh)	70	90	120
Batt. Life (years)	10	20	13
Efficiency (%)	64	80	68
Bal. of Sys. (10^6)	6	16	5
Cycles per Year	250	360	170

The low and high scenarios define the competitive range for low and high fuel and charging energy costs respectively. Other mixed scenarios will change the competitive range. The results clearly show that battery life and efficiency are the key parameters to be improved for competitive systems to be developed.

Acknowledgement:

This work is supported by DOE, Office of Energy Storage and Distribution.

Technology Screening Curves
Gas Turbine (C) Utility

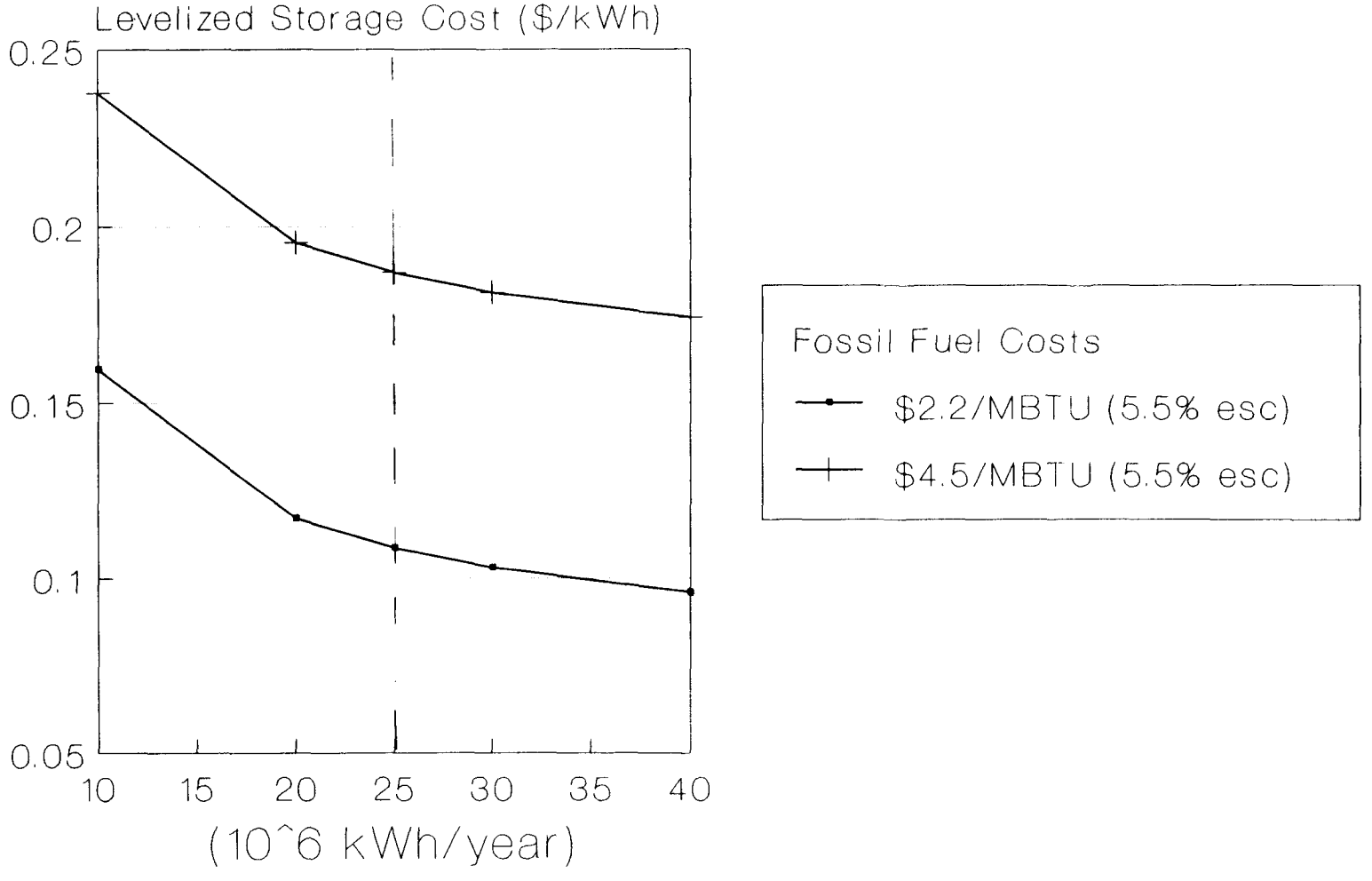

Na-S / Utility
Battery Purchase

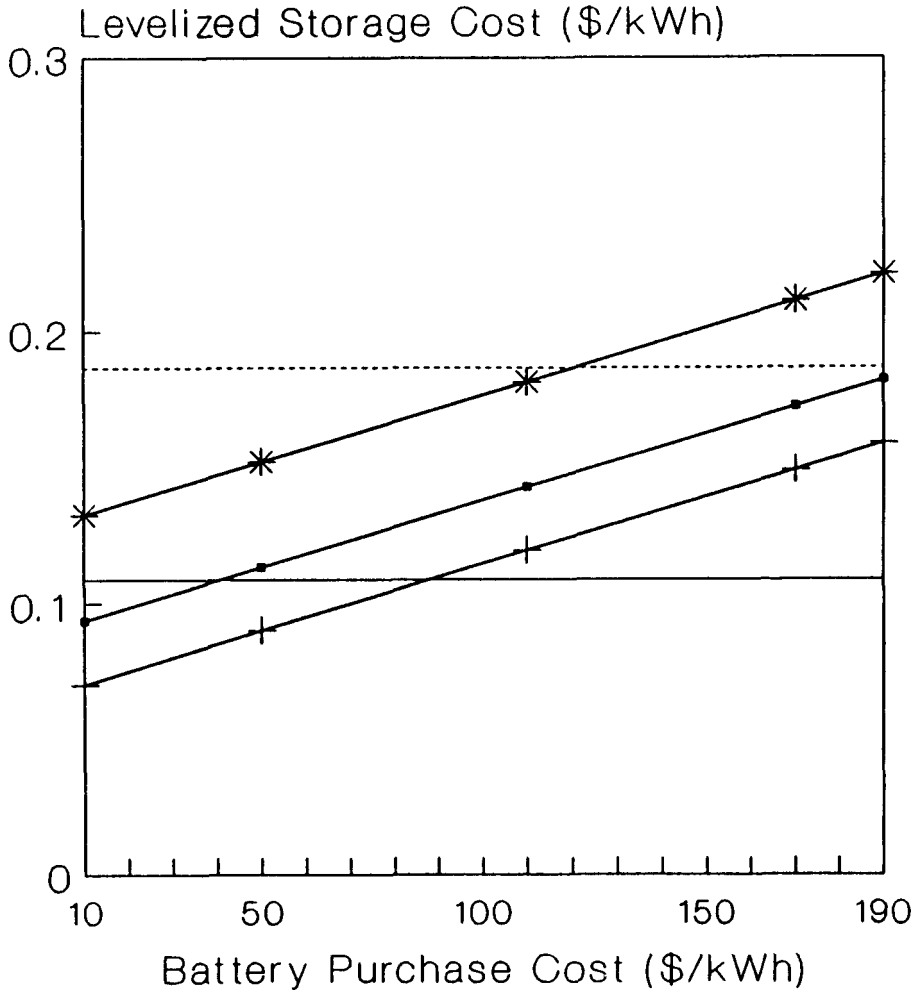

Energy Prices

Charging Electricity
- $.025/kWh
- $.01/kWh
- $.05/kWh

Fossil Fuel Gas Turb.
- $2.2/MBTU (5.5% esc)
- $4.5/MBTU (5.5% esc)

Na-S / Utility
Efficiency

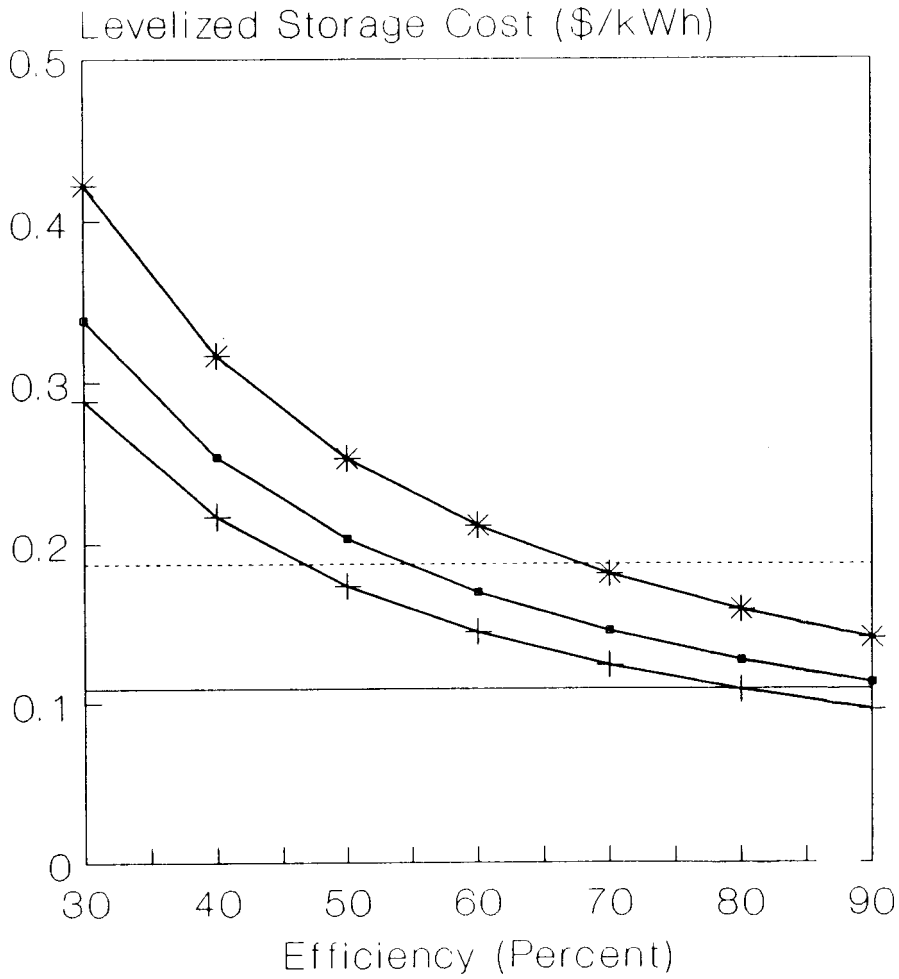

Energy Prices

Charging Electricity
- $.025/kWh
- $.01/kWh
- $.05/kWh

Fossil Fuel Gas Turb.
- $2.2/MBTU (5.5% esc)
- $4.5/MBTU (5.5% esc)

Na-S / Utility
Battery Life

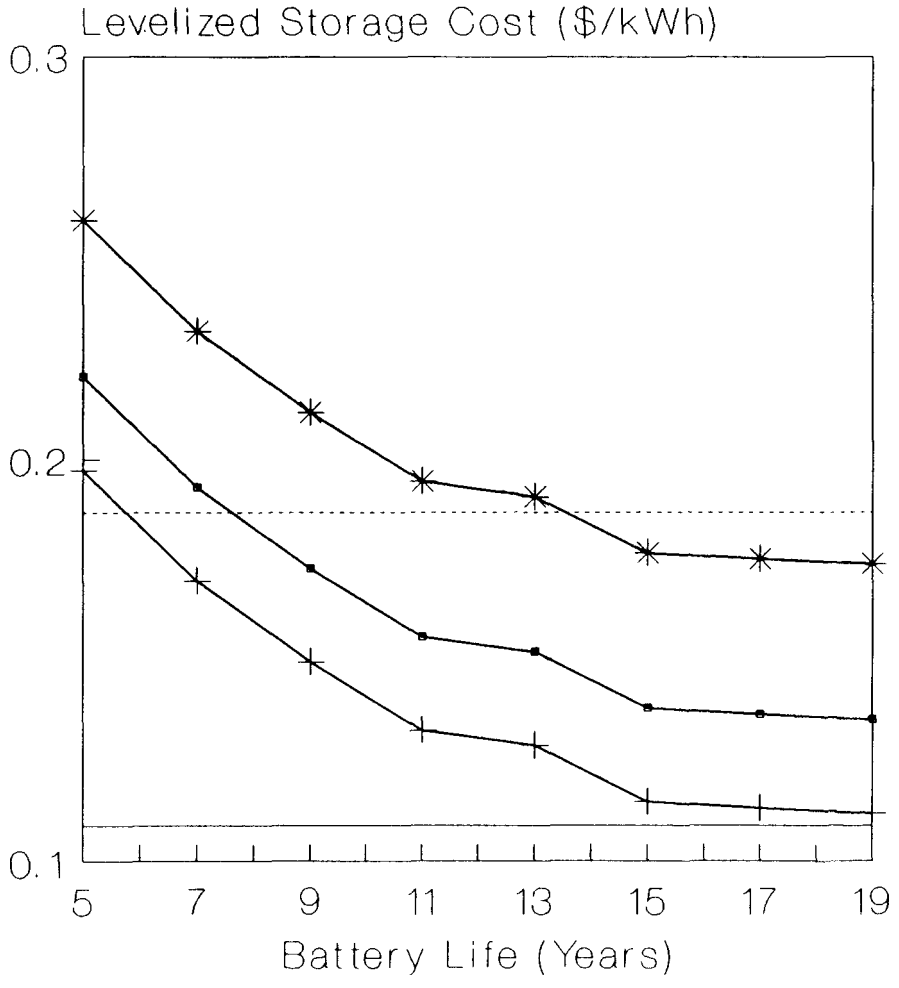

Energy Prices

Charging Electricity
- $.025/kWh
- $.01/kWh
- $.05/kWh

Fossil Fuel Gas Turb.
- $2.2/MBTU (5.5% esc)
- $4.5/MBTU (5.5% esc)

Na-S / Utility
Balance of System

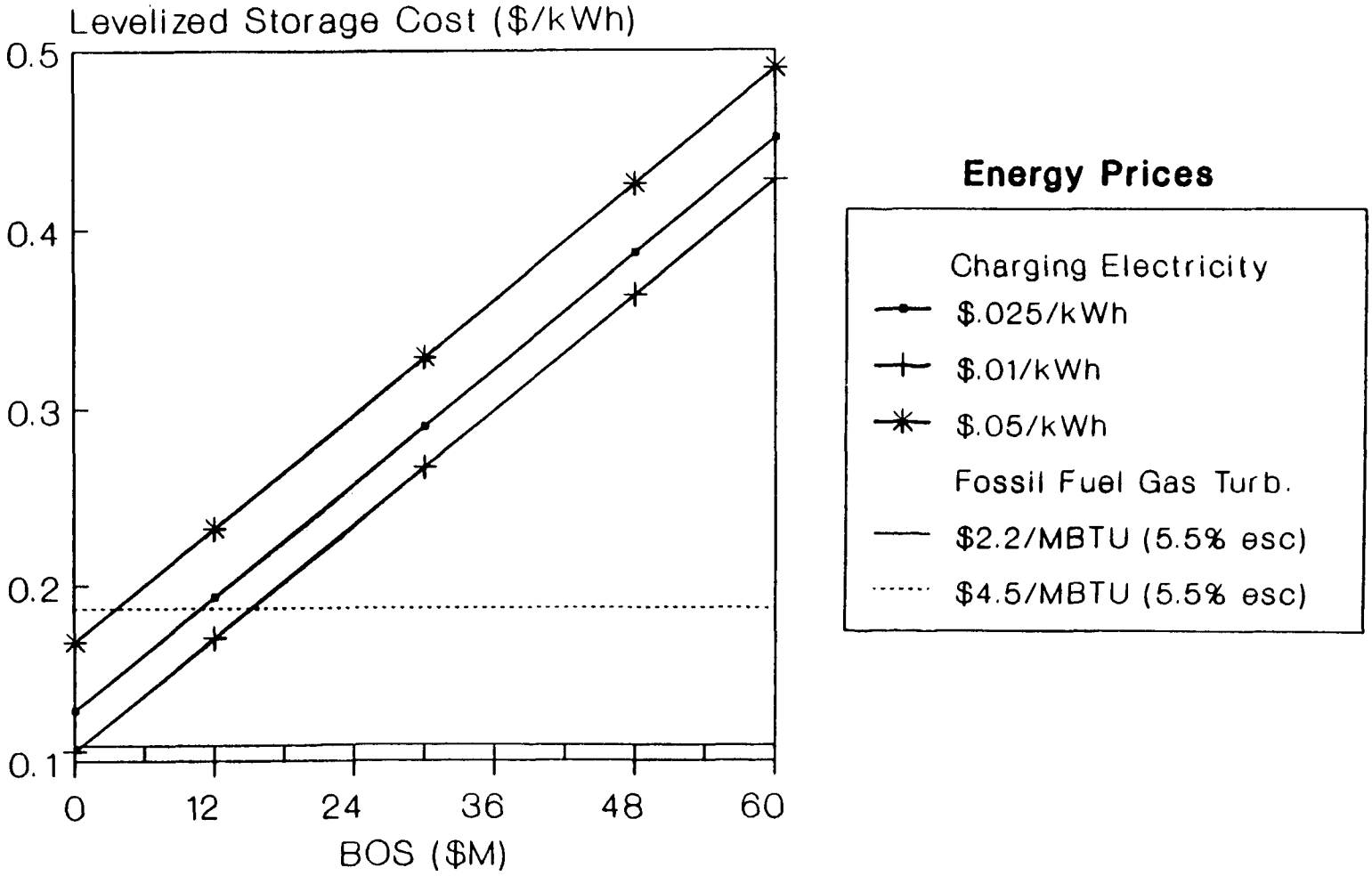

PROJECTED COSTS FOR SODIUM/SULFUR ELECTRIC VEHICLE BATTERIES

Philip C. Symons
Electrochemical Engineering Consultants, Inc.

Daryl R. Brown
Pacific Northwest Laboratory

The requirements for acceptance of batteries for electric vehicle (EV) applications include good performance characteristics, high reliability, customer-oriented systems, and competitive costs. Good progress has been reported for the first three of these, which are primarily technical in nature, but little has been made public to date concerning the more-speculative projected selling price for batteries. Cost projections are of particular importance to DOE, since they provide program managers with some reassurance that the systems being funded have the potential, ultimately, of being commercially successful. As a result, Pacific Northwest Laboratory (PNL), with Electrochemical Engineering Consultants Inc. (EECI) as a subcontractor, has been funded by DOE over the past few years to conduct assessments of the costs that might be expected for advanced batteries if and when these are commercialized.

During 1986-7, Chloride Silent Power Ltd. (CSPL), in conjunction with one of its parent organizations the Chloride Group, prepared and refined cost estimates for sodium/sulfur EV batteries. The projections were made by designing a manufacturing operation for the production of 6600 batteries/year, each battery having a nominal capacity of 69kWh, then estimating the costs for equipment, materials, energy, manpower, and other variable and fixed items. After allowing for selling, administrative, warranty, and disposal costs, plus appicable license fees, taxes, and return on investment, the required selling price using a pro-forma costing methodology was estimated to be $112/kWh. During 1988, PNL/EECI, with the participation of James E. Quinn of DOE, was permitted to review the CSPL cost projections. The review was done to assure that the cost estimation method had a good chance to reflect actual costs, and that the assumptions made were reasonable. We report on the results of this review herein.

In collaboration with CSPL, PNL/EECI aggregated the cost information presented here, so only combined costs are shown, in order to protect CSPL's proprietary information. In addition, factory overhead, rent, depreciation, return on investment, and taxes were recomputed using the standard methodology developed by the Electric Power Research Institute (George, 1984). This was done to protect corporate financial information for Chloride as well as to adjust data to better compare with likely overheads in the United States.

For purposes of estimating, a single manufacturing plant was assumed to have an annual production capacity of 453 MWh, corresponding to 6600, 69kWh batteries per year. Costs were estimated for distinct manufacturing plants producing two different batteries, one based on a 24-Wh "PB" cell and the other on an 81-Wh "XPB" cell. Cost data for the PB-based option only will be presented. An annual production capacity of 453 MWh translates into

approximately 19 million PB cells or 5.6 million XPB cells. This production level allows significant discounts for procuring raw materials and components in large quantities and makes automated production both practical and economically feasible. The majority of the processes are automated, scaled-up versions of processes currently existing at CSPL. Plant and equipment designs were developed for manufacturing processes dedicated to producing a single battery based on either the PB or XPB cell. The production of multiple cell sizes and/or batteries from a single facility was not considered. The production facility is presumed to operate 50 weeks per year, 24 hours per day, 5 days per week. Near continuous operation of the production facility is preferred because of the significant capital investment and the nature of some of the unit operations.

CSPL has fabricated experimental sodium-sulfur EV batteries for the CF Bedford (Griffon) van and is presently assembling a battery for the Ford ETX-II. The CSPL manufacturing and design engineering team, utilizing the experience base acquired from these demonstration battery builds, has developed a battery design which incorporates ease of manufacturing, low cost, and component optimization. The evolved battery design, the specifications for which are presented in Table 1, has a rating of 69 kWh at 192 volts nominal, and is suitable for a medium sized delivery van.

The projected selling price for the battery at a moderate annual production rate of 6600 batteries is $7700 or $112/kWh. The individual cost accounts which were used to develop this selling price are summarized in Table 2 and Figure 1. A detailed breakdown of the material costs is presented in Table 3 for both the cell and battery components. Included in the material costs are indirect as well as direct materials, process gases, tools and consumables, energy, and maintenance materials.

Factory costs and selling prices were also estimated for three alternative annual production rates. The results, which are presented in Figure 2, suggest that the selling price might be reduced by $670 or $10/kWh by doubling the annual output from the factory.

The DOE/PNL/EECI review of the cost estimation methodology and results involved the evaluation of proprietary reports, followed by a site visit to examine original design/cost information and other documentation, and to interview staff who performed the work. The review investigated comprehensiveness and reasonableness of the methodology, assumptions, and results, and the likelihood that the design and manufacturing processes would achieve desired specifications. The conclusion of the review was that the cost study was consistent with good cost estimation practice and the results were reasonable. Overall, the review team felt that the costs projected for sodium-sulfur EV batteries are achievable in the early to mid-1990s.

Reference

George, J.H.B. 1984. Guidelines for Estimating the Capital Costs of Battery-Based Energy Storage Systems. Research Project RP1198-12. Electric Power Research Institute. Palo Alto, California.

TABLE 1. EV Sodium-Sulfur Battery Specification

Design Consideration	Requirement
Delivered Energy	68.8 kWh @ 3 hr rate
Delivered Capacity	376 Ah
Nominal Voltage	192 Volts
Max Power @ 0.96 Volt Load	73 kW
Peak Power @ 1.6 Volt Load	58 kW
Total Weight	442 kg
Dimensions for Half-Battery (l w h)	1510 x 529 x 230 mm
Envelope for Half-Battery (l w h)	1643 x 559 x 230 mm
Volumetric Energy Density (delivered)	187 Wh/liter
Volumetric Power Density (peak)	157 W/liter
Gravimetric Energy Density (delivered)	154 Wh/kg
Gravimetric Power Density (peak)	129 W/kg

TABLE 2. EV Battery Manufacturing Cost and Selling Price Summary

Accounting Category	$/Battery	$/kWh	% of Factory Cost	% of Selling Price
Cell Production				
Direct Labor	219	3.18	3.9	2.8
Materials	2186	31.77	38.9	28.4
Battery Assembly				
Direct Labor	59	0.86	1.0	0.8
Materials	1084	15.76	19.3	14.1
Total Labor and Mat'ls	3548	51.57	63.1	46.1
Other Factory Costs				
Overhead on Mat'ls[1]	327	4.75	5.8	4.2
Overhead on Labor[2]	417	6.06	7.4	5.4
Rent[3]	108	1.57	1.9	1.4
Depreciation[4]	467	6.79	8.3	6.1
Total Other Factory Costs	1319	19.00	23.5	17.1
Selling & Admin. Expenses				
Distribution & Service	138	2.00	2.5	1.8
Marketing Costs	103	1.50	1.8	1.3
Warranty Costs	172	2.50	3.1	2.2
Battery Disposal[5]	344	5.00	6.1	4.5
Total Selling & Admin.	757	11.00	13.5	9.8
FACTORY COST	5624	81.74	100.0	73.0
License Fee[6]	231	3.36	4.1	3.0
ROI and Taxes[7]	1845	26.82	32.8	24.0
SELLING PRICE	7700	111.92	136.9	100.0

[1] Based on 10% of total materials.
[2] Based on 150% of total labor
[3] Based on $\$6/ft^2$
[4] Based on 10% "straight-line" depreciation of total equipment investment.
[5] Based on $5.00/kWh.
[6] Based on 3% of the selling price.
[7] Based on 30% of Total Investment Required, which is defined as the total equipment investment (see Table 3-3) plus working capital. Working capital is defined as 30% of Total Labor and Materials + Total Other Factory Costs. The Total Investment Required for the EV battery plant producing 6600 units annually is $40.583 million.

TABLE 3. PB Cell and Battery Assembly Materials and Direct Labor Costs

Component	Total M & L ($/Battery)	Material[1] ($/Battery)	Labor[2] ($/Battery)	Equipment[3] (K$)
Cell				
Sulfur Electrode	276	249	27	1,856
Sodium Electrode	191	165	26	4,416
Beta" Alumina	577	530	47	10,383
Seals and Containment	995	903	92	10,482
Cell and String Assembly	366	339	27	2,984
Total Cell	2405	2186	219	30,121
Battery Assembly				
Bank Parts and Assembly	285	279	6	290
Buses and Terminals	51	51	-	-
Thermal Enclosure	588	588	-	-
Thermal Management	12	12	-	-
Controls and Hardware	126	126	-	-
Battery Parts and Assembly	81	28	53	627
Total Battery Assembly	1143	1084	59	917
TOTAL	3548	3270	278	30,946

[1] Includes direct and indirect materials, process gases, tools, consumables, energy and maintenance materials.
[2] Based upon a labor rate of $13,500 per annum.
[3] Includes installation, commissioning and connection of services.

Figure 1: Breakdown of Projected Selling Price of $7700 for 69kWh Sodium/Sulfur EV Battery

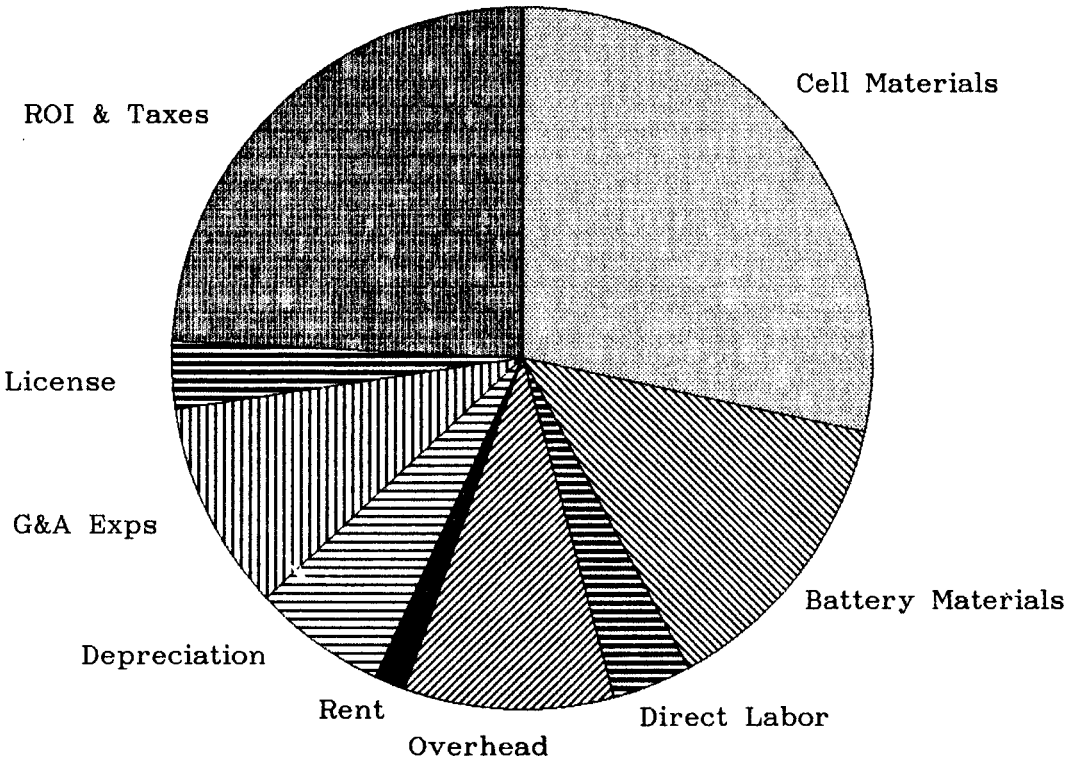

Figure 2: Projections of Factory Cost and Selling Price as Function of Production Volume

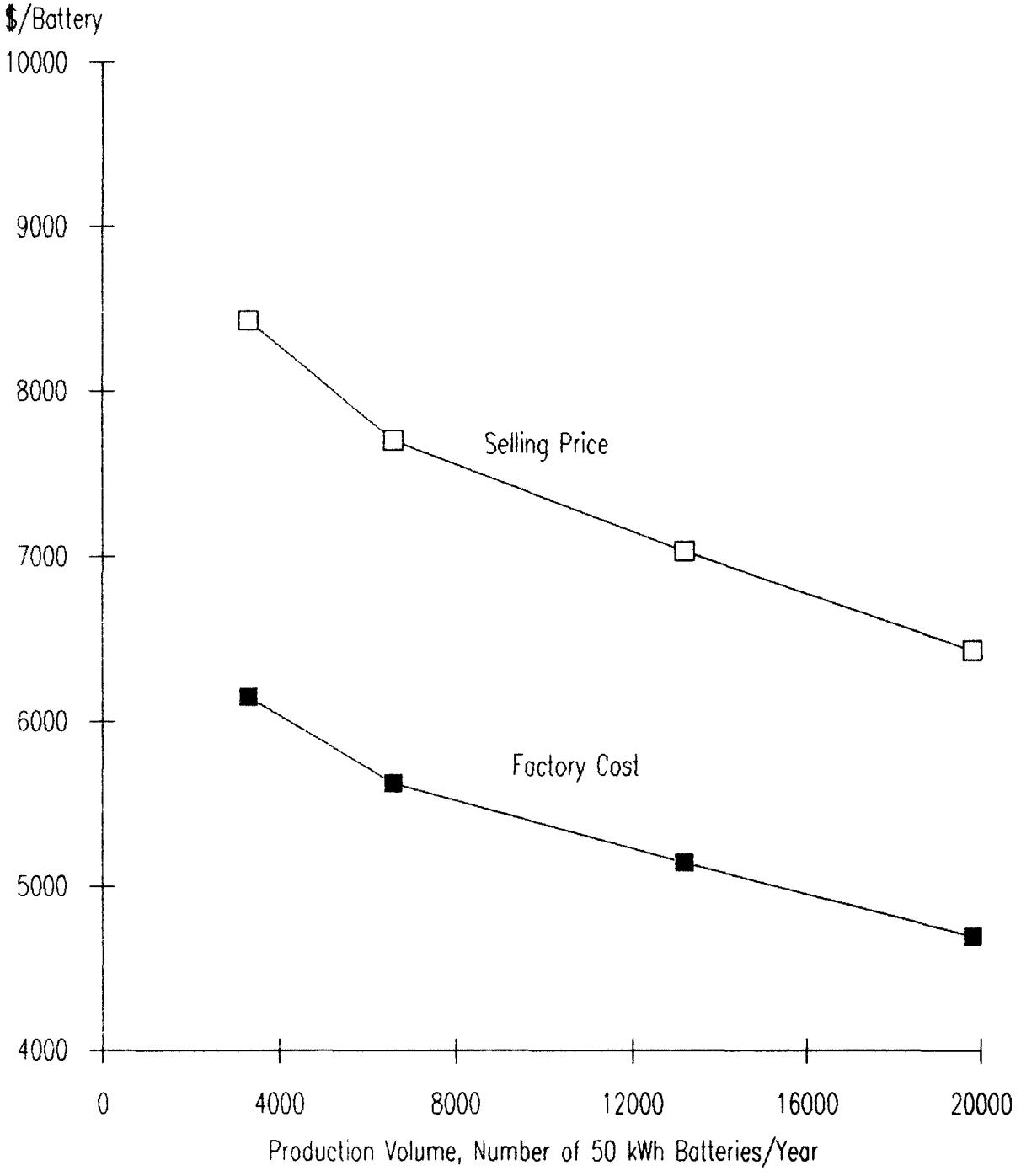

FUEL CELLS

CHAIRPERSON:

Pandit Patil
U.S. Department of Energy

THE AIR-COOLED PHOSPHORIC ACID FUEL CELL/ BATTERY HYBRID PROPULSION SYSTEM

Chang V. Chi, Donald R. Glenn, Sandors G. Abens
Energy Research Corporation
3 Great Pasture Road
Danbury, CT 06813

Energy conversion processes for power production are intimately related to our worsening air quality and global environmental balance. This situation is exacerbated by the increasing dependence in the U.S., once again, on petroleum fuels. The transportation sector alone accounts for 65% of this demand, with 50% coming from imports. One option to minimize this trend is to substitute batteries for gasoline and diesel engines. Electric vehicles (EV's) have not fulfilled this role mainly because current battery technology cannot provide the range and speeds produced by internal combustion engines (ICE). Additionally, recharge rates are too slow further limiting EV usage. A fuel cell integrated with an advanced battery (FC/B) provides a full performance capability with quiet, odor-free operation and dramatic reductions in polluting emissions.

The Energy Research Corporation (ERC) is pioneering a transportation application of a Fuel Cell/Battery (FC/B) hybrid power system for the first-of-a-kind electric system to be installed in a small urban mass transit vehicle. This program is funded by the Department of Energy (DOE) and Transportation (DOT) with cost sharing provided by ERC.

ERC and its team partners, Bus Manufacturing USA, Inc. (BMI) and the Los Alamos National Laboratory (LANL) were selected to develop the urban mass transit bus utilizing the Phosphoric Acid Fuel Cell (PAFC)/Battery hybrid system. The new system will, for the first time, fulfill the Electric Vehicle (EV) mission by providing range and speeds comparable to conventional vehicles, quietly, virtually pollution and odor free, using a non-petroleum based fuel, methanol.

The objective of the present phase (Phase 1) of the four phase program is to demonstrate the feasibility of the fuel cell/battery combination as a power source for a bus using a Brassboard (½ scale of FC/B Test Bed Bus) system. The performance of this brassboard unit is to be evaluated based on DOT White Book transit bus performance guidelines and on the Georgetown University Arlington route.

ERC's approach to the FC/B hybrid bus power source stresses low cost and reliability. The power source utilizes an air cooled phosphoric acid fuel cell which provides the lowest cost, most reliable and lightest weight fuel cell design available. The methanol reformer has a compact double annular concentric design which is compatible with low cost mass production techniques. ERC's non-sintered, polymer-bonded Nickel Cadmium battery was chosen because of its light weight, high discharge rate capability (3C) and outstanding charge acceptance which is very important for the frequent stop and go operation of the inner city transit buses. From the bus drive train trade-off analysis and prior experience with electric motors and controllers, a nominal system voltage of 128 V was chosen to maximize the use of available hardware.

Figure 1 shows ERC's simplified, functional concept for the FC/B hybrid power system. The parallel operation of fuel cell and battery provides the simplest system, thus lowest cost and highest reliability. During heavy load such as

acceleration and high speed cruising, the fuel cell and battery provide the maximum power together for the traction motor. Both the fuel cell and battery are at high currents and reduced voltage as seen in Figure 1A. During deceleration and idle, when the bus requires less power than available from the fuel cell, the excess fuel cell output is used to charge the battery. The voltage characteristics of the fuel cell stack must be matched carefully to the requirements of the battery in order to avoid an undercharged or overcharged condition. This matching is accomplished by the use of the appropriate ratio of cells in the stack and in the battery. We anticipate that the 240 to 100 fuel cell to battery ratio used for this application will be appropriate for most city bus driving conditions.

A typical driving cycle is depicted in Figure 2 (one Central Business District cycle from the DOT White Book Transit Bus Duty Route). As shown, the fuel cell power is modulated between 2/3 and full load which is well within its response capability.

The test-bed-bus chosen is a 27 foot long high quality bus which has 25 seats with a maximum capacity of 40. The bus is driven through its rear axle by a direct-current electric motor which receives its power from an on-board fuel cell and storage battery. With the bus weight estimate of 22,660 lbs., and an electric drive train capable of 70 hp continuous (105 hp intermittent duty) and an auxiliary power estimate of 18 kW of peak power in order to meet acceleration, over-the-road climb and cruising speed requirements. The peak power delivery is shared almost equally between the fuel cell and battery.

The air-cooled PAFC fuel cell stack has 240 cells and operates at a nominal 144 volts. On the fuel side, hydrogen rich gas (approximately 75% H_2 and 25% CO_2 on dry basis) reformed from methanol (58%) and water (42%) is used. About 1lb./min. of methanol is consumed for the nominal 0.6 V/cell for 60 kW fuel cell output.

Table 1 shows the test-bed-bus specification with the nominal 60 kW fuel cell and 24 kWh battery. Figure 3 shows the component layout in the bus, and Table 2 shows the anticipated FC/B bus performance. As shown in the table, the FC/B bus performance will exceed all the DOT White Book alternative power bus performance guidelines with a top speed of 55 mph which is well over any inner city speed limits.

Over a 12-year life cycle, the total cost of the FC/B powered bus is projected at $1.59/mile which is comparable with $1.57/mile diesel engine powered bus cost. This cost comparison does not include the environmental benefits or possible tax credits for the fuel cell bus.

The engineering analyses and the hardware verification testing conducted thus far indicate that the PAFC/Battery hybrid power source for a city bus is entirely feasible and well within the state-of-the-art component technologies comprising the propulsion system. The bus is competitive both in terms of performance and life cycle cost with an equivalent diesel powered bus, while providing the pollution abatement which will become mandatory in the not-to-distant future.

ACKNOWLEDGEMENT

This ERC co-shared program is largely funded through a DOE Contract, DE-AC08-87NV10714. ERC gratefully acknowledges the management team of Dr. Pandit Patil, DOE; Mr. Clint Christianson, Dr. James Miller and Dr. Michael Krumpelt,

Argonne National Lab and Mr. Sam Romano, Georgetown University. The authors also wish to thank our team members, Messrs. Robert Davis and Ferenc Pavlics, BMI and Dr. Hugh Murray, LANL, for their input.

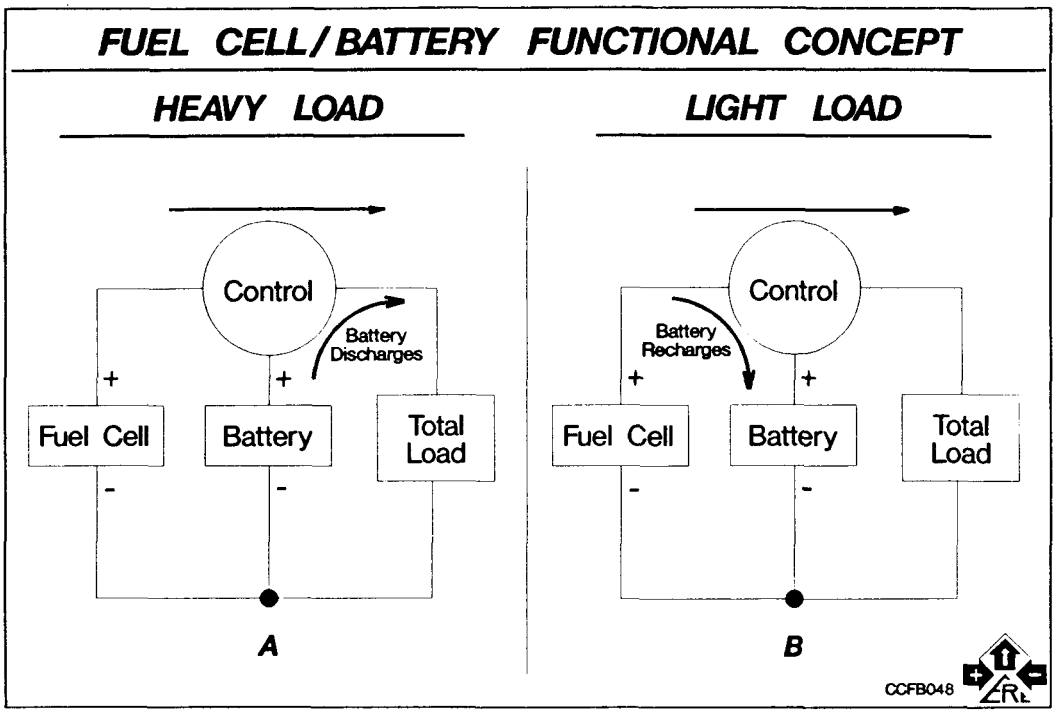

FIGURE 1

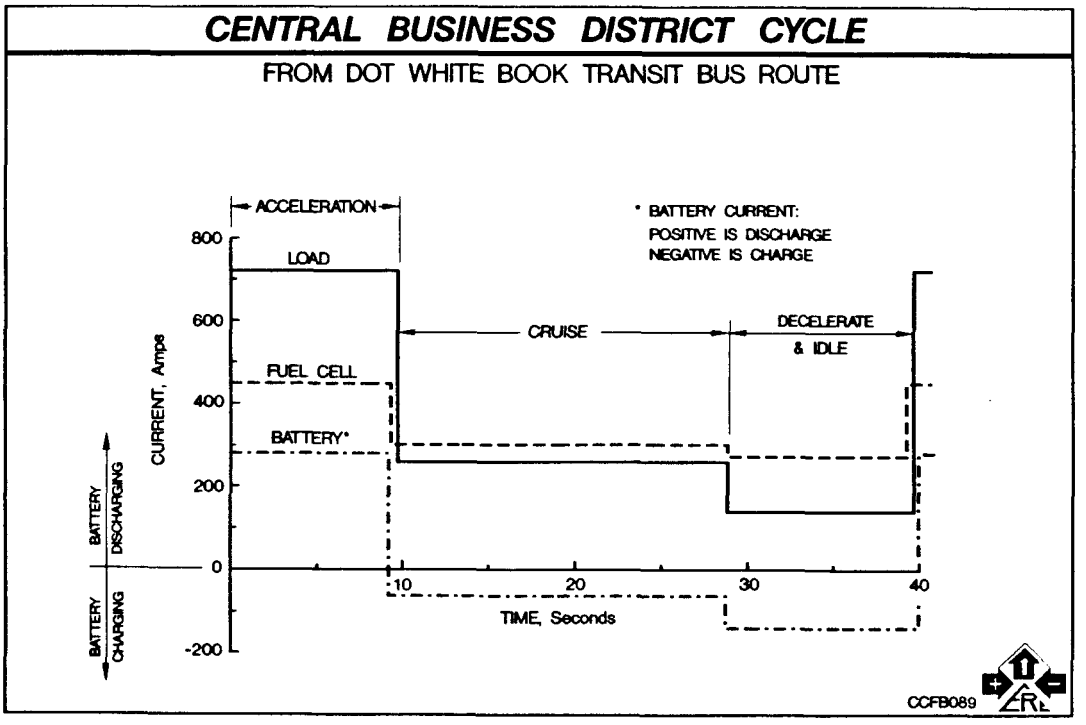

FIGURE 2

TEST BED BUS SPECIFICATION

PASSENGER CAPACITY, Seat/Max: 25/40

BUS DIMENSION, ft: 7.8 W x 8.75 H x 27.6 L

BUS GROSS VEHICLE WEIGHT, lb: 22,660

POWER, kW: 110 (PEAK), 18 (AUX.)

MOTOR: 70 HP/105 HP INTERMITTENT

AXLE: 2 SPEED REAR (5.38:1, 7.5:1)

FUEL CELL: 240 CELL PAFC, 60 kW

BATTERY: 100 CELL Ni-Cd, 24 kWh

CCFB076

TABLE 1

FUEL CELL / BATTERY POWERED TRANSIT OR SHUTTLE BUS

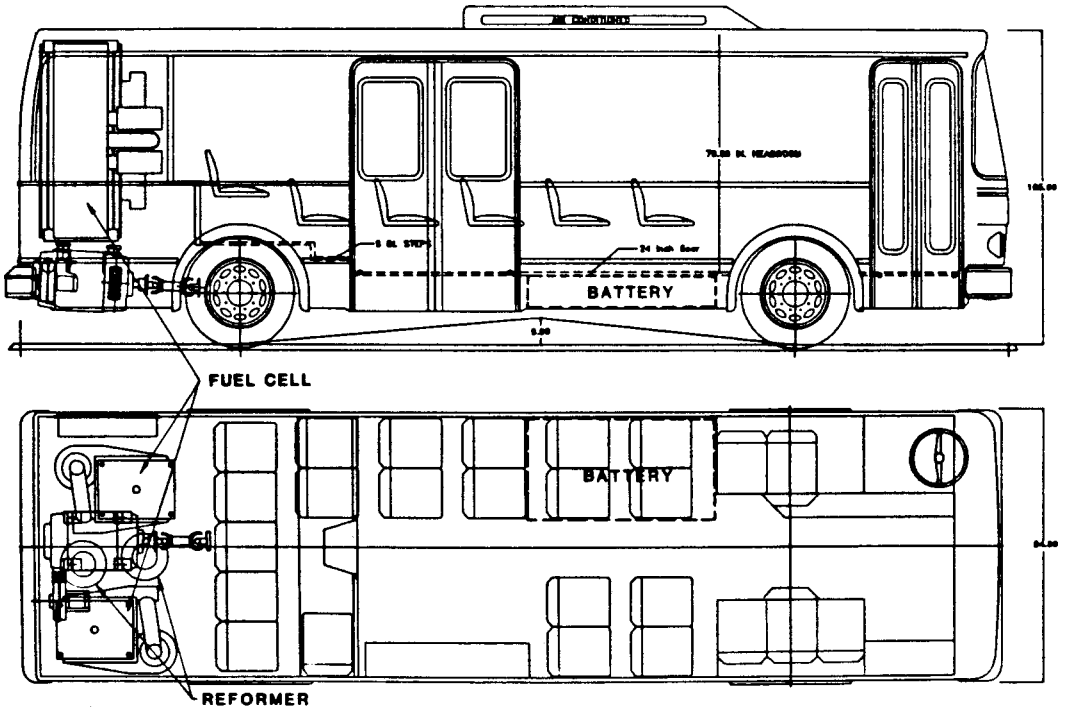

FIGURE 3

PREDICTED FC/B BUS PERFORMANCE

	FC/B BASELINE TBB	DOT ALTERNATIVE POWER
0-20 MPH	10 SEC.	12 SEC.
0-40 MPH	33 SEC.	46 SEC.
0-50 MPH	70 SEC.	90 SEC.
ACCELERATION, 0-15 MPH	0.115 g	0.06 g
TOP SPEED, LEVEL GROUND	55 MPH	50 MPH
TOP SPEED, 2.5% GRADE	38 MPH	34 MPH
TOP SPEED, 12% GRADE	13 MPH	7 MPH

CCFB017

TABLE 2

THE LIQUID-COOLED PHOSPHORIC ACID FUEL CELL/BATTERY PROPULSION SYSTEM

Russ J. Kevala and Daryl M. Marinetti
Booz, Allen & Hamilton Inc.

The current phase of the project is aimed at developing the specifications for a small (27-foot) urban transit bus with a liquid-cooled phosphoric acid fuel cell as the main power source. This will be achieved through the design, fabrication, and testing of a half-size brassboard propulsion system. The project is a collaborative effort of Booz, Allen & Hamilton, Chrysler Pentastar Electronics Inc. (PEI), the Engelhard Corporation, and Fuji Electric Company (FE). Booz, Allen is responsible for overall project management, system specification, economic assessment, and systems integration; PEI is responsible for the DC powertrain system, battery/fuel cell integration, and brassboard testing; and Engelhard and FE are responsible for the development and fabrication of the fuel cell subsystem.

Three batteries were evaluated for supplying the peak power requirements: nickel/iron, tubular lead-acid (deep cycle), and flat plate lead-acid (SLI). Trade-offs between battery type and capacity, fuel cell power rating, powertrain gear ratios and bus performance were conducted by means of a simulation program. Major trade-off considerations were:

- Bus performance equivalent to standard diesel bus acceleration and grade performance
- Ability to operate over the standard DOT urban bus cycle as well as over a specified Georgetown University route
- Availability of components
- Reasonable costs in relation to diesel bus costs.

As a result of the trade-offs, the following components were specified for the bus:

Fuel Cell	Nominal Power Rating	47.5 kW
Battery	Type	SLI Lead-acid
	Capacity (C/2)	80 Ah
	Peak Power	165 W/kg
Motor	Type	DC Separately Excited
	Shaft Power	40 HP Continuous
		70 HP Peak
Transmission	Torque	100 Ft-lb Peak
	First Gear	2:1
	Second Gear	Direct

The weight of the bus with these components is estimated at approximately 23,125 lb. with 20 passengers. Standard air-suspension, axles, brake and door actuation systems, and accessories will be employed, including an air conditioner.

Based on these specifications, a 25 kW fuel cell and half-size batteries and powertrain components have been assembled at PEI. Initial tests of the fuel cell subsystem indicate efficiency of the order of 36.5 percent at full power with all auxiliaries. A step-up chopper is used to ensure that the fuel cell supplies the power at the correct voltage for various system operating conditions. The fuel cell charges the battery when bus power requirements are lower than the nominal fuel cell power rating and the battery state-of-charge is below 89 percent. The SLI battery cannot withstand discharge below 65 percent. Hence its sizing is critical to ensure reliable bus operation.

Brassboard proof-of-feasibility tests currently underway will verify system operation under selected DOT cycle and Georgetown University route conditions. The simulation program is being updated as data from the brassboard becomes available. The findings will then be used to revise the bus specifications in preparation for the next phase, in which a full size propulsion system will be developed, tested, and installed in a test-bed bus.

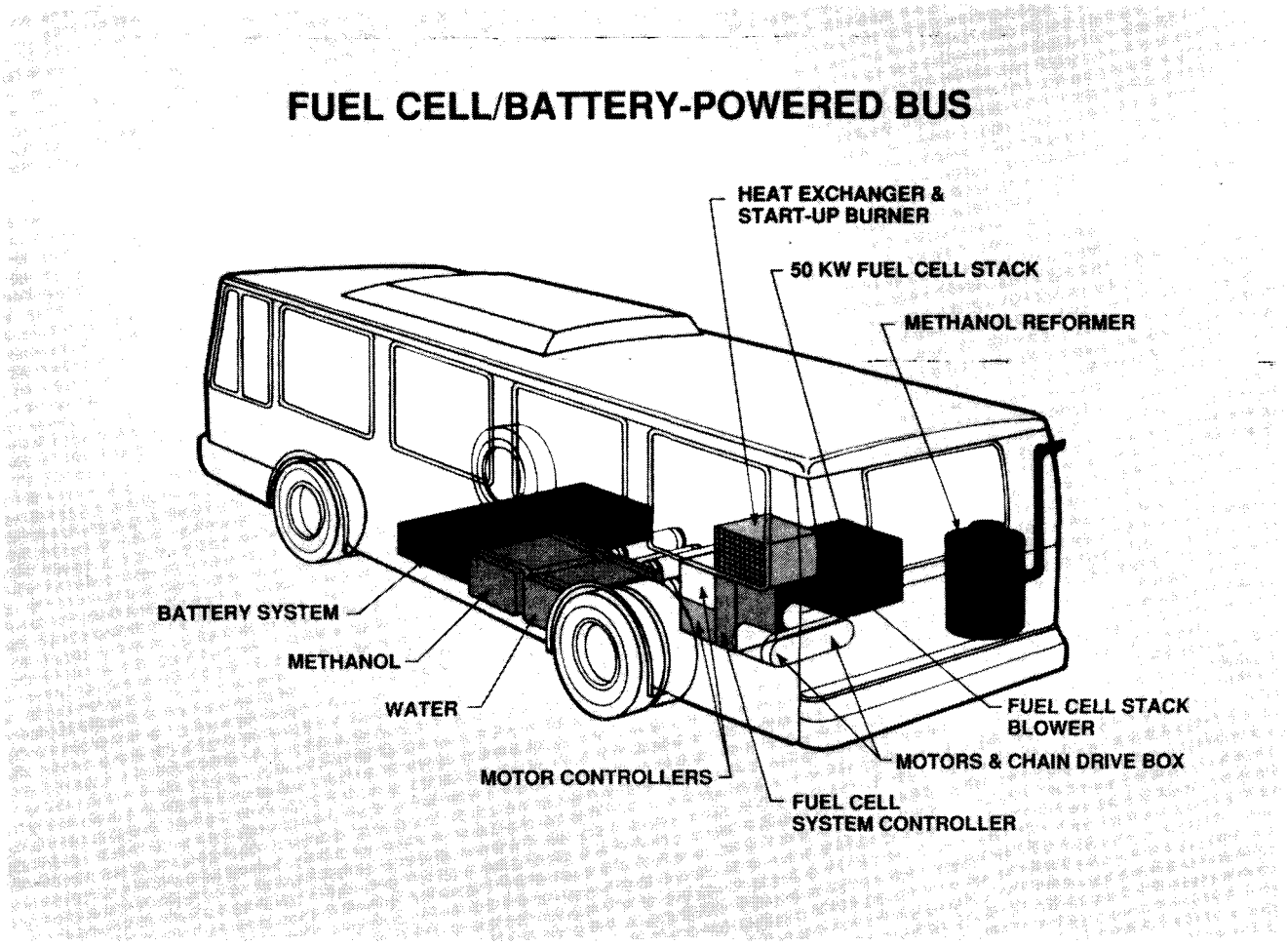

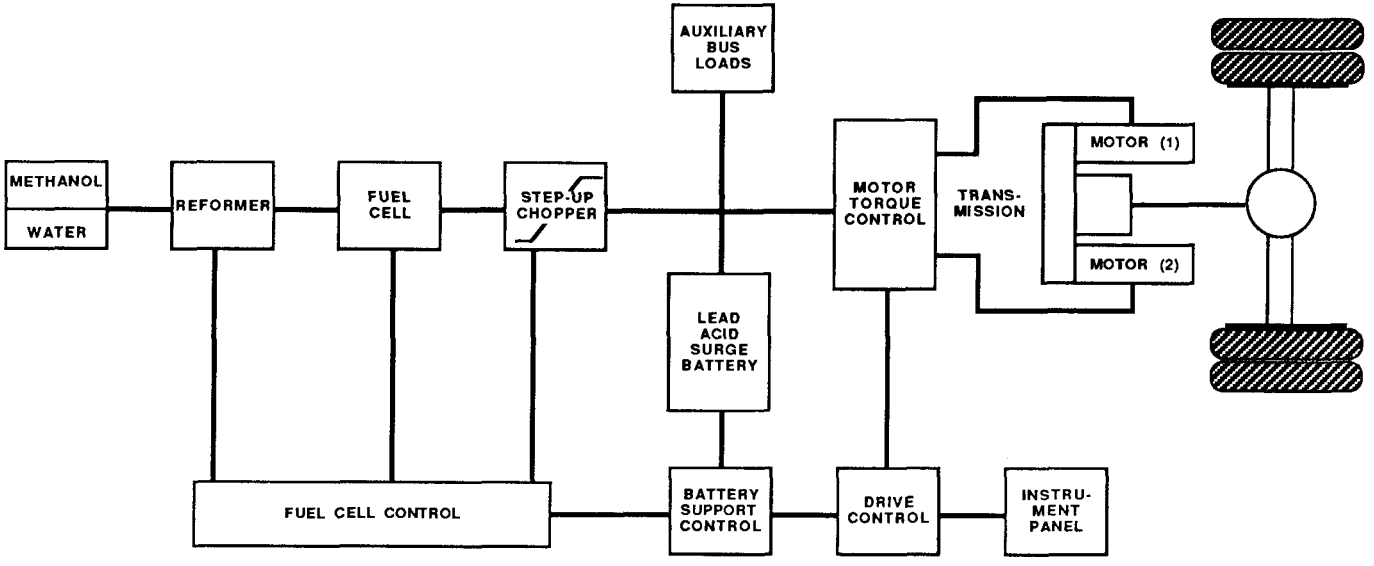
METHANOL
WATER
REFORMER
FUEL CELL
STEP-UP CHOPPER
AUXILIARY BUS LOADS
LEAD ACID SURGE BATTERY
MOTOR TORQUE CONTROL
TRANS-MISSION
MOTOR (1)
MOTOR (2)
FUEL CELL CONTROL
BATTERY SUPPORT CONTROL
DRIVE CONTROL
INSTRU-MENT PANEL

TRADE-OFF PARAMETERS

- **FUEL CELL**
  - 60 kW
  - 55 kW
  - 50 kW
  - 45 kW
- **BATTERY**
  - NICKEL/IRON NIF-170
  - SODIUM/SULPHUR
  - ZINC/BROMINE
  - LEAD-ACID SLI HP31E
  - LEAD ACID EV 3ET205
- **MOTOR PEAK POWER**
  - 120 kW, 153 HP
  - 100 kW, 127 HP
  - 80 kW, 102 HP
- **TRANSMISSION**
  - TWO-SPEED--1.5:1.0; 2.0:1.0
  - DIRECT DRIVE
- **REGENERATIVE BRAKING**
  - 500, 300, 100, 0 AMPS
- **PASSENGER PAYLOAD**
  - 10 PASSENGERS
  - 20 PASSENGERS
  - 30 PASSENGERS

LEVEL GRADE ACCELERATION PERFORMANCE
TWO-SPEED TRANSMISSION

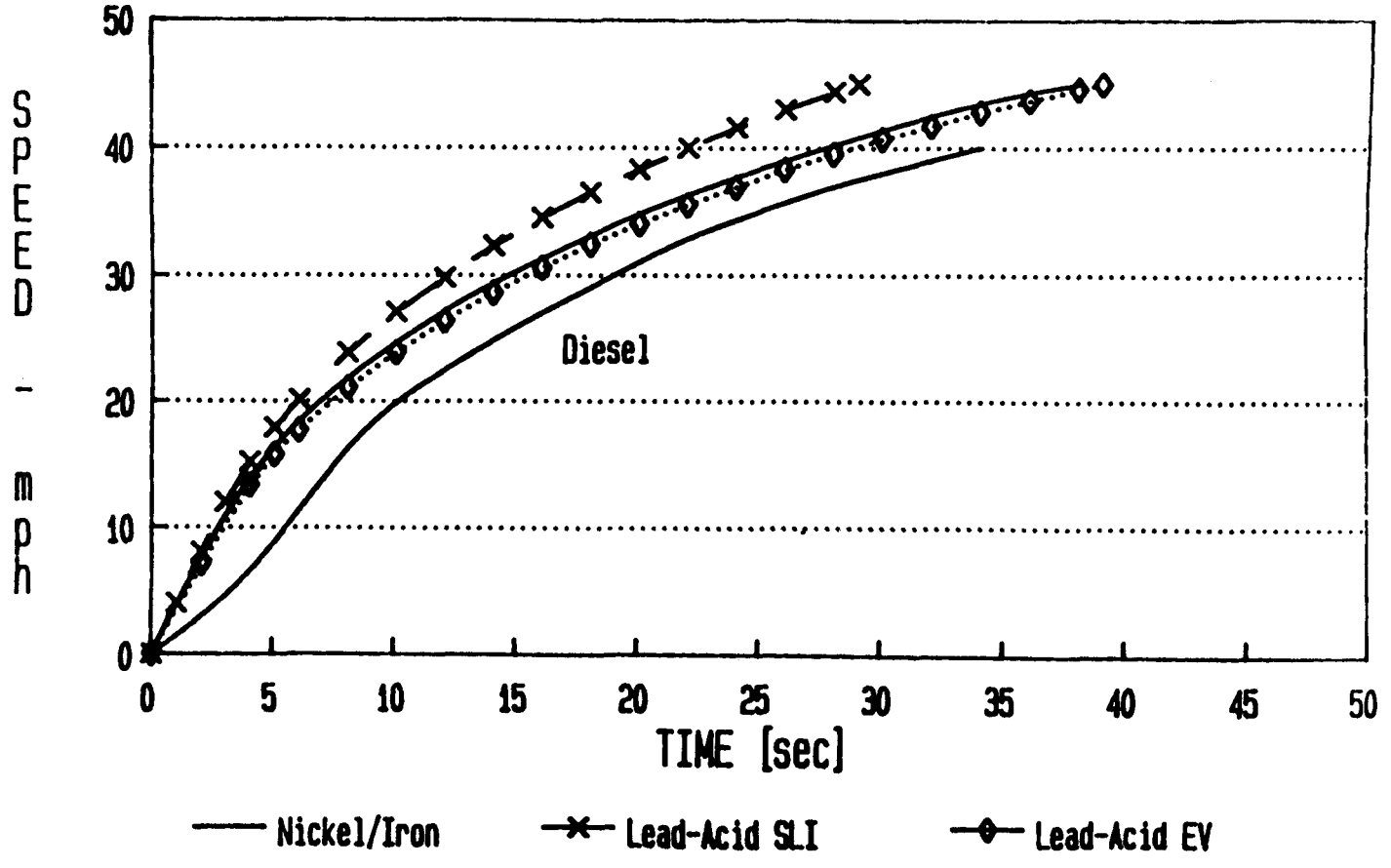

AN ASSESSMENT OF FUEL CELLS FOR TRANSPORTATION APPLICATIONS

Michael Krumpelt and Romesh Kumar
Argonne National Laboratory

INTRODUCTION

Experience over the past fifteen years has alerted the public to our extreme dependence on imported oil and our deteriorating air quality in urban areas. These concerns have led to the conclusion that we must eventually replace the petroleum fueled internal combustion (IC) engine used in transportation with a more efficient and cleaner power source.

Electric-powered vehicles have been suggested as a means of reducing reliance on petroleum in the transportation sector and of drastically reducing environmental emissions. However, for many applications user acceptance will only be forthcoming if such a vehicle has the same virtually unlimited range (through rapid replenishment of the fuel) as present automobiles.

Powering a vehicle with batteries alone cannot achieve an acceptable extended range through rapid refueling, but a fuel cell/battery hybrid system, or ultimately a stand-alone fuel cell, could have that capability. The fuel of choice for such vehicles would be either methanol derived from coal or ethanol obtained from biomass. Both can be converted efficiently and virtually free of emissions to electricity in fuel cell systems. Such vehicles would have the additional advantages of the smooth and quiet operation that is characteristic of trolleys and electric trains, compared with the noise and vibration of today's Diesel-powered urban buses. Such improvements in the "quality of service" would be welcomed by the public.

To eventually succeed in the market place, such fuel cell powered vehicles will have to compete with existing technology, mandating (1) a reasonably low capital cost, (2) an acceptably high power density, (3) a tolerably short startup time, (4) safety, and (5) a good dynamic response capability. The magnitude of that challenge becomes apparent by comparing the cost of a typical automobile engine of about $50/kW, with the cost of fuel cell systems. Although fuel cell systems for transportation have not been developed yet, the cost of stationary fuel cell power plants is currently about $2500/kW and is projected to decrease to about $750/kW when mass produced.

Power densities of fuel cell systems when packaged compactly range between 35 and 75 W/L,[1] compared to the power density of an IC 75W/L,[1] engine of about 100 W/L.

To start an IC engine takes only seconds, whereas fuel cell systems can take several minutes to over an hour before power can be drawn. This slow startup is largely due to the fact that continuous utility operation has been the development goal so far. Major improvements appear to be possible.

Safety and dynamic response capability of fuel cell systems are concerns that have not yet been addressed.

Five types of fuel cells are far enough developed to be considered for transportation applications: the alkaline fuel cell (AFC), phosphoric acid fuel cell (PAFC), proton exchange membrane (PEM) fuel cell, molten carbonate fuel cell (MCFC), and solid oxide fuel cell (SOFC).

AFC:

Alkaline fuel cells have been used routinely in space flight and are still used in the Space Shuttle. Alkaline cells were also used in the "Kordesch car" and in a tractor assembled by Allis Chalmers. They were chosen by Elenco in Europe for an experimental bus running on bottled hydrogen. The drawback of alkaline fuel cells is the need for carbon-dioxide-free fuel and oxidant. Being a strong base, the KOH electrolyte reacts with weak acids such as carbon dioxide to form potassium carbonate, consuming the electrolyte. Although it is possible to recirculate the electrolyte and remove the potassium carbonate, this is likely to be expensive and impractical in a vehicle operating on methanol.

PAFC:

Phosphoric acid fuel cells were developed primarily for the utility industry and are ready to be commercialized. The operating temperature of PAFCs is about 200°C. Three different designs using either water, air, or triethylene glycol coolant have been developed. The last is already being marketed in forklift trucks.

Phosphoric acid fuel cells cannot deliver electrical energy at room temperature but must be preheated to above 130°C before any current can be drawn. Further, the cells must always be maintained under partial load to prevent oxidation of the carbon support of the catalyst. The best use of PAFCs is, therefore, in steady operating modes.

As is the case with alkaline fuel cells, the PAFC requires hydrogen fuel, but it can tolerate CO_2 and small amounts of CO. It becomes possible, therefore, to make the hydrogen on board by steam reforming of methanol. PAFC stacks of 100-kW capacity have been built and operated.

PEM:

The proton exchange membrane technology was originally developed by the General Electric Company for space applications, using DuPont's Nafion membrane, but received new impetus in the past two years from the development of a new membrane by Dow Chemical. Dow's membrane has a lower electrical resistance than Nafion, which permits the current density to be increased. Given the high cost per unit area of fluorocarbon membranes, a high current density improves the economics.

PEM fuel cells operate at about 80°C, and have the advantage over PAFCs that some power can be delivered at ambient temperature, facilitating the startup. The negative consequence of having the relatively low operating temperature of 80°C is an extreme sensitivity to carbon monoxide poisoning of the electrocatalyst.

PEMs need to be operated under pressure (2-5 atm) to prevent dehydrations of the membrane. The technology is in an earlier stage of development than that of AFCs and PAFCs. Stacks of 20-kW capacity are currently being tested.

MCFC:

Molten carbonate fuel cells operate at a relatively high temperature of 650°C. This has the advantage that carbon monoxide is not an electrode poison and

can even be used as fuel. Moreover, methane and probably methanol can be fed directly to the MCFC if a reforming catalyst is added to the cells.

However, the MCFC cannot be thermally cycled. Once the electrolyte becomes solid, it is prone to develop cracks during reheating. The MCFC would have to be kept at its operating temperature over the life of the vehicle, unless the cyclability is improved. Prototype cells of 20-kW capacity have been built and operated.

SOFC:

Solid oxide fuel cells can operate on virtually any fuel without external fuel processing due to the very high operating temperature of 1000°C. Current densities are high, but the volume of the "tubular SOFC" is also high. The more recent cell designs, such as the monolithic and flat-plate configurations, can potentially provide high volumetric power densities. When contained in a thermal enclosure to maintain the system at operating temperature even at standby conditions, such SOFCs could be an option for transportation.

Although conceptually elegant, the new SOFC designs are still in an early stage of development, and stacks of only a few watts capacity have been made so far.

ASSESSMENT

To make a preliminary assessment of the five types of fuel cells for a transportation application relative to each other, we have evaluated four system designs: a liquid-cooled phosphoric acid (L-PAFC), an air-cooled phosphoric acid (A-PAFC), a proton exchange membrane (PEM), and a monolithic solid oxide (MSOFC). Schematic flow sheets and design considerations for these systems are described below. Alkaline fuel cells were not considered; in our view, the alkaline fuel cell is not compatible with alcohol or hydrocarbon fuels because the necessity of eliminating the CO_2 from the reformed anode gas makes the system complicated and expensive. Molten carbonate cells were not evaluated either, because we believe that they are unlikely to meet the shock and vibrational resistance required for a transportation application, and may not withstand the frequent thermal cycles.

All systems were assumed to produce 30 kWe net power and to operate on catalytically reformed methanol:

$$CH_3OH + H_2O \text{ ---- } CO_2 + 3H_2$$
$$\Delta H_{298} = +49.48 \text{ kJ/mol}$$

Figure 1 shows the schematic flow sheet for the L-PAFC system, which is similar to that proposed for the fuel cell/battery powered bus.[2] In this system the fuel, a mixture of CH_3OH and H_2O, is vaporized using part of the fuel cell stack waste heat via the circulating liquid coolant. The vaporized fuel is reformed to H_2 and CO_2 along with small amounts of CO and the excess H_2O. This gas mixture is fed to the fuel cell where 85% of the H_2 is oxidized electrochemically. The H_2 in the spent fuel is burned at the reformer to provide the energy for the endothermic fuel reform reaction. The liquid coolant circuit in the L-PAFC incorporates a radiator to dump the excess stack heat to the environment. Figure 1 also shows the temperatures of the various streams and the thermal energy transfers within the various components.

The A-PAFC system proposed for the fuel cell/battery bus[3] is shown schematically in Fig. 2. The CH_3OH/H_2O fuel mixture is vaporized and reformed

using the energy in the spent fuel. Typically 70% of the H_2 in the reformed fuel is oxidized electrochemically in the fuel cell stack; the remaining energy of the fuel is used at the reformer. The air-cooled system dumps all of the stack waste heat to the environment. Figure 2 also shows the various stream temperatures and thermal energy transfers.

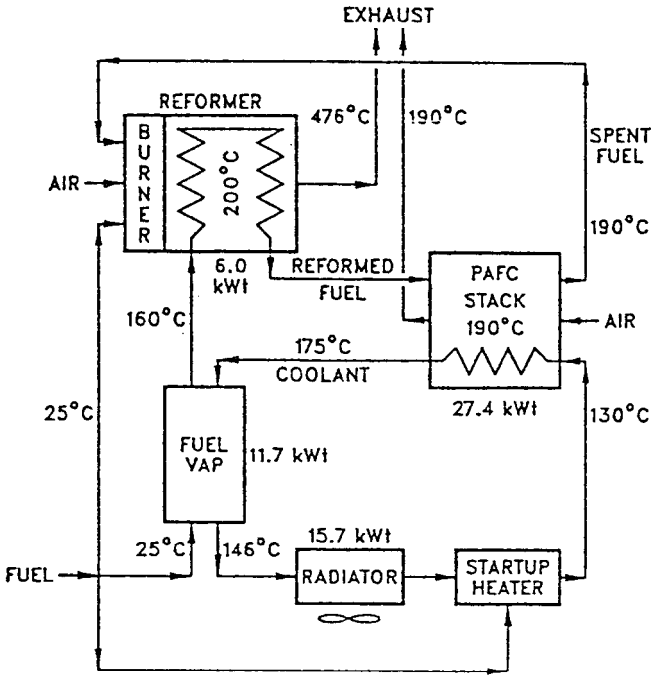

Figure 1. Flow sheet for the liquid-cooled phosphoric acid fuel cell system.

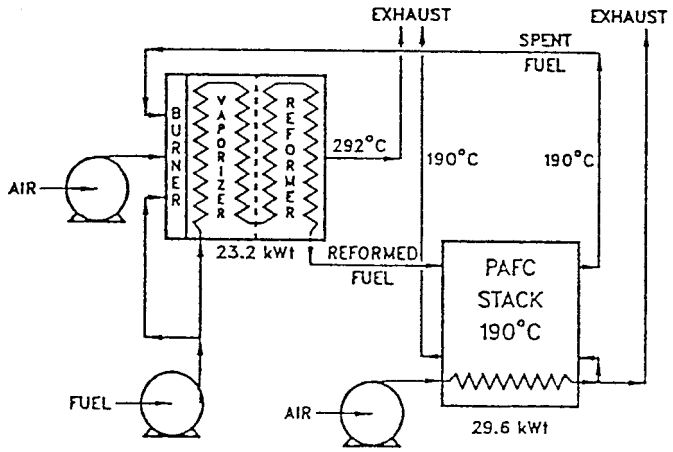

Figure 2. Flow sheet for the air-cooled phosphoric acid fuel cell system.

The schematic flow sheet for a PEM system is shown in Fig. 3.

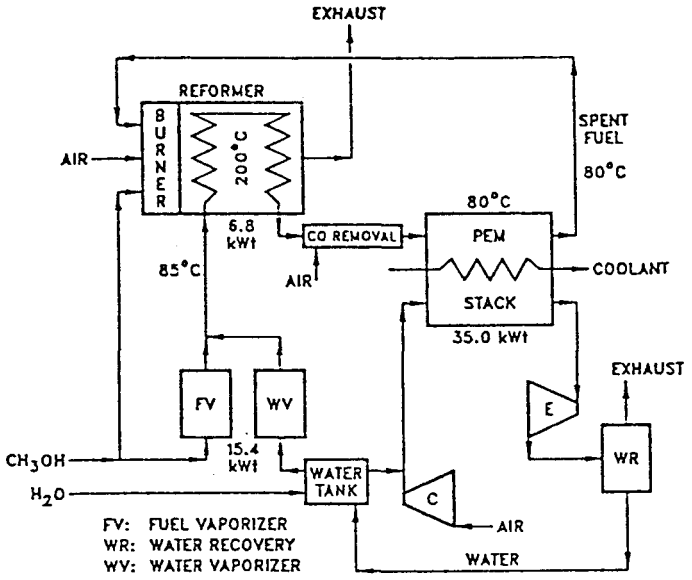

Figure 3. Flow sheet for the proton exchange membrane fuel cell system.

This system is more complex than the PAFC systems because the PEM cell is operated at 2 to 3 atm, and water must be added to and recovered from the fuel and oxidant streams. The CH_3OH and H_2O are vaporized and reformed at 2 atm, CO is removed by selective oxidation, and the reformed fuel gas is fed to the PEM anode. The spent fuel is used at the reformer to provide the enthalpy of reformation. The oxidant air is compressed to 3 atm, humidified, and fed to the PEM cathode; an expander on the exhaust air recovers part of the compression energy.

The MSOFC system represented in Fig. 4 assumes internal reforming of the

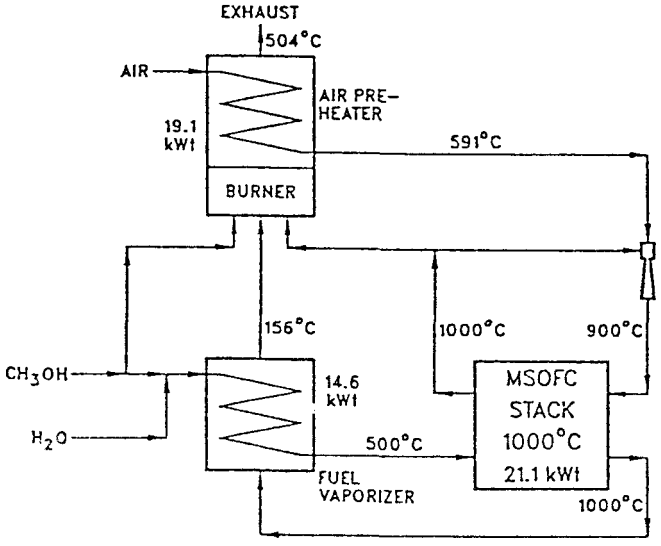

Figure 4. Flow sheet for the monolithic solid oxide fuel cell system.

methanol fuel within the fuel cell stack. Fuel can be vaporized using only the sensible heat in the spent fuel. Because of the high temperature of operation of the fuel cell, however, the air fed to the fuel cell must be preheated, which is accomplished by burning the spent fuel. In addition, to limit thermal stresses in the ceramic fuel cell stack, part of the exhaust air is recirculated through the MSOFC stack. The hot exhaust air provides the oxygen for combustion of the spent fuel.

The thermodynamic efficiency of the four systems was estimated using a spreadsheet and the design parameters shown in Table 1. The H_2O/CH_3OH ratios

Table 1. Design Parameters for the Fuel Cell Systems

	Fuel Cell System			
Parameter	L-PAFC	A-PAFC	PEM	MSOFC
Fuel H_2O/CH_3OH	1.3	1.3	2.22	1.0
Fuel Utilization, U_f	0.85	0.70	0.85	0.85
Oxidant Utilization	0.50	0.50	0.50	0.50
Cell Voltage, V	0.60	0.60	0.63	0.63
Pumping Losses, % of Gross Power	3.0	10.0	15.0	10.0

differ for the four systems because the fuel reformer for the phosphoric acid fuel cell systems (and for the PEM system) needs water in excess of the theoretical one mole per mole of methanol to ensure complete reforming of the fuel and to suppress the formation of CO. For the PEM, in addition to the water required for the reform reaction, the anode gas needs to be humidified to near saturation at the stack temperature. In the MSOFC, on the other hand, the electrolyte transfers oxygen ions from the cathode to the anode, thus introducing water into the anode gas as a result of the cell reaction. Therefore, the fuel itself does not need to contain as much water; indeed, it is possible that this system could operate with essentially no water in the input fuel.

The electrochemical fuel utilization (U_f) in the A-PAFC is lower than for the other systems since the spent fuel needs to contain enough energy to vaporize and reform the fuel. The same is true for the PEM as well; however, the efficiency could be slightly improved by operating at the higher electrochemical fuel conversion level, making up for the required thermal energy by burning methanol directly at the spent fuel combustor. Pumping losses are high in the PEM because this system operates at 2 to 3 atm and because the temperature-difference driving force for rejecting the waste heat to the environment is small. The A-PAFC and the MSOFC are likely to have comparable pumping losses because they are both air cooled systems. The L-PAFC is likely to have the lowest pumping losses among these four fuel cell systems.

The calculated base system parameters are shown in Table 2 for each system at steady state under full load. The net fuel conversion efficiencies based on the higher heating value of input methanol range from 29.7% for the PEM system to 39.4% for the L-PAFC system. The A-PAFC and the PEM system combine the fuel vaporizer and reformer into one component; therefore, the vaporizing and reforming duty breakdown is somewhat arbitrary. The MSOFC system does not use an external reformer; instead, an air preheater is needed for this system.

Table 2. Calculated Efficiencies and Component Duties

	Fuel Cell System			
Parameter	L-PAFC	A-PAFC	PEM	MSOFC
Net Efficiency, %	39.4	30.1	29.7	38.4
Vaporizer, kWt	11.69	12.98	15.39	14.58
Reformer, kWt	6.01	10.18	6.79	—
Air Preheater, kWt	—	—	—	19.10
Radiator, kWt	15.75	—	35.04	—
Losses, kWt	0.93	3.33	5.29	3.33

The L-PAFC and the PEM both need radiators to discard the waste heat, while the A-PAFC and the MSOFC reject the waste heat as hot air or combustion exhaust. The latter two systems may also require radiators if water recovery from the exhaust gases is desired to obtain water for blending with methanol to produce the initial fuel. It may be observed that in the PEM system, while the stack waste heat is comparable to that in the other systems, the DT available for cooling is rather small (only about 40°C); it may be necessary, therefore, to use heat pipes in the PEM stack to dissipate the waste heat with a reasonable-sized radiator.

The system cost is comprised of the cost of the fuel cell stack and the other components. We have not conducted a detailed cost analysis. In general, however, the more complex a system, the higher its anticipated cost. Other factors such as materials and fabrication techniques, operating temperature, enclosure requirements, and process control requirements also affect system cost. A very qualitative assessment of the four flow sheets shown in Figs. 1-4 indicates that the PEM is the most complicated of these four types of fuel cell systems. The complexity arises from the high pressure operation, the fuel and oxidant water management requirement, the low ΔT for stack heat rejection, and the need for CO removal from anode gas. The least complicated of the four is the A-PAFC. The L-PAFC and the MSOFC are comparable in complexity. Thus the anticipated system costs are likely to be the lowest for the A-PAFC and highest for the PEM, with L-PAFC and the MSOFC falling in-between the other two.

Relative to IC engines, a 40% efficient power source may conserve 2000-3000 gallons of gasoline over a 100 000 mile life of a passenger car. To be economically viable, the fuel cell system must, therefore, cost no more than $4000-5000. Less efficient systems must be less expensive. In buses, the fuel cost savings are much more substantial because the total number of miles driven is orders of magnitude higher. Fuel cell system costs of $30-40K become affordable.

Partial load operation of a fuel cell implies a lower current density and higher cell voltage than under full load conditions. As a result, the efficiency increases. Transient load operation, however, is more difficult to predict in the absence of any test data. The system designs presently being developed envisage the use of a "load-leveling" battery to isolate the fuel cell sub-system from load variations. Transient load operation still needs to be demonstrated with stand-alone fuel cell systems. It is expected, however, that fuel cell systems with external fuel reformers (L-PAFC, A-PAFC, and PEM) will have a relatively slow response to load changes due to kinetic limitations within the reformer. The high

temperature MSOFC with internal fuel reforming is expected to be much more responsive to load changes. On the other hand, it may be possible to improve the dynamic response of the systems with external reformers by engineering modifications, such as the inclusion of surge tanks for the reformed fuel.

Startup of fuel cell systems involves getting the reformer and the fuel cell to their respective operating temperatures. Cold startup could require several minutes for the low temperature PEM to several tens of minutes for the higher temperature PAFC and MSOFC systems. It may also be possible, particularly for municipal transportation and fleet applications, to keep the systems "idling" in a standby mode at all times, in which case the startup time becomes insignificant. The power loss during standby is likely to be 1-5% of the system's nominal power rating, presumably provided by consumption of the fuel.

CONCLUSIONS

Based on the above considerations, although the L-PAFC and the A-PAFC are presently being considered for the bus applications, the PEM and MSOFC systems may be viewed as having the potential for broader application. All four systems offer the potential of fuel efficiencies much greater than those of internal combustion engines and are expected to have much lower environmental emissions. They will be quiet, smoothly accelerating, and a pleasure to drive. In the large metropolitan areas of the country where air quality has been deteriorating in recent years, such fuel cell powered vehicles may indeed become a reality in the future.

Acknowledgment:

Argonne National Laboratory is operated by the University of Chicago for the U. S. Department of Energy (DOE) under contract W-31-109-Eng-38. This work was supported by DOE's Office of Transportation Systems.

References

1. R. Kumar et al., "Fuel Cells for Vehicle Propulsion", Ext. Abstracts 1988 Fuel Cell Seminar, Long Beach, Ca.

2. R. Kevala, "Development of a Liquid-Cooled Phosphoric Acid Fuel Cell Powered Bus System", ibid.

3. Chang Chi, D. Glenn, "Air-cooled PAFC and Ni-Cd batteries - A marriage that works" Proceedings of the 23rd IECEC, Denver, Co. 1988.

PEM FUEL CELL RESEARCH PROGRAM

Ross A. Lemons
Los Alamos National Laboratory

The Mechanical and Electronic Engineering Division at Los Alamos National Laboratory in conjunction with industrial and university subcontractors and collaborators is conducting an integrated research and exploratory development program on fuel cells for transportation applications. This program, sponsored by the Department of Energy (DOE) Office of Energy Storage and Distribution, has the objective of bringing fuel cell technology from its present status to a proof-of-concept level where it becomes a practical alternative to internal-combustion engines for vehicular propulsion.

The need for and interest in an alternative transportation technology are rapidly increasing. Both the growing national petroleum dependency and the need to reduce air pollution and carbon dioxide production are motivating this interest. Proton-exchange-membrane (PEM) fuel cells, because of their high efficiency and low operating temperature, can contribute significantly to the solution of these problems. However, to make this contribution the fuel cell must be competitive with internal-combustion engines in both cost and performance.

This is a difficult challenge. The requirements for transportation applications are extremely stringent. The fuel cell must be sufficiently inexpensive on an adjusted life-cycle cost basis to appeal to the consumer. It must have sufficient power density to meet the performance specifications of the vehicle and fit within the available engine space. It must operate efficiently on reformed methanol and air, and it must tolerate impurities in the fuel, such as carbon monoxide. It must be able to start rapidly and to respond quickly to changes in power demand. And it must be safe and reliable with comparable or better lifetime than an internal-combustion engine.

The specific goals of the program are (1) to reduce the catalyst requirements to 0.2 g Pt/kW, (2) to increase the power density to 0.75 W/cm^2 at 1 atm H_2 and 1.7 atm air, (3) to achieve this performance with 85% H_2 utilization and 33% air utilization, (4) to sustain performance with 500 ppm CO in the fuel stream, and (5) to achieve >7500-h life under load cycle testing.

Over the past two years we have made major strides toward achieving these goals. By thinning the catalyst layer on the electrode and impregnating it with a protonically conducting polymer, the Pt catalyst requirements have been reduced to <0.25 mg/cm^2 on the cathode. Using experimental membranes, the power density has been increased to 0.9 W/cm^2 on H_2 (3 atm) and air (5 atm) at a current density of 2.0 A/cm^2 with low catalyst loading electrodes. Hydrogen utilization >80% has been demonstrated with no degradation in performance. The severe fall in cell voltage caused by 100 ppm of CO in the fuel stream has been completely eliminated by injecting 2% oxygen into the fuel stream.

Moreover, recent experiments give us substantial confidence that the ambitious goals of the program can be met. For example, Rutherford backscattering and electron microprobe data indicate that only the outer 10% to 20% of the catalyst is being used effectively. This offers the potential for a substantial further reduction in catalyst loading without adversely affecting performance. High-frequency resistance data indicate that the overall cell resistance is substantially greater than the intrinsic resistance of the components. If this extra resistance can be eliminated, much higher power densities can be achieved. The transport of water within the membrane and the electrodes is much better understood, and this understanding should facilitate sustaining performance over the full dynamic range required for transportation applications. Operational data as a function of pressure and flow have given clues to the design of electrodes with good performance at lower pressures. And the life data collected so far indicate excellent stability for this type of fuel cell.

Increasingly the challenges will be in the system integration and development of manufacturing methods. Recently a new contract was awarded to International Fuel Cells Corporation to investigate designs and manufacturing methods for low-cost fabrication of high-efficiency, high-power-density, PEM fuel cell power plants. This is a first step toward realizing an economically manufacturable PEM fuel cell technology.

In summary, PEM fuel cells offer an attractive alternative power source for transportation applications. They provide much higher efficiency and lower pollution than internal-combustion engines. Recent achievements in the program have overcome many of the technical obstacles to realizing this potential, and there are strong indications that the remaining challenges can also be overcome.

LOS ALAMOS NATIONAL LABORATORY

FUEL CELLS FOR TRANSPORTATION PROGRAM

SPONSOR: DOE/OFFICE OF ENERGY STORAGE AND DISTRIBUTION

MOTIVATIONS

- TRANSPORTATION ACCOUNTS FOR OVER 60% OF U.S. PETROLEUM USAGE, AN AMOUNT COMPARABLE TO TOTAL DOMESTIC PRODUCTION.

- FUEL CELLS PROVIDE APPROXIMATELY TWICE THE ENERGY EFFICIENCY OF INTERNAL COMBUSTION ENGINES, NEGLIGIBLE POLLUTION, AND POTENTIALLY COMPARABLE RANGE AND PERFORMANCE.

- METHANOL, WHICH IS EASILY REFORMED FOR FUEL CELL USAGE, IS EXPECTED TO REPLACE PETROLEUM AS THE PRIMARY LIQUID FUEL.

Fig. 1. Primary motivations for the Los Alamos Fuel Cells for Transportation program.

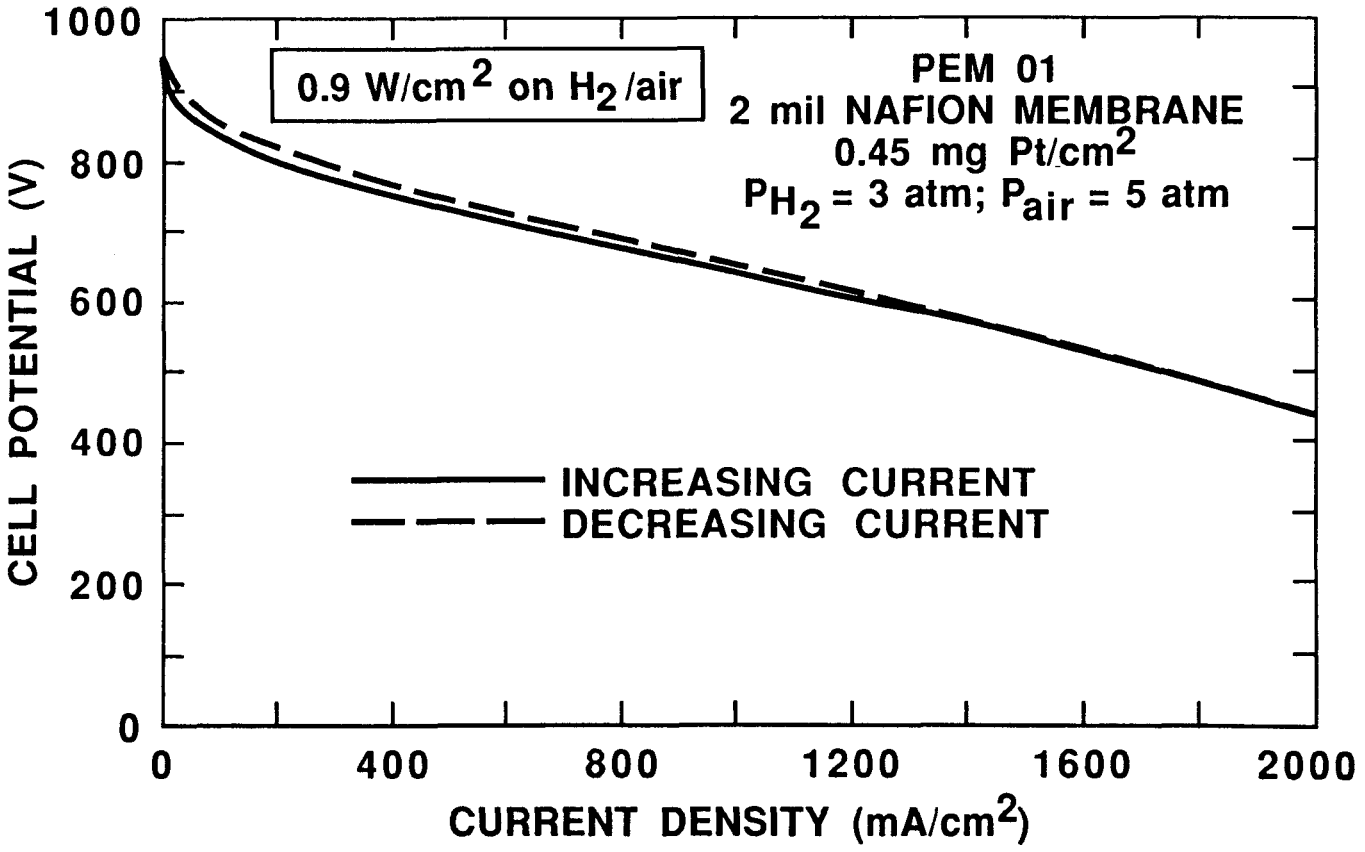

Fig. 2. Current-voltage performance of a proton-exchange-membrane fuel cell operating on H_2 and air at 80° C with 0.45 mg Pt/cm^2, showing that current densities in excess of 2 A/cm^2 can be achieved with low catalyst loading electrodes.

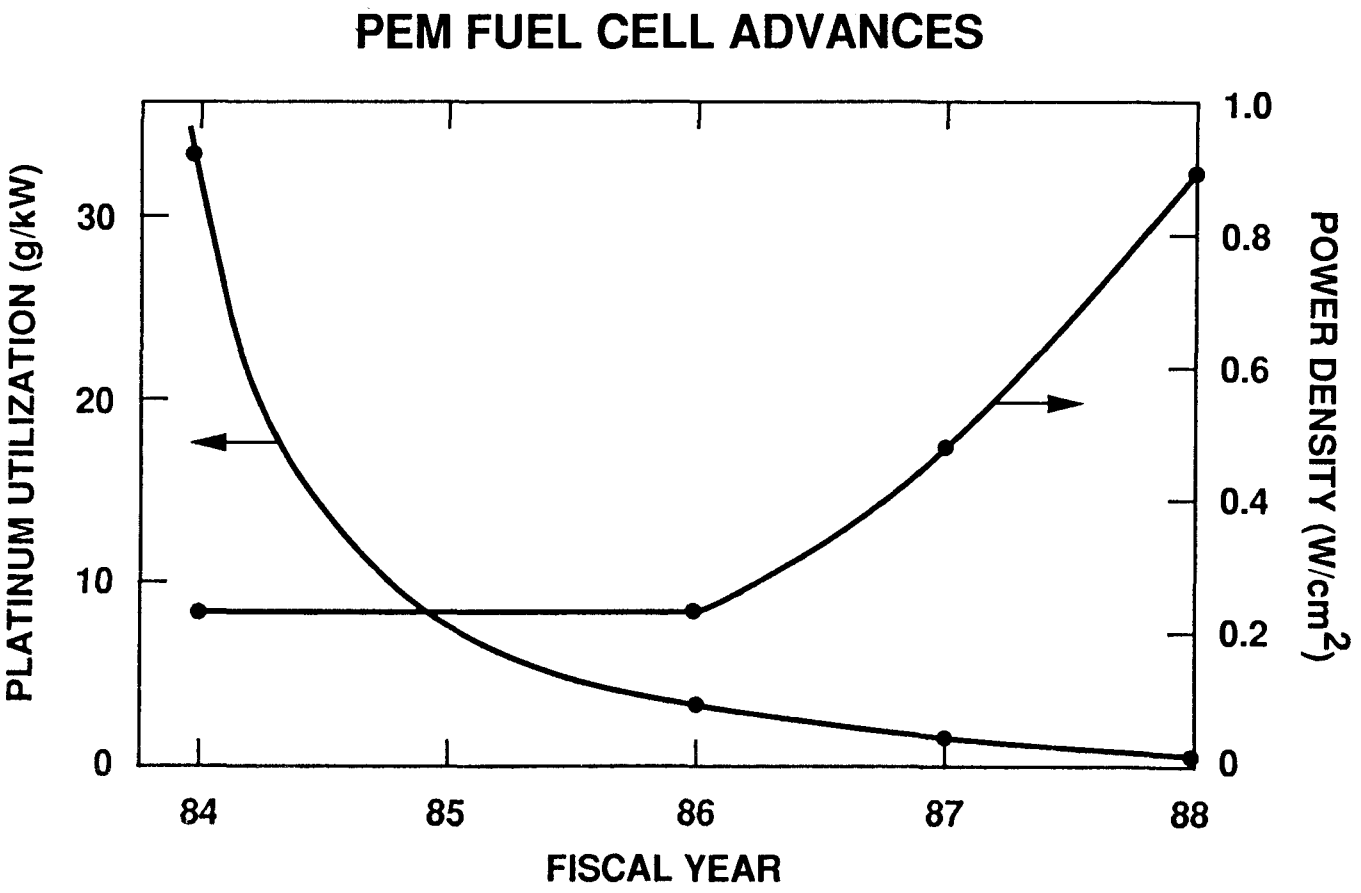

Fig. 3. These curves show that a 30-fold reduction in Pt catalyst requirements and a fourfold increase in power density have been achieved in the program over the last few years.

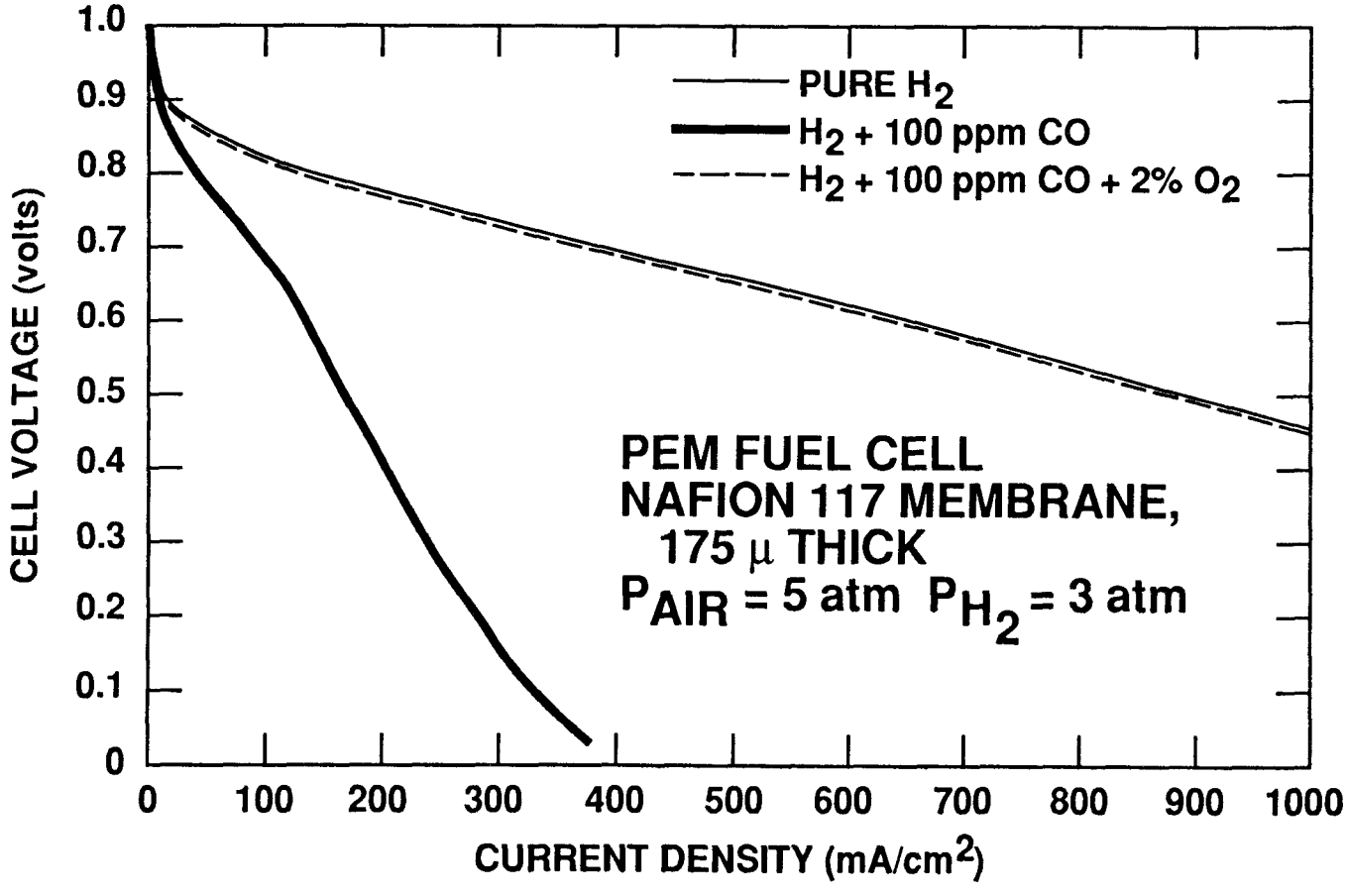

Fig. 4. The once severe problem of CO poisoning has been overcome by a combination of selective oxidation of the reformate and injection of small amounts of oxygen or air into the fuel cell anode. This curve shows that the poisoning effects of 100 ppm CO can be completely removed with a 2% oxygen addition to the anode.

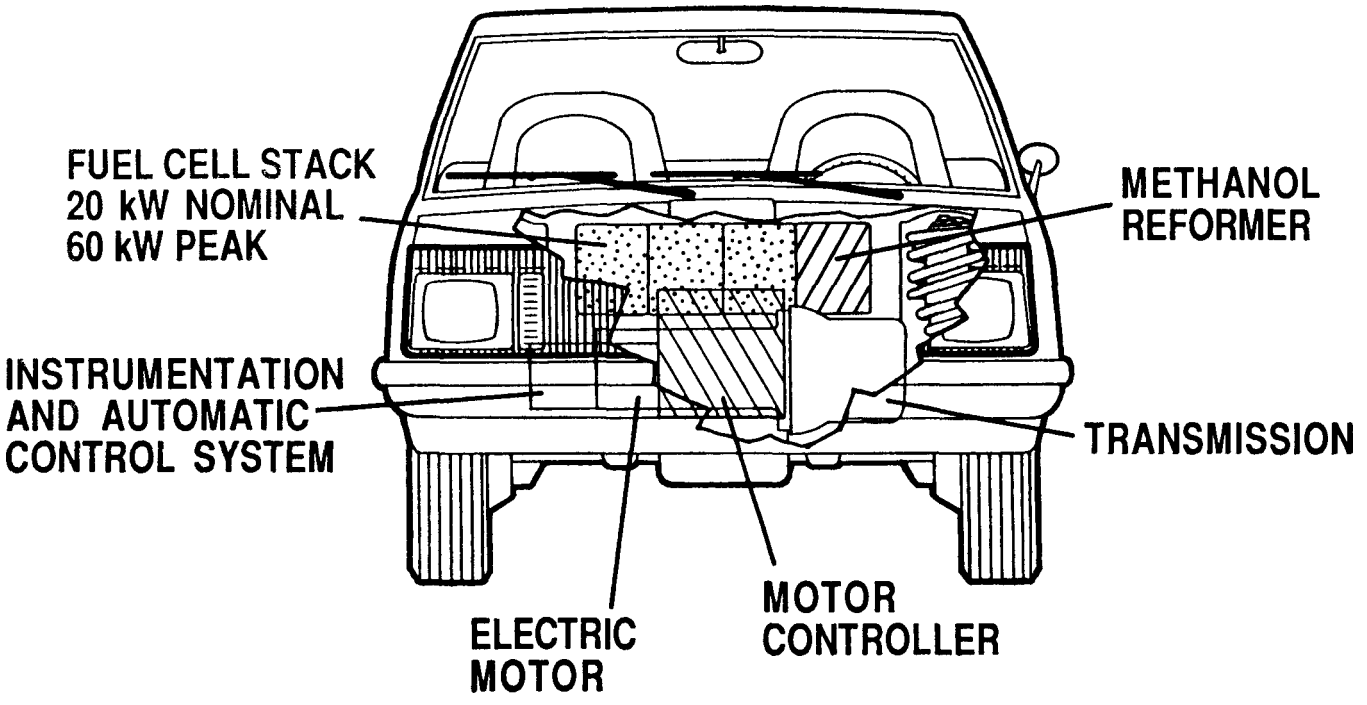

Fig. 5. Schematic diagram of a fuel cell power plant in a passenger car.

FUEL CELL PARAMETERS FOR A PASSENGER CAR

OPERATING POINTS

PEAK	0.50 V	1.8 A/cm^2	0.9 W/cm^2
CONTINUOUS	0.75 V	0.4 A/cm^2	0.3 W/cm^2

STACK SIZE

ACTIVE AREA	500 cm^2	DIAMETER	25 cm
CROSS SECTION	1000 cm^2	DIAMETER	35 cm
CELL THICKNESS	0.5 cm	--	
NUMBER OF CELLS	133	--	
STACK LENGTH	66 cm	TOTAL	75 cm
STACK VOLTAGE (NOM)	100 V	--	
STACK VOLUME	0.072 m^3	--	
STACK DENSITY	1.0 g/cm^3	--	
STACK WEIGHT	75 kg	--	

Fig. 6. Estimate of the volume and weight for a fuel cell stack large enough to power a compact passenger car, based on the performance data shown in Fig. 2.

PEM FUEL CELLS MATERIALS AND PROCESSES

Shimshon Gottesfeld
Electronics Research Group
Los Alamos National Laboratory

A central challenge of the "fuel cells for transportation" project at the Electronics Research Group, LANL, has been to cut down the Pt loading in PEM fuel cells while maximizing cell performance. The lowering of the Pt loading is an essential prerequisite for terrestrial transportation applications, but it has to be achieved without compromising the power and energy densities of the PEM fuel cell. The approach adopted to achieve these goals is based on the development of a new type of membrane-electrode assembly, fabricated by hot pressing an ionomer-impregnated gas-diffusion-electrode onto an ionomeric membrane. The impregnated gas-diffusion-electrode (made by Prototech) and the ionomeric membrane (usually Du-Pont's Nafion®) have been central components of our PEM fuel cells and, thus, the central targets of investigation. An important recent finding from our work on the impregnated gas-diffusion-electrode has been that only the very thin outer layer of the impregnated catalyst (a few microns) is utilized, and, therefore, the thickness of the catalyst layer can be lowered further without loss of performance. "Planarization" of the carbon cloth electrode with carbon powder before the application of the catalyst layer resulted in a successful reduction of the catalyst layer thickness down to 25 microns without loss of performance. This means that a loading of only 0.22 mg Pt /cm^2 on each electrode can provide the performance demonstrated in Fig. 1, which is indistinguishable from that obtained with twice that loading.

In recent tests of experimental membranes we have examined effects of membrane thickness and of the equivalent weight of the ionomer. Thinner membranes provide improvements in cell performance beyond the linear effects of ohmic losses. In cells with thinner membranes, the onset of the excessive (superlinear) loss of cell voltage is shifted to higher current densities (Fig. 2). This behavior is believed to be caused by improved water transport toward the anode in cells with thinner membranes, which prevents excessive dehydration near and within the anode at high current densities. We have recently tested a new ionomeric membrane, which is a Nafion-like material (copolymer of perfluorovinyl ether and tetrafluoroethylene), with an equivalent weight lower than that of the Nafion 117 - EW 900 instead of 1100. The beneficial effects of the lowered EW (plus, possibly, some other membrane manufacturing parameters) can be clearly seen in Fig. 3. The lower EW means a higher state of membrane hydration, which result in better conductivities and lower sensitivity to dehydration at high current densities.

Water is perhaps the most important material in the PEM fuel cell, and water management in this cell at high and varying current densities is probably the most difficult problem. However, recent testing has demonstrated that humidification conditions have been defined to allow continuous cell operation for hundreds of hours at 300 mA/cm^2 without dehydration failures. To further optimize water management for higher currents and varying loads, we have measured the water drag under relevant conditions, i.e., for PEM cells without any free electrolyte. The results are summarized in Fig. 4. NMR measurements are under way aiming at a comprehensive evaluation of the water profile in the membrane in an operating cell.

Out of the techniques employed to learn about the state of the materials and about processes in the PEM cell, impedance spectroscopy has proved to be a powerful diagnostic tool. Distinction between poor cell performance brought about by dehy-

dration of the impregnation additive or, conversely, by excess water in the catalyst layer (electrode flooding) is quite difficult to make based only on steady-state polarization curves. The impedance spectrum has special features that help distinguish between these opposite cases. Examples of impedance spectra for operating PEM cells will be presented.

Materials considered for the current collector plates in PEM cells have included graphites of various densities as well as appropriate metallic plates. Results of tests with a cell based on stainless steal current collector plates will be described. No significant corrosion problems have been identified, but the "cathode flooding" problems were quite severe, apparently because of the absence of a cathode porous backing.

The final subject of this presentation will be a method for treating CO anode poisoning at the temperature of a PEM fuel cell by in situ oxygen injection. Recent results have demonstrated the high reproducibility of this approach, which never failed to give satisfactory results in any of the PEM cells tested. The practicality of the approach will be discussed.

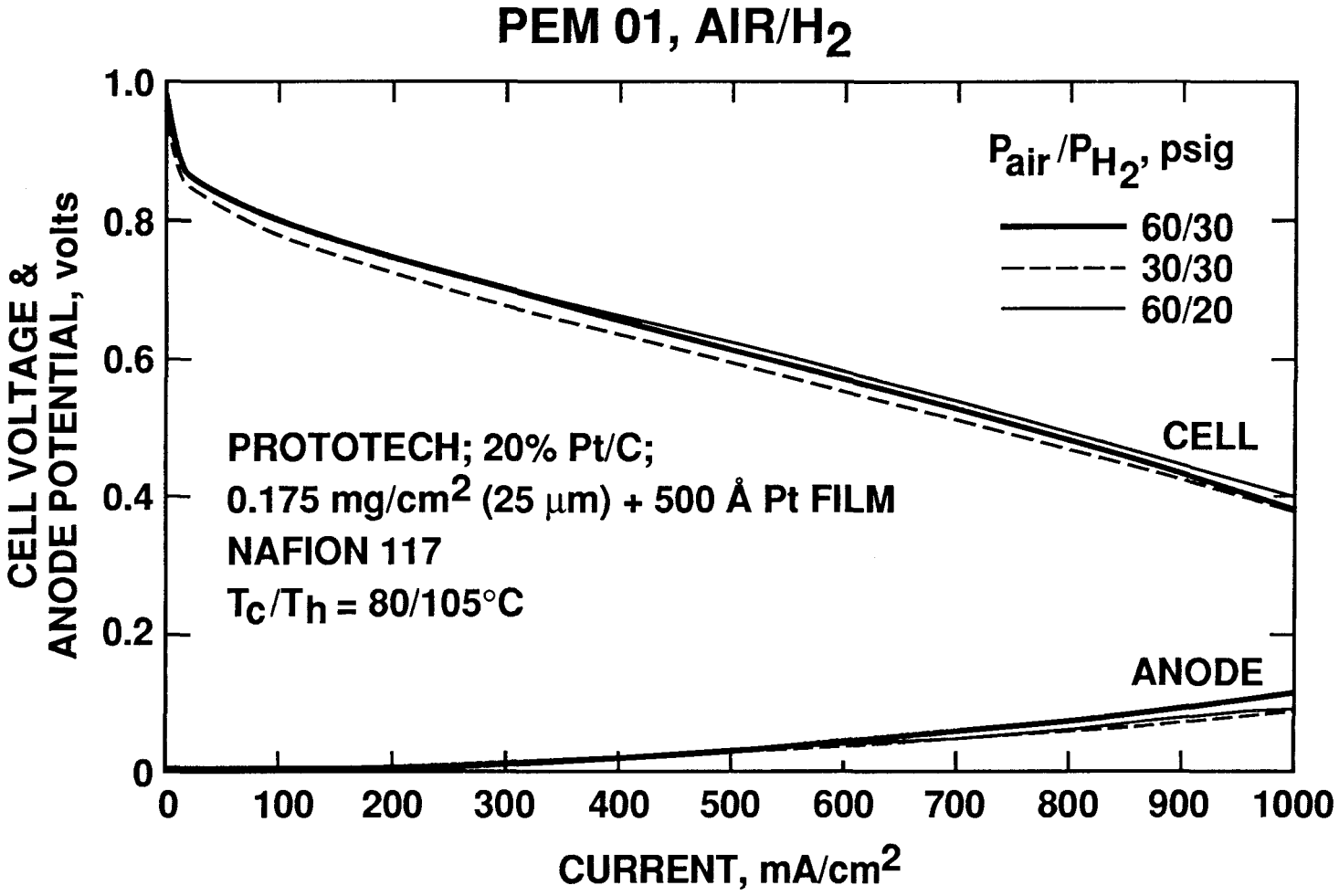

Fig. 1. Polarization curve for a PEM single cell based on a 117 Nafion membrane and modified Prototech electrodes with only 0.22 mg of Pt/cm^2 on each electrode.

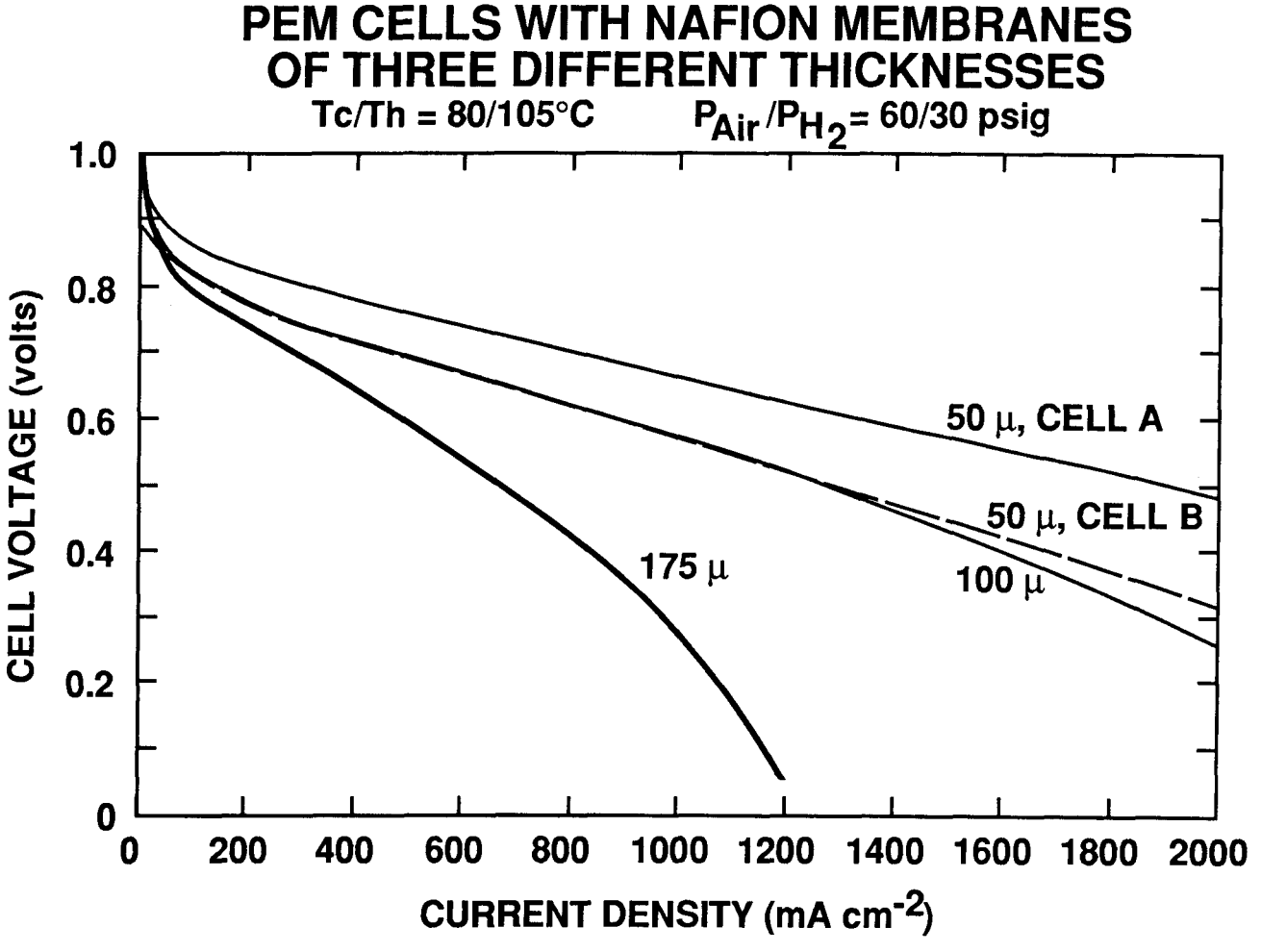

Fig. 2. Effect of membrane thickness on the polarization curve of a PEM single cell.

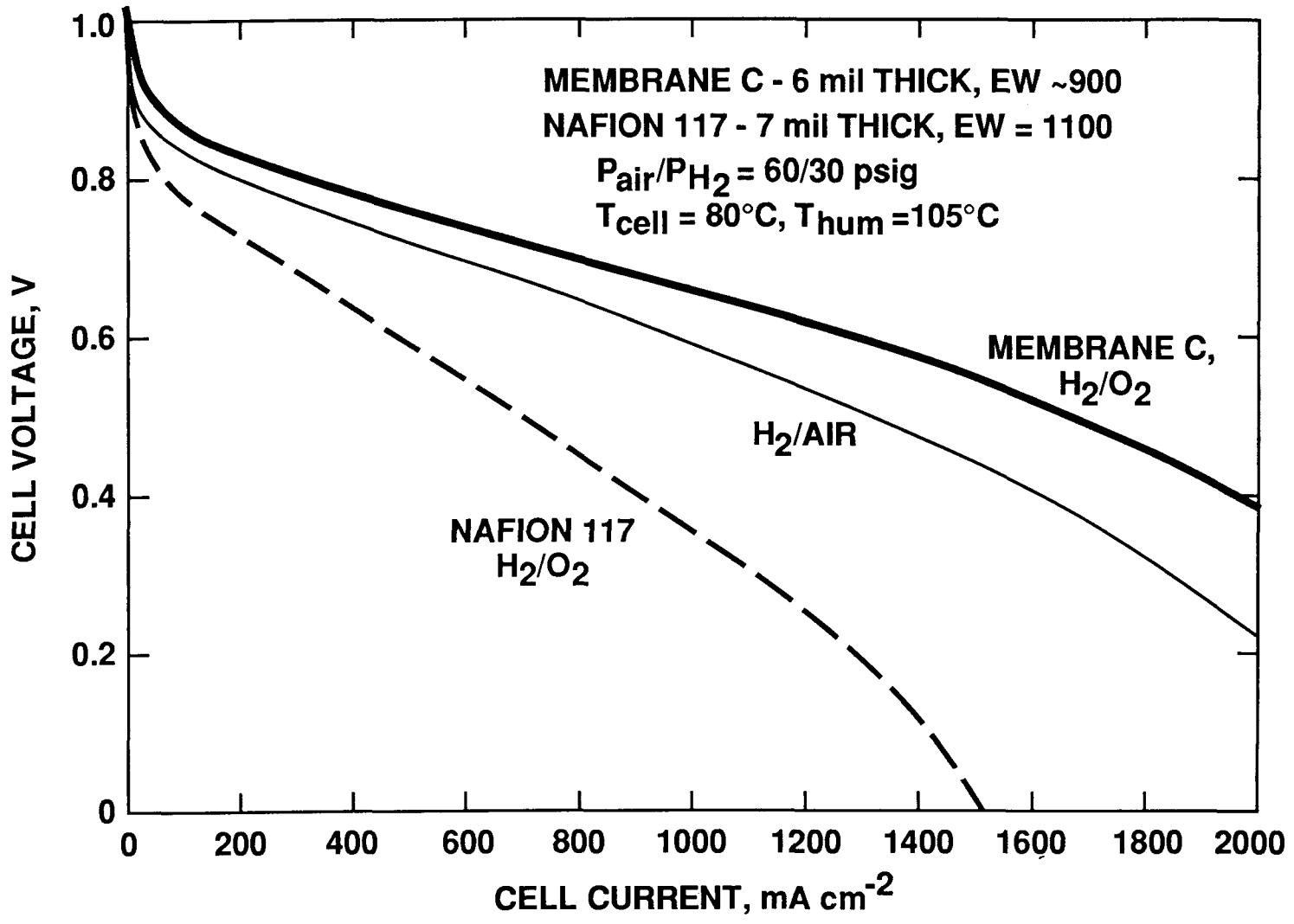

Fig. 3. Polarization curves for a PEM cell with a perfluorosulfonic acid membrane of EW of 900, compared with a polarization curve for a PEM cell with a 117 Nafion membrane.

WATER "DRAG" IN PEM CELL UNDER DIFFERENT EXPERIMENTAL CONDITIONS

CELL CONFIGURATION	LIQUID OF IMMERSION	T, °C	MAXIMUM CURRENT DENSITY mA/cm^2	APPARENT DRAG H_2O/H^+
Pd(H)/Nafion/Pd(H)	H_2O	25°	5	2.5 ± 0.5
Pd(H)/Nafion/Pd(H)	0.1M H_2SO_4	25°	100	2.5 ± 0.5
Pd(H)/Nafion/Pd(H)	1M H_2SO_4	25°	150	1.1 ± 0.3
Pd(H)/Nafion/Pd(H)	4M H_2SO_4	25°	50	0.5 ± 0.3
Pd(H)/Nafion/Pt/C, H_2(g)	H_2O on Pd(H) side	25°	5	~ 0.5
Pd(H)/Nafion/Pt/C, H_2(g)	H_2O on Pd(H) side	50°	5	~ 0.5

Fig. 4. Apparent water drag through Nafion membranes in PEM cells with no free electrolyte.

ECONOMIC EVALUATION OF PEM FUEL CELLS

J. R. Huff
Los Alamos National Laboratory

Estimates have been made for the current and expected (1995-2000) costs of proton-exchange-membrane (PEM) fuel cell stacks. These estimates are limited to materials costs because the lack of an industrial base limits the establishment of reasonable manufacturing costs estimates.

Eight different cases of PEM fuel cell performance were examined and the effect of performance on cost is clearly demonstrated. The performance data used were taken from recent publications by Ballard Technologies Corporation. A brief description of each case is given below, followed by discussion and tabulation of characteristics, performance, and costs.

Case 1 - A contemporary Nafion operating point on hydrogen/oxygen.
Case 2 - A contemporary Nafion operating point on reformate/air.
Case 3 - Nominal performance with a Dow experimental membrane using hydrogen/oxygen.
Case 4 - High performance with a Dow experimental membrane using hydrogen/oxygen.
Case 5 - Projected continuous performance for a Dow experimental membrane using reformate/air in the present configuration.
Case 6 - Projected maximum performance for a Dow experimental membrane using reformate/air in the present configuration.
Case 7 - Projection from Case 3 using reformate/air with reduced catalyst loading and improvements in reactant distribution and cell resistance.
Case 8 - Projection from Case 4 using reformate/air with reduced catalyst loading and improvements in reactant distribution and cell resistance.

Characteristics for each of these cases are given in Table 1. In cases 7 and 8, platinum loading is maintained at the level of 2 mg/cm²/cell. Lower levels than this are possible, but this level may be required for adequate lifetime of the hardware. In the Ballard tests, steam-reformed methanol (reformate) was simulated with a gas containing 0.3% CO, 25% CO_2, and the balance H_2 (dry basis). The gas was "conditioned" to reduce CO content to 2 to 10 ppm before being passed into the fuel cell.

In calculating materials costs, platinum cost was taken as $16/g. The membrane cost was assumed to be fixed at $500/m² for both Nafion and the Dow experimental material. In all cases, materials costs were assumed to benefit from high-quantity purchases.

The parameters in Table 2 were derived by fixing the power rating and the cell active area and using the performance levels given in Table 1. The power levels indicated are rated-power, not peak-power capabilities. The costs derived illustrate that high power density is a necessary goal to cut system costs. Although not shown, this goal is also necessary to reach appropriate volumes for some applications. The values suggest that membrane-electrode assemblies could reach a materials cost minimum approaching $40/kW. As would be expected (see Case 1), power plant size does not affect the $/kW cost of the catalyst and membrane.

*Nafion is a Registered Trademark of the E.I. du Pont de Nemours & Co., Inc., Wilmington, DE

To complete the stack materials costs, it was assumed that the other repeating stack components would be the same or very similar to those already being used. Thus, these remaining elements are the carbon-based separators, anode supports, and electrically conductive wetproofing for the cathode. It was also assumed that there has not been any significant change in the cost of these items since 1981, when a feasibility study was performed for Los Alamos by the General Electric Company (GE). Therefore, the GE costs of $\$5.70/ft^2$ for the carbon/Kynar molded separator plates, $\$5.00/ft^2$ for the carbon paper anode support, and $\$2.86/ft^2$ for the electrically conductive wetproofing were used. The costs of these elements for each case are given in Table 3.

The cost for the balance of the stack (end plates, tie rods, insulation, etc.) was assumed to be 5% of the total cost in $/kW of the repeating elements of the stack. A summation of costs for each case is presented in Table 4.

Reformer designs for transportation applications will be significantly different from those presently used in utility applications. When these new designs are finalized, cost estimates for reformer manufacture will probably decrease. However, most of the power-plant manufacturing cost is in the cell stack, which will be most strongly affected by performance improvements.

Manufacturing costs will have to consider such items as labor for cell fabrication, separator molding, and stack assembly, as well as the burden on these operations. Manufacturing yields will also have to be a factor. In addition, it has been estimated that a factor of 1.7 times the manufacturing costs should be used to obtain the installed cost. Thus, the final installed costs of the fuel cell power plant may well be twice the manufacturing cost.

Acknowledgment:

This work is supported by DOE, Office of Energy Storage and Distribution.

TABLE 1
PEM FUEL CELL CHARACTERISTICS

Case	Cell Voltage V	Current Density ma/cm²	Membrane	Pt Loading/Cell mg/cm²	Reactants
1	0.69	970	Nafion	8	H_2/O_2
2	0.67	430	Nafion	8	Ref/Air
3	0.82	1076	Dow	8	H_2/O_2
4	0.57	4306	Dow	8	H_2/O_2
5	0.70	970	Dow	8	Ref/Air
6	0.60	1507	Dow	8	Ref/Air
7	0.74	1076	Dow	2	Ref/Air
8	0.49	4306	Dow	2	Ref/Air

TABLE 2
PEM PARAMETERS AND COSTS

Case	Power Rating kW	Stack Voltage V	Stack Current A	# of Cells	Active Cell Area cm²	Pt Cost $/kW	Membrane Cost $/kW
1	20	22	901	32	929	190	74
	20	89	225	129	232	190	74
2	20	200	100	299	232	444	173
3	20	80	250	98	232	146	57
4	20	20	1000	35	232	52	20
5	20	89	225	127	232	189	74
6	20	57	350	95	232	141	55
7	20	80	250	108	232	40	63
8	20	20	1000	41	232	15	24

TABLE 3
REPEATING ELEMENT COSTS AS A FUNCTION OF PERFORMANCE

Case	Separator Plates $/kW	Anode Support $/kW	Cathode Wetproofing $/kW
1	16	8	5
2	37	19	11
3	12	6	4
4	4	2	1
5	16	8	5
6	12	6	3
7	13	7	4
8	5	3	1

TABLE 4
SUMMATION OF MATERIALS COSTS FOR PEM STACKS
($/kW)

Case	1	2	3	4	5	6	7	8
Catalyst	190	444	146	52	189	141	40	15
Membrane	74	173	57	20	74	55	63	24
Separator Plates	16	37	12	4	16	12	13	5
Anode Support	8	19	6	2	8	6	7	3
Cathode Wetproofing	5	11	4	1	5	3	4	1
Total ($/kW)	293	684	225	79	292	217	127	48
Balance of Stack	15	34	11	4	15	11	6	2
Total ($/kW)	308	718	236	83	307	228	133	50

ELECTRODE CHARACTERIZATION

J. McBreen
Brookhaven National Laboratory
Upton, NY 11973

The goal of this project is to understand electrocatalysis of fuel cell reactions at the molecular level and to apply the results to the development of new catalysts for oxygen reduction and direct oxidation of methanol. Work has focused on the use of the National Synchrotron Light Source (NSLS) at Brookhaven National Laboratory (BNL) for doing X-ray Absorption Spectroscopy (XAS). This has included both X-ray Absorption Near Edge Structure (XANES) and Extended X-ray Absorption Fine Structure (EXAFS) studies. EXAFS spectra provide information about the local environment of an absorbing atom while XANES spectra yield information about local coordination symmetry and the electronic state (e.g. valence state) of the absorbing atom. The work has included (1) a XANES and EXAFS study of underpotential deposited (UPD) copper on carbon supported platinum catalysts, (2) the coupling of cyclic voltammetry and XAS to study carbon supported platinum in several acidic electrolytes, (3) an EXAFS study of poisoned platinum electrocatalysts in methanol/H_2SO_4 electrolytes, and (4) XAS investigations of pyrolysed metal macrocyclics on various carbon supports.

XAS Studies of UPD Cu on Pt

UPD layers of foreign metals on Pt are known to catalyse oxidation of small organic molecules such as methanol or formic acid. A recent review (R. Parsons and T. VanderNoot, J. Electroanal. Chem. 257, 9(1988)) has enumerated possible explainations for this. These are.

(1) Modification of electronic structure of catalyst.
(2) Modification of physical structure of catalyst.
(3) Adsorption of OH^- ions to oxidize CO poison.
(4) Catalysis via a redox process of the UPD species.
(5) Physical blocking of poisons or H adsorption.

Any of the first four items should be apparent in the XAS spectra. XANES spectra at the Cu K-edge indicated that the UPD Cu was in the Cu(I) state. XANES at Pt L_3-edge indicated that there was electron transfer from the UPD layer and a concomitant filling of the Pt d-bands. The EXAFS spectra indicate that the UPD Cu is associated with either water or attached OH^-.

XAS Studies of Carbon Supported Platinum

XAS measurements were made on carbon supported Pt in several acidic electrolytes at various potentials. In addition time resolved XAS measurements were made while doing cyclic voltammetry on these electrolytes. The formation and reduction of the oxide could be plainly seen. On adsorption of hydrogen there was a concomitant reduction in the filled Pt d-bands.

XAS Studies of Poisoned Pt Catalysts

A comparative XAS study was made on carbon supported Pt catalysts in 1M H_2SO_4 and in 1M H_2SO_4 + 1M C_2H_5OH. The EXAFS spectra were different. However, elucidation of the structure of the poison will require much more data analysis.

XAS Studies of Pyrolyzed Macrocycles

An extensive XAS study has been made on the products of the pyrolysis of Fe and Co teteramethoxyphenylporphyrin (TMPP) on both Cabot Vulcan XC-72 and Black Pearls carbon. The results indicate that the catalyst has a structure similar to the core of the original macrocycle. The catalyst concentration is much higher on the Black Pearls material.

PROJECT GOALS/FUEL CELL R&D

PROJECT GOAL	R&D ACTIVITY
REDUCE PLATINUM LOADING	CURRENT GENERATION MECHANISM SPE FUEL CELLS
PLATINUM SUBSTITUTES	EXAFS STUDIES OF PYROLYZED MACROCYCLES *Fe and Co Teteramethoxyphenylporphyrins (TMPP)*
	EXAFS STUDIES OF PLATINUM FUEL CELL ELECTRODES
DIRECT METHANOL OXIDATION	STUDIES OF CATALYST POISONS HREELS, EXAFS
	XANES STUDY OF UNDERPOTENTIAL DEPOSITED (UPD) METAL SUB-MONOLAYERS ON CARBON SUPPORTED Pt CATALYSTS

XANES FOR Cu, Cu_2O AND UPD Cu ON Pt

UPD Cu IS MONOVALENT COPPER

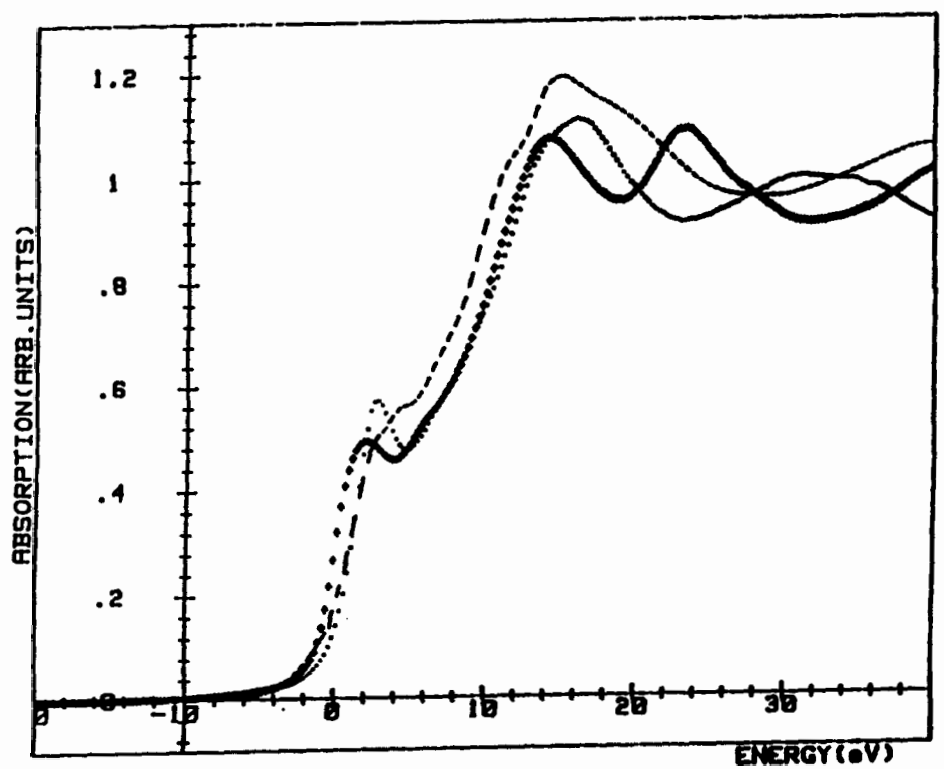

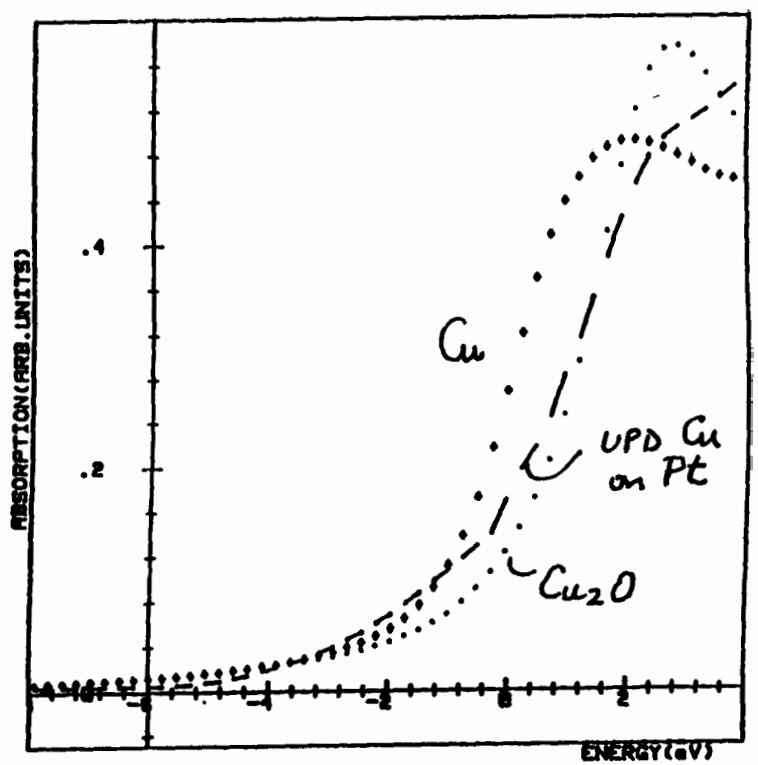

EFFECT OF ADSORBED Cu ON Pt XANES

REDUCTION OF WHITE LINE

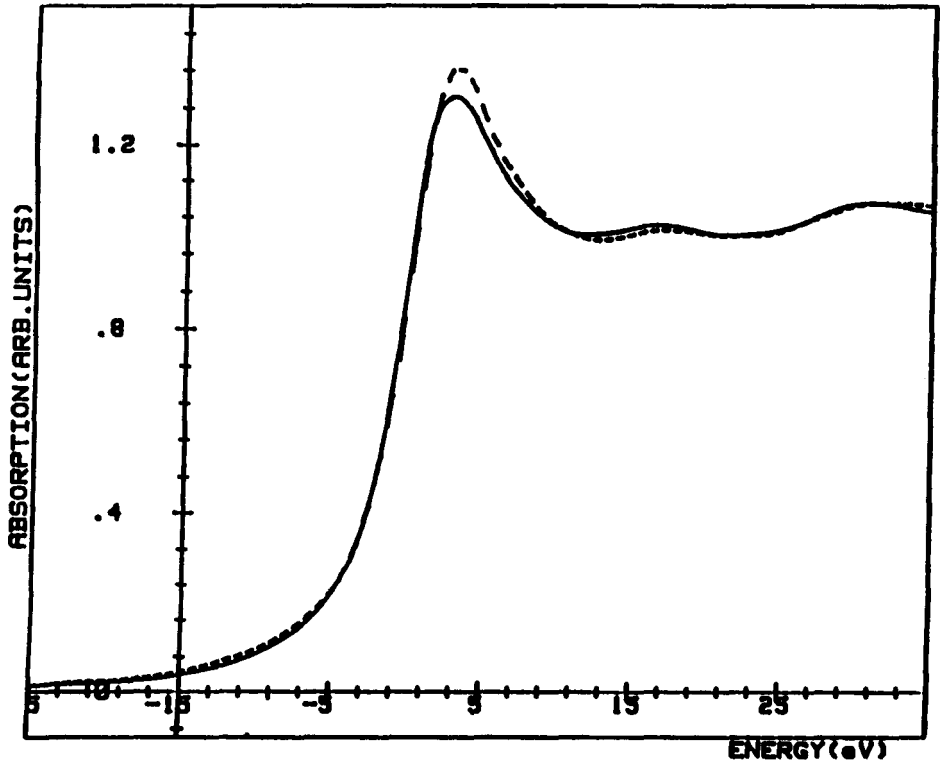

Pt XANES IN 1N H_2SO_4
-0.250V, 0.183V and 1.0V SCE

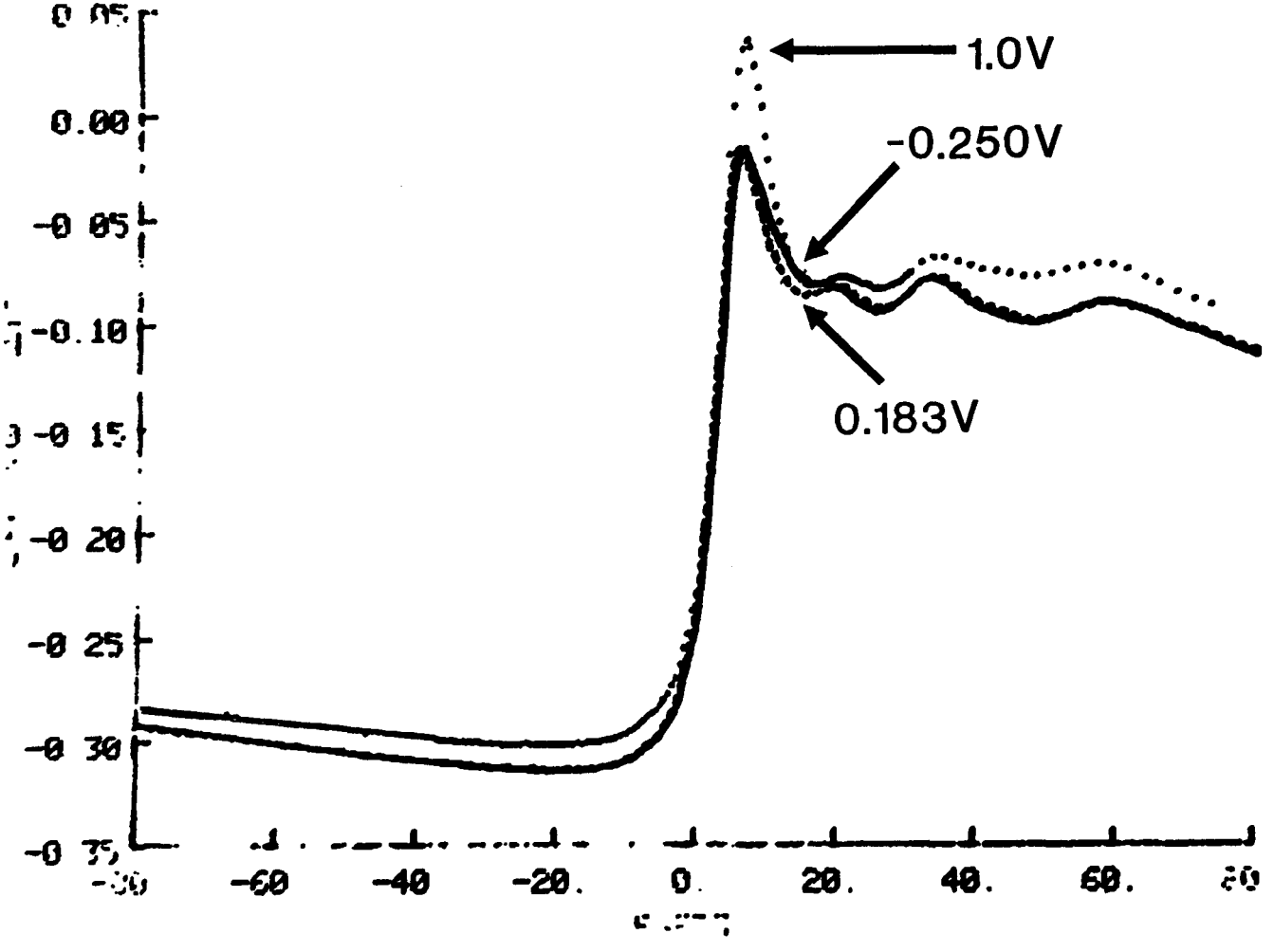

CONCLUSIONS

XANES STUDY OF UPD Cu ON Pt

- STUDIES CAN BE DONE IN THE TRANSMISSION MODE IN 4s
- AT 50mV SCE UPD Cu IS IN Cu(I) STATE
- PEAK AT L_3 X-RAY ABSORPTION EDGE OF Pt PROPORTIONAL TO d-ELECTRON VACANCIES
- UPD Cu DECREASES PEAK
- ADSORBED HYDROGEN BROADENS PEAK
- XANES CLEARLY SHOWS ELECTRONIC EFFECTS
- STRUCTURE AWAITS EXAFS RESULTS

AQUEOUS CARBONATE ELECTROLYTES FOR FUEL CELL APPLICATIONS

Elton J. Cairns, Kathryn A. Striebel and Frank R. McLarnon
Applied Science Division
Lawrence Berkeley Laboratory
Berkeley, California 94720

Novel carbonate-containing alkaline electrolytes have been evaluated for possible use in high-performance alkaline fuel cell cathodes [1]. Three complementary studies have been carried out to evaluate these promising electrolytes: (*i*) rotating disk electrode (RDE) and rotating ring-disk electrode (RRDE) techniques were used to measure kinetic currents and hydrogen peroxide production rates; (*ii*) the performance of PTFE-bonded gas diffusion electrodes were measured in a half-cell with a very small uncompensated solution resistance; and (*iii*) a mathematical model of the porous gas-diffusion electrode, based on the flooded-agglomerate model [2], was constructed to aid in the understanding of the observed electrode behavior. Parallel studies of oxygen reduction kinetics, and experimental and theoretical cathode performance, were carried out with potassium carbonate and potassium hydroxide electrolytes at similar ionic strengths. These studies revealed that the local electrolyte composition in the pores of the electrocatalyst does not remain invariant, with respect to the alkaline-carbonate electrolyte elsewhere in the cell.

Kinetic RDE and RRDE studies were carried out on bright Pt in controlled-temperature electrolytes prepared from ultrapure salts and ultrapure water. Disk currents were corrected for variable rates of mass transfer according to a first-order model and for electrode roughness (determined from the charge due to hydrogen desorption at the absence of oxygen). The results at a constant potential of 900 mV *vs* RHE for several electrolyte compositions are shown in Figure 1(a). For both electrolytes, there is a general decrease in kinetic current with increasing ionic strength, due to the lower oxygen solubility at higher electrolyte concentrations. However, when such plots are corrected to a constant oxygen concentration according to first-order reaction kinetics, the kinetic currents can be seen in Figure 1(b) to *increase* with increasing ionic strength. Lower peroxide-ion production rates were observed in the lower-pH carbonates over the entire concentration range, consistent with the prior work of Appel and Appleby [3].

PTFE-bonded Pt-on-carbon electrodes were used as received from Prototech Inc. These electrodes contained 0.3-0.4 mg of Pt per cm^2 in the active layer and were supported on a hydrophobic carbon paper gas supply layer. Figure 2 shows steady-state galvanostatic polarization curves recorded on electrodes with approximately 220 cm^2 of active Pt. Significant hysteresis is observed with the alkaline-carbonate electrolyte. It is suggested that this behavior is due to an increase in the local pH of the electrolyte in the electrode pores, consistent with a cathodic shift of ~200mV of the entire voltammogram recorded immediately following the polarization measurements. This behavior is less pronounced at higher carbonate-ion concentrations and higher temperatures.

A steady-state one-dimensional mathematical model was constructed to aid in the study of electrolyte composition changes in the alkaline-carbonate electrolyte. In this model, diffusion and migration effects in the liquid phase, carbonate solution chemistry and the negative reaction order with respect to pH (when the reference electrode potential is held constant) are accounted for. The results of the model will be presented, along with suggestions on how to overcome the pH-gradient effect.

References

1. K.A. Striebel, F.R. McLarnon and E.J. Cairns, "Oxygen Reduction in Fuel Cell Electrolytes," Lawrence Berkeley Laboratory Report No. LBL-24340 (1987).

2. J. Giner and C. Hunter, *J. Electrochem. Soc.* **117**, 1124 (1969).

3. M. Appel and A.J. Appleby, *Comptes Rendus Acad. Sc. Paris*, Ser.C, 551 (1975).

Acknowledgement

This work was supported by the Assistant Secretary for Conservation and Renewable Energy, Office of Energy Storage and Distribution, Energy Storage Division of the U.S. Department of Energy under Contract No. DE-AC03-76SF00098.

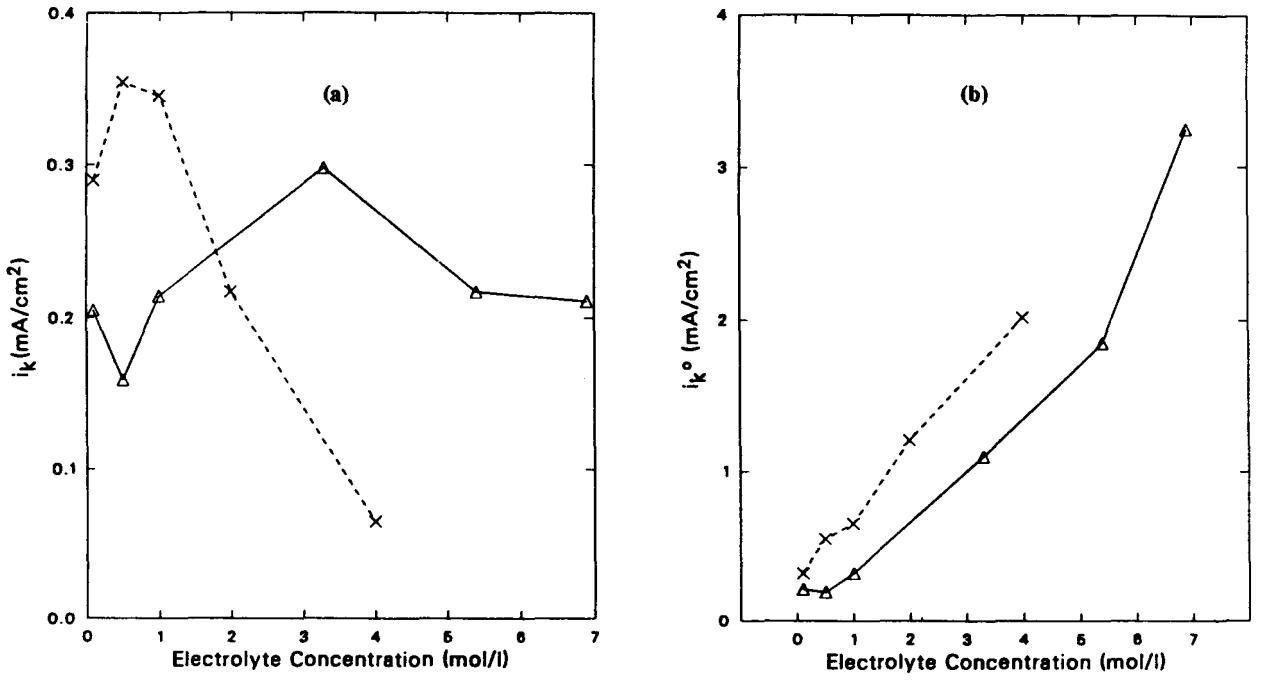

Figure 1. Comparison of mass-transfer-corrected current density in KOH and K_2CO_3 electrolytes, at 900mV *vs* RHE, 23°C.
(a) i_k corrected for electrode roughness.
(b) Normalized current density, i_k^o, corrected for roughness and $C_{O_2}^{\infty}$ differences.
_____Δ, KOH; ------×, K_2CO_3.

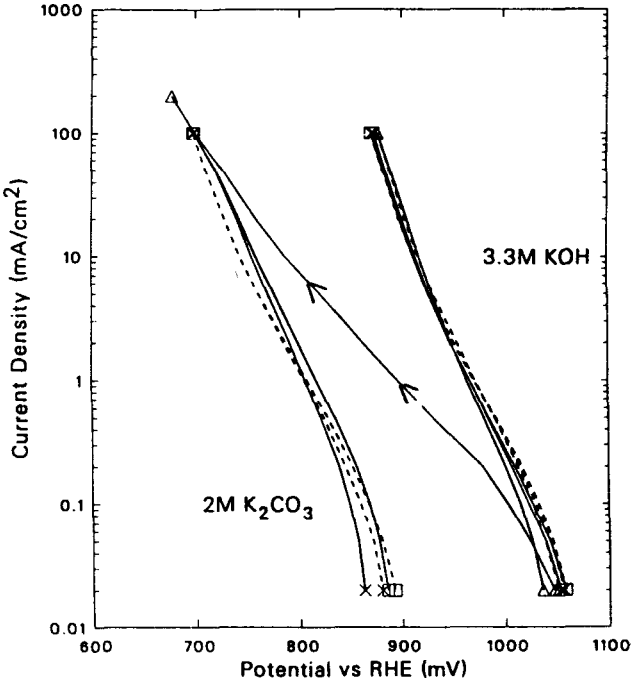

Figure 2. "Cycling" polarization measurements in alkaline electrolytes 23°C; Prototech electrode with 3.3M KOH and 2.0M K_2CO_3.
_____ cathodic direction; ------ anodic direction;
Δ, first cycle; ×, second cycle; □, third cycle.

MODELING A FUEL CELL/BATTERY HYBRID SYSTEM FOR VEHICLE APPLICATIONS

Samuel Romano
Georgetown University
Advanced Vehicle Development
Washington, DC 20057

The fuel cell/battery hybrid propulsion system under development by the Department of Energy is being designed for transit bus applications. This selection was made because the transit application offers the best environment for the introduction of this promising technology. The route structure is defined and an infrastructure exists for a controlled evaluation. A phosphoric acid fuel cell (PAFC) was selected for this first application because it represents the only technology that has demonstrated performance on reformed fuels suitable for transportation applications.

The fuel cell/battery powered vehicle offers all the advantages of a battery powered vehicle without the restrictions or limitations in range because it uses liquid methanol which permits rapid refueling. However, the thermal inertia of the phosphoric acid fuel cell system, primarily due to fuel processing, does not allow the rapid power level changes required by a transit bus in its stop and go operation. To meet the resulting cyclic power demands, a hybrid system combining both fuel cell and battery power is used. In addition, at the present state of development, the power density of PAFC is not adequate to provide the peak power required for hill climbing and acceleration without excessive weight and size penalties. The battery is used to meet these two requirements. The fuel cell energy characteristics and the battery peak power characteristics should be determined by the operational requirements of the mission. Optimum performance of this hybrid combination is achieved by selecting the proper combination of fuel cell and battery sizes to match the application.

A computer program has been developed which can be used to match the combined power output of the FC and battery to a defined operational requirement. Or working from a mission profile it can be used to size the fuel cell and battery to meet the power and energy requirements. A mathematical model was developed and programmed for digital simulation of vehicle performance along any specified route. The program is written in the Fortran language and compiled with the Microsoft Fortran Compiler for MSDOS computers. Figures 1, 2 and 3 shows the organization of the input and output data and the internal logic. Eighty input parameters describing the vehicle, drive/transmission, motor/generator (for regenerative braking), motor controller, battery and fuel cell are required for a simulation together with a route description consisting of the length of each segment, grade, the allowable maximum speed along the segment, and dwell times along the route.

This input data is read in and stored in arrays, for example the route information and gear shift points. After reading and storing of data, certain initialization of program variables is

performed. Following data input and the initialization, the computation path is repeated until the entire route has been traversed. At each time interval in the simulation, the road load is determined and computations proceed ultimately to determine the total power requirements consistent with the tractive effort necessary for the desired performance, system losses being taken into account (e.g. battery, controller,motor, transmission, axle, accessories, etc.). Excessive power demands require additional computations for obtainable performance. Integration routines (Runge Kutter methods) are then used to update the vehicle status. The vehicle position and speed are checked and the computational scheme is repeated.

The power source consisting of the fuel cell and battery were modeled independently. Both models were configured for operational use in the program rather than for battery or fuel cell design purposes. Considerations for the battery simulation include dependency of the battery voltage on the state of charge, battery capacity as a function discharge current, internal resistance characteristics as a function of state of charge and battery gassing voltage.

In modeling this particular power system it was necessary to consider the rapid changes in power required in vehicular applications. Phosphoric acid fuel cells are usually considered for steady state power sources where response times for increases or decrease in power are well below that required for vehicular operations. In the hybrid system the battery will accommodate the more rapid changes in power demands and will act as a sink for FC power when power demands are below FC output. Unfortunately, this does not eliminate the need for some modulation of FC power output. It does however, permit much lower response times. The program will model the response time of the FC system and will only allow modulation of power within the FC capability.

The program effectively operates the vehicle, whose characteristics have been defined including the fuel cell\battery power source along a prescribed route and records data suitable for sizing power components or adapting a power system to a specific mission. The program is expected to be invaluable in matching the initial fuel cell/battery powered buses developed for the current DOE program to transit properties throughout the country.

Figure 1

FUEL CELL/BATTERY POWERED BUS COMPUTER SIMULATION

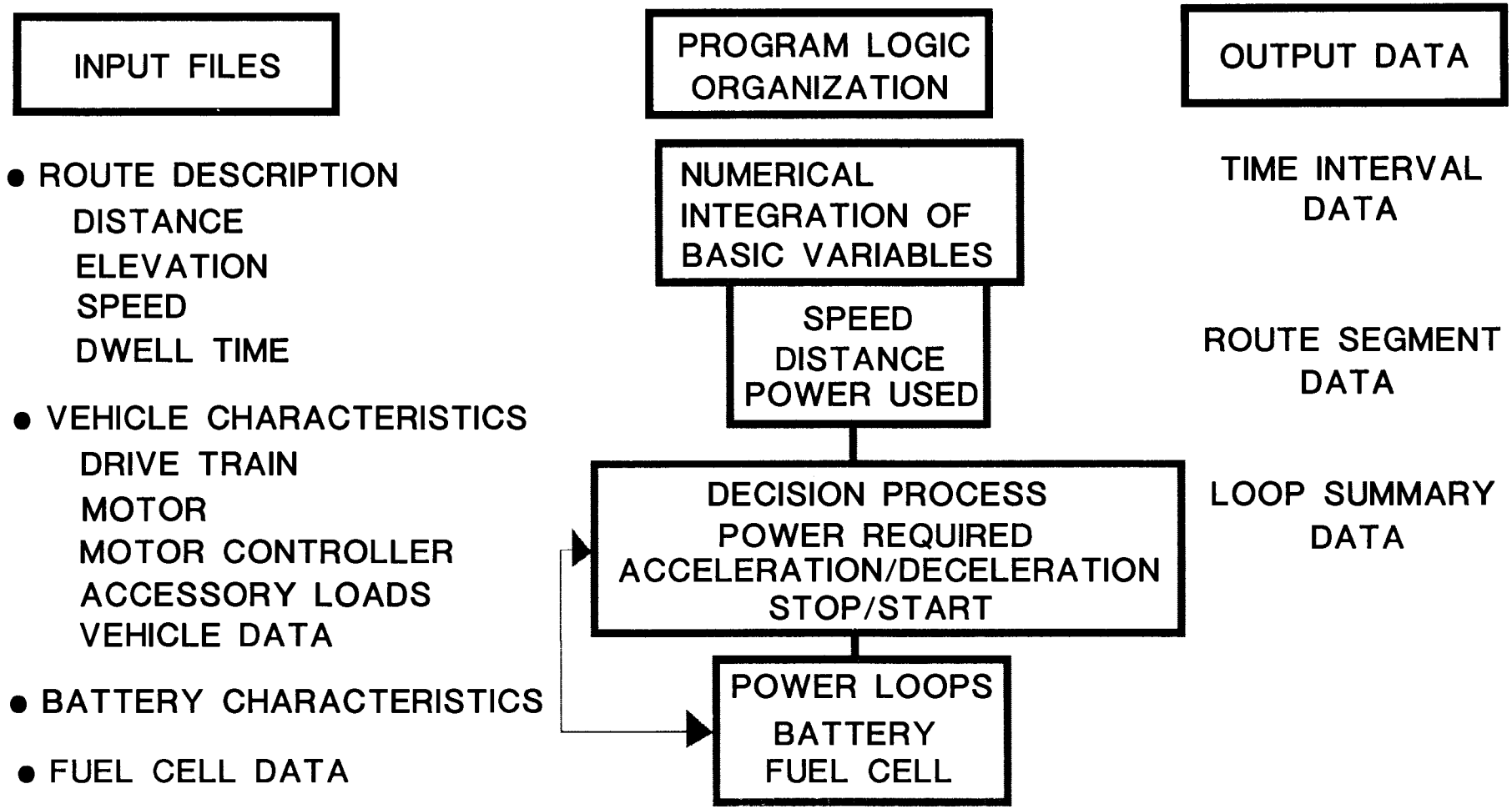

Figure 2

FUEL CELL/BATTERY POWERED BUS COMPUTER SIMULATION

DATA OUTPUT

• TIME INTERVAL DATA

TIME

SPEED

DISTANCE

MOTOR CURRENTS & VOLTAGE

MOTOR OUTPUT POWER

FUEL CELL POWER OUTPUT

FUEL CELL CURRENT & VOLTAGE

BATTERY OUTPUT/INPUT

• ROUTE SEGMENT DATA

BATTERY POWER USED - (AMP HR)

AVERAGE BATTERY CURRENT - (AMP)

AVERAGE BATTERY HEAT LOSS (KW)

BATTERY STATE OF CHARGE (%)

BATTERY ENERGY OUTPUT (KW-HR)

FUEL CELL ENERGY OUTPUT (KW-HR)

FC FUEL CONSUMPTION (MI/GAL)

AVERAGE ARMATURE POWER LOSS (KW)

Figure 3

FUEL CELL/BATTERY POWERED BUS COMPUTER SIMULATION

DATA OUTPUT

- **LOOP SUMMARY**

TOTAL DISTANCE TRAVELED (MI)
TOTAL DWELL TIME USED (MIN)
RATE OF ENERGY CONSUMPTION (KW-HR/MI)
TOTAL REGENERATIVE ENERGY (KW-HR)
RATE OF METHANOL CONSUMPTION (MI/GAL)
BATTERY STATE OF CHARGE (%)

ZINC/BROMINE BATTERY DEVELOPMENT

CHAIRPERSON:

Stephen Lott
Sandia National Laboratories

ZINC-BROMINE BATTERY DEVELOPMENT AT ENERGY RESEARCH CORPORATION

Anthony Leo
Energy Research Corporation
3 Great Pasture Road
Danbury, Connecticut 06813

Energy Research Corporation is involved in a program to develop the zinc-bromine battery system for stationary energy storage applications. Technology development work is being done under a project supported by the U.S. Department of Energy through Sandia National Laboratories. We are presently in the final year of the project, which began in September, 1985. The first three years of work focused on improving the cell component technology and developing reliable stack and process system hardware. In the fourth year the program activities have centered on battery testing and the evaluation of a new generation of stack hardware.

The new design scales up electrode active area from 872 cm^2 to 1500 cm^2, and significantly changes the design approach used. The new flow frame was designed to address problems which have been encountered with the 872 cm^2 cell hardware, such as flow channel blockage, frame cracking and poor cell-to-cell flow uniformity.

The design of the flow frame was done using a flow model which predicted shunt current losses, pumping power losses and flow distribution among stacked cells. Dye injection flow tests and single cell electrochemical tests were done to insure that flow was uniform over the cell area and that good deposit quality was obtained with high capacity density zinc plating. The dye injection tests were done using machined flow frame prototypes, and iterations were made on the flow plenum area of the flow frame to achieve a uniform velocity profile over the active cell area. Single-cell testing done after the dye injection tests verified that zinc deposits were dense and uniform with capacity densities as high as 200 mAh/cm^2. After the flow tests and zinc deposition tests were completed, an injection mold was fabricated to produce the new frame.

Evaluation of the larger flow frame hardware has recently begun in 5-cell battery tests. Energy efficiencies of 60 to 70% have been obtained on a baseline cycle which consists of a 5-hour charge at 35 mA/cm^2 followed by a discharge at 37.5 mA/cm^2. Fabrication of a 52-cell, 18 kWh system was recently completed and testing is now beginning. The stack has required initial cycling at low rates to facilitate wetting of the Daramic separators.

One of the design changes built into the 1500 cm^2 frame was the allowance of slightly more space in the zinc electrode channel. This was done to provide a more loose cell package to eliminate the frame cracking problem that had been encountered in the 872 cm^2 stack hardware. This has led to slightly lower voltaic efficiency due to catholyte flow bypassing the carbon felt bromine electrodes, which are compressed less in the new frame. This problem is being addressed in a revision of the cell component thickness specifications.

As the development of the 1500 cm^2 stack hardware has progressed, cycle life testing has continued on stacks built using the 872 cm^2 active area hardware. Two stacks are currently on test, a 5-cell and a 30-cell 1.4 kW stack, which have each logged over 350 cycles. Both of the stacks have gone through two repair operations, in which the end electrode current collectors at the ends of the stack were replaced with new designs.

The baseline cycle used with the 872 cm^2 stacks consists of a 30 A (34.4 mA/cm^2) 5-hour charge followed by a 30 A discharge to a voltage cut off of 1.2 V per cell. The 5-cell stack currently on test is operating at 68% energy efficiency on the baseline cycle. The 30-cell stack is delivering about 65% energy efficiency.

Future work in the program will include continued life testing of the 872 cm^2 stacks currently on test. Testing will continue on the 1500 cm^2 stacks and new batteries will be built utilizing the improved cell component specifications to increase the voltaic efficiency of the large stacks. These tests will include operation on the baseline cycle described above, (150 mAh/cm^2 capacity density) as well as tests utilizing 200 mAh/cm^2 discharge output.

Acknowledgment:

This work is supported by the U.S. Department of Energy and managed through Sandia National Laboratories.

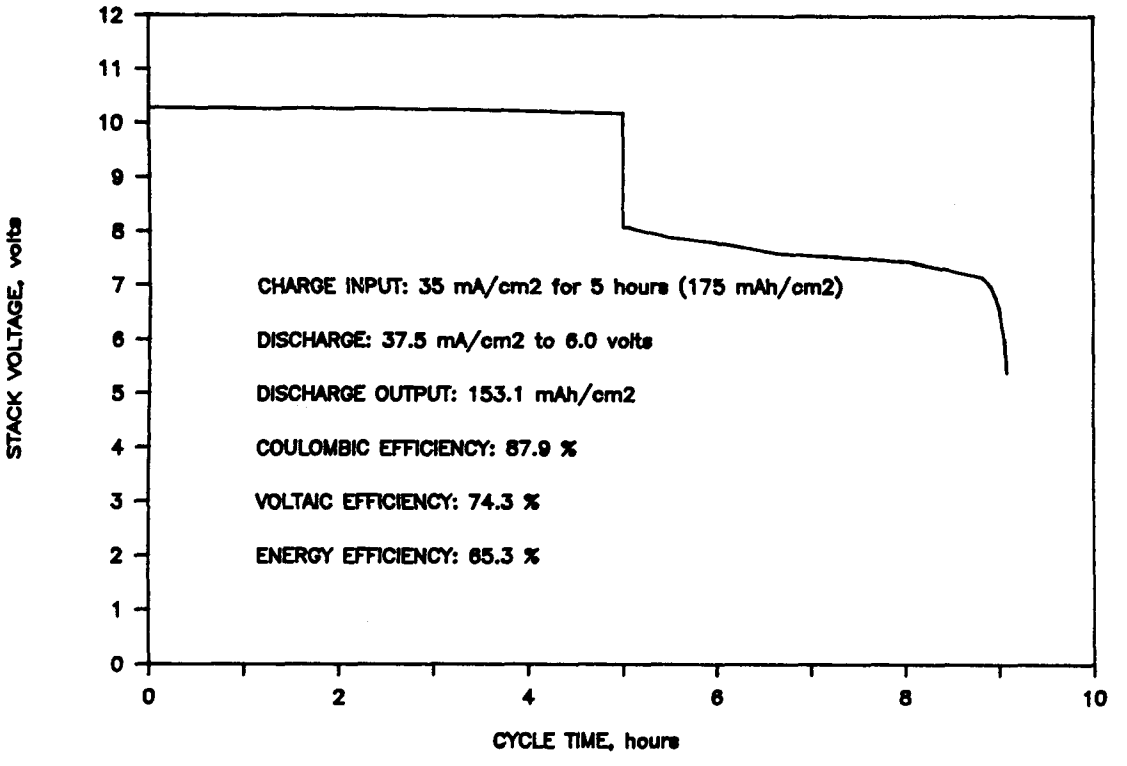

1500 cm² 5-CELL STACK 1500-5-3 - VOLTAGE PERFORMANCE ON CYCLE 10

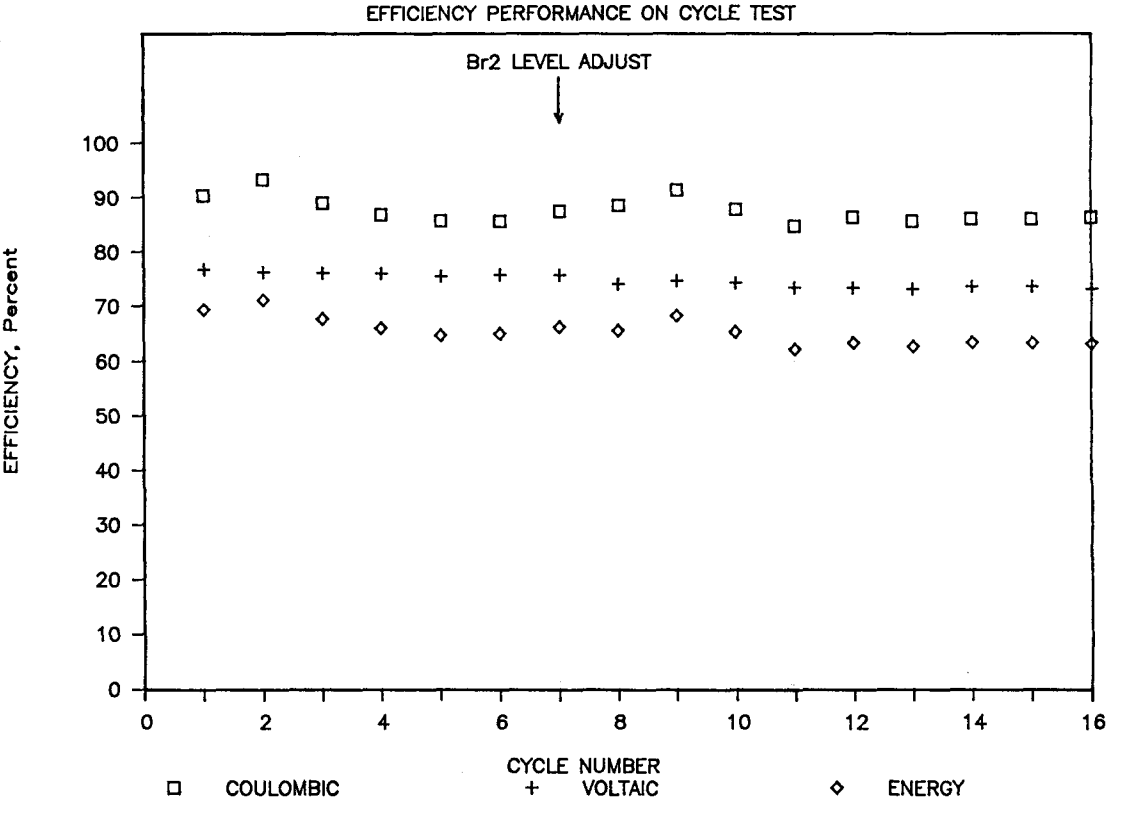

1500 cm² 5-CELL STACK 1500-5-3 - EFFICIENCY PERFORMANCE ON CYCLE TEST

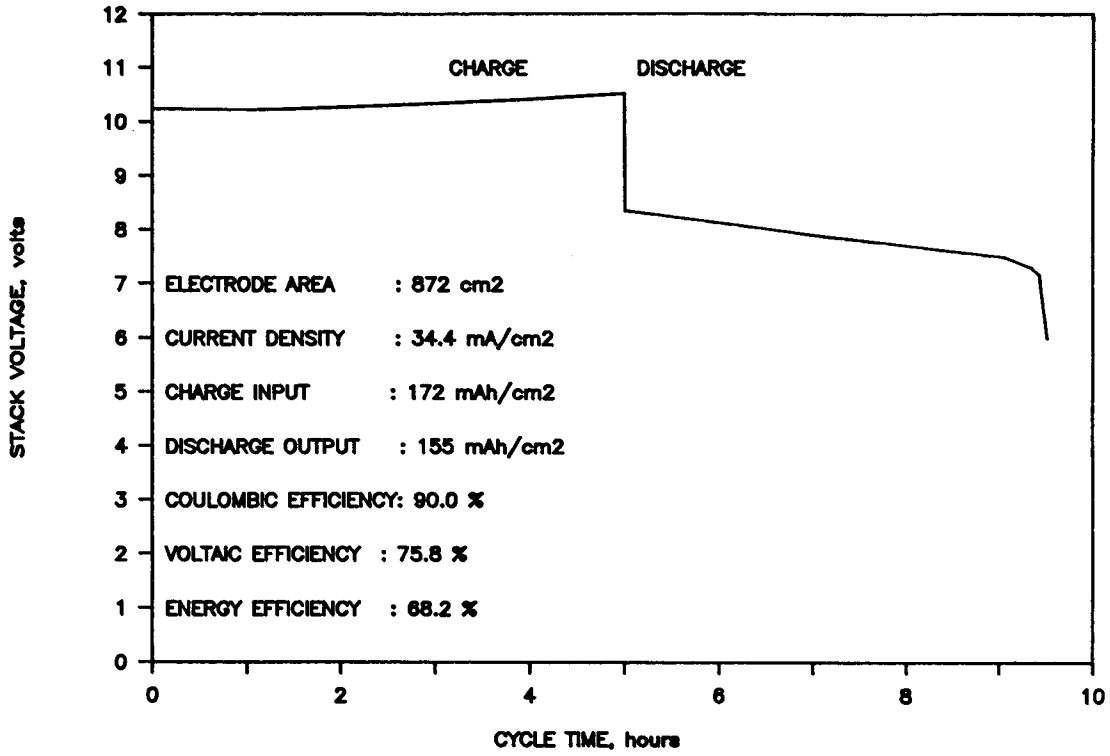

5-CELL STACK SNL-5-4 - VOLTAGE DATA FOR CYCLE 247

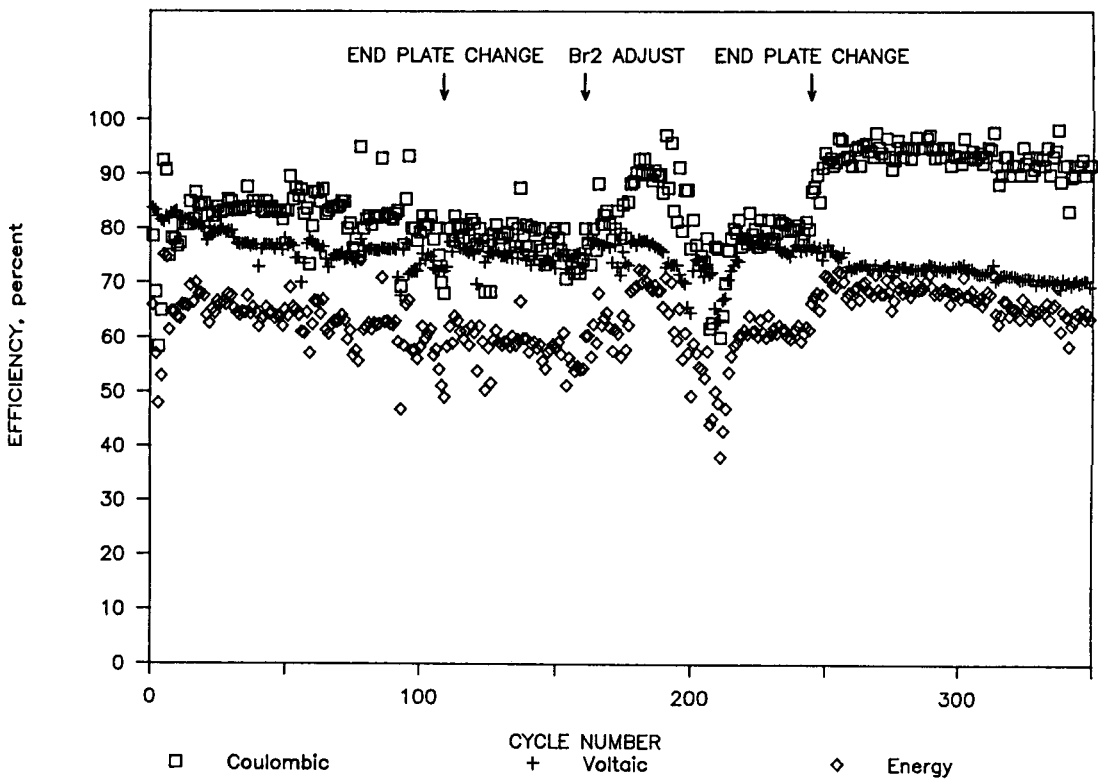

5-CELL STACK SNL-5-4 - EFFICIENCY PERFORMANCE ON CYCLE TEST

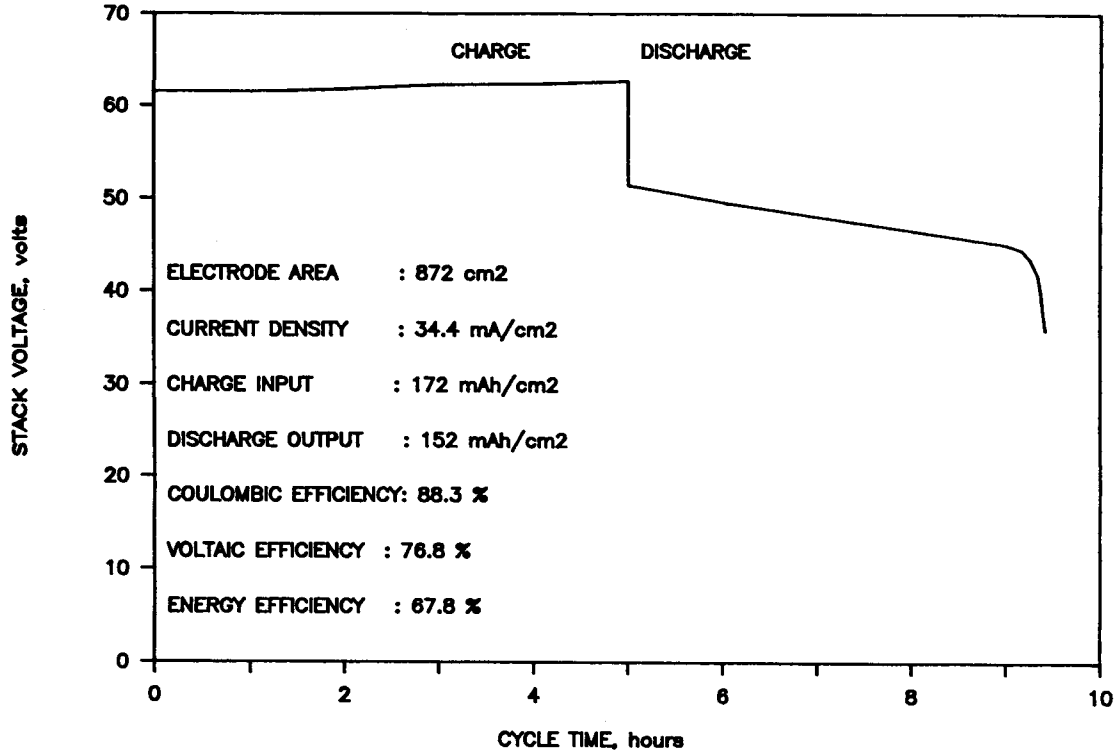

30-CELL STACK SNL-30-2 - VOLTAGE DATA FOR CYCLE 270

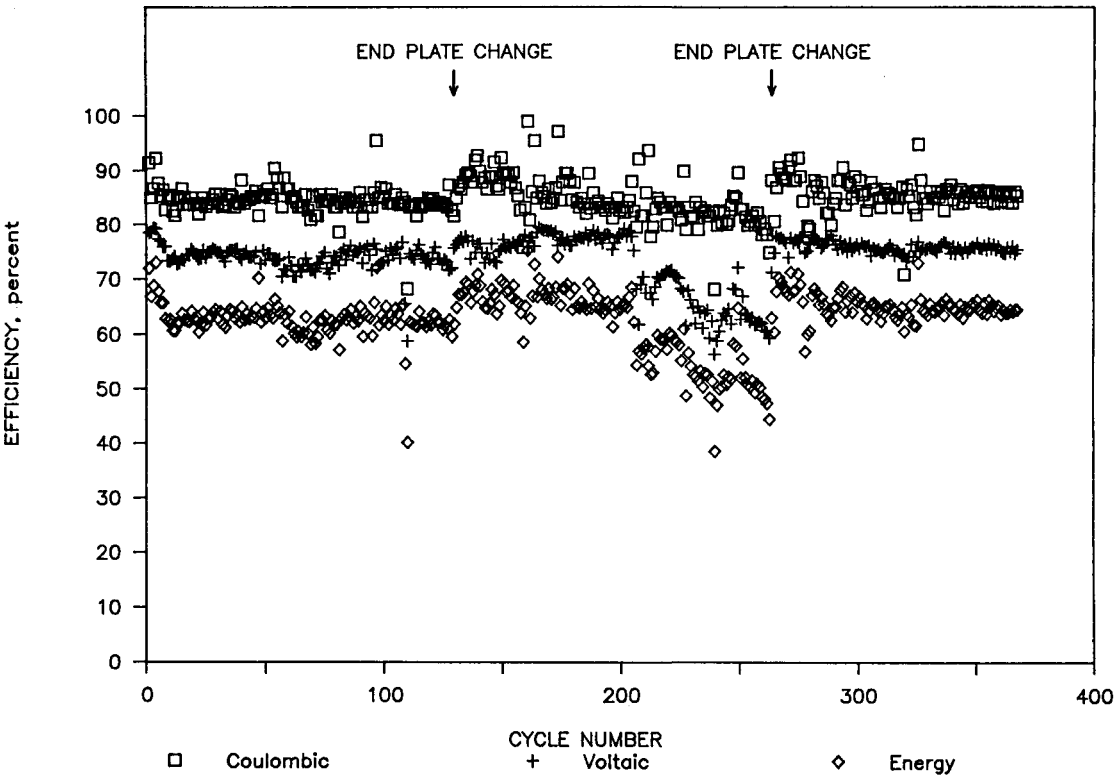

30-CELL STACK SNL-30-2 - EFFICIENCY PERFORMANCE ON CYCLE TEST

ZINC/BROMINE BATTERY DEVELOPMENT

P. A. Eidler
Johnson Controls, Incorporated
5757 North Green Bay Avenue
P. O. Box 591
Glendale, WI 53201

The advanced battery business unit at Johnson Controls, Inc. is developing Zinc/Bromine battery technology for electric vehicle (EV), load management, and pulse power applications. This battery system was selected for development due to its' attractive energy density, potential for long cycle life, and its' low anticipated manufacturing costs. Design flexibility make this system an attractive candidate for both mobile and fixed base applications.

The Zinc/Bromine EV program at JCI, under a cost share program with DOE-Sandia, is focusing development efforts on a 50 kWh electric vehicle system to be delivered in January 1990 for eventual testing in a Ford Aerostar minivan. Battery performance is required to meet 35kW sustained power and 65kW peak power at 80% DOD. Meeting these requirements necessitates optimization of the zinc bromine battery. This was initiated by using JCI's proprietary computer model to select the optimum thickness of the electrode, separator, and electrolyte gap to maximize efficiency. The model calculates energy consumed by the shunt current protection system and calculates battery performance based on a constant current discharge.

An early load management battery was designed and built by JCI as a proof-of-concept system to demonstrate the feasibility of zinc/bromine for load management applications. This system is not as weight sensitive nor does it have the peak power requirements as in the EV program. This allows design parameters to focus on efficiency and cycle life. This system contained two 78-cell stacks to be connected in parallel resulting in an open-circuit voltage of 1.6 volts per cell and a battery voltage of 125 volts. This battery was cycled once each day using a 45 amp 5 hour charge and a 56 amp discharge which lasted about three hours. After every discharge, the battery was placed into a strip mode which removed all of the excess zinc from the anodes insuring ideal plating conditions for the next charge cycle. A typical charge/discharge cycle is illustrated in figure 1. This battery displayed a coulombic efficiency of about 80%, and an average energy efficiency of approximately 60%.

A separate computer program determines the drop in pressure for a given battery design with parameters used in the initial modeling program. It is recognized that this analysis is on a dynamic system in which the viscosity and density are constantly changing variables. Thus, the pressure drop is analyzed for both the anolyte and catholyte from 0% to 100% depth of discharge (DOD). Calculations for diverter spacing, to achieve uniform flow across the face of the separator/electrode, are also performed based on a specific electrolyte flow rate. This program provides an adequate analysis of pressure changes in the battery, however, the main shortcomings have been in the analysis of two phase flow, complex curves, channel expansions, and channel contractions.

These shortcomings have been addressed by using finite element analysis to model the flow channels geometrically complex sections. Turbulent flow regions have been minimized, and critical radii of curves have been recognized. Velocity

and pressure profiles of channels and complex curves were calculated accurately enabling several design iterations to occur in a short time frame. The next refinement of the flow model will address the two phase flow of the catholyte at the batteries various states of charge.

Peak power tests and SFUDS (Simplified Federal Urban Driving Schedule) discharge cycles were used to support the initial computer model results in identifying the optimum electrolyte in an EV application (see Table 1). The initial computer model predicts performance based on a constant current discharge, so modifications have been initiated to incorporate peak power discharge test data and SFUDS data. These two testing methods provide additional insight regarding battery performance relating to acceleration capabilities and battery performance late in the discharge cycle.

Emphasis is focused on battery energy efficiency when selecting load leveling electrolyte. A study examining the efficiencies of various electrolytes is shown in figure 2. These results indicate that the best unsupported electrolyte for a load leveling applications is 2.25M $ZnBr_2$, 0.8M MEP, and 0.5M $ZnCl_2$.

The requirements for this battery necessitate a continual development effort pertaining not only to battery components, but manufacturing techniques as well. Evaluation of various plastics as potential candidates for electrodes and frames is a continuous process. Separator development and various carbon coating techniques are also continually being assessed. The cell dimensions suggested by the model require that the electrode and separator are inserted in a frame that is .041" thick. This frame would include sections for the fluid flow channels, manifold, diverters, and a leak free seal for the separator/electrode. This required sections of plastic .010" thick to be injection molded. A finite element analysis of the mold filling and cooling capabilities was performed to determine the appropriate manifold configuration and the drop locations.

Self discharge is an important criteria in common manifold batteries that must be minimized. This was accomplished by using JCI's patented shunt current protection system. Minimizing the shunt currents by using this SCP system necessitates higher battery operating pressures, thus, a means of support is required to reduce the deflection that is observed at the endblocks. The endblocks of the battery are vibration welded to the terminal electrodes and are reinforced with an insert. These inserts are designed to reduce deflection of the battery to less than .012" at 15 psi. The deflection was examined both experimentally and modeled by using finite element analysis.

In summary, many design parameters are modeled to determine the effect they will have on battery performance and functioning. Modeling system performance, based on established limitations, allows our development team to test these limitations and advance the battery technology in a focused and cost efficient manner.

Acknowledgement:

This research is supported by DOE, Sandia National Laboratories

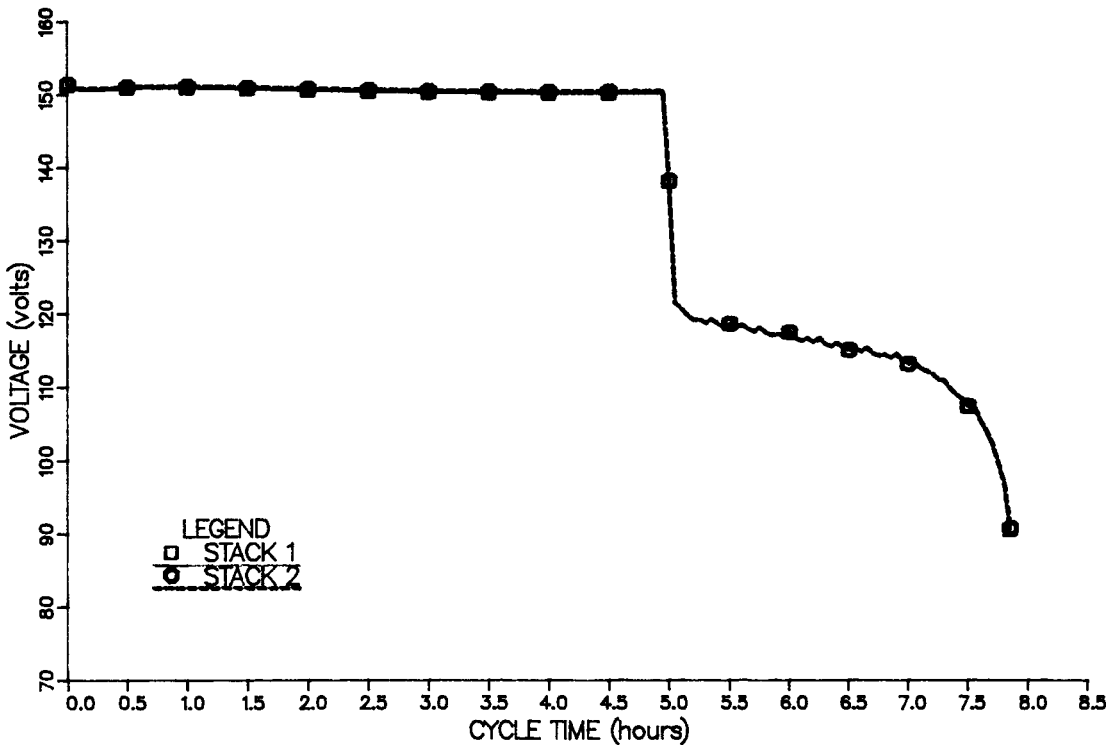

FIGURE 1: BATTERY VOLTAGE DURING CYCLE TIME
Z-20 LOAD LEVELING BATTERY
CYCLE #180

Table 1

ELECTROLYTE STUDY RESULTS

	Methods of Discharge		
Electrolyte	Constant Current (% EE)	SFUDS (% EE)	Power Test* (W/cm2 at 80% DOD)
Unsupported	69.4	63.8	0.1003
NH_4Cl Supported	62.7	66.5	0.1349
KCl Supported	58.5	67.2	0.1071

NOTE: * Contract requires power test results at 0.1343 W/cm^2 at 80% DOD f 20 seconds above a 1.07 volt/cell cutoff.

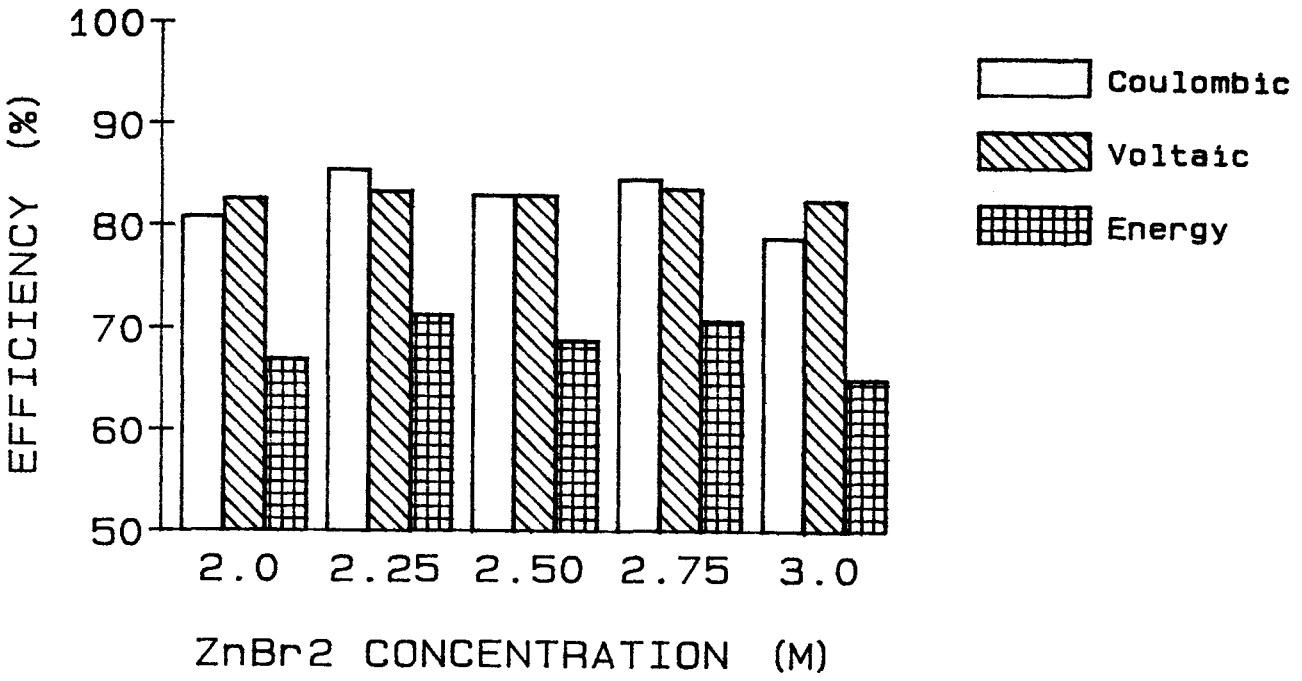

FIGURE 2: LOAD LEVELING ELECTROLYTE STUDIES
ZnBr2 Concentration Analysis
(base solution: [ZnCl2] = 0.5M, [MEP] = 0.8M)

MEMBRANE AND DURABILITY STUDIES FOR THE ZINC/BROMINE BATTERY

C. Arnold, Jr., R. A. Assink and P. C. Butler
Sandia National Laboratories, Albuquerque, NM

Zinc/bromine flow batteries are being developed for vehicular and utility load leveling applications by Johnson Controls Co. and Energy Research Corp. under DOE sponsorship. A schematic diagram of this battery is shown in Figure 1. Problems that have been encountered with the zinc/bromine battery are loss of coulombic efficiency brought about by permeation of bromine through the separator and limited life caused by attack of the bromine-containing electrolyte on plastic parts, particularly the flow frame. In this paper, the results of our recent efforts to address these problems are presented.

In current battery designs, microporous separators are used because of their low cost, mechanical robustness and proven durability. The primary disadvantage of these separators is that they are not selective; crossover of electroactive negatively charged bromine complexes as well as uncomplexed bromine takes place which leads to self-discharge and loss of coulombic efficiency. Our approach to this problem was to impregnate and/or coat the microporous separators with a polyelectrolyte. This should serve to reduce the rate of bromine transport by two mechanisms: 1)Donnan exclusion of the negatively charged bromine moieties, and 2)physical closure of some fraction of the pores. It was anticipated that the resultant hybrid membranes would have higher resistivities but that the increase in resistivity would be minimal because the impregnated polyelectrolytes are ionically conductive in an aqueous environment. The polyelectrolyte selected for this study was sulfonated polysulfone (SPS). SPS is soluble in organic solvents, which facilitates the impregnation process. In addition, SPS is stable but not soluble in the battery electrolyte.

The effect on area resistivity and bromine transport of impregnating a silica-filled microporous polyethylene separator (Daramic^{R}) with SPS is summarized in Table I. These data indicate that very large decreases in the bromine transportation rate were achieved at the cost of relatively modest increases in area resistivity. In preliminary battery cycle tests, a 13% increase in coulombic efficiency was noted with Daramic that had been impregnated with a 20% solution of SPS in dimethylformamide (DMF)

Figure 2 shows the sulfur profiles across the thickness dimension of the membrane impregnated at room temperature three times and the membrane impregnated under vacuum at 90°C. While the internal concentration of SPS was the same for both membranes, the concentration of SPS in the multiply-immersed membrane was considerably higher at or near the surface. The data of Table I indicate that the detrimental effect of this coating on area resistivity was apparently more than counterbalanced by its benefical effect on bromine transportation.

One of the plastics used to fabricate flowframes for the zinc/bromine battery is poly(vinyl chloride) (PVC). PVC is fairly stable toward aqueous bromine and can be easily fabricated into complex parts. Because of its thermal instability and brittleness, it is impractical to use pure PVC in battery applications. Therefore, the PVC used in the zinc/bromine battery contains several proprietary additives. ^{13}C NMR plots shown in Figure 3 indicate that these additives contain both aliphatic and aromatic carbons (peaks in the range of 31-34 and 140 ppm, respectively), and that their concentration is greatly reduced after aging in the electrolyte for 18 weeks at 60°C. Tefzel^{R}, a copolymer of ethylene and tetrafluoroethylene, is reported to be stable in aqueous bromine. Although Tefzel^{R} is more expensive than PVC, it does not contain any additives. Long term stability tests are being carried out to determine if Tefzel^{R} might be a viable replacement for PVC. Two week aging data at 70°C, which look promising, are shown in Figure 4.

Daramic^{R}-Trademark of W. R. Grace Co.
Tefzel^{R}-Trademark of E. I. DuPont De Nemours & Co.

Acknowledgement: This work was supported by the U.S. Department of Energy's Office of Energy Storage and Distribution.

TABLE I

Effect of Impregnation of Sulfonated Polysulfones on the Area Resistivity and Bromine Transport of a Microporous Separator

SPS Conc (%)	Weight Gain (%)	Resistivity (Ω cm^2) (R)	Br_2 Transport ($mol/cm^2 s \times 10^9$) (P)	R×P (10^9)
No Treatment				
-	-	1.1	5.2	5.6
Immersion 3×/Ambient				
20	66.8	5.0	0.05	0.25
SPS Cast Membrane/0.07mm				
100	-	99.3	<0.05	-
Vacuum Immersion/90°C/H^+ Form				
10	17.3	1.6	1.7	2.7
20	39.1	2.8	0.4	1.1
30	97.7	41.9	<0.05	-
Vacuum Immersion/90°C/Na^+ Form				
10	16.9	1.4	2.4	3.4
20	51.8	4.1	0.4	1.6
30	159.0	28.3	<0.05	-

ZINC-BROMINE CIRCULATING BATTERY

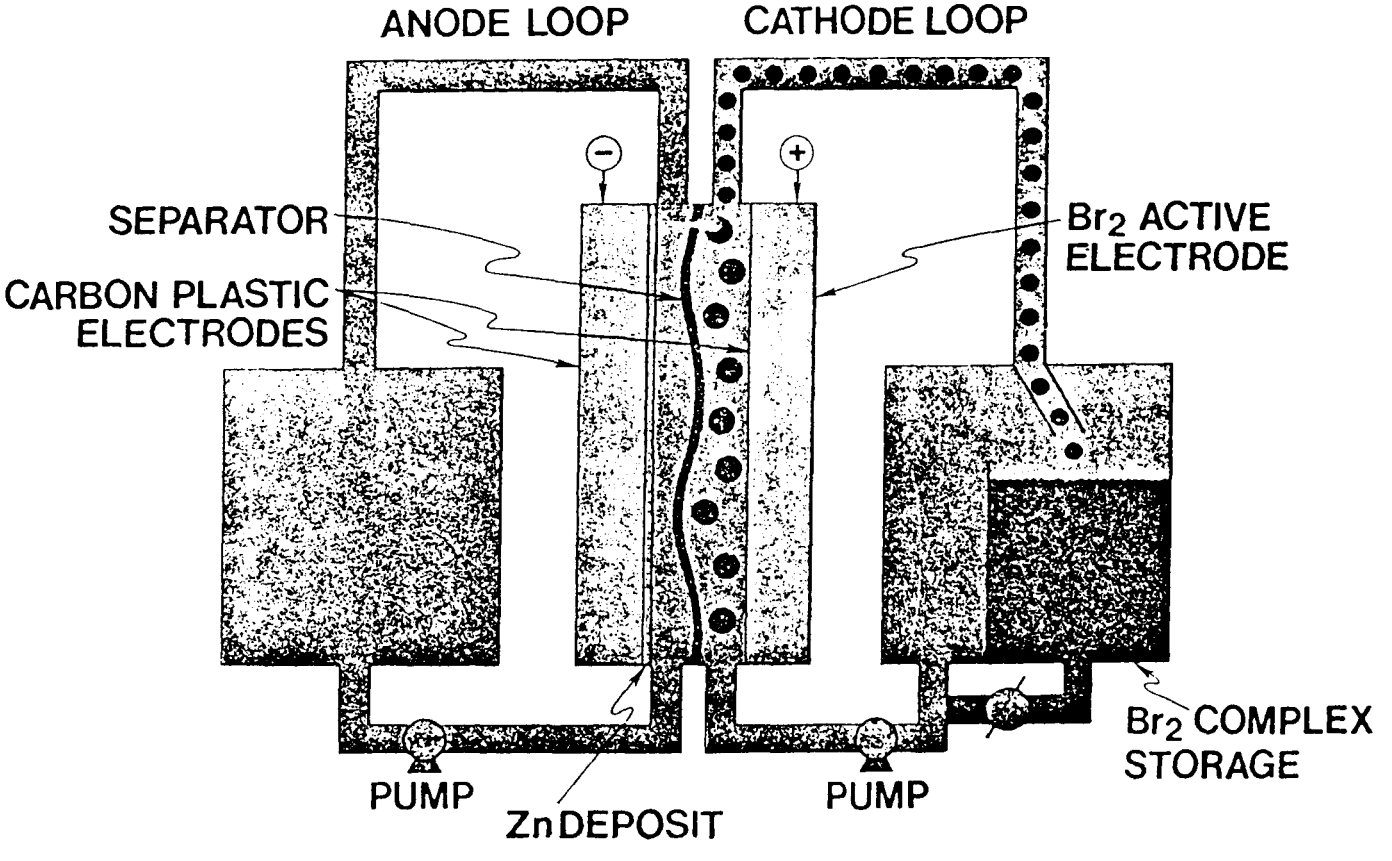

Electrochemical Reactions:

$$Zn^{\circ} \rightleftharpoons Zn^{++} + 2e^{-}$$

$$Br_2 + 2e^{-} \rightleftharpoons 2Br^{-}$$

Self discharge:

$$Zn^{\circ} + Br_2 \rightarrow ZnBr_2$$

Figure 1. Schematic diagram of the zinc/bromine flow battery

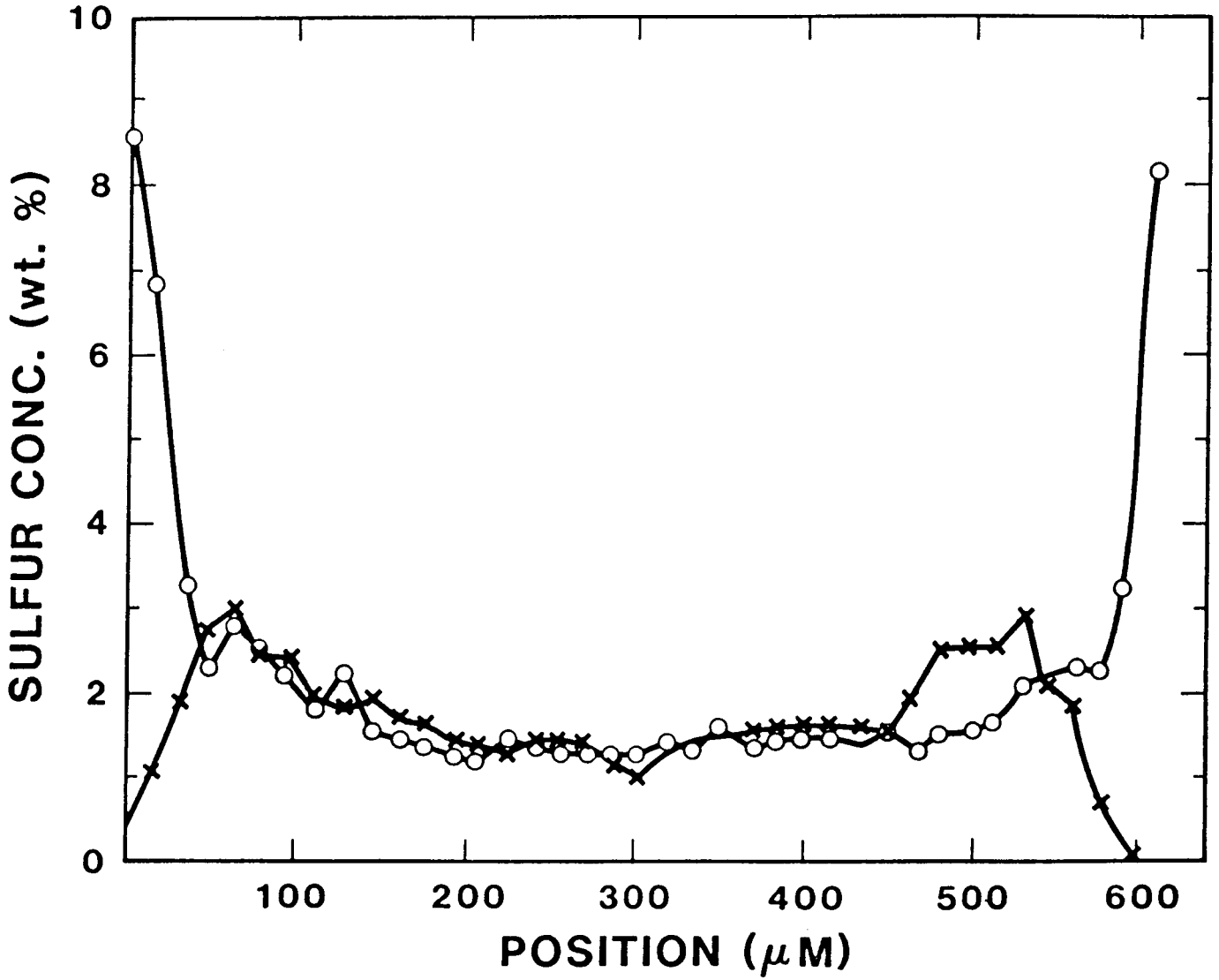

Figure 2. Sulfur content as function of depth across the thickness dimension of two membranes: -O- impregnated at room temperature three times; -x- impregnated under vacuum at 90°C.

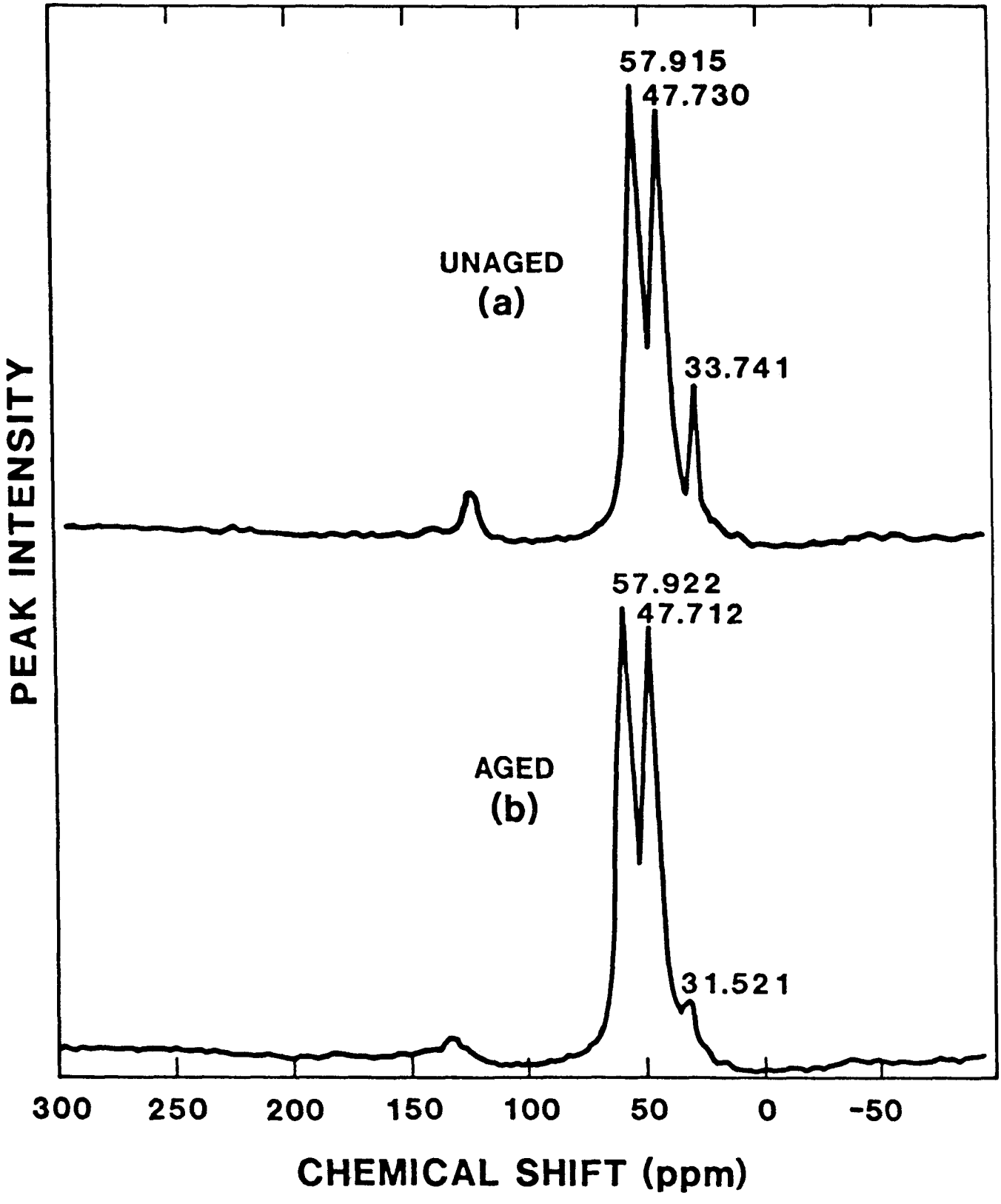

Figure 3. ^{13}C NMR spectra of unaged (a) and aged PVC-1 (solid) (b). Aging conditions: 60°C for 18 weeks in a bromine-containing electrolyte.

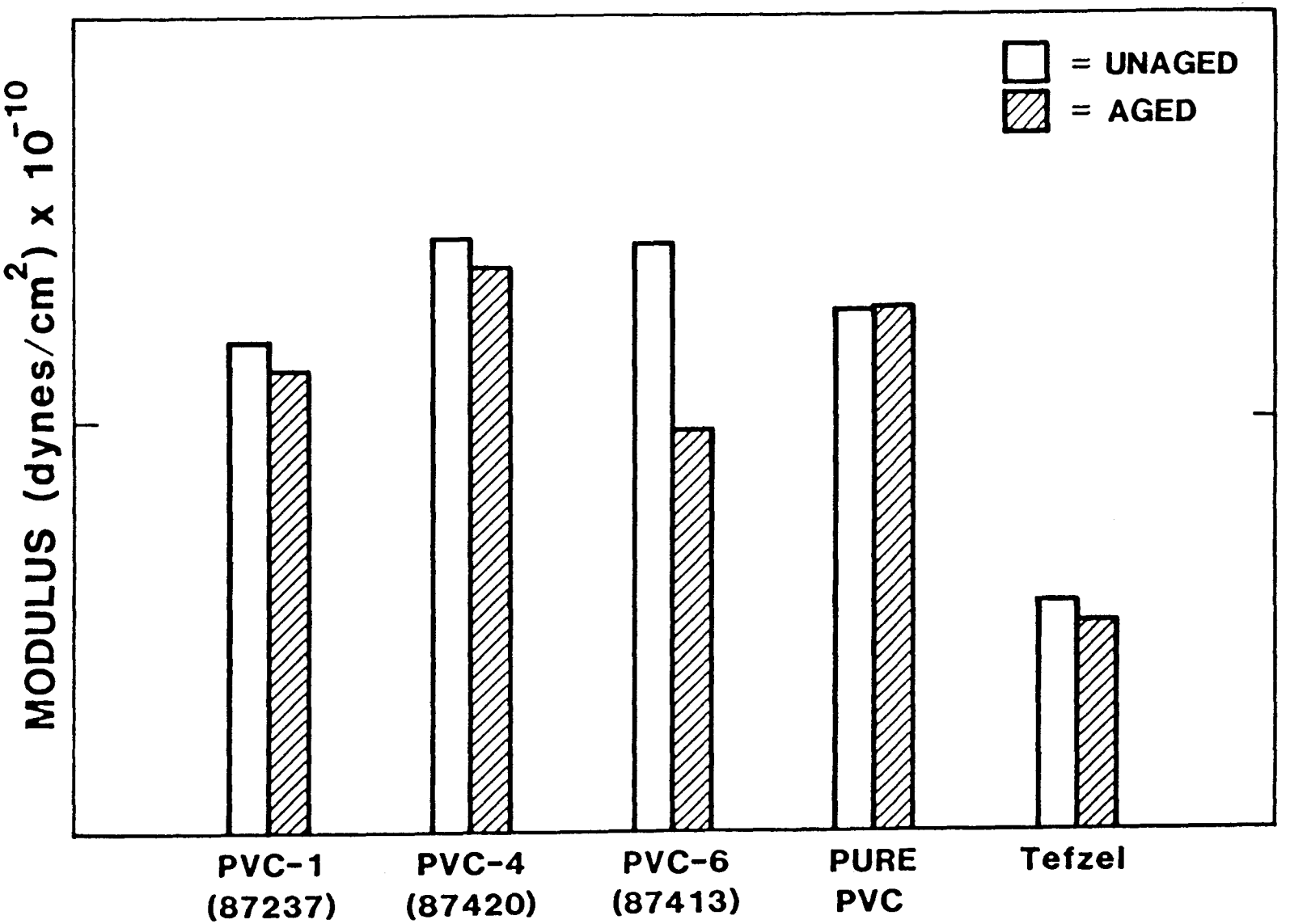

Figure 4. Effect of aging on the shear modulus of various thermoplastics. Aging conditions: 70°C for two weeks in a bromine-containing electrolyte.

EXAFS STUDIES OF ELECTROCHEMICAL SYSTEMS

J. McBreen
Brookhaven National Laboratory
Upton, NY 11973

Since 1985 several in-situ techniques have been developed at Brookhaven National Laboratory (BNL) for X-ray absorption Spectroscopy (XAS) of electrodes. This has included X-ray Near Edge Absorption Spectroscopy (XANES) and Extended X-ray Absorption Fine Structure (EXAFS) investigations. Conventional EXAFS studied have been done using a stepped monochromator at The National Synchrotron Light Source (NSLS) at Brookhaven National Laboratory (BNL). In addition time resolved EXAFS have been done using a dispersive beamline at LURE-CNRS (Laboratoire pour l'U-tilisation Rayonnment Electromagnetique) in Orsay, France. The in-situ investigations included XANES and EXAFS studies of several electrodes under actual operating conditions. This included nickel oxide battery electrodes in strong alkali, the formation of supersaturated zincate solutions at discharging zinc electrodes in 12M KOH and platinum fuel cell electrodes in several acids. Preliminary studies have been done on underpotential deposited (UPD) monolayers of Cu and Pb and the products of methanol oxidation on carbon supported platinum in acid electrolytes. Time resolved EXAFS has been coupled with cyclic voltammetry on nickel oxide and carbon supported platinum electrodes. In addition extensive ex-situ EXAFS studies have been done on complexes in zinc bromide electrolytes and on the pyrolysis and products of adsorbed Fe and Co macrocyclics on various carbons.

XAS

XAS in its simplest form is the accurate measurement of the X-ray absorption coefficient (μ) of a material, as a function of photon energy, in an energy range that is below and above an adsorption edge of one of the elements in the material. The absorption edge is due to the liberation of a K-shell or L-shell electron. At low photon energies (<50 eV) the excited electron undergoes multiple scattering in the vicinity of the excited atom. This part of the spectrum is the XANES and it provides information about the local coordination symmetry and the electronic state (e.g. valence state) of the absorbing atom. At higher energies the electrons are excited to the continuum and there are oscillations in μ due to a final state interference effect between the outgoing photoelectron wave of the excited electrons and the backscattered wave from neighbouring atoms. This is the EXAFS region and it can be explained the basis of local spatial structure alone. The parameters that can be found from EXAFS analysis are coordination numbers, coordination distances and the relative measures of the static and dynamic disorder in the system. Fortunately, the theory of EXAFS has been worked out in detail. XAS is very useful for in-situ electrochemical studies since both the probe and the signal are X-rays. The great advantage is that the actual structure probe is the scattered electrons, hence the ability to get short range characteristics.

Thus it is excellent for investigating amorphous materials and and electrolytes. Another advantage is that it is element specific and as a result is very useful in the study of composites such as fuel cell and battery electrodes.

EXAFS Studies of Zincate Electrolytes

Three EXAFS investigations were made on zincate electrolytes. This included (1) a preliminary study of 8.4 M KOH + 0.74 M ZnO, (2) an in-situ study of zincate formation in Zn/AgO cells with a 12 M KOH electrolyte and (3) studies of 0.74 M ZnO in 8.4 M NaOH, KOH, RbOH and CsOH. In the case of the in-situ studies measurements were done in electrolytes with various additions of silicate or sorbitol.

The EXAFS results were the same in all cases irrespective of the degree of supersaturatiopn or the alkali used. In some cells the solubility exceeded 4 M. The k^1 weighted radial structure functions displayed two peaks. Analysis of the first peak is consistent with the presence of $Zn(OH)_4^=$ and a Zn-O bond length of 1.97 Å. The second peak in the radial structure function was at 2.8 Å. Three possibilities for the second peak are (i) dimerization of zincate, (ii) ion pairing with the alkali ions, or (iii) waters of hydration. The fact that the second peak almost dissappears in the k^3 weighted transform eliminates the first option. The abscence of an increase in this peak in RbOH or CsOH eliminates ion pairing with the alkali ion. So the second peak must be due to waters of hydration around the zincate ion.

XAS Studies of the Nickel Oxide Electrode

The utility of XAS was demonstrated in in-situ studies of the nickel electrode. Hitherto, only the structure of β-$Ni(OH)_2$ was known in detail. α-$Ni(OH)_2$ and?the charged materials are amorphous and their structure was unknown. Analysis of the EXAFS has elucidated the detailed structure of α-$Ni(OH)_2$ and the charged β- $Ni(OH)_2$ for the first time.

PROJECT GOALS/BATTERY R&D

PROJECT GOAL	R&D ACTIVITY
STABLE HIGH CAPACITY DENSITY ZINC ELECTRODES	ZINC MORPHOLOGY AND DEPOSITION KINETICS STUDIES
	EXAFS STUDIES OF COMPLEXES IN $ZnBr_2$ AND ALKALINE ELECTROLYTES
IMPROVE BATTERY EFFICIENCY	BROMINE TRANSPORT IN SEPARATORS
IN SITU TECHNIQUES	EXAFS AND XANES STUDIES OF BATTERY AND FUEL CELL MATERIALS - Nickel Oxide Electrode

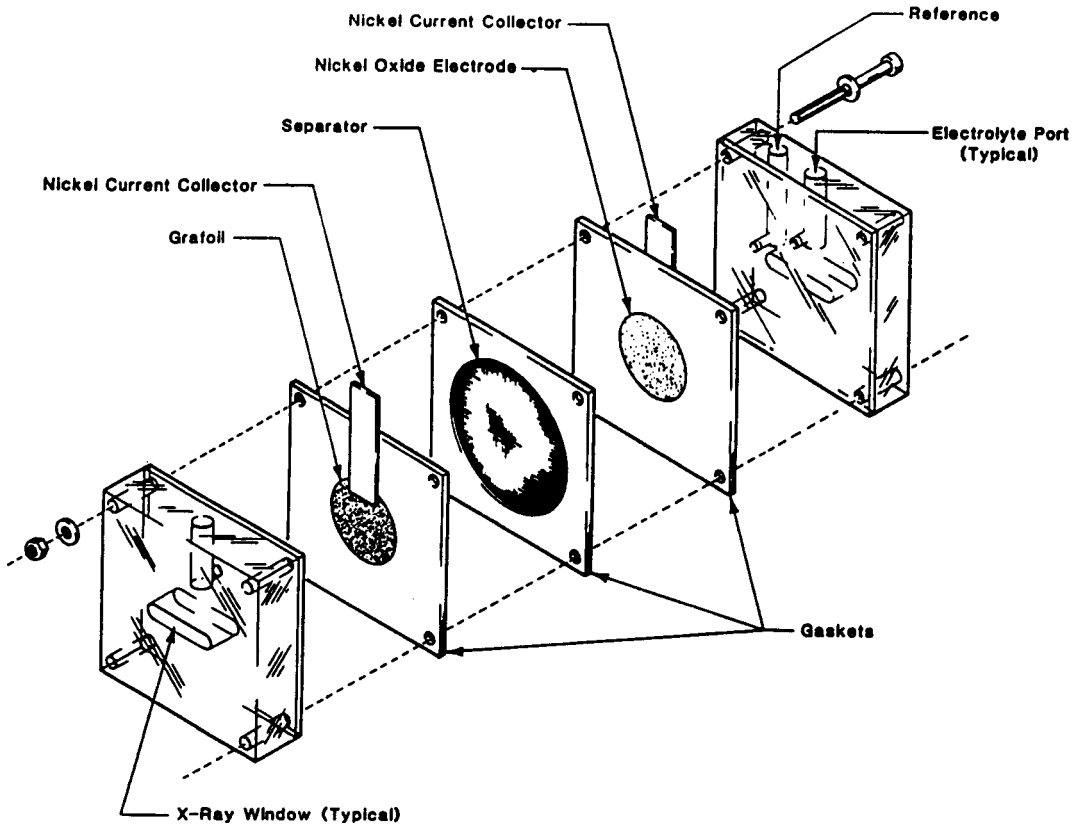

Cell for in-situ X-ray absorption measurements on nickel oxide electrodes.

STRUCTURE OF $Ni(OH)_2$; (A) BASAL PLANE, (B) STACKING ALONG c-AXIS

Ni-Ni COORDINATION SHELLS ARE INDICATED 1,2,3.

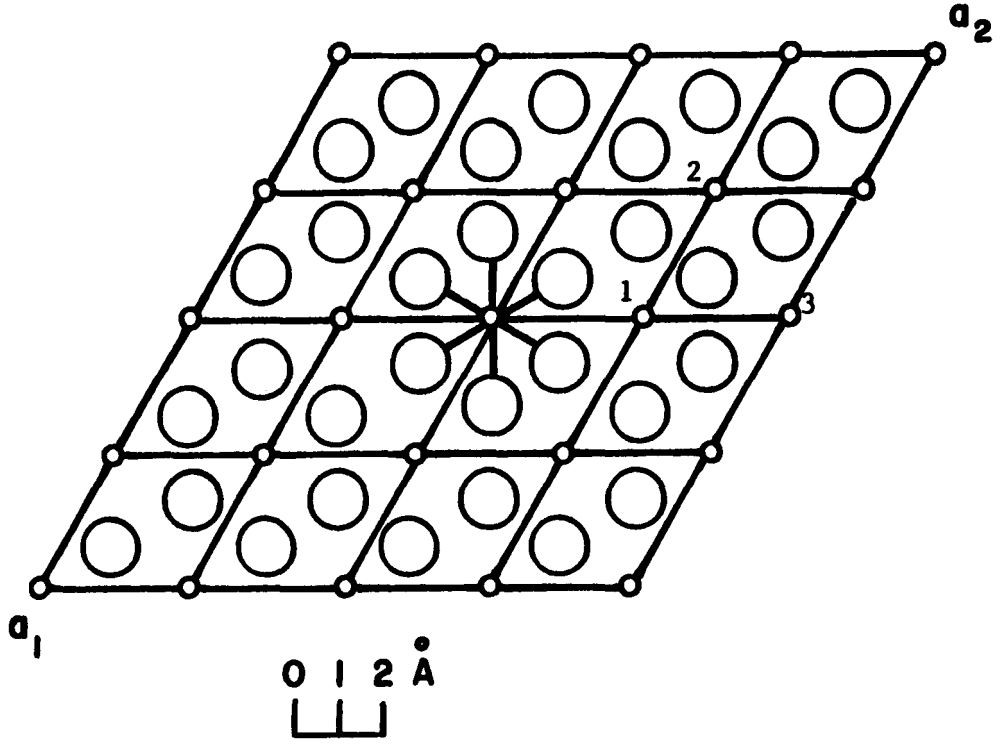

A

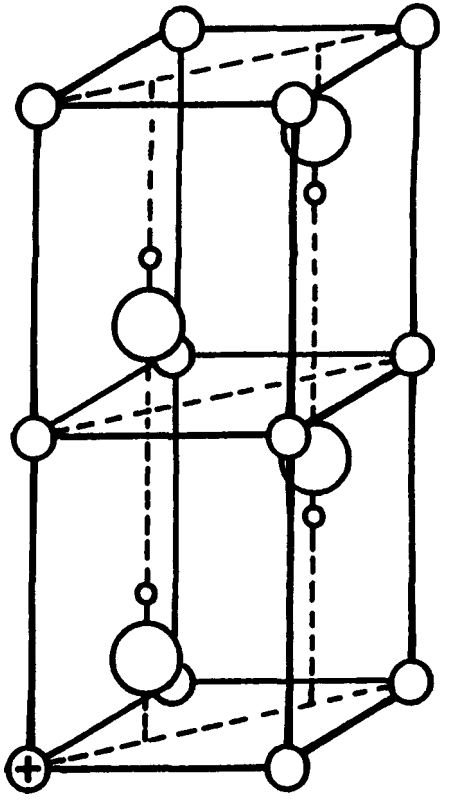

B

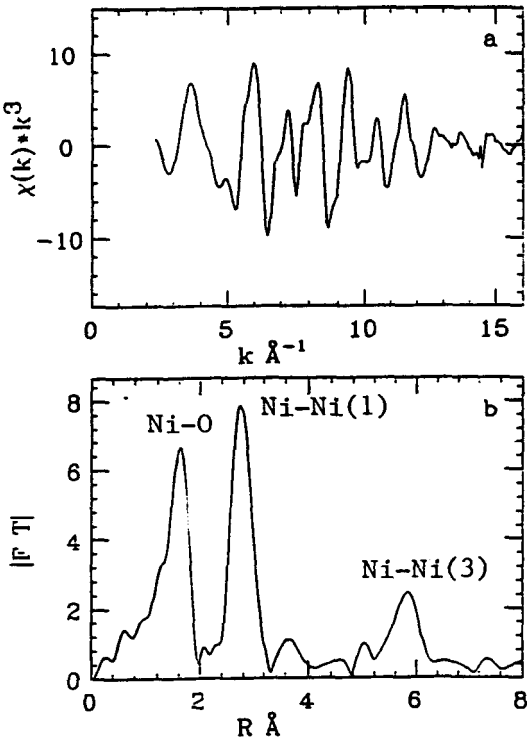

(a) EXAFS and (b) radial structure function for a dry β-Ni(OH)$_2$ electrode.

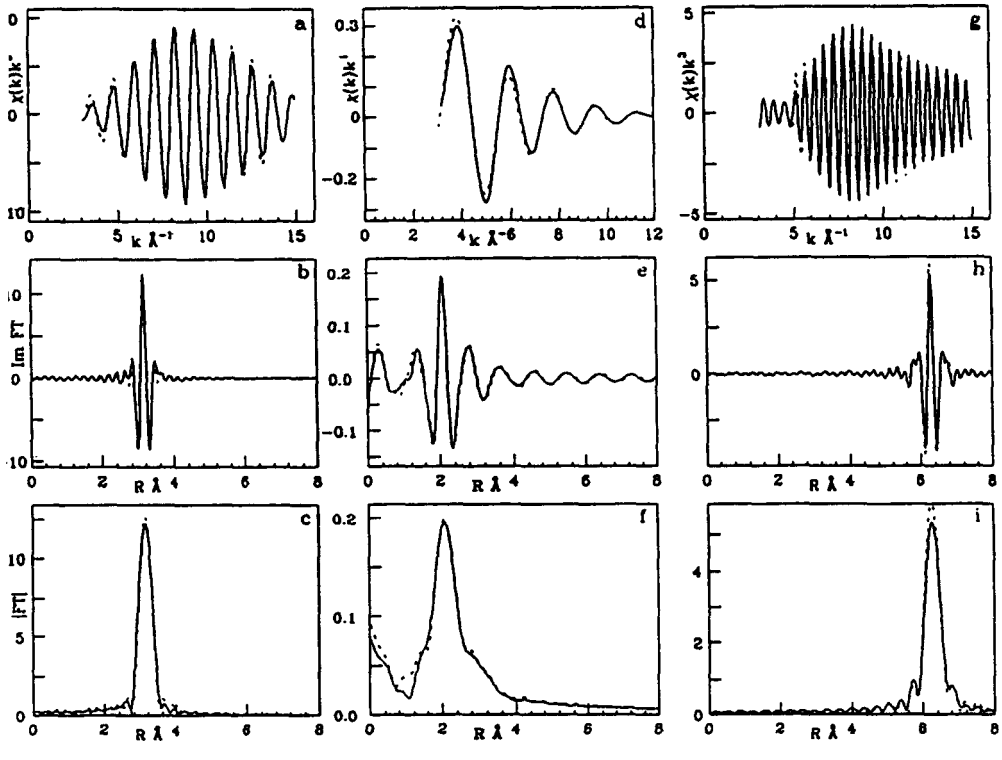

Calculated fits (- - -) to experimental EXAFS results (——) for β-Ni(OH)$_2$ at 77K using Ni foil and NiO as the reference compounds.

Structural parameters obtained from <u>in-situ</u> EXAFS on cycled nickel oxide electrodes (NOE).

Sample	Shell	R	N	$\Delta\sigma^2$, $Å^2$	ΔE_o eV
NOE charged once	$Ni-O_1$	1.88	4.1	-0.0039	7.01
	$Ni-O_2$	2.07	2.2	0.010	0.32
	$Ni-Ni_1$	2.82	4.7	-0.0023	6.55
	$Ni-Ni_2$	3.13	1.0	0.0072	-0.09
NOE Charged + Discharged	Ni-O	2.05	5.7	0.0016	1.92
	$Ni-Ni_1$	2.82	1.0	0.0009	-7.92
	$Ni-Ni_2$	3.13	5.0	0.0007	0.08
	Ni-Ni(3)	6.25	5.7	0.0029	-2.65
NOE Recharged	$Ni-O_1$	1.88	4.1	-0.0039	7.05
	$Ni-O_2$	2.07	2.2	0.009	0.48
	$Ni-Ni_1$	2.82	4.7	-0.002	6.63
	$Ni-Ni_2$	3.13	1.0	0.006	0.11

Accuracies: N:±15%, $\Delta\sigma^2$:±15%, R:±0.01 Å

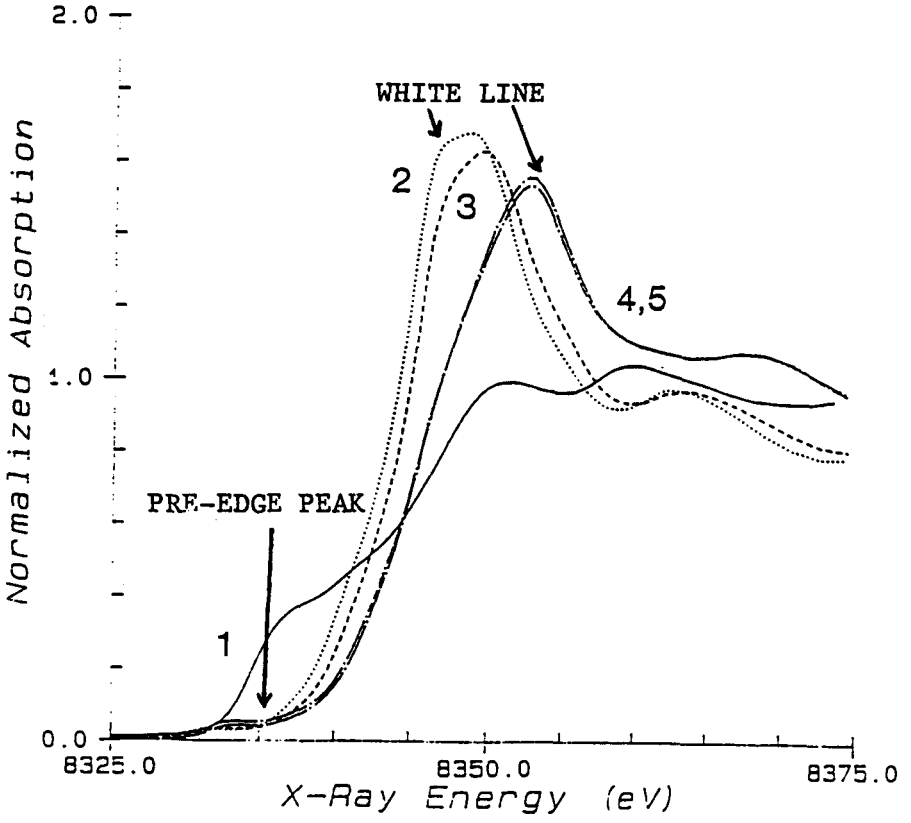

Nickel K-absorption edges for (1) Ni foil, (2) dry electrode, (3) after first discharge, (4) after first charge, and (5) after second charge.

XAS STUDIES OF $Ni(OH)_2$ ELECTRODES
CONCLUSIONS

- $Ni(OH)_2$ STRUCTURE DETERMINED BY EXAFS AGREES WITH BEST NEUTRON DIFFRACTION DATA
- STRUCTURE OF CHARGED MATERIAL WAS UNKNOWN BECAUSE IT IS AMORPHOUS
- XAS DATA INDICATE THAT IN THE CHARGED MATERIAL THE Ni ATOMS HAVE A DISTORTED OCTAHEDERAL COORDINATION
    - EXAFS ANALYSIS REQUIRES A TWO SHELL FIT
    - XANES SPECTRA INDICATES A DISTORTED COORDINATION
        - INCREASED PRE-EDGE PEAK
        - DECREASE IN WHITE LINE INTENSITY
- IN-SITU TIME RESOLVED XANES DEMONSTRATED
- FURTHER WORK SHOULD BE DONE ON IN-SITU STUDIES OF TOPOTACTIC ELECTROCHEMICAL REACTIONS OF THIS TYPE

AQUEOUS BATTERY DEVELOPMENT

CHAIRPERSON:

Glenn Cook
Electric Power Research Institute

BIPOLAR LEAD/ACID BATTERY DEVELOPMENT

T. J. Clough,
ENSCI Inc.
R. L. Scheffler,
Southern California Edison

The bipolar lead/acid battery design was originally developed by the Jet Propulsion Laboratory (JPL) and Atlantic Richfield Company and is now being developed for commercial applications by ENSCI Inc. Southern California Edison (SCE) is contributing support to current development efforts as part of SCE's electric transportation research, which is focused on accelerating development of commercially viable electric vehicles to improve air quality and increase off-peak electrical demand.

The key to widespread market acceptance of electric vehicles is the development of an economical battery which could overcome the vehicle range and performance limitations imposed by conventional lead/acid batteries. The ENSCI bipolar battery could increase fleet van range up to 100 miles, a 60-70% increase over current levels. Power capacity would be even more dramatically improved (by at least a factor of four.)

The battery is a sealed maintenance free design with oxygen recombination. It makes use of a bipolar configuration with a light weight conductive polymer composite bipolar plate for increased energy and power density. It incorporates electronically conductive tin dioxide coated glass fibers in the positive active material and as part of the bipolar plate composite structure. These fibers enhance current flow (power capability) and improve battery life.

Projections based on laboratory developed data show bipolar battery energy densities could be in excess of 50 Wh/kg, similar to levels achieved by nickel/iron batteries. Performance and cycling information was obtained at JPL on a 4-volt bipolar battery assembled with ENSCI's newest bipolar substrate. ENSCI's battery cycled in excess of 1200 cycles at the 5-minute rate to 80% depth-of-discharge with essentially no change over time in the constant current polarization curve.

One of the most significant manufacturing advantages of the bipolar battery is that it features conventional polymer composite and battery assembly manufacturing processes. The bipolar manufacturing process consists of producing preforms and molded 2-volt cells and end plates using conventional equipment and existing commercial capacity. The cells and end plates are then assembled into batteries using a process plan analogous to the manufacture of a conventional lead-acid monopolar battery. These processes translate directly into commercially competitive manufacturing costs, low capital, and short lead times to establish commercial manufacture.

The bipolar lead-acid battery offers a near term high performance energy storage system that can be cost competitive with conventional lead-acid batteries. It significantly out performs conventional batteries, yet takes advantage of the existing manufacturing and market infrastructure for lead-acid batteries.

- **HIGH CAPACITY AND ENERGY**
- **50+% REDUCTION IN WEIGHT AND VOLUME**
- **HIGH POWER**
- **LIGHTWEIGHT COMPOSITE STRUCTURE AND RUGGEDNESS**
  - NO HEAVY LEAD GRIDS
  - NO HEAVY INTERCELL CONNECTS
- **SEALED MAINTENANCE FREE**
  - NO WATERING SYSTEM
  - NO HIGH TEMPERATURE THERMAL INSULATION
  - NO HYDROGEN GASSING

SBLA Battery Module

Voltage - 12 volt
Capacity - 10 A.hr. to 200 A.hr

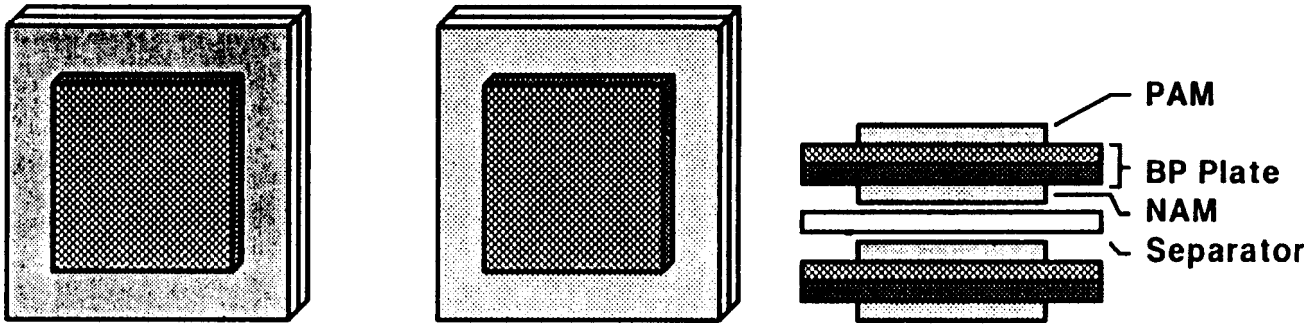

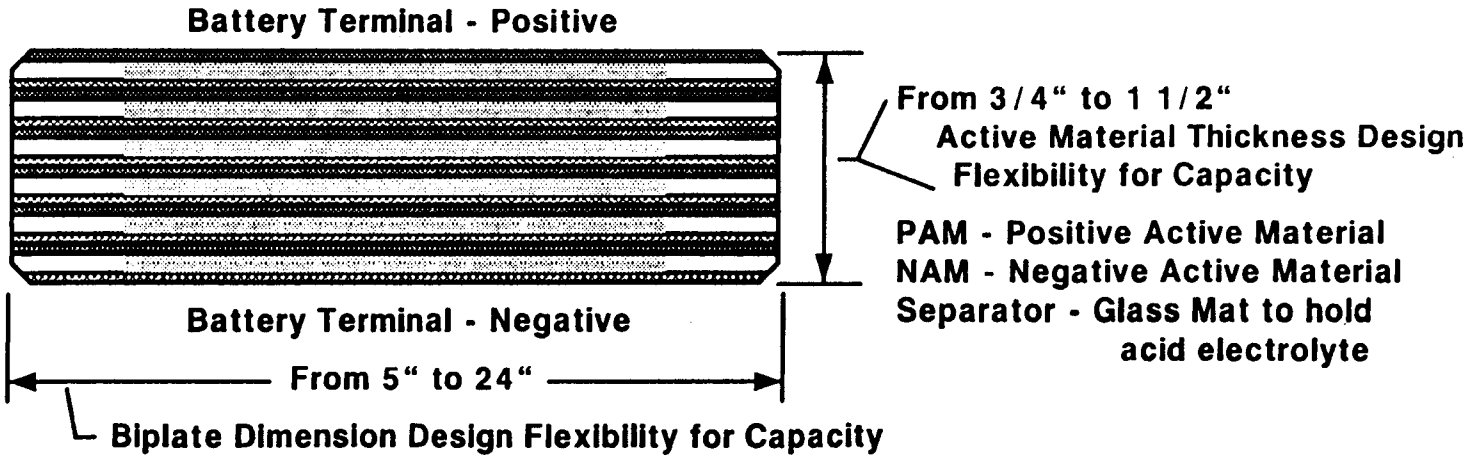

EV Battery Comparison of Specific Energy

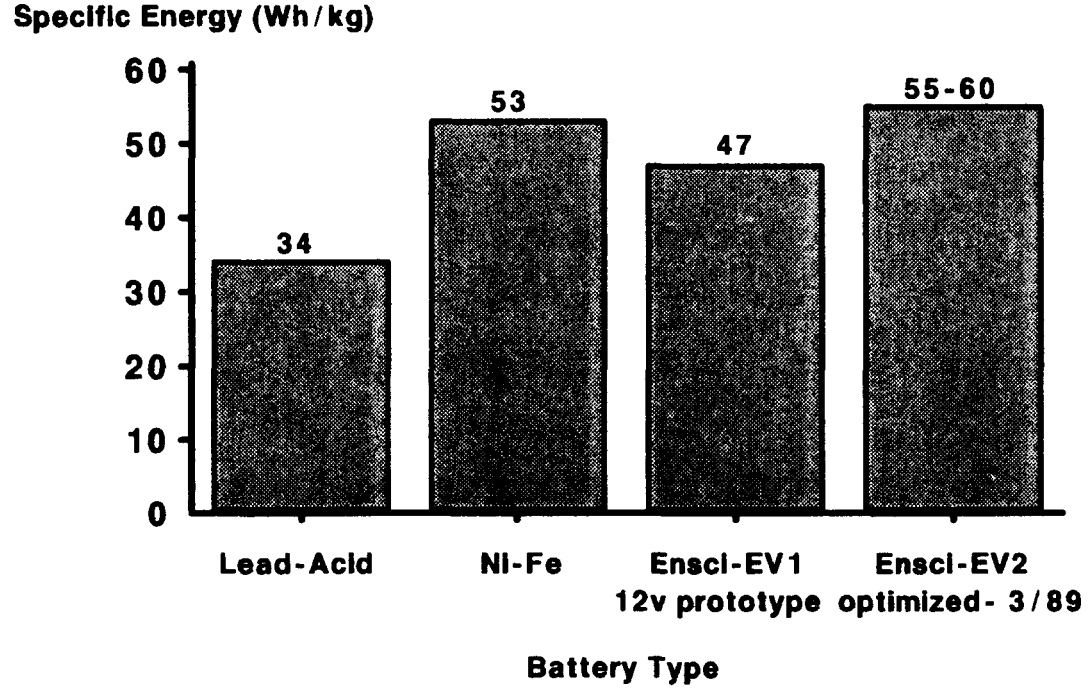

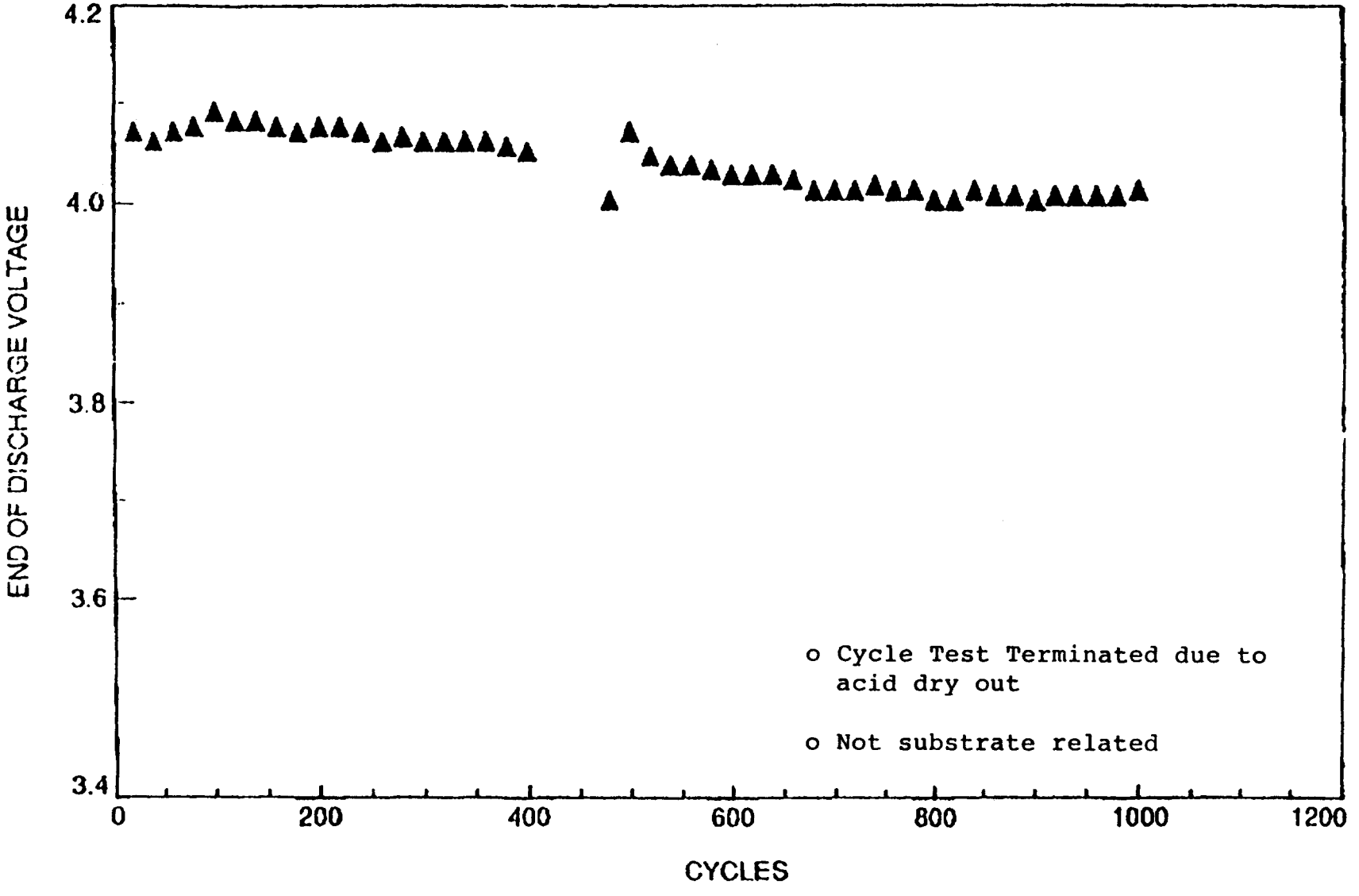

Cycle Life Data on 2-Cell Bipolar Battery with Improved ENSCI Bipolar Substrate #120. Discharge at 120 mA/cm^2. (Source JPL)

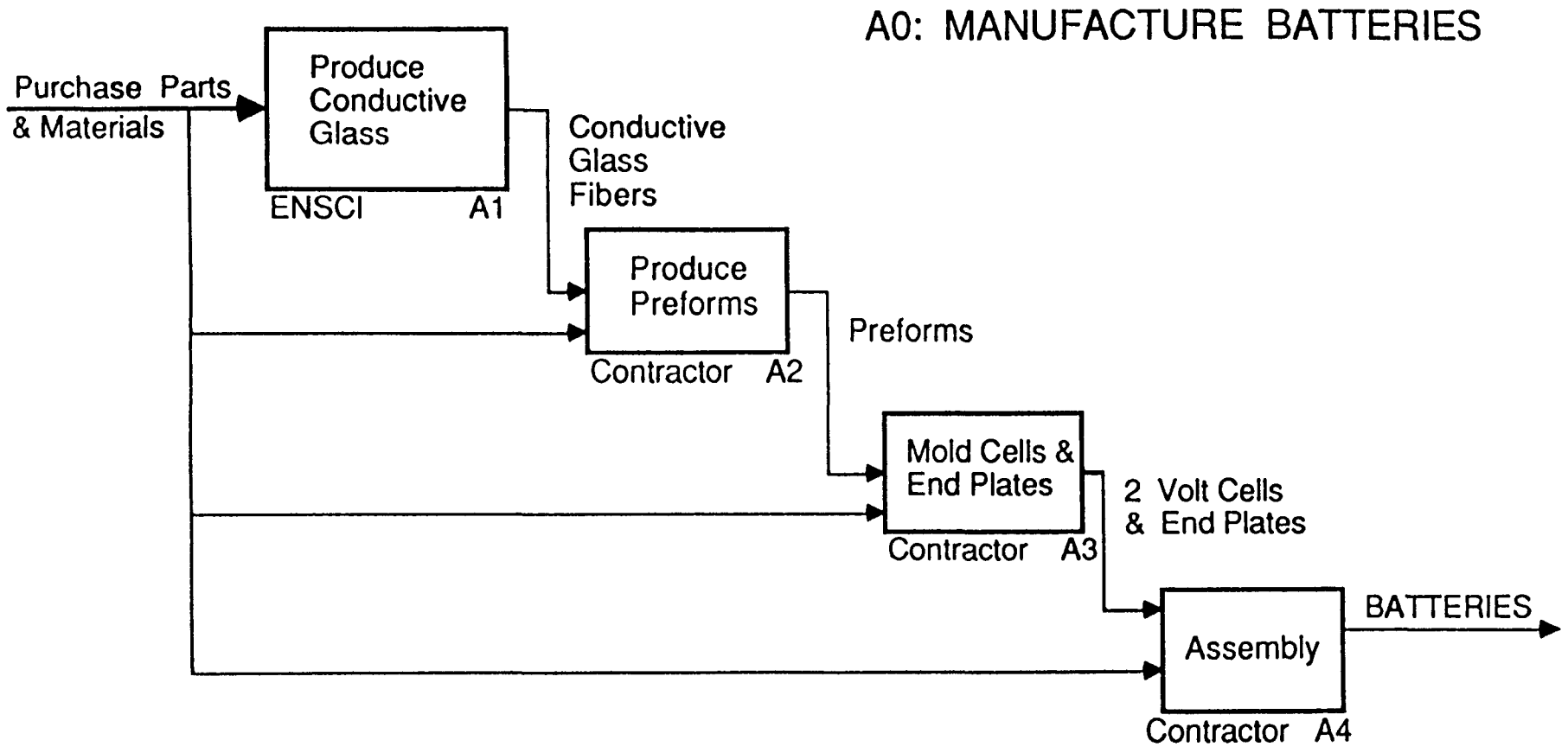
A0: MANUFACTURE BATTERIES
Purchase Parts
& Materials
Produce
Conductive
Glass
ENSCI
A1
Conductive
Glass
Fibers
Produce
Preforms
Contractor
A2
Preforms
Mold Cells &
End Plates
Contractor
A3
2 Volt Cells
& End Plates
Assembly
Contractor
A4
BATTERIES

Bipolar Battery Manufacturing Plan

- **Conductive glass fibers**

  Semi-continuous pilot plant - operation early 1989

- **Component production battery assembly**

  Existing capacity and conventional equipment - to be contracted for in 1989

FLOW-BY LEAD ACID BATTERY DEVELOPMENT

M.G. Andrew
Johnson Controls, Inc.
Advanced Battery Business Unit
5757 N. Green Bay Avenue/P.O. Box 591
Milwaukee, WI 53201

The Advanced Battery Business Unit (ABBU) of Johnson Controls (JCI) is working on a contract sponsored by the United States Department of Energy (DOE) for the design and development of an advanced lead-acid battery system for electric vehicles. Progress to date is based on the concept of flow-by electrolyte circulation through the cells comprising the battery pack. In this configuration the electrolyte flows parallel to the electrode surfaces in order to provide stable electrical performance throughout cycle life. Significant improvements in module based specific energy during the last year have positioned this technology within 7% of the contract goal. Present activities are directed towards achieving the formidable life goal of 450, 80% DOD cycles. Ultimately, a 180 volt, 39 kWh battery system will be fabricated for evaluation in an electric delivery van.

The performance goals for the flow-by battery are very ambitious. Development efforts have been focused on providing significant increases in active material (AM) utilization, while minimizing non-reactive and peripheral component mass, in order to maximize module specific energy. The aggressive specific energy goal of 56 Wh/kg requires a 40% increase compared to the best established lead acid technology, and it is based on the SFUDS discharge profile, a series of constant power steps in which the power levels are a function of battery system weight. The life goal of 450 cycles at 80% DOD is extremely challenging, and due to the transient power nature of the SFUDS profile, it is considerably more difficult to achieve than if evaluated under constant current discharge conditions, even if the average discharge power is the same.

JCI's proprietary Lead-Acid Battery Mathematical Model (LABMM) has been a key tool in determining the optimal values for critical electrochemical design parameters. Advances during the last six months have resulted in the achievement of a module based SFUDS specific energy of 52.4 Wh/kg. Scale-up of the present module design to satisfy the battery system capacity specification will result in an additional 5% improvement in specific energy to 55 Wh/kg.

The interim 1990 life goal of 100 cycles is based on the present status of 50 cycles and recent design modifications resulting in a one-third increase in the PAM mass fraction to 25%. Current engineering efforts are coordinated around a single objective: achieving the ultimate life goal of 450 SFUDS cycles without compromising specific energy. Preserving the integrity of the positive active material (PAM) is the main thrust of these efforts. A two-pronged approach is being pursued: (i) increasing the stress threshold of the PAM, and (ii) refining cell parameters to ensure that the PAM stress threshold is not reached. Computer-aided engineering design (CAEDS) has been used to optimize the electrolyte flow parameters inside the cell stack in order to minimize PAM erosion and deleterious morphological changes that contribute to premature failure. A statistically designed experiment to determine the main effects of and interactions between nine design variables known to affect life is nearing completion. Preliminary results suggest that element compression is a major factor in extending life. Tasks are underway to develop a

subsystem capable of mechanically buttressing the active materials on a battery system scale in order to achieve a factor of three improvement in life. Other experiments are in progress to determine the interactions between compression level and peak voltage during the critical gassing onset phase of recharge.

Thermal modelling of the projected full size, 180 volt battery system is underway. A forced air cooling/heating system will complement the heat transfer advantage offered by the flow-by circulation. Laboratory experiments are in progress to determine the feasibility of an electrolyte circulation subsystem that derives its power from the vehicle dynamics. Operating/maintenance safety features are given priority consideration as this project moves toward the battery system deliverable.

FLOW-BY LEAD-ACID
PERFORMANCE GOALS

Battery Performance	Goals
Specific Energy (SFUDS)	56 Wh/kg
Peak Specific Power (SFUDS)	79 W/kg
Electric Van Range (SFUDS)	94 miles
Cycle Life (80% DOD)	450 cycles
Energy Efficiency	75%

DEVELOPMENT STRATEGY

* Limits of PAM Utilization
* New Baseline Cell
* Specific Energy Milestone
* Cycle Life Improvement
* Battery System Design

FLOW-BY DESIGN

* Parallel to Electrode Surface
* MTC Equivalent to Flow-through
* Uniform Distribution via Diverter
* Thermal Management
* High Specific Energy

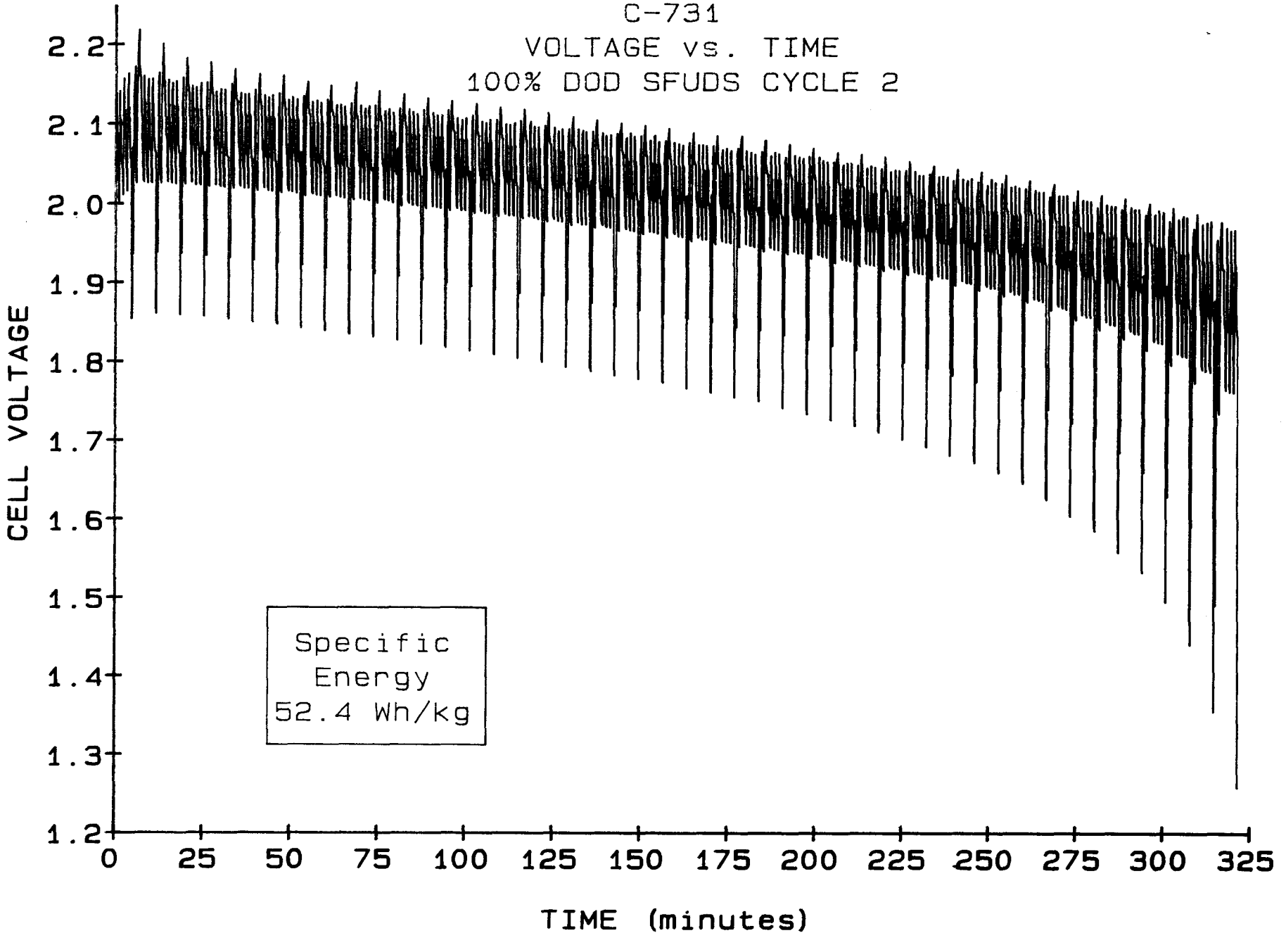
C-731
VOLTAGE vs. TIME
100% DOD SFUDS CYCLE 2
CELL VOLTAGE
2.2
2.1
2.0
1.9
1.8
1.7
1.6
1.5
1.4
1.3
1.2
0
25
50
75
100
125
150
175
200
225
250
275
300
325
TIME (minutes)
Specific
Energy
52.4 Wh/kg

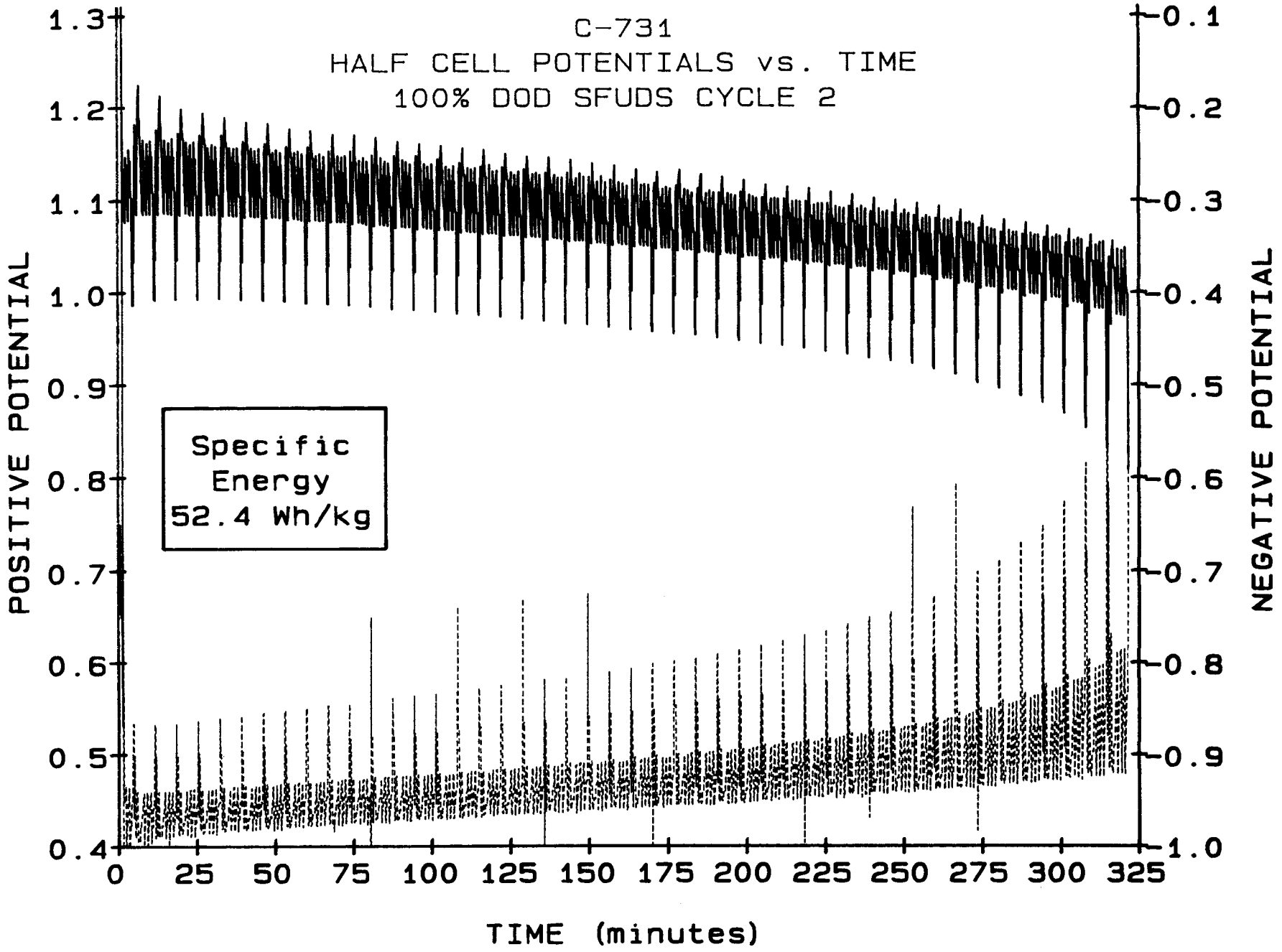
C-731
HALF CELL POTENTIALS vs. TIME
100% DOD SFUDS CYCLE 2
Specific
Energy
52.4 Wh/kg
POSITIVE POTENTIAL
NEGATIVE POTENTIAL
TIME (minutes)
1.3
1.2
1.1
1.0
0.9
0.8
0.7
0.6
0.5
0.4
0.1
0.2
0.3
0.4
0.5
0.6
0.7
0.8
0.9
1.0
0
25
50
75
100
125
150
175
200
225
250
275
300
325

FLOW-BY LEAD-ACID
PERFORMANCE GOALS and STATUS

Battery Performance	Goals	Status
Specific Energy (SFUDS)	56 Wh/kg	52.4 Wh/kg
Peak Specific Power (SFUDS)	79 W/kg	79 (210) W/kg
Electric Van Range (SFUDS)	94 miles	70.2 miles
Cycle Life (80% DOD)	450 cycles	52 cycles
Energy Efficiency	75%	79%

NICKEL/IRON BATTERY DEVELOPMENT

Gary G. Paul
Eagle-Picher Industries, Inc.

The goals and objectives for the development of the Nickel/Iron battery is to establish a battery that a) has an energy density greater or equal to 56 Wh/Kg, b) has a volumetric density of 100 Wh/L, c) has an optimum configuration, d) has an energy efficiency of 70%, and e) has displayed a cycle life of 1200 Cycles.

The Nickel/Iron battery has demonstrated performance which nearly meets these goals. Early performance exceeding 60 Wh/Kg and a volumetric density of 120 Wh/L. This was accomplished within the overall design constraints of the DSEP battery; a practical, production feasible module.

Energy efficiency numbers of over 70% have been demonstrated in the laboratory presently. Cycle life is still being evaluated at this time. Previous designs of the Nickel/Iron battery have demonstrated an excess of 2000 cycles.

Other development goals are to move toward cost reductions through design improvements through efficient materials utilization along with improved manufacturing methods.

The cost driver of the battery is the positive electrode. This is because it contains the majority of the nickel used in the battery. The possibilities for cost reduction in this area have been improved recently with the introduction a non-woven mat of nickel fiber. The material is manufactured by the National Standard Company under the trade name Fibrex (TM). It has the potential for substantial improvements in energy density along with material cost reduction.

Early work with the material was unsuccessful because of problems in loading the active material and the resulting dimensional instability of the finished nickel electrode. The major problems appeared to be due to the open structure and large pore size of the mat and its lack of mechanical strength.

The material has been improved by the introduction of cross-linking the mat with carbonyl nickel powder. This new material has the potential for providing the necessary mechanical strength and dimensional stability required for long cycle life battery electrodes.

The problem associated with loading the active material into the fiber mat have been overcome in part by applying a periodic reverse impregnation process. The method is essentially the same as the normal aqueous electrochemical process except that the polarity of the electrodes is periodically reversed during impregnation. Periodic current reversal is commonly used in the metal plating industry to promote a more uniform deposited film on the work piece. It appears to have similar load leveling effect in impregnating nickel electrodes with active material.

Work is underway to continue investigation of plating/deplating current densities and cycle times to achieve optimum results. This method has an additional benefit of yielding a 20% higher ampere-hour efficiency in loading the plate over the normal constant current process.

Testing was performed comparing the rate capability of sintered and fiber nickel plates at various states of charge (SOC) but the fiber-based plate supported higher current densities at the lower SOC of 25%. The impregnation loading level of the fiber nickel plate was much lower than the standard sintered plate, with a consequent reduction of capacity.

The marked differences in scope and ability to sustain heavy loads at a low state of charge may be only a consequence of the relatively low active material content of the fiber plate. However, it seems likely that the fiber material can be loaded higher and still perform as well as a sintered plate of comparable active material density.

CONCLUSIONS

Test results have shown that fiber-based electrodes can provide performance levels comparable to sintered electrodes, with potential for further weight and cost reductions.

ACKNOWLEDGMENTS

This work was supported by the U.S. Department of Energy/Office of Transportation Systems under Contract DE-AC08-86NV10510

	NIF-170	NIF-200	NIF-220
SPECIFIC ENERGY (C/2)	45 Wh/Kg	49 Wh/Kg	53 Wh/Kg
SPECIFIC PEAK POWER (50% DOD)	139 W/Kg	132 W/Kg	121 W/Kg
VOLUMETRIC DENSITY	90 W/L	107 W/L	117 W/L
DISCHARGE CAPACITY (C/2) 4.5 VOLT CUT-OFF	175 A-hr	199 A-hr	220 A-hr
SIMULATED RANGE (FUDS)	50 MILES	70 MILES	80 MILES

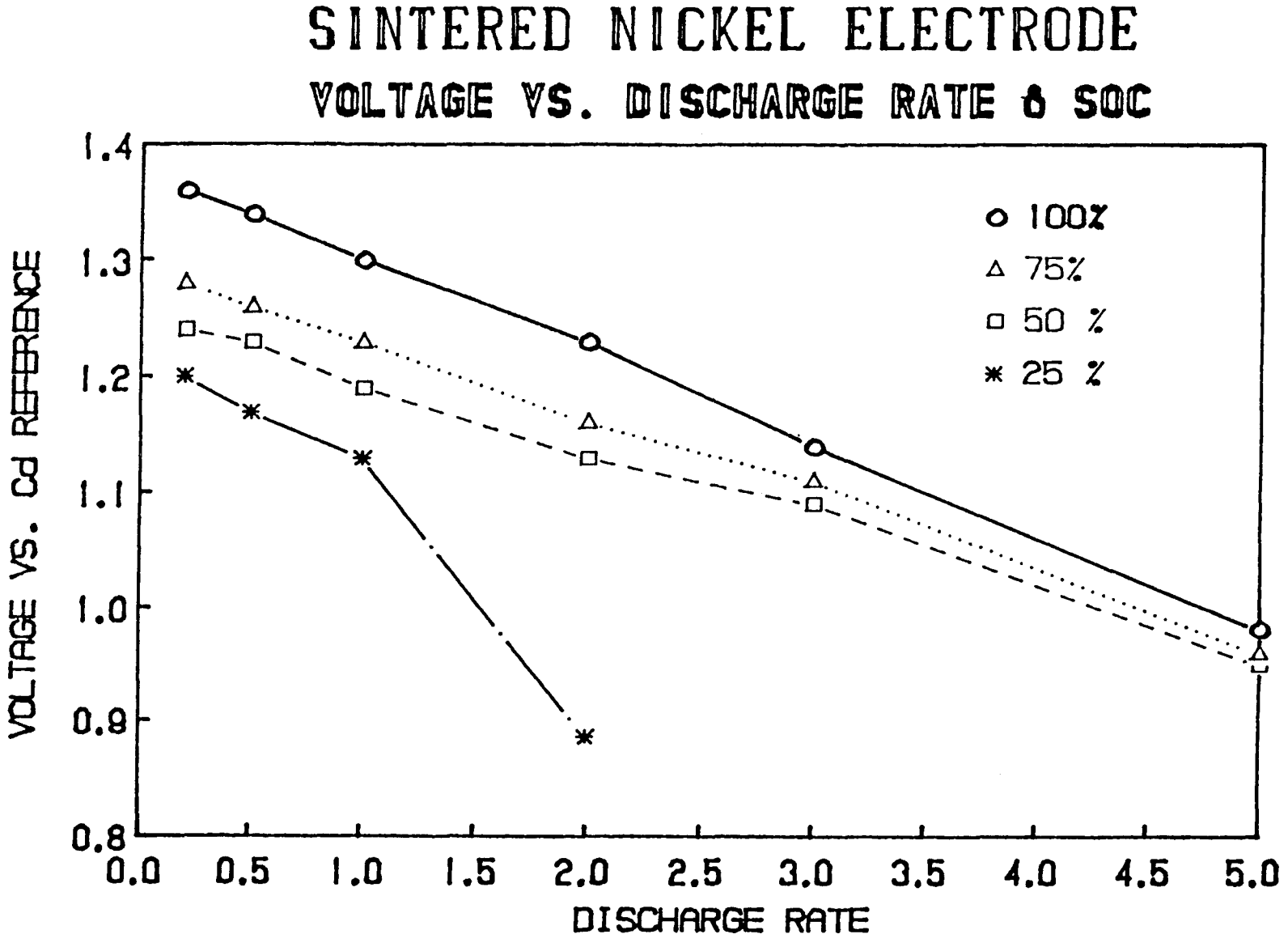
SINTERED NICKEL ELECTRODE
VOLTAGE VS. DISCHARGE RATE & SOC
VOLTAGE VS. Cd REFERENCE
DISCHARGE RATE
100%
75%
50 %
25 %
1.4
1.3
1.2
1.1
1.0
0.9
0.8
0.0
0.5
1.0
1.5
2.0
2.5
3.0
3.5
4.0
4.5
5.0

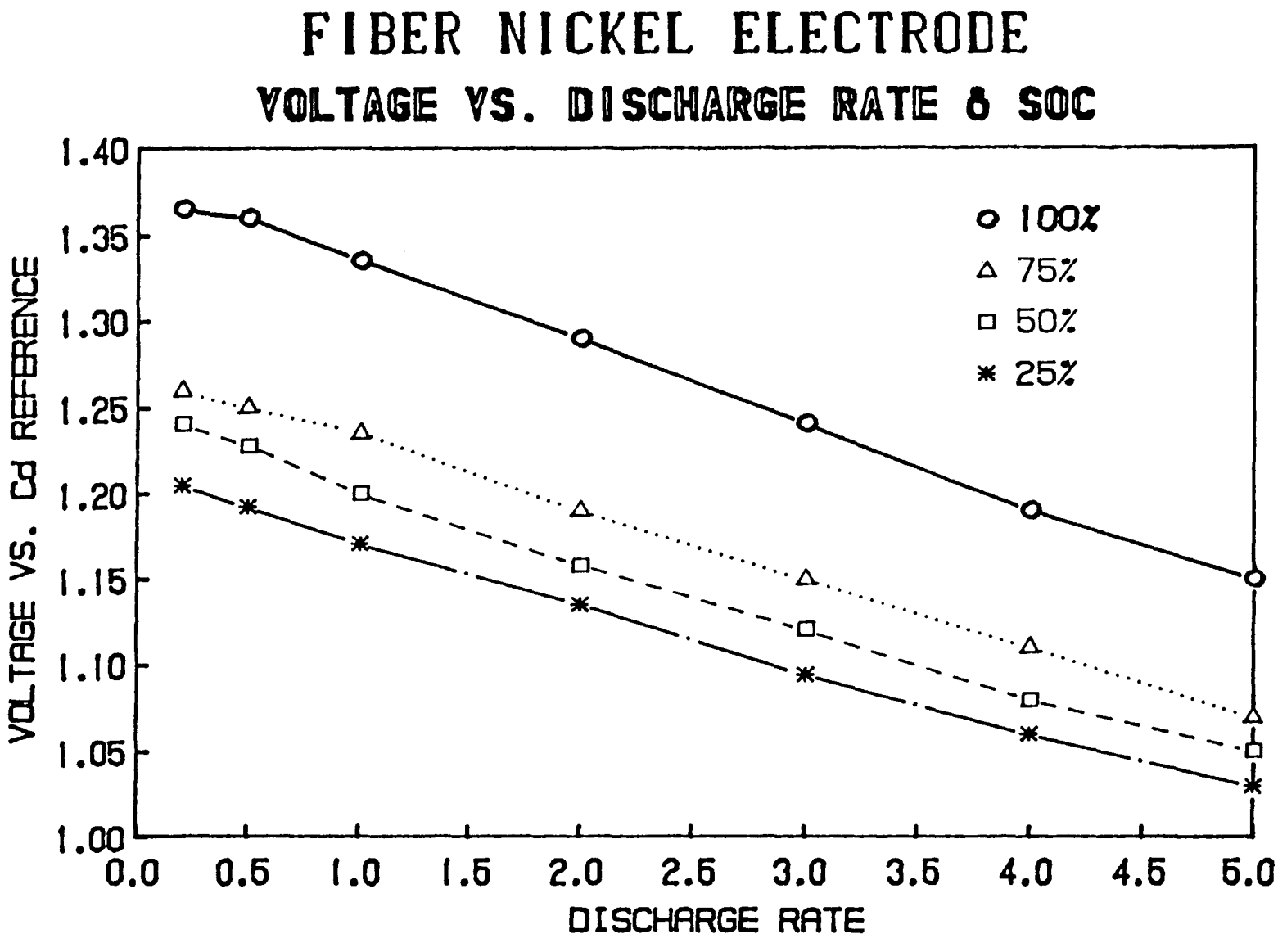
FIBER NICKEL ELECTRODE
VOLTAGE VS. DISCHARGE RATE & SOC
VOLTAGE VS. Cd REFERENCE
1.40
1.35
1.30
1.25
1.20
1.15
1.10
1.05
1.00
0.0
0.5
1.0
1.5
2.0
2.5
3.0
3.5
4.0
4.5
5.0
DISCHARGE RATE
100%
75%
50%
25%

TERRESTRIAL NICKEL/HYDROGEN BATTERY DEVELOPMENT

R. L. Beauchamp, J. P. Zagrodnik
Johnson Controls, Inc./Advanced Battery Business Unit

The Nickel/Hydrogen battery has several advantages over other battery systems, including significantly longer cycle life, no maintenance, high reliability, and an accurate state-of-charge indication. Despite the relatively high initial cost of the system, these advantages can be translated into a competitive life cycle cost (3.9 cents/kWh/cycle), making the system an excellent candidate for photovoltaic and other remote energy storage applications (1).

A program to design, fabricate, and deliver an 8 kWh Nickel/Hydrogen photovoltaic storage battery is continuing at Johnson Controls, Inc. (JCI) under a cost share contract with Sandia National Laboratories (SNL). The program objective is to further reduce the cost of the system and to demonstrate an 8 kWh prototype design which is field deployable.

The JCI terrestrial Nickel/Hydrogen cell module design (Figure 1) consists of a back-to-back configuration of two sintered nickel positives, each with an adjacent separator and a catalytic negative electrode. An absorber is located between the positives to act as an electrolyte reservoir. Several modules are connected in parallel and enclosed in a case to form a 160 Ah cell (Figure 2) and ten cells are connected in series to form a 2 kWh, 12 volt battery (Figure 3). The battery is then enclosed in a fiber wound pressure vessel which acts as the hydrogen reservoir (Figure 4). Four independent 2 kWh batteries, which can be combined in series/parallel to form an 8 kWh deliverable, will be completed in the Fall of 1989.

Cells currently on test at JCI have demonstrated over 1,800 cycles at 83%-84% energy efficiency for an outdated 120 Ah design. More recent 160 Ah design cells have been operating steadily at 83%-86% energy efficiency (98%-99% coulombic efficiency) after nearly 500 cycles (Figure 5). Similar results are being achieved with cells tested at SNL. In addition, SNL has been successfully demonstrating the operation of a JCI 7 kWh battery in a photovoltaic application over the past two years.

Prior to the JCI developmental effort, cost estimates for aerospace Nickel/Hydrogen batteries were well above the level at which any consideration could be given for terrestrial applications (2). Past efforts at JCI had already reduced this cost to $823/kWh (3) and results from the most recent studies have further reduced the cost to $676/kWh (Figure 6). The most significant contributions to the recent cost reductions were the use of a lower cost catalyst and the replacement of the hydrophobic backing membrane on the negative electrode with a lower cost alternative. No detrimental effect on performance has been observed with either of these modifications. Consideration of additional improvements from ongoing core research and further adaptation of proven lead-acid automotive battery mass production techniques indicates that the $375/kWh program goal is achievable.

ACKNOWLEDGEMENT

This development work is funded, in part, by the U.S. Department of Energy and Sandia National Laboratories, under contract No. 57-4683.

REFERENCES

1. D. M. Bush, "Evaluation of Terrestrial Nickel/Hydrogen Cells and Batteries," SAND88-0435, May, 1988.

2. L. J. Burant, W. O. Gentry, "An Interim Cost Study of a Terrestrial Hydrogen/Nickel Oxide Battery," Proceedings of the Eighteenth IEEE Photovoltaic Specialists Conference, October, 1985.

3. R. L. Beauchamp, J. F. Sindorf, "Cost Reductions in the Nickel-Hydrogen Battery," Journal of Power Sources, Volume 22, pp.229-241, 1988.

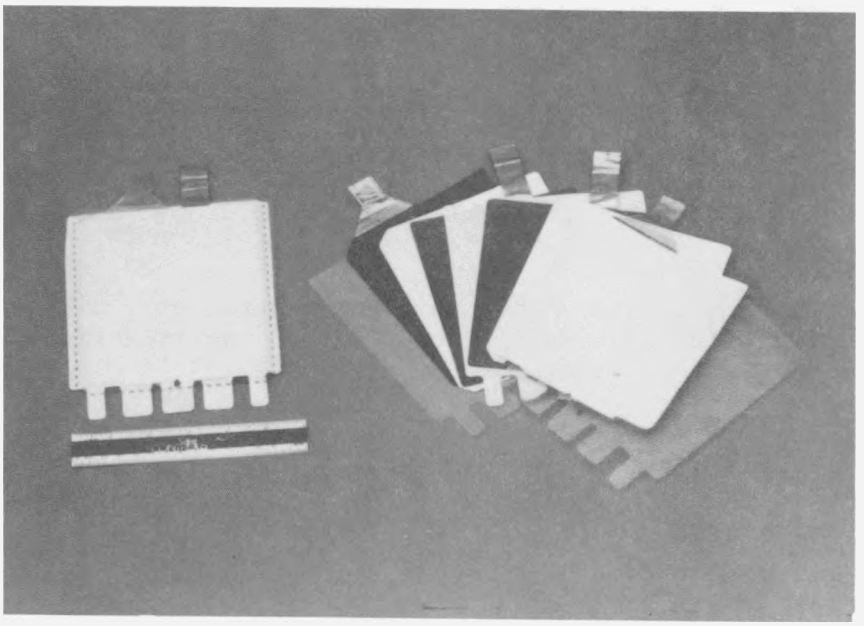

Figure 1

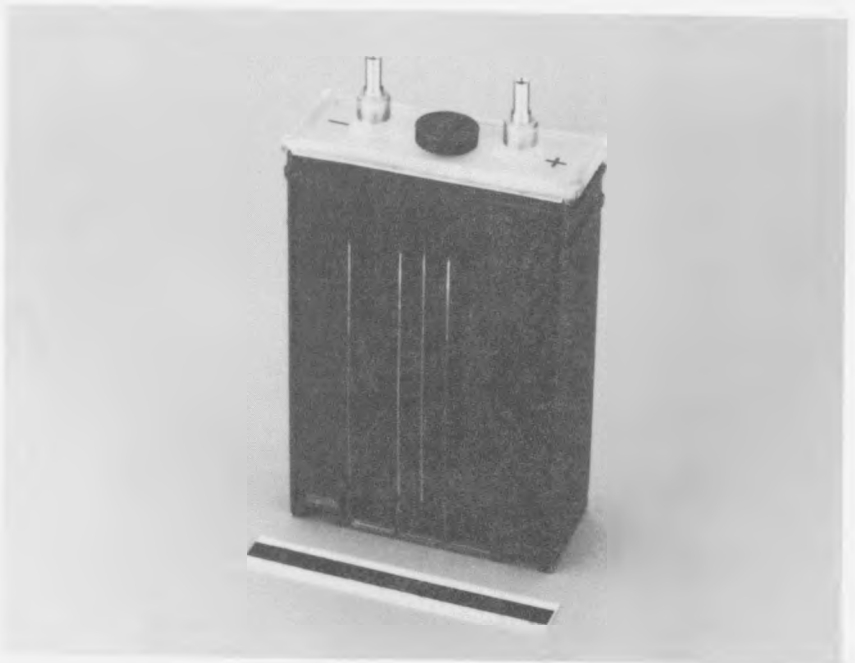

Figure 2

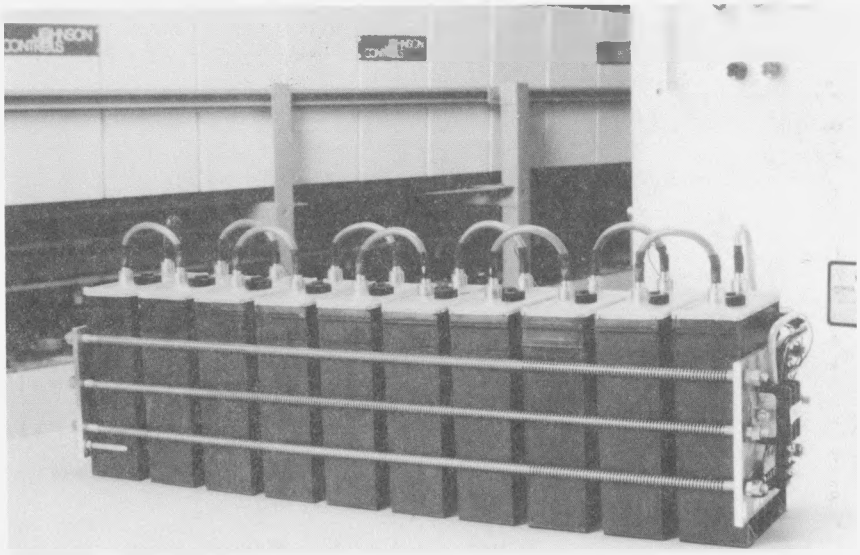

Figure 3

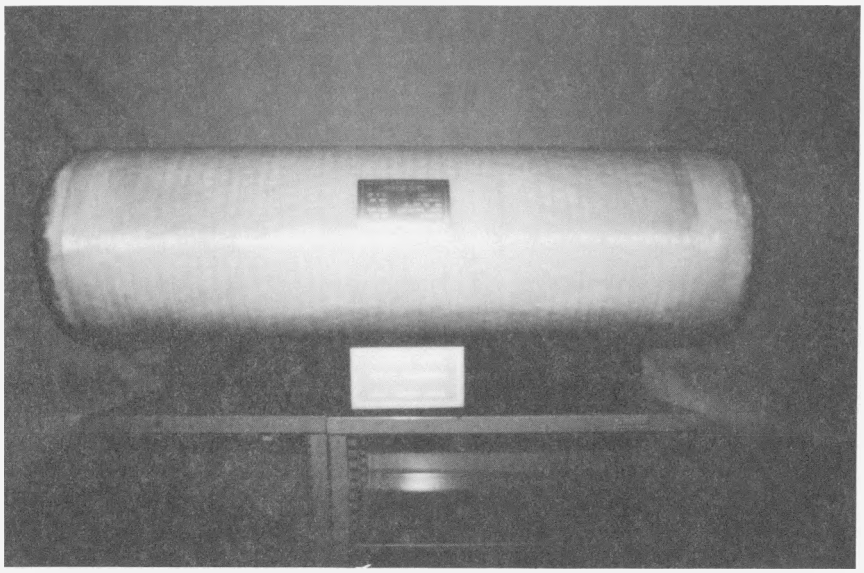

Figure 4

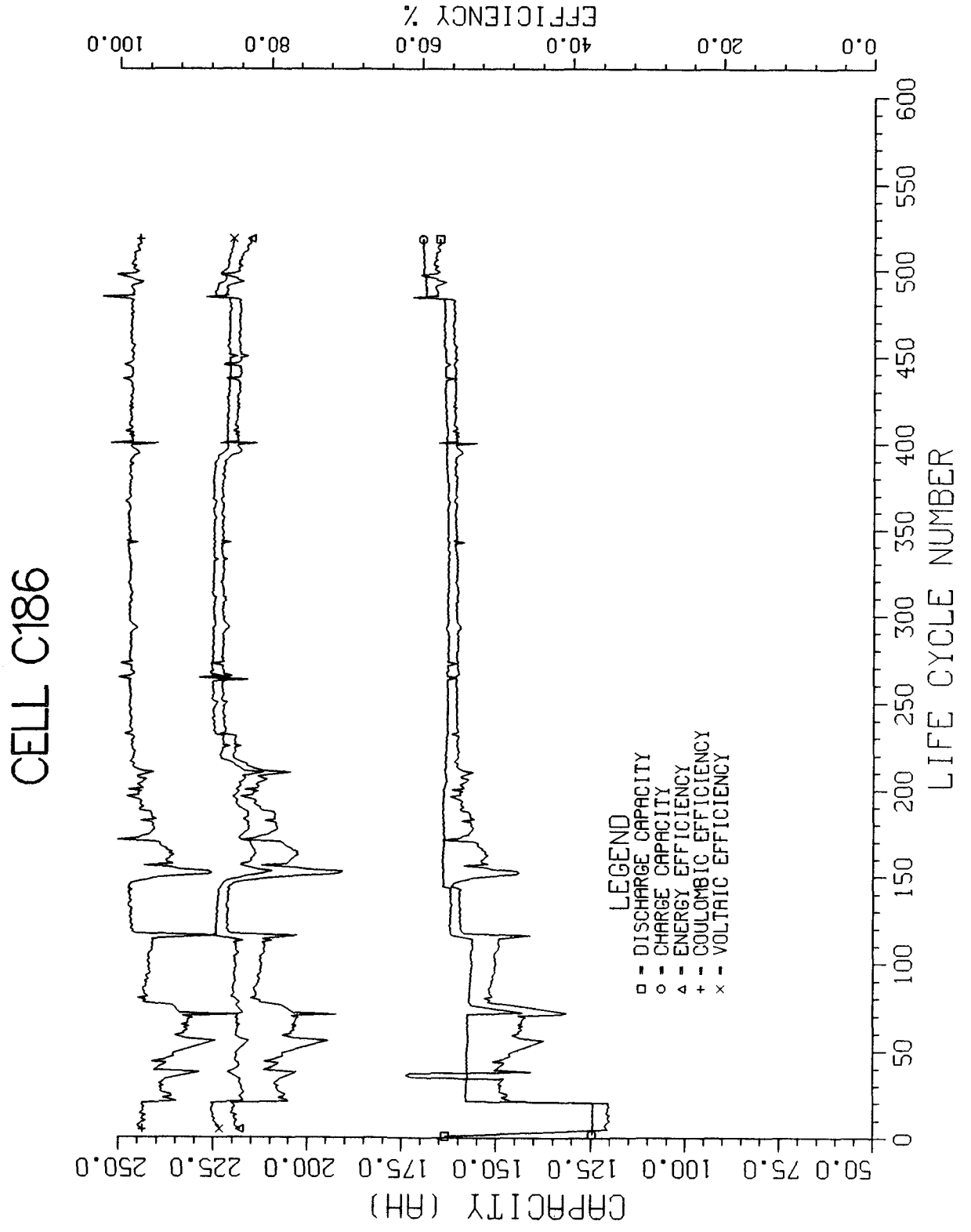
CELL C186
CAPACITY (AH)
EFFICIENCY %
LIFE CYCLE NUMBER
LEGEND
□ = DISCHARGE CAPACITY
○ = CHARGE CAPACITY
△ = ENERGY EFFICIENCY
+ = COULOMBIC EFFICIENCY
× = VOLTAIC EFFICIENCY

Figure 5

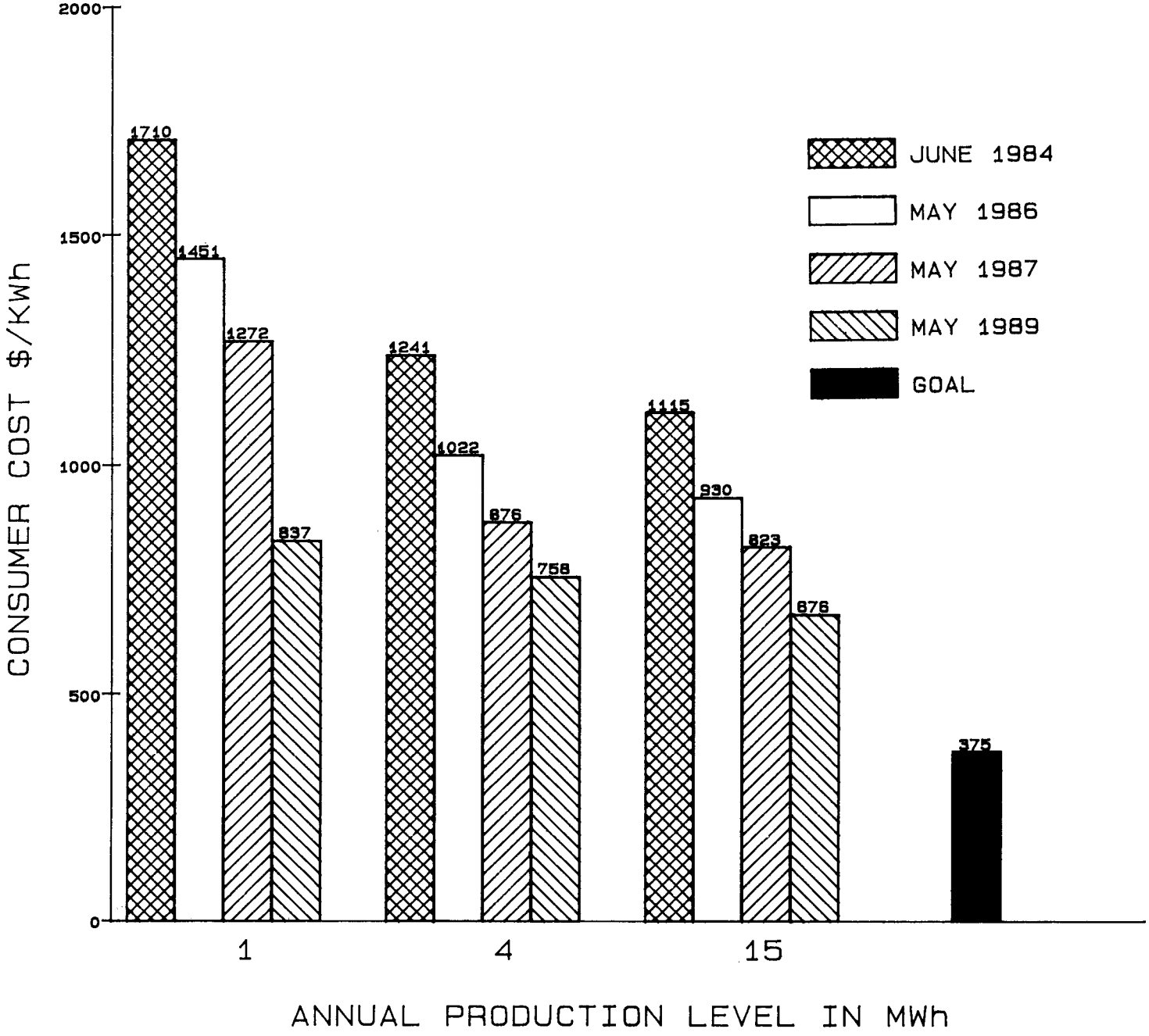
2000
1500
1000
500
0
CONSUMER COST $/KWh
1710
1451
1272
837
1241
1022
876
758
1115
930
823
676
375
JUNE 1984
MAY 1986
MAY 1987
MAY 1989
GOAL
1
4
15
ANNUAL PRODUCTION LEVEL IN MWh

Figure 6

CHINO 10 MW LEAD ACID BATTERY UTILITY LOAD LEVELLING DEMONSTRATION

George D. Rodriguez
Southern California Edison Company

ABSTRACT

The Chino 10 MW-40 MWh Battery Energy Storage Project has been operating since July 21, 1988, undergoing a series of tests aimed at demonstrating the costs and benefits of the facility for energy management purposes.

Some of the more important Chino Battery Plant performance characteristics are given in Table 1. The battery storage system is comprised of 8,256 individual two-volt cells rated at 5 kWh at the four-hour rate. The cells are arranged into eight parallel strings of 1,032 cells in series for a nominal 2,000 Vdc rating. A one-line diagram of the plant is shown. The converter is a self-commutated, 18-pulse stepped-wave, GTO-thyristor-based system rated at 10 MW with a one-way efficiency of at least 97%. The system was built by the General Electric Company.

A Test Plan Outline for the two-year demonstration is described in Table 2. As of the end of June, the plant has completed 96 cycles at an 80% depth of discharge. From July 1988 to May 1989, the facility has been operated in a block loading mode, i.e., 10 MW discharge for four hours. After a software program change in June 1989, the battery plant has been operated in a load following mode, i.e., responding to load changes above a predetermined set-point level. Monthly maximum, minimum, and average cycle efficiencies for the battery, power conditioning system, and total plant are presented. The facility has consistently performed at a 70% AC-AC turnaround efficiency.

The Chino Battery plant underwent a significant outage from January 1989 to March 1989 to perform planned capital improvements; to complete remaining plant design items; and to repair damage from a December 21, 1988, short-circuit incident. These changes are also described. Significant operation and maintenance items, such as cell watering, cell emission tests, and control system outages, are described.

The Chino Battery Facility is owned and operated by the Southern California Edison Company. The Electric Power Research Institute and the International Lead Zinc Research Organization are project participants having supplied the 10 MW converter and 2,000 tons of lead for the batteries, respectively.

Table 1. Design Characteristics of the Chino 10 MW-40 MWH Battery Energy Storage System

Rated Power Capacity	10 MW
Rated Energy Capacity	40 MWH @ C/4 rate
Battery Voltage	2000 Vdc
Output Voltage	12 kVac
Footprint	50,000 square feet
Lead-Acid Battery System	
• Battery	Exide GL-35, 2 Volt 3250 Ah(5h)
• No. of Cells	8,256 cells arranged in 8 strings
	6 cells per module
Power Conditioning System	
• Type	Bidirectional 18-pulse voltage-source, stepped wave, gate turn-off thyristor-based converter
• Power - Real Reactive	10 MW, charge/discharge 10 MVA, leading/lagging
• Efficiency	97 percent - one way

Chino 10 MW Battery Energy Storage Project

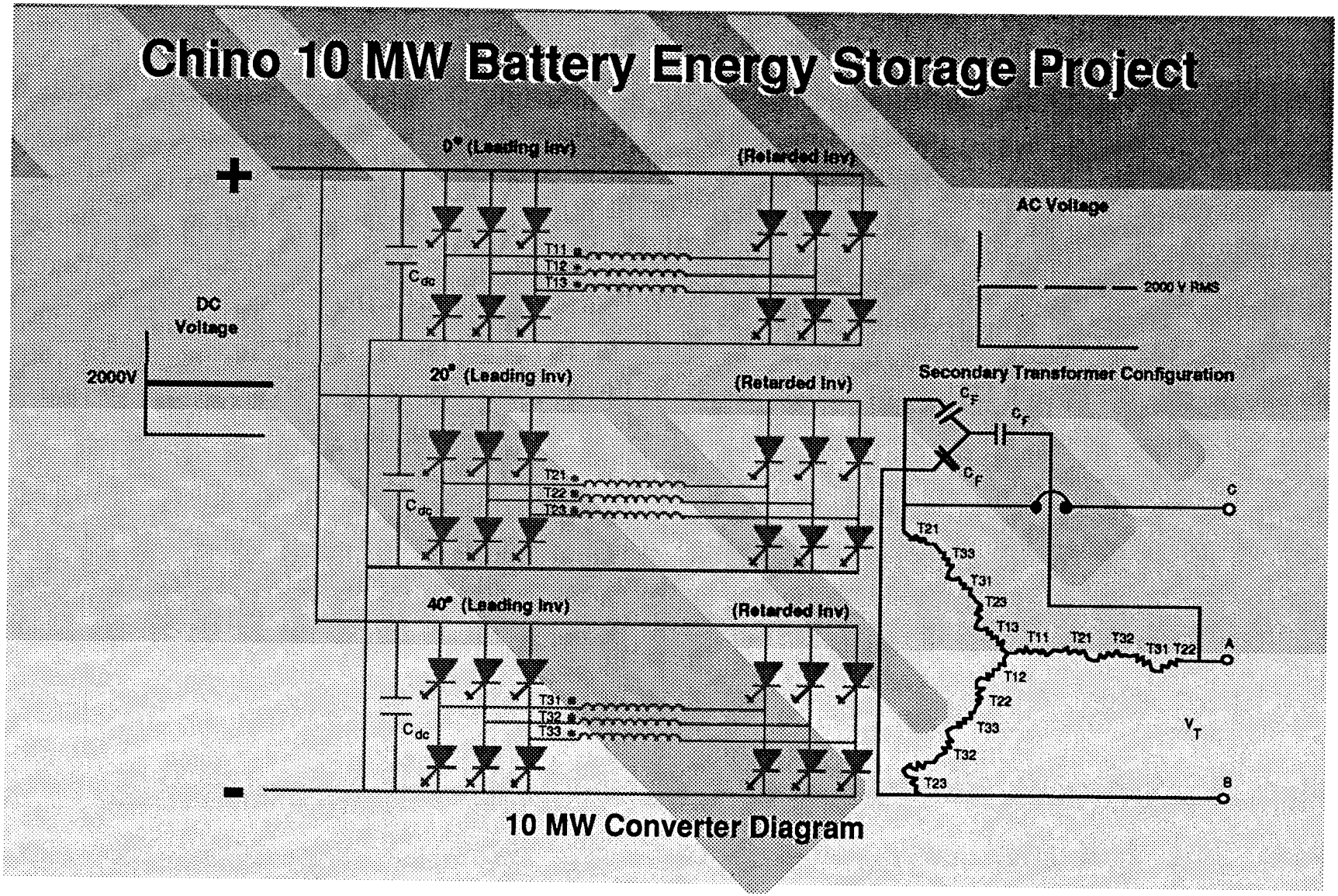

10 MW Converter Diagram

Table 2. Two-Year Test Plan Elements

Type of Test	Description	Duration
1. Parametric/Benchmark	Various Block Loading and Charging Schemes to establish performance parameters	6 months
2. Baseline	Normal Utility Mode of On/Off Peak Operation (i. e. 10 MW Discharge/8 hr Recharge)	8 months
3. Load Following	Peak Shaving Operation at various thresholds	4 months
4. Voltage/VAR Regulation	Operation to maintain set voltage/VAR level	1 month
5. Major Equipment Evaluation	Design Validation Tests, including thermal response tests	2 months
6. Special Operating Tests	Spinning Reserve, Black Start, other programmed tests	2 months
7. Combined Operation	Integrated Load Levelling or Peak Shaving and Spinning Reserve or Regulating Operation	1 month

Table 3. Chino Battery Energy Storage Project Monthly Performance Statistics

	PCS DC-AC Discharge Eff.	PCS AC-DC Charge Eff.	Battery DC-DC Eff.	PCS + Battery AC-AC Eff.	Total Cycle Aux. Energy (MWh)	Overall Plant Eff.
August 1988						
Average	98.9	95.7	78.5	74.3	11.7	64.2
Minimum	98.4	90.1	71.4	63.3	4.0	31.3
Maximum	99.5	97.4	85.1	81.1	86.4	70.7
September 1988						
Average	98.7	96.3	76.2	72.4	5.8	65.9
Minimum	98.1	95.3	72.9	69.2	4.4	57.3
Maximum	99.4	96.7	79.3	75.6	12.2	69.9
October 1988						
Average	98.6	96.3	79.0	75.0	8.60	68.0
Minimum	97.3	94.6	68.9	65.5	4.52	46.9
Maximum	99.2	98.7	82.5	79.3	32.04	73.1

Table 3. Chino Battery Energy Storage Project Monthly Performance Statistics

	PCS DC-AC Discharge Eff.	PCS AC-DC Charge Eff.	Battery DC-DC Eff.	PCS + Battery AC-AC Eff.	Total Cycle Aux. Energy (MWh)	Overall Plant Eff.
December 1988						
Average	99.1	95.6	83.8	79.5	5.6	72.2
Minimum	98.5	93.6	81.3	76.2	4.4	63.7
Maximum	99.5	96.3	90.0	85.3	12.2	78.0
March 1989						
Average	98.7	96.8	82.9	79.2	4.0	73.8
Minimum	98.1	96.1	82.1	78.9	3.4	72.9
Maximum	98.9	97.3	83.3	79.6	4.8	74.8
April 1989						
Average	98.1	96.8	80.8	76.7	3.8	71.7
Minimum	97.0	96.1	76.3	72.7	3.2	68.2
Maximum	98.7	97.3	83.9	79.1	4.3	73.7

ADVANCED METHODS TO CHARACTERIZE ELECTRODE SURFACE LAYERS

Rolf H. Muller
Materials and Chemical Sciences Division
Lawrence Berkeley Laboratory

Experimental in situ methods have been used to provide new insights into the composition, structure and mechanism of formation of surface layers on electrodes.

Spectroscopic ellipsometry is used to determine spectral properties of surface materials and to derive wavelength-independent parameters pertaining to film structure. Measurements at different wavelengths serve as independent monochromatic input, and film parameters are derived by the optimization of multidimensional optical models. By minimizing the difference between measurements and model predictions, spectral variations in film optical properties as well changes in film thicknesses and structure are obtained.

The early stages of the anodic oxidation of Ag(111) in 1M KOH during the application of potential steps, current steps, and potential sweeps have been investigated by spectroscopic ellipsometry. Film thicknesses and surface coverages have been derived from the measurements by use of a dual-layer optical model. The results are supported by SEM observations on selected specimens. Oxide crystals are found to nucleate from an initially-formed homogeneous oxide layer. A decrease in number density of crystals of several orders of magnitude during film growth has been found and is attributed to the growth of larger crystals at the expense of smaller ones.

Raman spectroscopy of surface layers for their chemical characterization is conducted with equipment sensitive enough to observe unenhanced emission. This high sensitivity is achieved by use of a multilayer optical filter for removing the elastically scattered incident wavelength, a single monochromator to disperse the light, and a multichannel detector for observing the entire spectrum simultaneously.

Laser Raman spectroscopy has been used for the identification of surface species during the anodic oxidation of Cu in 1M KOH. Two major anodic peaks are observed in the cyclic voltammogram at -350 mV and 0 mV vs Hg/HgO. Near the first anodic peak, a Raman band associated with the formation of Cu_2O is clearly observed around 633 cm^{-1}. At a potential of around -100 mV vs. Hg/HgO, $Cu(OH)_2$ is identified by a band at 488 cm^{-1}. This observation coincides with the beginning of the second anodic voltammetry peak. As the potential is increased further, the Cu_2O band intensity slowly diminishes and the $Cu(OH)_2$ band increases slightly. At 650 mV, oxygen evolution begins and a broad Raman band centered around 550 cm^{-1} is observed together with the 488 cm^{-1} band. The appearance of this band may be due to the formation of a trivalent copper surface species, possibly Cu_2O_3. Although CuO is thermodynamically favored over $Cu(OH)_2$, the CuO band is not observed. The reduction of the oxides is complex and affected by illumination.

In situ angularly-resolved light scattering equipment has been built for collecting elastically scattered light over the angles of 5-85 from the

incident direction in 1 increments with fiber optic probes. Elastic light scattering has been used to measure changes in the spectral power density function (SPDF) of the surface during anodic oxidation. The integral of the SPDF is a measure of the RMS roughness of the surface, and the angular dependence of the SPDF is related to the size of the growing particles.

Light scattering measurements during the anodic oxidation of silver have confirmed the redistribution of the oxide from small to large crystallites derived from the ellipsometer measurements. They have also confirmed the compact nature of Cu_2O and the porous, microcrystalline structure of $Cu(OH)_2$ formed on Cu.

Scanning Tunneling Microscopy (STM) allows the topographical investigation of metal surfaces with atomic resolution. A commercially available STM (Digital instruments, Inc. Nanoscope I) with a 0.6 μm scanner was interfaced with an AST personal computer. Both a digital to analog (x/y position control) and analog to digital (z height data) converter were employed. A 320x200 point array was used to store the data. Epoxy insulated etched platinun-iridium tunneling tips were used (Longreach Scientific Resources, Orr's Island, Maine 04066). Smooth silver surfaces (RMS roughness about 50 Å) were prepared by vapor deposition of silver on glass substrates.

Deposition of Pb from 5mM lead acetate, 1M sodium acetate was followed by STM. The initial surface was smooth, with roughnesses of long wavelength (1000 Å) and low amplitude (100 Å). Near the potential of underpotential Pb deposition, no obvious changes in the surface topography were evident. This lack of observed change is due to the relatively large roughness of the original surface and the relatively low resolution (about 2.0 Å) at which the images were taken. Once bulk deposition begins, a large number of small (50-100 Å) growth center are seen to form near the rougher portions of the substrate. These centers grow, reducing the short range roughness of the surface. Later, longer range (about 500 Å) waviness of the surface becomes evident and the amplitude and wavelength of the surface roughness continues to change. Preferential growth near the recesses of the surface is observed, and the surface undergoes a number of roughening and smoothing cycles.

Quantitative data an surface microtopography were derived from the STM by use of the amplitude density and autocorrelation functions of the surface profiles.

ACKNOWLEDGMENTS: This work was supported by the Assistant Secretary of Conservation and Renewable Energy, Office of Energy Storage and Distribution of the U.S. Department of Energy under Contract no. DE-AC03-76SF00098.

NON-AQUEOUS BATTERIES

CHAIRPERSON:

Al Landgrebe
U.S. Department of Energy

ADVANCED SODIUM/METAL CHLORIDE CELL RESEARCH

D. R. Vissers, S. K. Orth, M. C. Hash, L. Redey, P. A. Nelson, and I. D. Bloom
Electrochemical Technology Program
Chemical Technology Division
Argonne National Laboratory

The objective of the program is to establish a research base for the development of high performance Na/MCl_2 (M = Fe or Ni) cells that utilize solid electrolyte configurations with large surface areas. This effort, initiated late in FY 1988, is broken down into three subtasks: (1) MCl_2 Electrode development, (2) Composite Electrolyte Development, and (3) Cell Research.

Our MCl_2 electrode studies have thus far focused on enhancing the overall performance of the $NiCl_2$ electrode[1,2]. In these studies, 2-3mm thick, annular $NiCl_2$ electrodes are used inside of a β''-Al_2O_3-tube electrolyte. We investigated the effects of electrode porosity in annular 16-, 18-, and 20-vol %-Ni electrodes, of additives, such as sulfur which is used in the current technology, of cycling rates, and of temperature. High-capacity density electrodes, 0.5-0.55 Ah/cm^3, made from a sintered mixture of Ni and NaCl (3:1 in terms of capacity) are being developed. It should be noted here that this capacity loading is considerably higher than that used in the current technology.

The results of these studies have clearly indicated the charge rate, sulfur addition, electrode porosity, and temperature have a marked effect on electrode performance. Those cells that were charged quickly tended to have lower utilizations than those charged more slowly. In some cases, the effect of charge rate is more pronounced than the effect of temperature on the performance of the electrode. Sulfur seems to enhance the utilization of NaCl in the electrode at all discharge current densities. In cell studies conducted at 260°C and the C/8 charge rate, marked effects of the sulfur additive and the vol % Ni used in the electrode were observed. For example, there was a 95% utilization of materials at the C/2 discharge rate in the sulfur-containing 18-vol%-Ni electrode as compared to 50% in a similar electrode without sulfur. Sulfur seems to enhance the charge acceptance of the Ni electrode by, perhaps, retarding Ni particle growth or by changing the chemistry of the electrode.

In the 20-vol%-Ni electrode (with sulfur), utilization of the active materials was not as good as that of the 18-vol% electrode with sulfur. At the C/2 discharge rate, the 20-vol% electrode utilized 79% of the active materials. On the other hand, the 18-vol% electrode utilized 95%. This variance is most likely due to differences in porosity of the two electrodes. Increasing the temperature to 300°C had little or no effect on the performance of the 20-vol% nickel electrode (78% utilization).

The area-specific impedance values at 15 s after current interrupt (ASI_{15s}) of the 18-vol%-Ni electrode with sulfur at 20% of theoretical $NiCl_2$ utilization was found to be 1.6 Ω cm^2 at 260°C. Currently, we are studying the effect of temperature on the ASI_{15s} values for this electrode design. In the 18-vol% electrode without sulfur, the ASI_{15s} measurement decreased as the temperature was raised. At 20% of theoretical $NiCl_2$ utilization, the 15 s measurements at 220, 260, and 300°C were about 6.1, 3 and 2.8 ohm-cm^2, respectively. In the 20-vol %

Ni electrode with sulfur, the same relationship was also true. At 20% of theoretical $NiCl_2$ utilization, the 15 s measurements at 220, 260, and 300°C were about 5.2, 2.7, and 1.6 ohm-cm^2, respectively.

In some cases, ASI_{15s} values do not seem to have a strong dependence on temperature. The interfacial resistance due to poor wetting of β''-Al_2O_3 by Na at the lower temperatures may be partially masking the true temperature dependence of the ASI_{15s} values.

The Na/MCl_2 electrode development studies are being continued and will be addressing both the $NiCl_2$ and $FeCl_2$ systems in the future. Key elements in the studies will focus on enhanced active metal (Ni, Fe) utilization in the respective electrode to improve the specific energy of each system.

In subtask 2, work is directed toward the development of a sodium-ion conducting glass-cramic (β-Al_2O_3) composite electrolyte that can be easily and inexpensively formed into high-surface-area prismatic configurations[3]. It is hoped that the resulting composite would have an ionic conductivity close to that of β-alumina and the ease of fabrication close to that of a glass.

During this past year, we have decreased the resistivity of our composites from 1000 to about 200 Ω-cm at 250°C by carefully controlling the particle size distribution of the glass used. Properly sized glass particles change the composite microstructure from a very coarse, obviously phase-separated to one with a very fine structure with intimate uniformity of the glassy and solid β''-alumina phases. We are continuing to refine our fabrication techniques to study the properties of composites made with less glass. Reducing the glass volume fraction from 50 vol% to about 10-25 vol% should correspondingly decrease the resistivity of the resulting composite.

The cell research subtask has been focused on the analysis of voltage losses in the cell. Three different cell configurations have been modeled to estimate their voltage-loss characteristics. The results of these analysis indicated that the voltage losses of the cell can be reduced markedly by shifting from a low-surface-area single electrolyte tube design to a higher-surface-area design. The projected specific energy and specific power of such cells is ~200 Wh/kg and 300-500 W/kg, respectively.

While this initial analysis indicates the potential of the system, further work is needed to refine the calculations and to experimentally obtain performance values closer to the projected values.

Acknowledgment

This work supported by the U.S. Department of Energy, Energy Systems Storage Branch under Contract No. W-31-109-Eng-38.

References

1. I. Bloom, S. K. Orth, and D. R. Vissers, Extended Abstracts, Vol. 89-2, p. 145, 176th Electrochemical Society Meeting, Hollywood, FL, Oct. 15-20, 1989.

2. L. Redey and D. R. Vissers, Extended Abstracts, Vol. 89-2, p. 143, 176th Electrochemical Society Meeting, Hollywood, FL, Oct. 15-20, 1989.

3. I. Bloom and M. C. Hash, Extended Abstracts, Vol. 89-2, p. 766, 176th Electrochemical Society Meeting, Hollywood, FL, Oct. 15-20, 1989.

Effect of Sulfur Addition on the Performance of 18 v/o $Ni/NiCl_2$ Electrode at 260°C

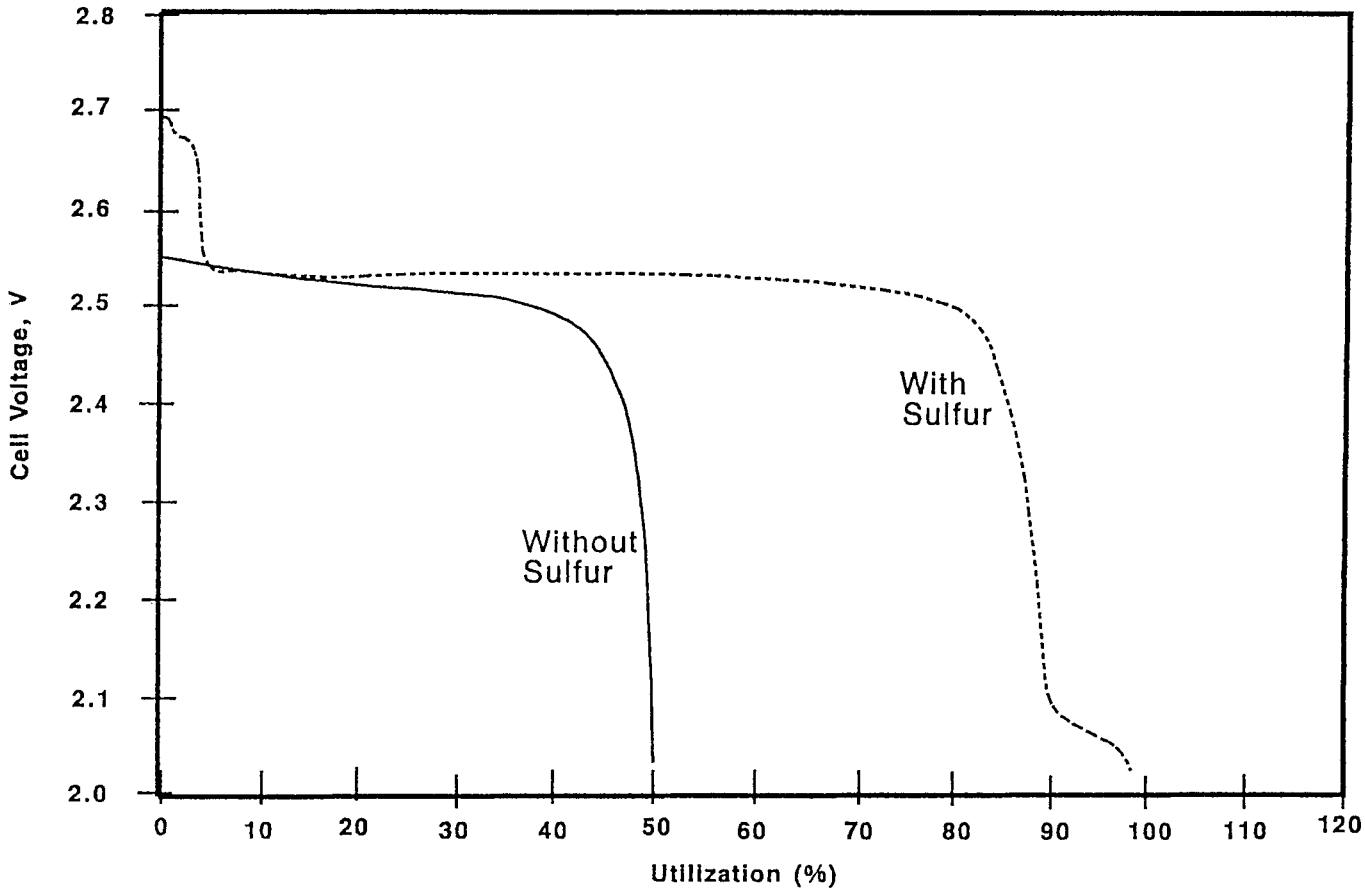

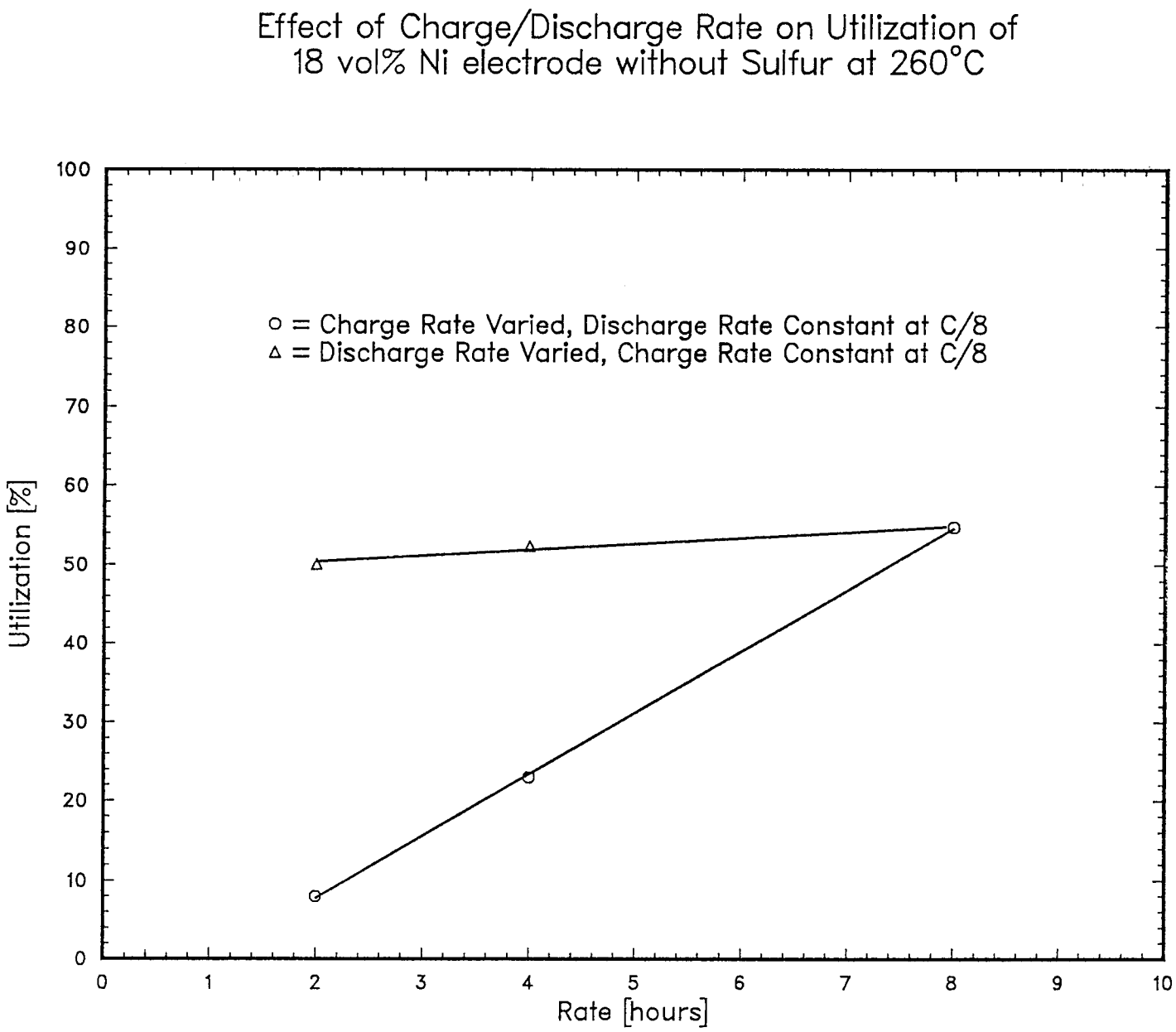
Effect of Charge/Discharge Rate on Utilization of
18 vol% Ni electrode without Sulfur at 260°C
○ = Charge Rate Varied, Discharge Rate Constant at C/8
△ = Discharge Rate Varied, Charge Rate Constant at C/8
Utilization [%]
Rate [hours]
0
10
20
30
40
50
60
70
80
90
100
0
1
2
3
4
5
6
7
8
9
10

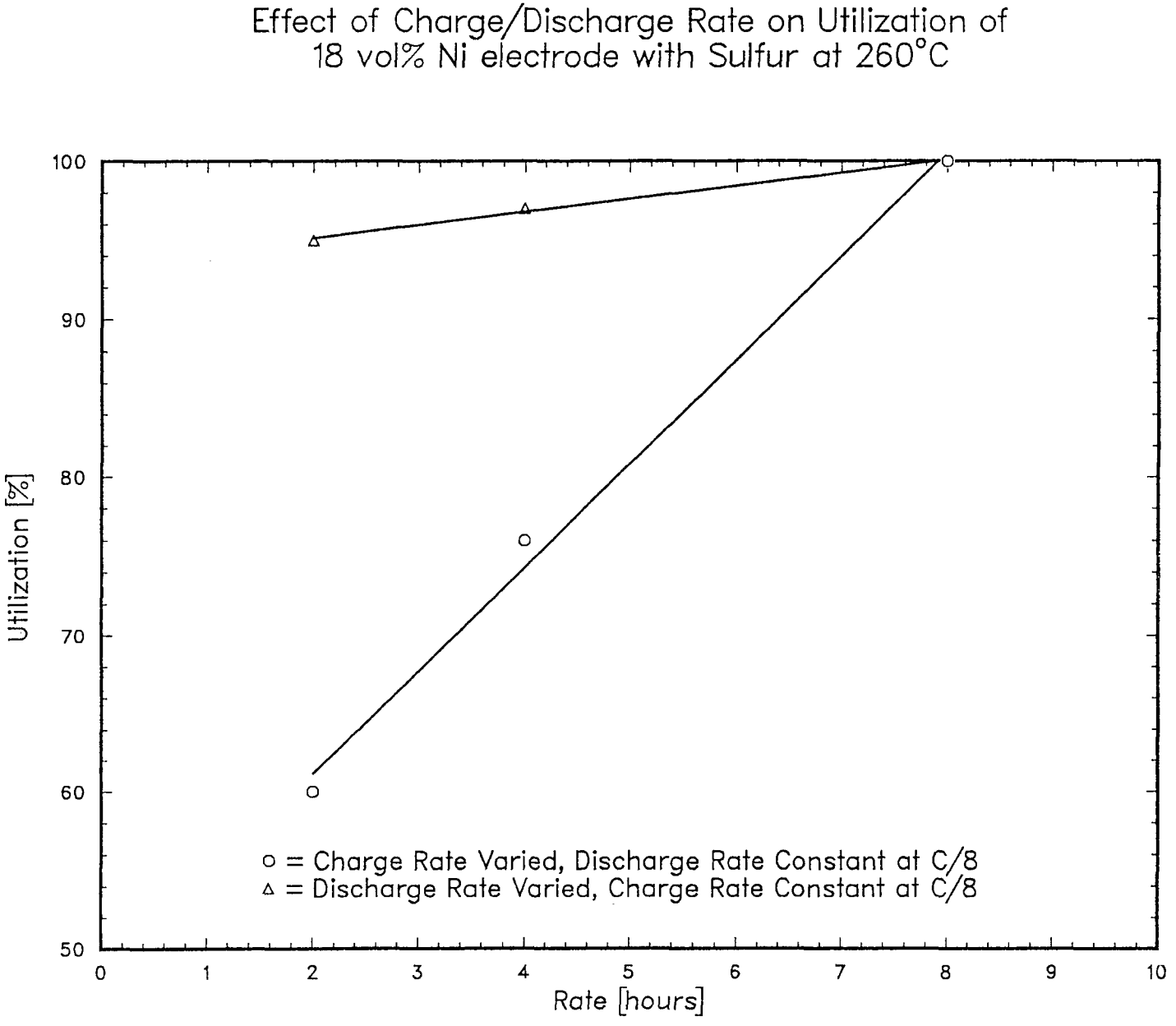
Effect of Charge/Discharge Rate on Utilization of
18 vol% Ni electrode with Sulfur at 260°C
Utilization [%]
100
90
80
70
60
50
0
1
2
3
4
5
6
7
8
9
10
Rate [hours]
o = Charge Rate Varied, Discharge Rate Constant at C/8
Δ = Discharge Rate Varied, Charge Rate Constant at C/8

Cyclic Voltammagrams at 260°C for 18 v/o Ni Electrode (no sulfur)

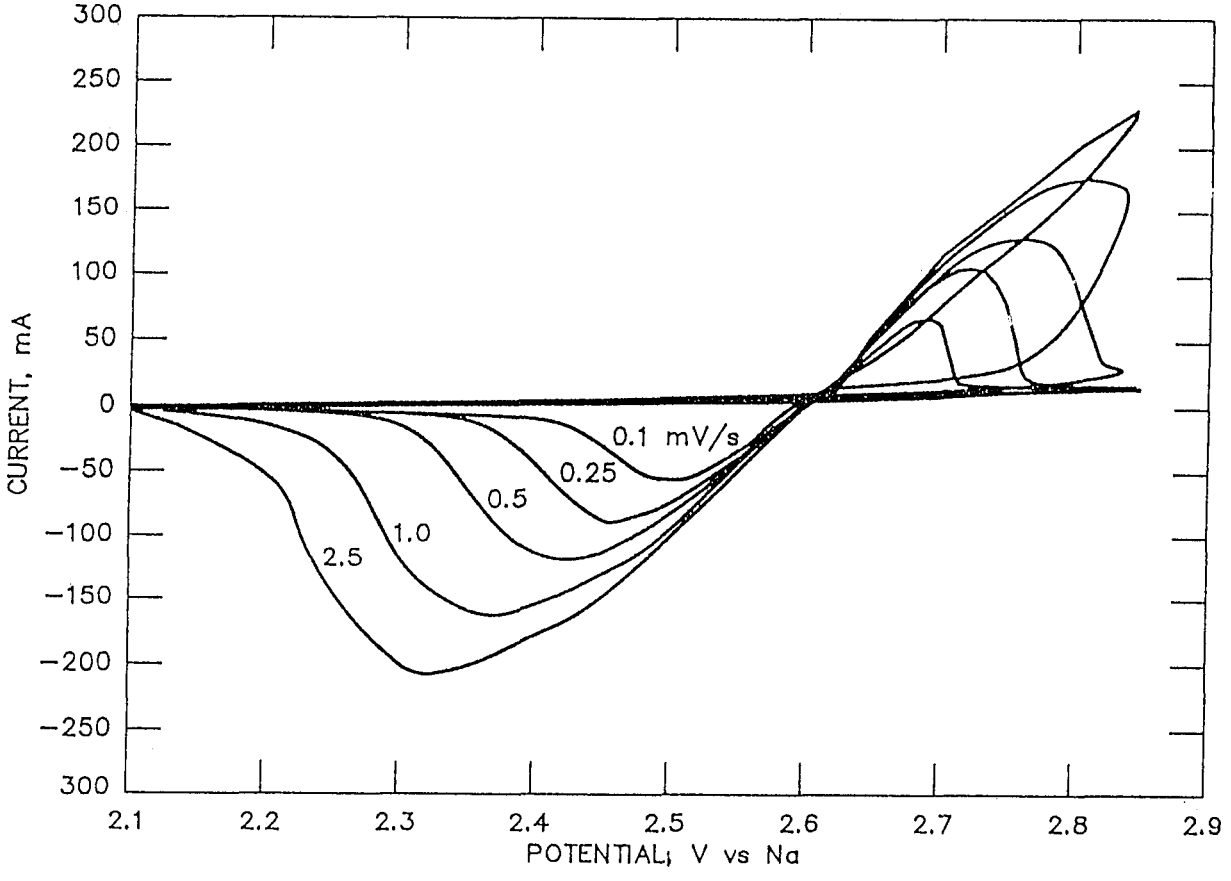

02270

Effect of Volume Fraction Ni on Performance at 260°C

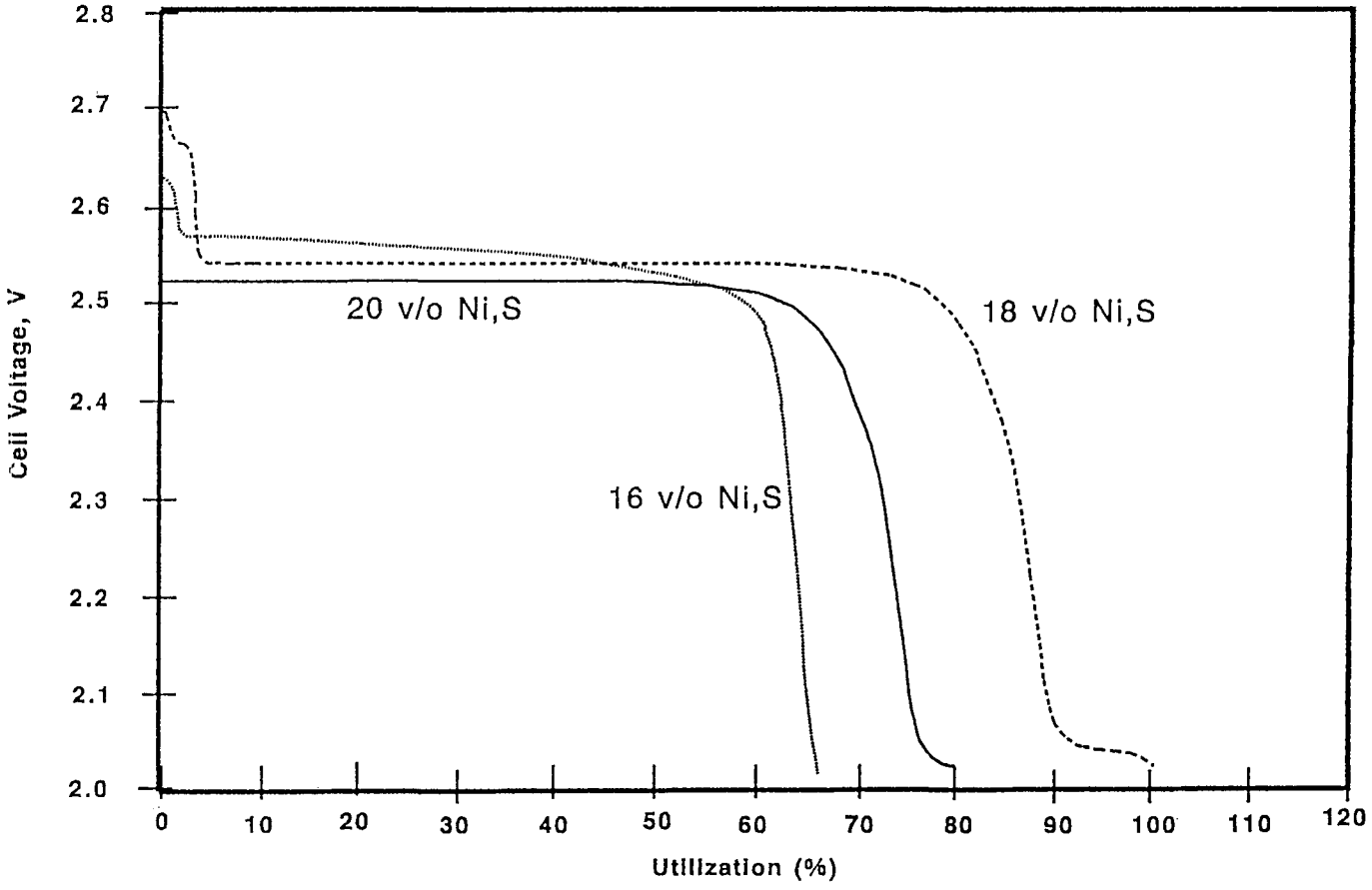

Effect of Temperature on the Performance of an 18 v/o $Ni/NiCl_2$ Electrode

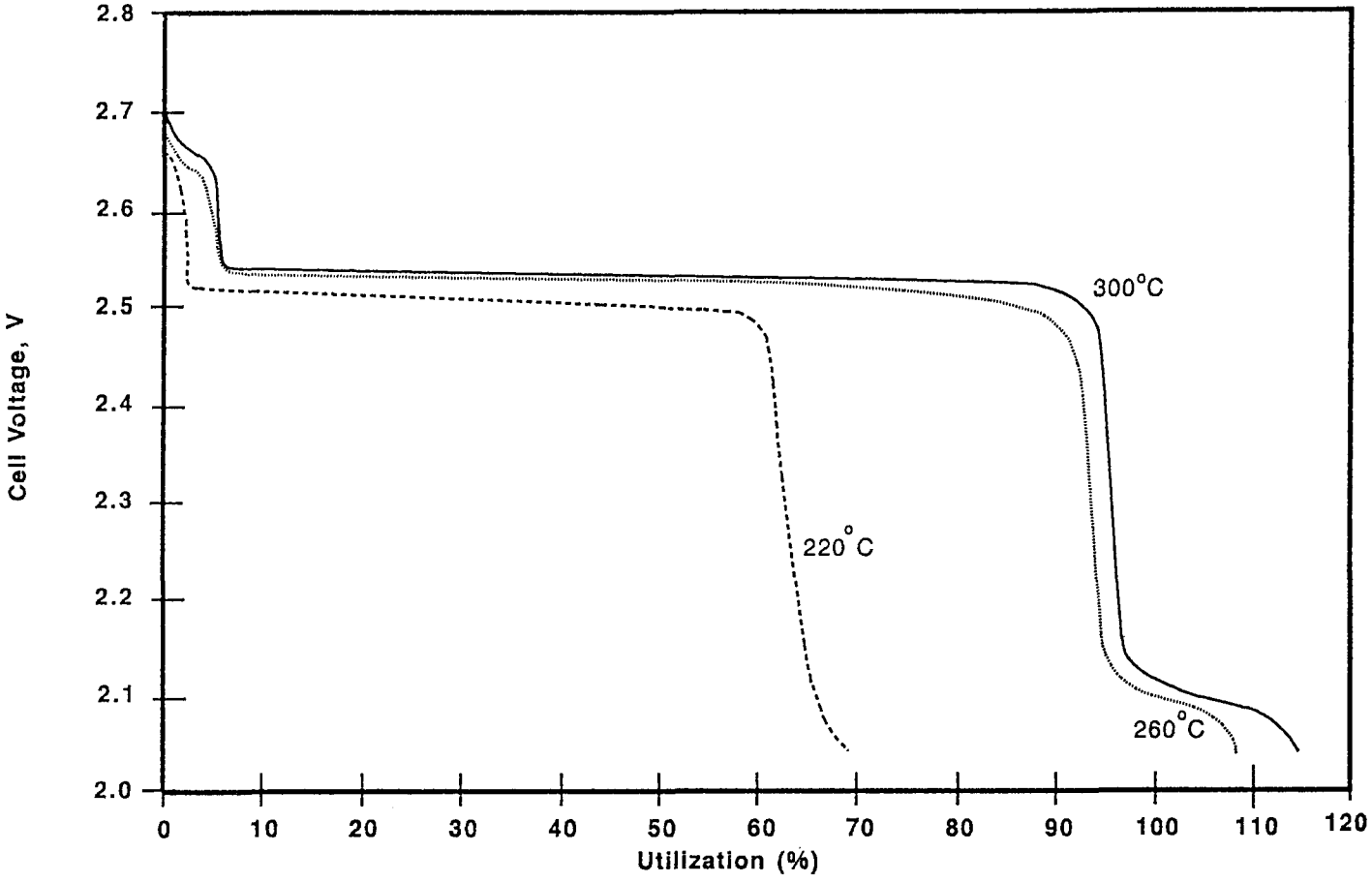

Photomicrograph of Glass-β"-Al_2O_3 Composite

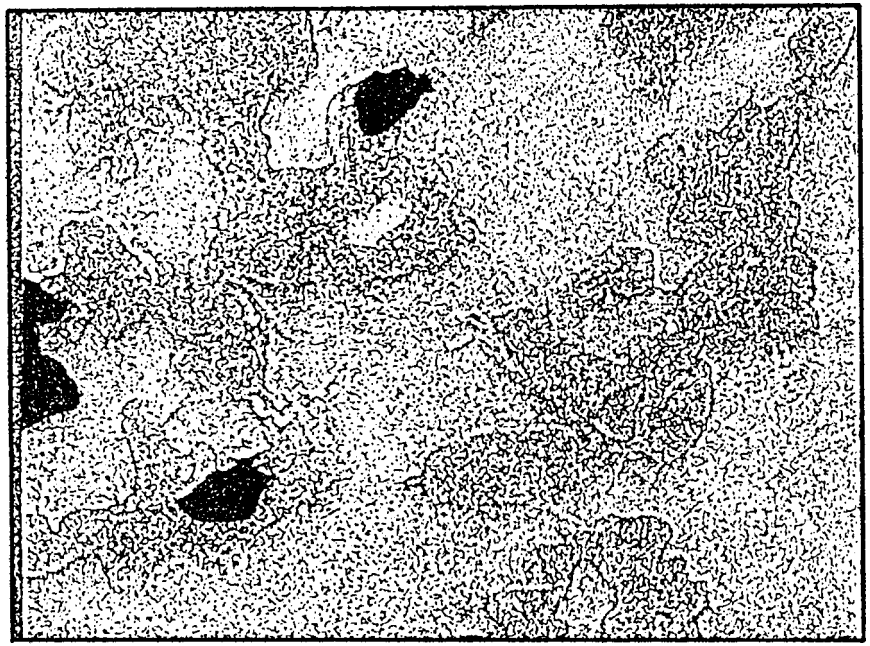

NOVEL HIGH-RATE, ALL SOLID-STATE, SODIUM AND LITHIUM/ORGANOSULFUR BATTERIES

Steven J. Visco, Meilin Liu, Michel B. Armand, and Lutgard C. De Jonghe

University of California at Berkeley
Materials and Chemical Sciences Division
Lawrence Berkeley Laboratory
1 Cyclotron Road
Berkeley, CA 94720

The pursuit of thin-film solid-state batteries for energy storage applications has greatly accelerated in the past few years. The inherent advantages of all-solid-state cells include negligible self-discharge, long cycle life, high reliability, and virtual absence of container corrosion. Although elegant work on polycrystalline and vitreous electrolytes has led to solid electrolytes with suitable ionic conductivities for battery development, the superior mechanical properties of elastomeric electrolytes combined with the simplicity of fabrication of thin films from these materials, has led to active pursuit of solid-state cells based on solid polymeric electrolytes (SPEs). Although solid polymer electrolytes generally have lower ionic conductivities than their polycrystalline and vitreous counterparts, the ability to cast thin films (10 to 100 m) from dilute solutions, compensates somewhat for this limitation. The majority of cells based on SPE's have utilized lithium foil negative electrodes and composite positive electrodes containing finely ground intercalation compounds (such as TiS_2) dispersed in the polymeric electrolytes. While many polymeric electrolytes have been described in the literature, the best known SPE is undoubtably polyethylene oxide (PEO)[1]. The operating temperature of SPE cells generally falls in the range of amient to 100°C, with the highest levels of performance occuring in the higher temperature regime. Reported results for a number of Li/PEO/X cells have indicated that such solid-state batteries are very close to actual commercialization[2]. The remaining skepticism with regards to SPE-based batteries are the relatively low attainable current densities and associated poor cathode utilization at high drain rates, particularly at low temperatures. This has generally been attributed to the low conductivity of the electrolyte, and consequently a number of groups have been exploring a variety of polymeric materials and/or dopant electrolyte salts in an attempt to increase the conductivity of SPE's. However, recent results in our laboratory have implied that composite cathodes based on intercalation compounds may contribute far more of a limitation to the performance of these cells than has been previously recognized. In fact, by replacing the costly TiS_2 intercalation cathode by an inexpensive polymer/polymer matrix composed of PEO and a solid-redox-polymerization electrode (SRPE), current densities far in excess of those reported for TiS_2 electrodes have been realized. These SRPE's are not "conducting polymers" such as polyacetylene-type materials, but are in fact electronic insulators, necessitating the inclusion of dispersed carbon black in the composite matrix*. Moreover, the gravimetric and volumetric energy and power densities of Li/SRPE

* the exact chemical nature of these materials and their synthesis will be discussed at the presentation.

and Na/SRPE cells are significantly higher than for analogous intercalation compound based cells. Furthermore, the solid-redox-polymerization electrodes (SRPEs) have been shown to have high thermal and chemical stabilities, as well as fast mass transport and electrode kinetics. One battery based on these materials, a Li/PEO/SRPE cell, has achieved over 75 cycles (still cycling), at a sustained power density of 150 W/kg (144 W/l), and a sustained energy density of 260 Wh/kg, with little evidence of deterioration of performance at 77 to 80°C. At 100°C, the Li/PEO/SRPE cell demonstrated a complete discharge cycle (100% of available capacity) at a current density of 10 mA/cm^2 (12 c rate) and a power density of 2400 W/kg. At ambient temperature, the Li/PEO/SRPE cells could be discharged at current densities of over 250 $\mu A/cm^2$. Furthermore, the analogous Na/PEO/SRPE cells have achieved the highest energy and power densities as well as longest cycle lives of any solid state sodium cells to date. The properties of this novel redox system are most clearly illustrated by comparison to the mechanism of protein folding as will be explained in the presentation. The SRPE materials can be generated as 1, 2, or 3-dimensional networks, depending on the mechanical, and electrochemical properties desired. Efforts are currently underway to synthesize a 2-dimensional ladder polymer which will unfold upon discharge of the Li/PEO/SRPE and Na/PEO/SRPE cells.

ACKNOWLEDGEMENT

This work was supported by the Assistant Secretary of Conservation and Renewable Energy, Office of Energy Storage and Distribution of the U.S. Department of Energy under Contract No. DE-AC03-76SF00098.

1. M. Gauthier, M. B. Armand, and D. Muller, in "Electroresponsive Molecular and Polymeric Systems," pp. 41-95 Marcel Dekker, 1988.

2. M. Gauthier et al, *J. Electrochem. Soc.*, **132**, 1333 (1985).

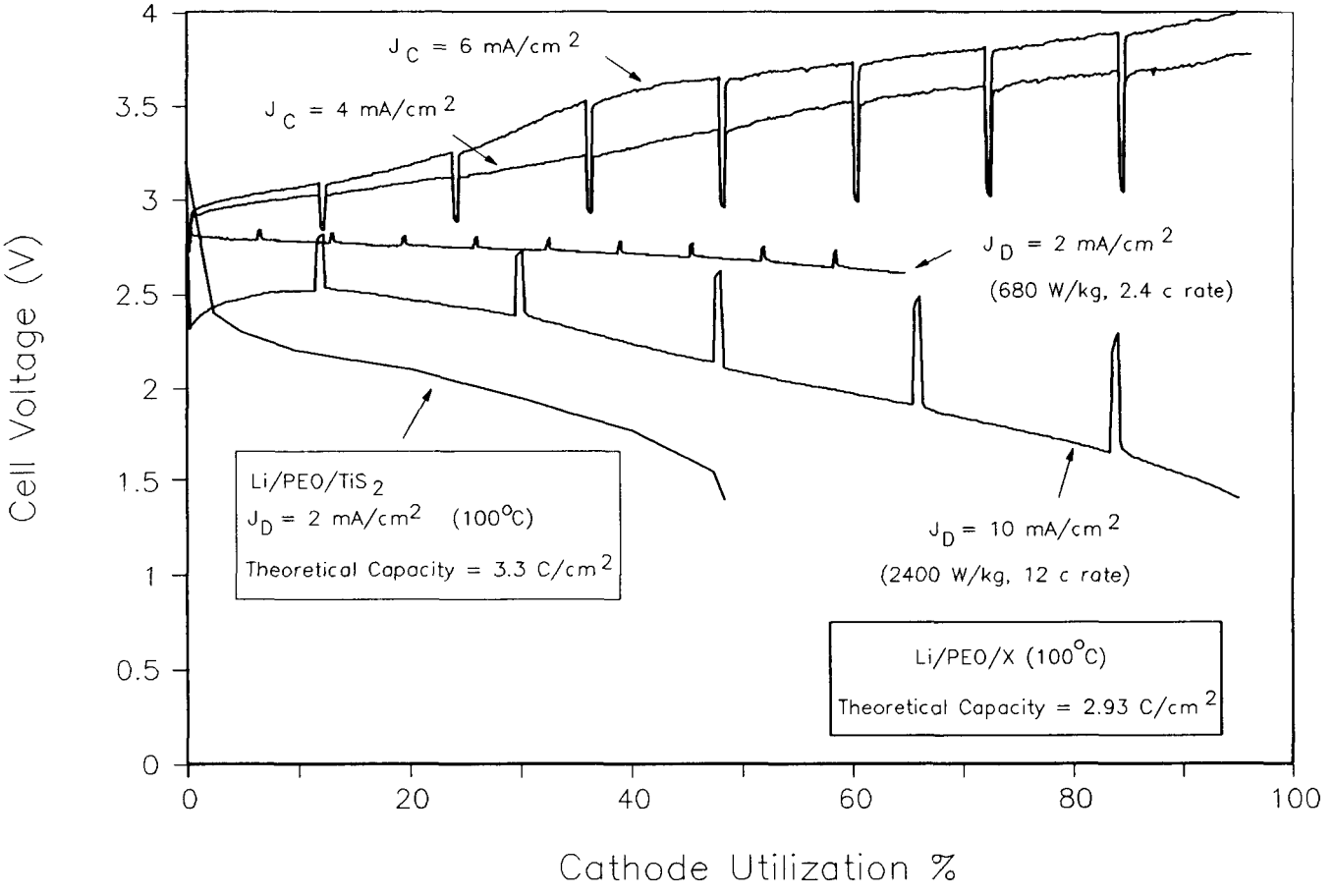

Fig 1. Rate capabilities of all-solid-state Li/PEO/SRPE and Li/PEO/TiS_2 cells.

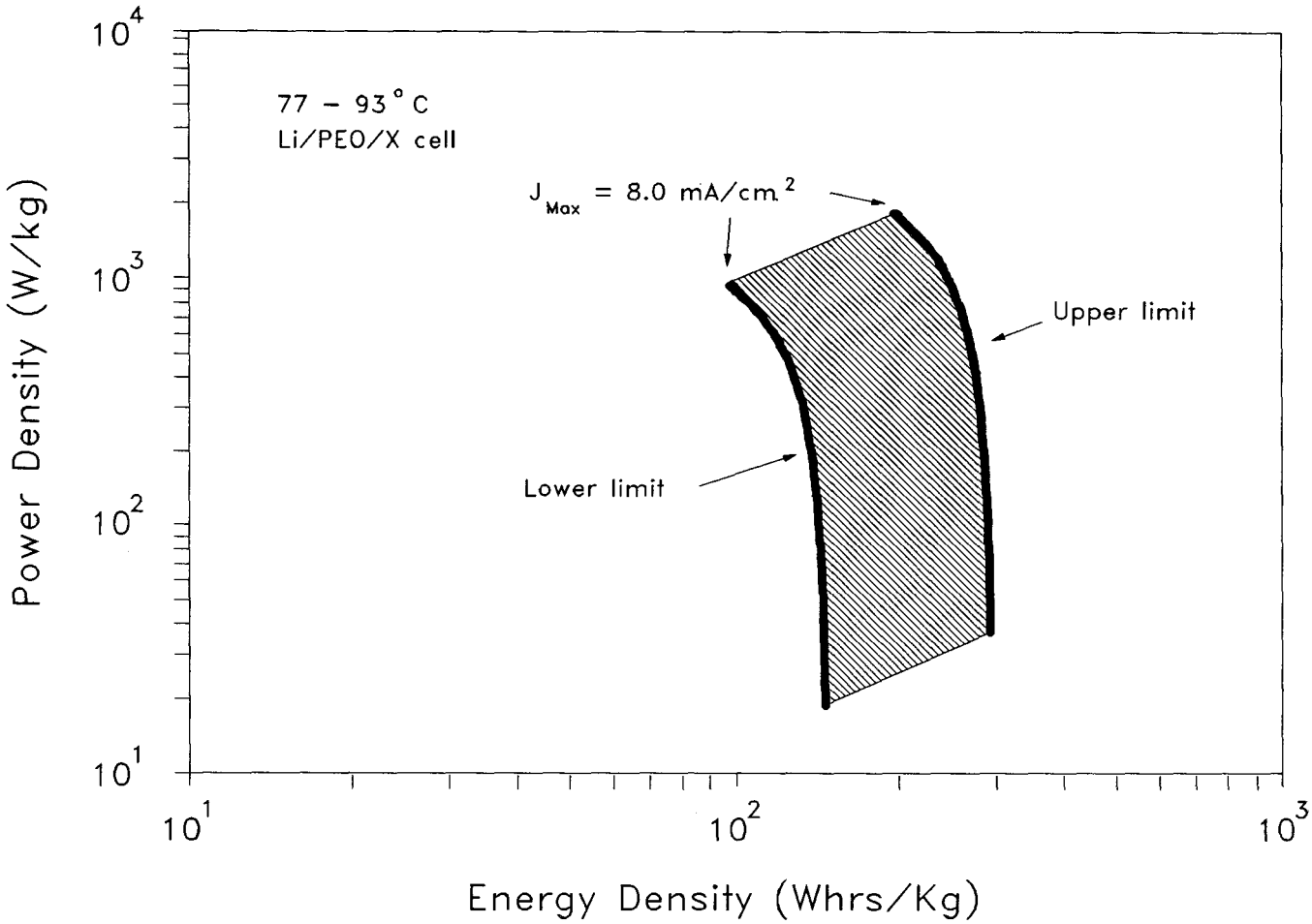

Fig. 2 Gravimetric Ragone plot for Li/PEO/SRPE cells.

DEVELOPMENT STATUS OF LITHIUM-ALLOY/IRON SULFIDE BATTERIES

Albert A. Chilenskas
Argonne National Laboratory

The development of lithium-alloy/iron sulfide batteries for electric vehicles and other applications is underway worldwide. The most advanced programs are the (1) U.S. DOE/EPRI program for electric vehicles, (2) British Admiralty-industry program for submarines, and (3) Canadian Government-industry program for on-road and off-road vehicles.

In the U.S. program, a just completed collaboration between Argonne National Laboratory (ANL) and Westinghouse Oceanic Division included the design, fabrication, and test of several fractional-scale (36-V/7.5-kWh) batteries designed for an electric van. Tests were also done with full-scale (12-V/250-Ah) modules, a quarter-scale vacuum-insulated battery case, a quarter-scale heating/cooling system, and a full-scale battery charger.

The tests provided verification of a conceptual van battery design for a full-scale battery. Only minor modifications were required to successfully operate the fractional-scale battery and to verify the basic design.

Thermal management studies with the vacuum-insulated case showed that the required heat loss values were achieved, as well as the required temperature uniformity. The heating and cooling system, after a modification to improve temperature measurements, performed according to design expectations.

Electrical performance tests of the battery showed that the cells achieved a specific energy of >110 Wh/kg in driving profile testing (J227a/C) and a specific power of >95 W/kg at 50% depth of discharge and 300 A. These values met or exceeded our goals for a van battery. Cycle life expectations, however, were not met. Separate tests of two 12-V modules and two 36-V sub-batteries were performed, and the average lifetime was about 120 cycles, compared to 350 cycles for the same cells tested individually.

Reliability tests showed that the battery could be cycled with one or more failed cells. A battery with failed cells cycled normally except for a loss of about 2 V per failed cell. The I^2R heating associated with a failed cell was found to be about equal to that of a normal cell.

The batteries were operated without any evidence of safety problems, as expected based upon previous tests experience and our analysis of the chemistry and electrochemistry of the system.

With completion of the fractional-scale battery tests, the U.S. program is ready to begin the final step in the development of a proof-of-concept Li-alloy/iron monosulfide van battery. A collaborative ANL-industry program, sponsored by DOE/EPRI, is underway to test a full-scale van battery in 1992.

Acknowledgment:

This research is supported by the U.S. Department of Energy, Office of Transportation Systems, Electric and Hybrid Propulsion Division.

WORLDWIDE LITHIUM-ALLOY/IRON SULFIDE DEVELOPMENT PROGRAM

Developer	Status
ANL/Westinghouse Oceanic Division	• Quarter-scale (36-V/7.5-kWh) batteries tested. • Battery design for electric vans verified.
British Admiralty/Vickers Hawker-Sidley	• Full-scale battery components tested. • Five-year program initiated 1989.
Electrofuel Mfg. Co. Canadian Government	• 100-Ah cells tested, 300–700 cycles. • Low-cost manufacturing.

QUARTER-SCALE LITHIUM-ALLOY/IRON SULFIDE BATTERY

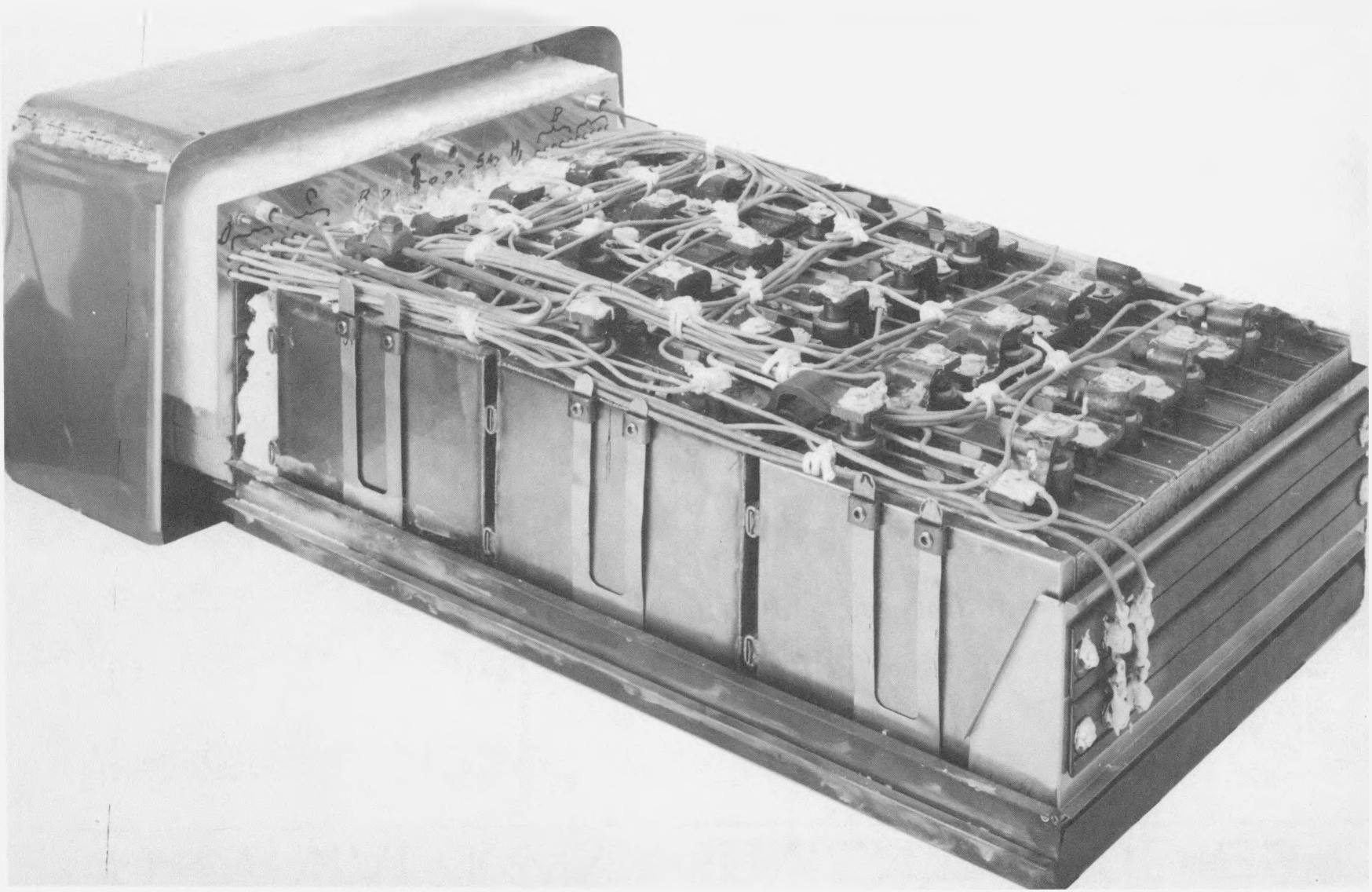

THERMAL MANAGEMENT STUDIES

Parameter	Status
Heat Loss	Achieved approximately 200 W with 36-V batteries. Some improvement needed in penetration losses.
Cell Temperature Variation	Design goal is $\pm 5^{\circ}C$. Tests achieved ± 5 to $\pm 10^{\circ}C$.
Battery Heat Up	Designed for 12-16 hour heating. Electrical resistance heaters are reliable.
Battery Cooling	Heat removed via cell bottom. Minor modifications needed to improve top-to-bottom temperature gradient.

BATTERY COMPONENT DESIGN VERIFICATION

Component	Status
Van Battery Design	• Concept design completed (Westinghouse Report). • Component design verification completed.
12-V/250-Ah Modules	• Energy and power adequate. • Life cycle needs improvement.
Vacuum Insulated Battery Case	• Weight, volume, and heat loss adequate. • Ready for scale-up to full size.
Heating/Cooling System	• Excellent performance. • Ready for scale-up.
Charger	• Excellent performance using electronic shunting. • Electrochemical overcharge control being tested.

BATTERY TEST RESULTS

Parameter	Test Results
Specific Energy, Wh/kg*	
40-A	110
J227a/C	112
J227a/D	104
Specific Power, W/kg*	
50% /DOD/300 A	97
Life Cycle	
Cells	350
Batteries	120
Reliability	• Operated batteries with one or more failed cells • Loss of 2 V/failed cell • I^2R heating no problem
Safety	• Operated without incident as expected

*Cell weight basis.

Li-Al/FeS_2 RESEARCH AT ANL

T. D. Kaun, M. J. Duoba, and K. R. Gillie
Argonne National Laboratory

Research is being conducted to bring a high-performance secondary battery containing Li-Al/FeS_2 cells with molten-salt electrolyte closer to commercial development. To maintain the electrolyte in the molten state, cells are normally operated at temperatures of 375-425°C. The objective of this research is the development of lithium-alloy/FeS_2 cells that will attain high performance (~200 Wh/kg and 400 W/kg) and long cycle life (>1000 cycles) and will have the potential for low-cost fabrication. Recent efforts have been concentrated on developing an electrolyte-starved (ES) cell design that is both overdischarge and overcharge tolerant (OCT). Also under investigation is a bipolar configuration that will substantially increase battery performance.

As reported earlier, an improved lithium-alloy/FeS_2 cell has shown promise of achieving the performance and cycle-life goals. Our improved FeS_2 cell has a low melting electrolyte, 25 mol % LiCl-37 mol % LiBr-38 mol % KBr (mp, 320°C), and a densely loaded FeS_2 electrode containing 15 mol % CoS_2, which is operated only on the upper voltage plateau (U.P.). Recent cell tests have demonstrated excellent capacity stability. A prismatic bicell (12 Ah) operated at a 2-h discharge rate and a 4-h charge rate has achieved 1027 cycles and 7000 hours of operation (see Fig. 1). After 1000 cycles, the cell operated with greater than 80% of its initial capacity and had a coulombic efficiency of about 96%. The FeS_2 electrode retained at least 90% of its initial capacity, as indicated by a reference electrode, throughout these 1000 cycles.

Overdischarge tolerance of the Li-alloy/U.P. FeS_2 cell in future battery applications will be handled by use of a Li-alloy electrode that limits the cell discharge capacity. Such cells, commonly referred to as "lithium limited," are necessary to avoid excessive expansion of the U.P. FeS_2 electrode if discharged into the lower voltage plateau. The capacity stability of such a cell design has been verified. A 12-Ah (100 cm^2 separator) cell has been operated for >900 cycles with stable capacity and >98% coulombic efficiency. By design, the electrode capacities of the cell are matched in such a way that, at 90% utilization of the U.P.-FeS_2 electrode, an 80% utilization of the Li-Al electrode needs to be achieved, at which point it becomes highly polarized and ends the discharge cycle by causing a sharp drop in cell voltage. The polarization of the Li-Al electrode at this point is about 300 mV. This abusive operation of the Li-Al electrode in the cell does not markedly affect its capacity or result in the long-term deposition of aluminum in the separator.

Conventional Li-alloy/metal sulfide battery cells require an electronic charger/equalizer to protect the cells from destructive overcharging. Overcharging generally results in oxidation of the active material in the positive electrode so that the FeS_2 is oxidized to sulfur and $FeCl_2$, which leads to cell short circuiting by the deposition of iron particles in the separator. Among the several chemical overcharge tolerance options that we examined, the lithium-shuttle mechanism was found to offer the best promise. The basis of this mechanism is the dissolution of lithium into the electrolyte from a high lithium-activity negative electrode and its diffusion to, and chemical reaction with, the positive electrode at the end of charge. Tests of Li-alloy/FeS_2 cells (25-Ah capacity) have demonstrated that the lithium-shuttle mechanism provides sufficient levels of overcharge tolerance. Figure 2 shows the electrode potentials of a Li-alloy/U.P. FeS_2 cell (operated at ~400°C) during a charge-discharge cycle in which a bulk charge at 25 mA/cm^2 to 2.03 V is followed by a trickle charge of 3.0 mA/cm^2. As seen, the potential for the LiAl + 10% $Li_5Al_5Fe_2$ electrode undergoes about a 200-mV transition near full-charge capacity. As is crucial for the preservation of cell longevity, the U.P. FeS_2 electrode indicates negligible change in potential; that is,

it is protected from the deleterious polarization of overcharge. Also, the Li-alloy electrode potential is little changed from -200 mV [vs. $\alpha+\beta$(Li-Al)] during the trickle-charge period. The self-discharge rate undergoes a stepwise increase (a 20-fold increase by the lithium-shuttle mechanism) to become equal and opposite in effect to the trickle-charge rate. In this test, the trickle-charge period (4 h) charged 5% more coulombs than the "rated" capacity. In confirmation, the extended trickle charge did not contribute additional capacity in the subsequent discharge. A coulometric and galvanic analysis indicated approximately 0% charge acceptance for a trickle charge at 2.5 mA/cm^2 with a Li-alloy/U.P. FeS_2 cell operated at 400°C.

The high lithium activity in the OCT cell requires the increased chemical stability of an MgO powder (Maglite S) rather than BN felt separator. (Likewise, the BN feedthrough packing has been replaced by AlN from Electrofuel, Toronto, Canada.) To maintain a mechanically strong MgO powder separator, an electrolyte-starved cell design had to be developed. By way of a modified electrolyte composition, the capacity utilization of the ES cell is now within 90% of the electrolyte-flooded cell. Although the electrolyte content continues to impose a trade-off in performance and cycle life. The chief improvement for the present ES U.P. FeS_2 cell was the reduced internal cell impedance. Our electrolyte development studies indicated that the off-eutectic LiCl-LiBr-KBr composition (34:32.5:33.5 mol %) has a 25% higher ionic conductivity at 400°C than that of the eutectic previously used. Studies have indicated that the higher ionic conductivity of the electrolyte approximately compensates for the reduced electrolyte content. As in Fig. 3, the area specific impedance at one second after current interrupt ($ASI_{t=1s}$) of 0.9 to 1.0 Ω-cm^2 for the ES U.P. FeS_2 cell is within 10% of the 0.8 to 0.9 Ω-cm^2 achieved by earlier electrolyte-flooded (with BN felt separator) cells. Moreover, the impedance curves with depth of discharge are virtually flat (Fig. 3). This is an especially desirable feature for a high-performance electric vehicle battery. Recent ES U.P. FeS_2 cells (20-Ah capacity) with OTC have been assembled with commercially pressed (Westinghouse Oceanic, Cleveland, OH) MgO-powder separator and electrode plaques. The successful operation of these cells indicates the ease of technology transfer and provides further demonstration of our FY89 milestone task.

In an effort to significantly improve the performance of the U.P. FeS_2 battery, work is being initiated on a bipolar configuration. One of the major challenges in this development effort is electrolyte containment. A new bipolar battery design (Fig. 4), which is hermetically sealed, is expected to provide long-term stability. Earlier versions used a gasket-type peripheral seal and were short lived. The hermetic peripheral seal relies upon the use of new ceramic materials that are chemically stable to the molten electrolyte, which has a high sulfide and lithium ion activity. Cell seals prepared with this sealant material should provide an electrically insulating, gas-tight bridge between the metallic housings of the electrode assemblies. To maintain structural integrity, the coefficients of thermal expansion of the ceramics are being matched to those of the metal components. In a bipolar battery, cells are stacked so that the positive and negative electrodes have a common current collector, the bipolar plate. This arrangement greatly reduces the weight contribution of the nonactive cell components (Table 1). Additionally, a uniform current distribution improves electrochemical performance. Based on a 100-cycle test of an FeS version, specific energy is increased by 30% and specific power is doubled compared with those of a monopolar cell. Projected performance for a five-passenger automobile powered by a bipolar Li-alloy/ FeS_2 battery is outstanding: a 640-km range and acceleration comparable to that achieved with a gasoline engine.

Acknowledgments:

This work was supported by the U.S. Department of Energy under Contract No. W-31-109-ENG-38. The authors are grateful for the support and encouragement of K. M. Myles, C. C. Christianson, and D. R. Vissers.

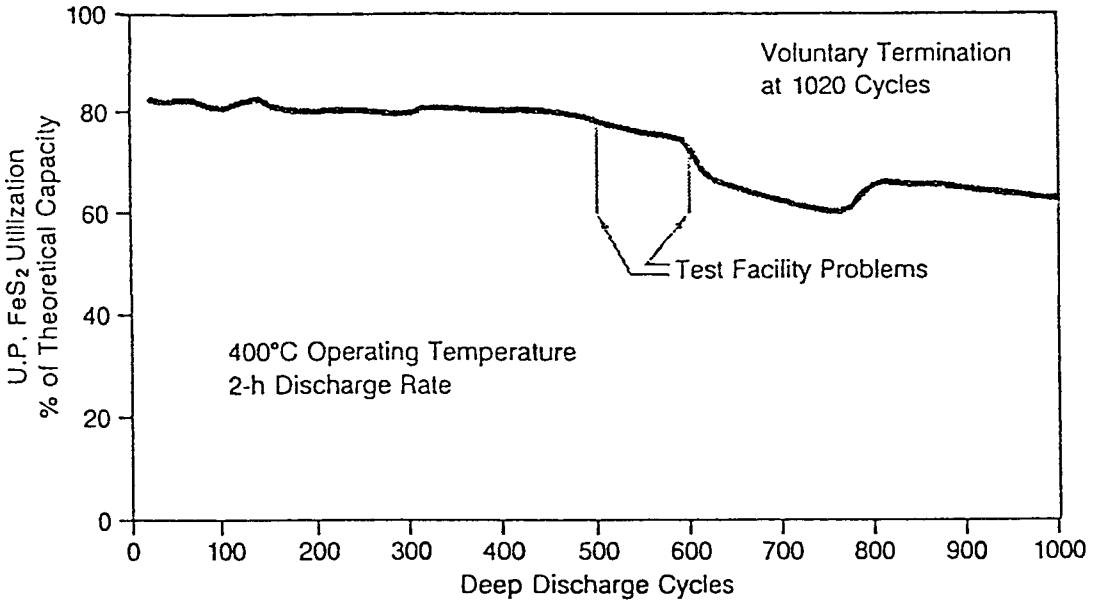

Fig. 1. Lifetime Test of Li-Alloy/U.P. FeS_2 Cell where Cell Capacity is Limited by the Li-Al Electrode After Cycle 500.

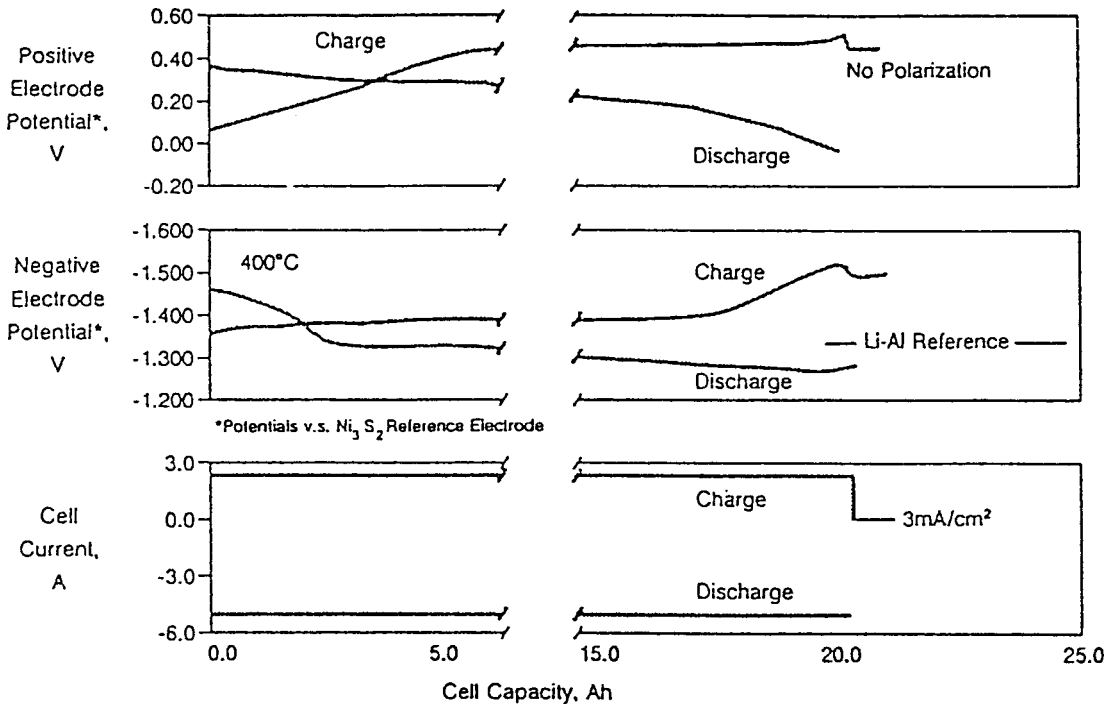

Fig. 2. Demonstration of Trickle-Charge Tolerance for U.P. FeS_2 Cell in which 5% Additional Capacity is Charged without Polarizing the Positive Electrode.

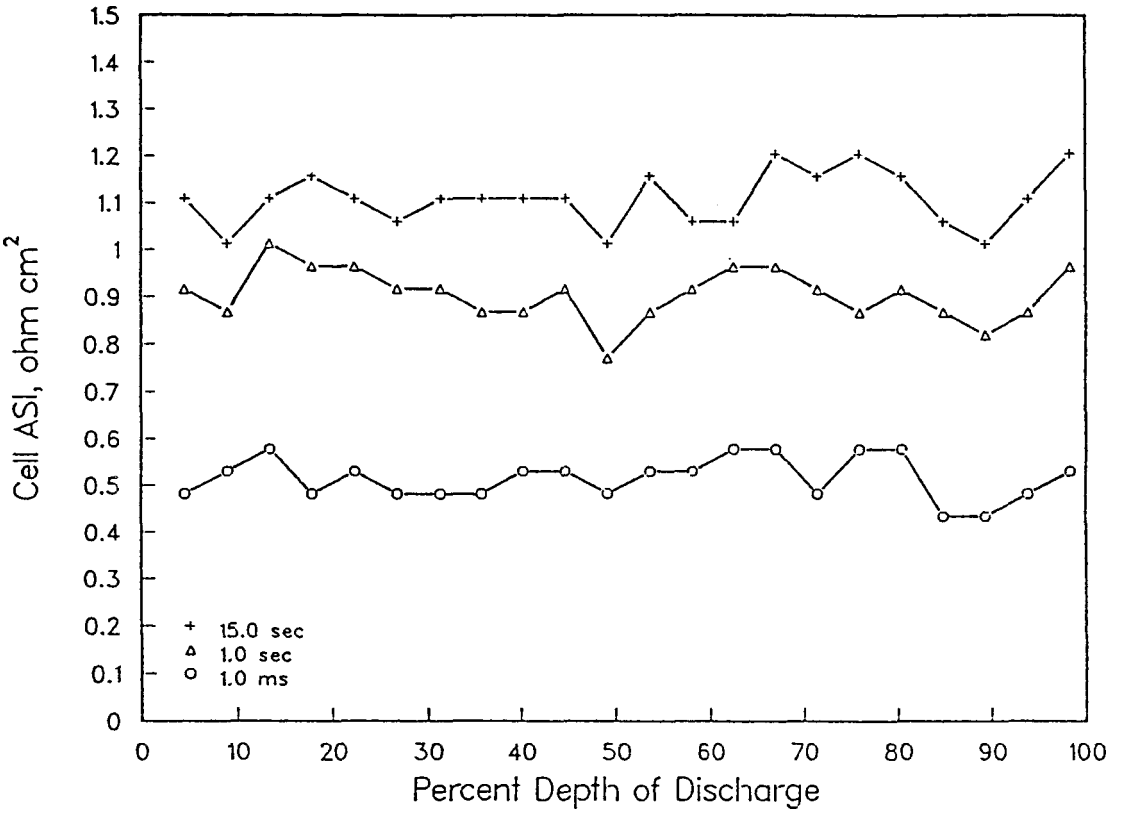

Fig. 3. Cell Impedance (in three time domains) for an Electrolyte-Starved U.P. FeS_2 Cell with LiCl-Rich LiCl-LiBr-KBr Electrolyte.

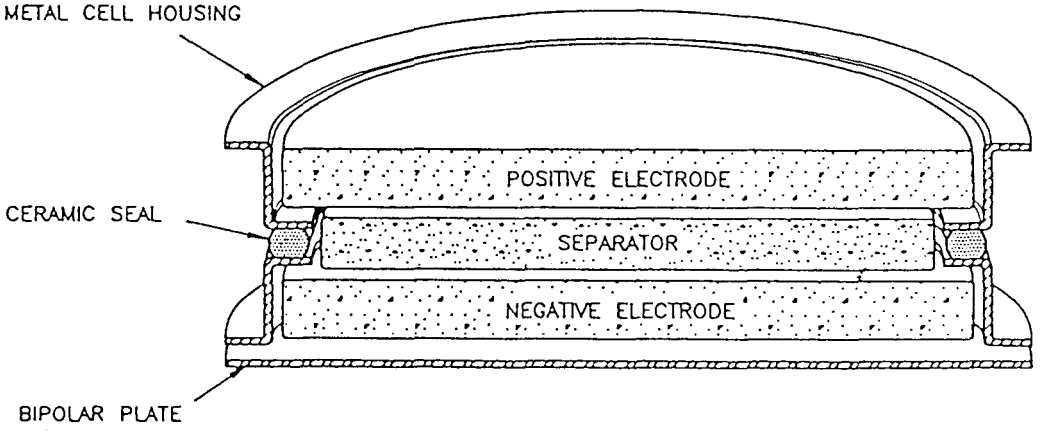

Fig. 4. Bipolar Lithium/Iron Sulfide Cell Design with Hermetic Peripheral Seal.

Table 1. Weight Breakdown and Performance of Li-Alloy/FeS Developmental Cells

Component	Weight %	
	Monopolar (Westinghouse)	Bipolar ANL
Electrode Active Materials		
Positive	16.5	27.7
Negative	13.6	19.3
	(30.1)	(47.0)
Electrolyte	23.9	35.0
Separator	6.2	8.0
Hardware		
Current Collector	27.0	7.5 - bipolar plate
Cell Container	12.8	2.5 - seal
	(39.8)	(10.0)
Cell Performance		
Cell Impedance	1.0 $\Omega \cdot cm^2$	0.6 $\Omega \cdot cm^2$
Specific Capacity	76 Ah/kg	99 Ah/kg
Specific Energy	94 Wh/kg	127 Wh/kg
Specific Power	100 W/kg	220 W/kg

BATTERY TESTING AND EVALUATION

CHAIRPERSON:

Robert Swaroop
Electric Power Research Institute

STATUS AND RESULTS OF ANL LIFE EVALUATION OF VALVE-REGULATED LEAD-ACID LOAD-LEVELING BATTERIES

W. H. DeLuca, J. F. Miller, C. E. Webster, and R. L. Hogrefe
Argonne National Laboratory
Chemical Technology Division
Argonne, Illinois

Argonne National Laboratory has developed and initiated a three-year life evaluation of both gelled-electrolyte and absorbed-electrolyte valve-regulated lead-acid (VRLA) battery technologies for deep-discharge applications. The objectives are (1) to use accelerated testing techniques to obtain data within 6 months on VRLA battery life expectancy, and (2) to determine VRLA battery life within a 2-3 year time period under temperature and depth-of-discharge (DOD) conditions that simulate those encountered in a utility load-leveling environment. The accelerated life test uses a matrix of operating conditions designed to increase the stress of known failure modes, thereby accelerating the mechanisms that cause battery end-of-life. The primary failure mode is expected to be active material changes caused by charge-discharge cycling (i.e., microstructural and morphological changes, sulfation, mass isolation, loss of surface area, loss of porosity, etc.). The test matrix consists of four sets of operating conditions (80% and 100% DOD and 30°C and 50°C temperature), which include the stress factors to accelerate failure.

There are two types of VRLA batteries being tested: (1) 12-V modules manufactured by Johnson Controls, Inc. (JCI), with a gelled electrolyte; and (2) 6-V modules manufactured by GNB, Inc., with an absorbed electrolyte. Each module undergoes acceptance, baseline performance, and life testing. After failure, a teardown examination/analysis is conducted to identify the failure mode. End-of-life is defined as the inability to furnish 80% and 64% of rated capacity for the 100% and 80% DOD tests, respectively.

The GNB modules were received at ANL in November 1988, and four were installed in the test system for evaluation. Those modules have successfully completed their acceptance and baseline performance tests. Two of the modules were placed on life test at 30°C, and a third is undergoing 100% DOD accelerated life testing at 50°C. The fourth module is on float charge and awaiting 80% DOD life testing at 50°C while the high-temperature charge data are being examined.

The JCI modules were received in February 1989, and testing was initiated on four of the modules. Acceptance and baseline performance tests were completed in April. The four JCI modules were placed on the same test regime as the GNB modules.

Constant-current/constant-voltage (CI/CV) charging was initially recommended by both manufacturers (CV = 2.35 V/cell with -5 mV/°C temperature compensation at >25°C). The time needed to achieve the desired 105% charge return from 100% DOD was excessive for both the GNB (~18 h) and JCI (~26 h) modules. These results were discussed with each manufacturer, and GNB requested that their charge procedure be changed to a CI/CV/CI method to ensure an 8-h daily charge return of 105%. JCI was satisfied with an 8-h charge return of ~103% and recommended the continued use of CI/CV charges with a CV of 2.35 V/cell.

Results of the acceptance and baseline tests (Table 1) show that the percentage weight variation among the GNB modules was a factor of four greater than that for the JCI modules. However, the capacities of the GNB modules matched to within 2% and

were about 17% higher than their specified ratings at both the 8-h and 3-h discharge rate. A 23% decline in module capacity resulted with increased discharge rate (130 ⇉ 272 A); this decline is in close agreement with that specified by GNB.

The average capacity of the JCI modules was within 1% of the manufacturer ratings at both the 8-h and 3-h discharge rates. Their capacity decreased by only 12% as the discharge rate was increased from 135 to 318 A. However, individual module capacities at the 8-h rate varied (minimum to maximum) by ~7%. At the 3-h rate, the variation increased to ~12%. The module-to-module capacity variations were discussed with the manufacturer, who recommended that the weakest module be given a special 24-h charge with a CV level of 2.45 V. Following the special charge, the capacity of the weakest module increased by ~9%, and the variation between modules decreased to 7.4%. The manufacturer did not deem a 7% variation in module capacities to be excessive.

Life cycles were performed with discharges at a 3-h rate to a voltage limit and daily charges limited to 8 h or 105% return. A 3-h discharge and 8-h charge were selected to maximize the total Ah per day of life testing. Battery resistance ($R_B = \Delta V/\Delta I$) and IR-free voltage vs. DOD will be periodically derived from pulse discharge test data. Variations in these parameters with life will be studied for possible early identification of battery failure.

Two GNB modules (EG03LL03 and EG03LL04) and two JCI modules (EJ90LL01 and EJ90LL02) were placed on life test at 30°C in May 1989. An 80% DOD discharge cut-off voltage (DCOV) of 5.64 V and 11.54 V is being used for the GNB and JCI modules, respectively. The capacity history of these modules is given in Fig. 1. The GNB module has retained ~100% of its initial 770-Ah (4583-Wh) capacity after accumulating a total of 158 test cycles. The JCI module retains ~101% of its initial 802 Ah (9705 Wh) after accruing 138 cycles. The GNB and JCI modules being cycled to 100% DOD at 30°C use a DCOV of 5.25 V and 10.5 V, respectively. The GNB module has retained ~95% of its initial 1009-Ah (5885-Wh) capacity after accruing 125 cycles, and the JCI module has increased its capacity by ~2% to 960 Ah (11.34 kWh) after 115 cycles. Equalization charges (24 h or 110% return) are being performed about every 25 cycles. The GNB modules show a slight drop in capacity on the first discharge after an equalization charge. This is the result of a decline in their operating temperature caused by the long charge period. Subsequent discharges show that their capacity has improved with equalization charging. In comparison, the equalization charges have had no noticeable effect on the capacity of the JCI modules to this point in their life.

Accelerated life testing at 50°C and 100% DOD was initiated on a third GNB and JCI module. The capacity history of these modules is given in Fig. 2. Both modules had an initial 30°C capacity of ~1000 Ah prior to high temperature operation. With the start of 50°C operation, the capacity of the GNB module increased by ~13% and the JCI module by only ~3%. These increases in capacity are less than those of flooded-electrolyte types of lead-acid batteries (>20%) for the same temperature rise (20°C). However, the capacity of both VRLA modules started to rapidly decline with cycling at a rate of >1%/cycle. The initial CI charge rate was reduced from 300 to 150 A, but this had no effect on the rate of capacity loss. The charge return was then increased from 105% to 110%, which stopped the rapid decline in capacity on both modules. Continued cycling with 110% charge return at 50°C recovered some of the lost capacity, but not all.

Returning to an operating temperature of 30°C and cycling with a charge return of 110% has increased the capacity of both modules to almost its initial level. The initial results indicate that both battery types need a higher charge return (≥110%) at 50°C to maintain reproducible performance. Hence, the 8-h daily charge time limit will be removed, and the needed overcharge at 40 and 50°C will be identified for both 80% and 100% DOD operation. The results will be reviewed with each manufacturer, and a charge regime will be defined for 50°C cycling.

Acknowledgment:

This research is sponsored by the Electric Power Research Institute (EPRI) and, in part, by the International Lead Zinc Research Organization (ILZRO).

PRELIMINARY RESULTS OF VRLA BATTERY ACCEPTANCE AND BASELINE PERFORMANCE TESTS

Manufacturer	GNB	JCI
Model Number	85A25	15-LL12-70
Average Weight, kg	248.4	517.5
Variation	1.6%	0.4%
Capacity To 1.75 V/cell @ 25°C		
Mfr. 8-h Rating (Ah)	1040	1080
Average (Ah/Wh)	1234/7297	1077/12863
@ CI Rate (A)	130	135
Variation	1.9%	7.0%
Mfr. 3-h Rating (Ah)	816	954
Average (Ah/Wh)	947/5510	964/11450
@ CI Rate (A)	272	318
Variation	1.0%	7.4%
Volts @ 80% DOD (V)	5.644	11.451
Variation	0.3%	0.4%

CAPACITY HISTORY OF VRLA MODULES AT 30°C

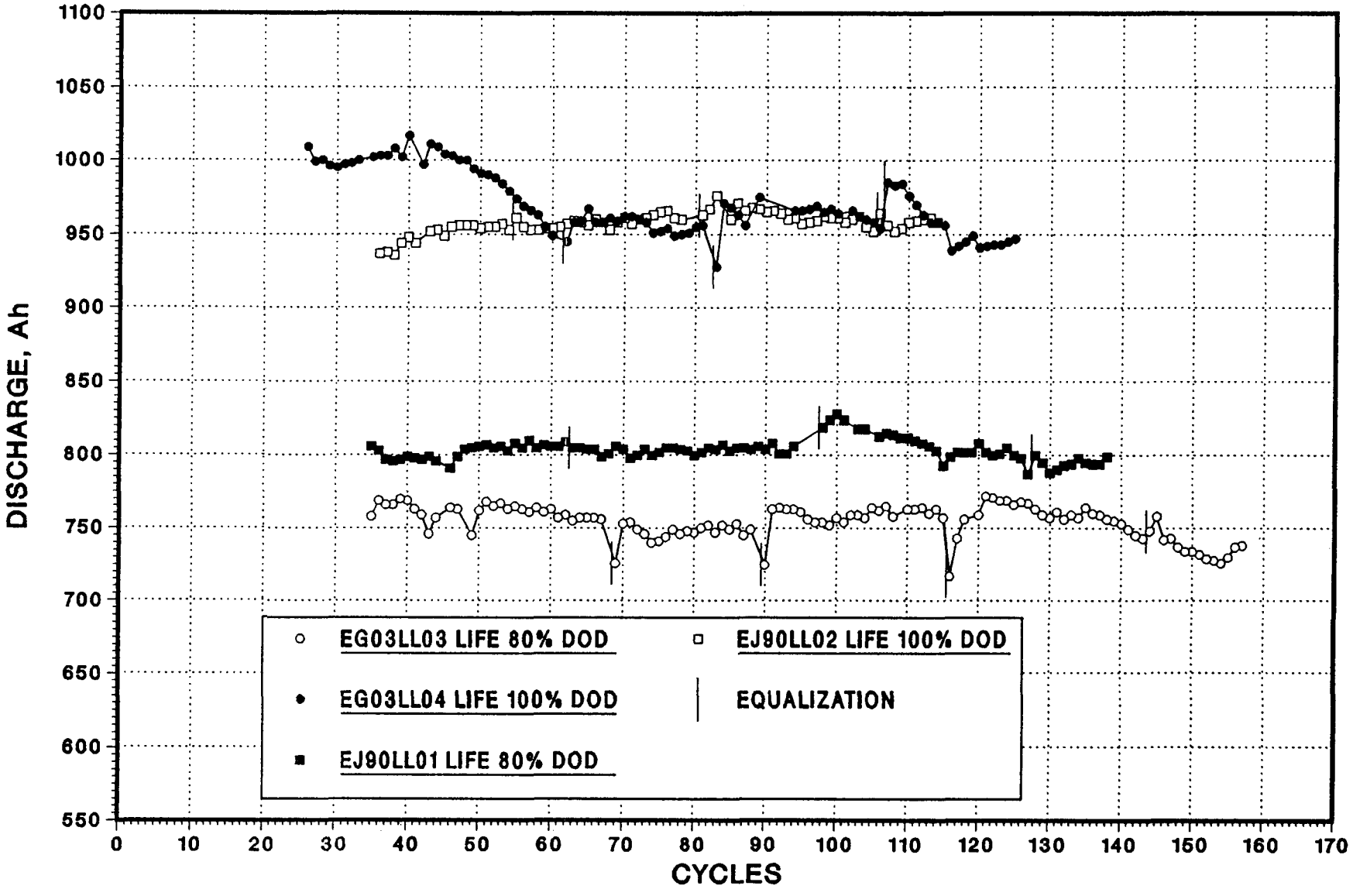

CAPACITY HISTORY OF VRLA MODULES AT 50C

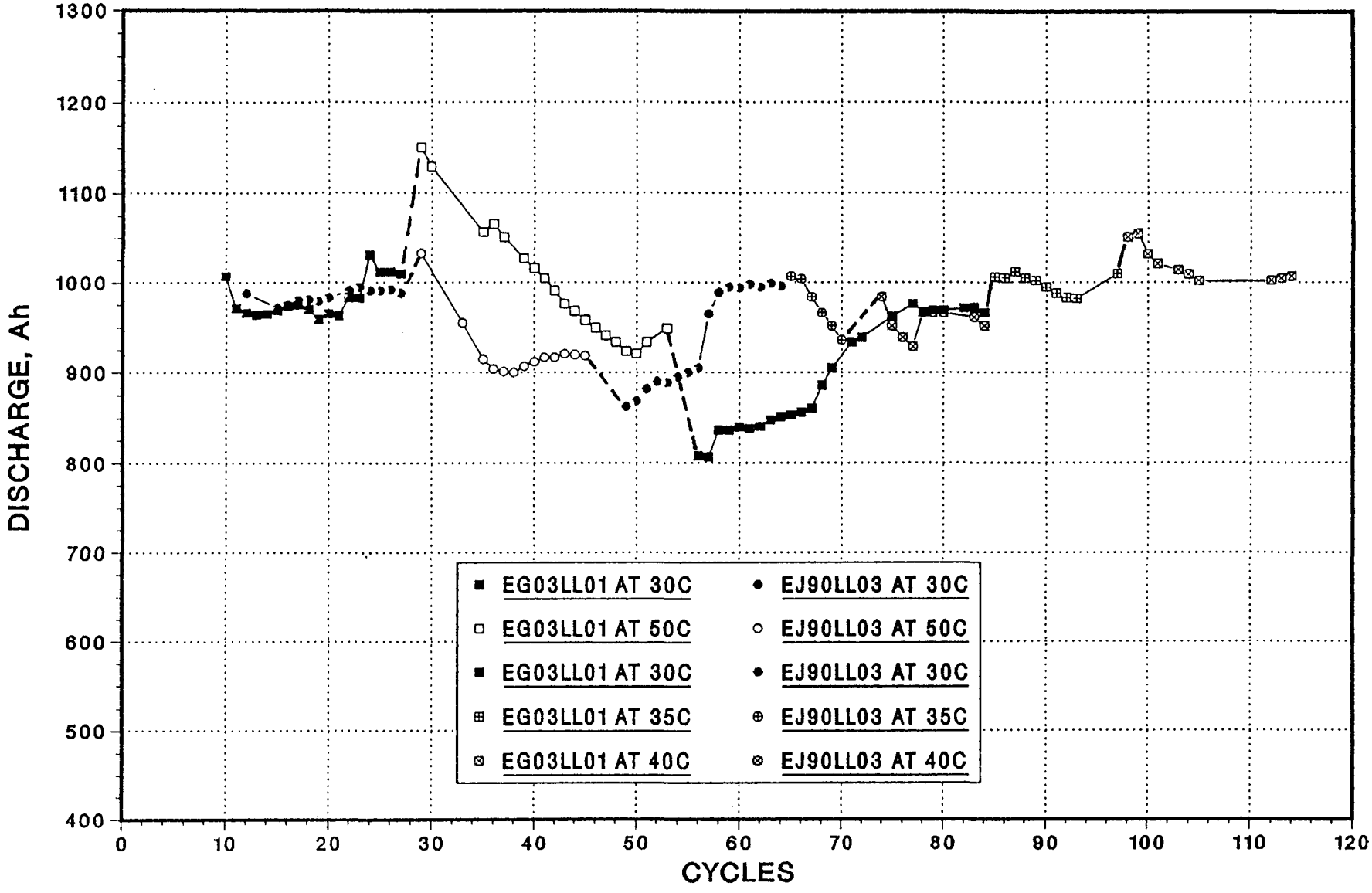

EVALUATION OF TWO STACKED VALVE-REGULATED BATTERIES FOR UTILITY CYCLING APPLICATION

G. R. Grefe, E. A. Hyman, B. M. Radimer, D. E. Marusiak
Public Service Electric and Gas Company
Somerville, NJ 08876

Many lead-acid battery manufacturers now offer valve-regulated batteries for standby and some cycling applications. These batteries are sometimes referred to in manufacturer's literature as being "sealed" or "maintenance-free". The potential advantages, if they are found suitable for bulk energy storage, include: reduced footprint, reduced maintenance, fewer auxiliary systems, easier installation and removal, and safer operation. Reduced footprint is also an important advantage in control battery applications for utilities to meet expansion needs in presently available space.

To help utilities and developers to better understand the applications, advantages, and promise of valve-regulated lead-acid batteries for utility cycling application, EPRI has funded the evaluation of two specific batteries of contrasting design sized at about 100 kWh each (8-hour rate) at the BEST Facility. Tasks include procurement, installation, acceptance, testing in utility and customer-side applications, performance evaluation, and preparation for a PSE&G field demonstration. Applications to be tested include both cycling and float service. Cycling service includes both energy storage, the profitable resale of energy acquired and stored at low cost, and power regulation: regulating tie-line flow (area requirement), frequency demand shaving, and UPS applications.

The batteries included in the test program are GNB, Inc. 1040 Ah absorbed glass fibre battery modules, model number 85A25 and Johnson Controls, Inc. 1080 Ah gelled battery modules, model number LL12-70. Both batteries were sized to nominally 120V. Each battery was delivered with a battery charger specified and purchased by the battery manufacturer.

The batteries were tested in a variety of applications by discharging the two battery systems in series and recharging them separately.

The dc/dc efficiency was 85% for JCI and 83% for GNB. However, forced cooling for the JCI battery would reduce the overall system efficiency.

Initial testing has proven that fundamental design concepts of the 2-VRLB systems are consistent with requirements for utility energy storage applications. Daily cycling which meets utility requirements for these storage applications maintains battery parameters within manufacturers' operating limits of temperature and charge-back. Energy and power density due to the stackable design made possible by freedom from water addition is excellent. Ease of installation and access for maintenance are also good, reducing installation and O&M costs.

Battery energy efficiency is greater than flooded cell systems previously tested, but the impact of blower energy consumption for the JCI battery must be evaluated. JCI has redesigned the blower system to minimize impact on efficiency. The effects of reduced cooling air flow and thermostatic blower operation on battery temperature will need to be evaluated.

Gas emissions and water loss which can shorten life and degrade performance have not been evaluated. Performance of battery valves and post-to-battery top seals which can effect gas emissions and water loss will be evaluated over the duration of the test. Gas emissions from three GNB cells and nine JCI cells are being metered and water loss will be measured by module weight loss.

TABLE 1

VALVE-REGULATED BATTERY SYSTEM SPECIFICATION SUMMARY

	GNB	JCI
Cell/Battery Model Number	85A25	LL12-70
Number of Cells/Batteries/Module	3 cells	15, 6-cell Batteries
Module Voltage (Nominal)	6	12
Number of Modules	20	10
Positive Plate Alloy	Antimony	Calcium
Electrolyte Immobilization	Absorbed (Glass Fibre)	Gelled (Fumed Silica)
Electrolyte SpGr	1.280	1.280
Module Rating, 1.75V, 8 hr (Ah)	1040	1080
Battery System kWh Rating	100	100
Predicted Cycle Life	1700[1]	1700[1]
Module Short Circuit Current (amps)	8,400	30,000
Cooling	Natural Convection	Blower
Module Dimensions(M) WxDxH	0.85x0.65x0.22	1.1x1.1x0.5
Footprint of Test Batteries (M^2)	1.1	4.0
Battery Stack Height (M)	2.3	3.4
Modules/Stack	10	5
Floor Loading (Kg/cm^2)	0.24	6.6

Note [1] At 77°F, 760 Ah maximum discharge

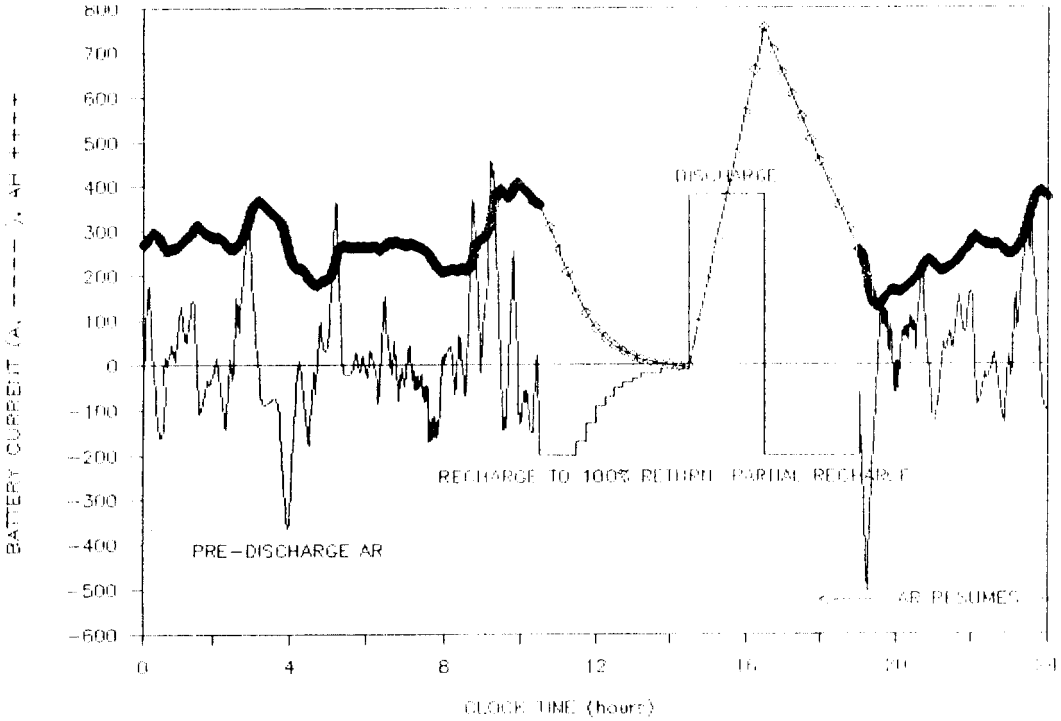

FIGURE 13: CONCEPTUAL SCHEME FOR OPERATING A SHARED CUSTOMER/UTILITY POWER REGULATING PLANT

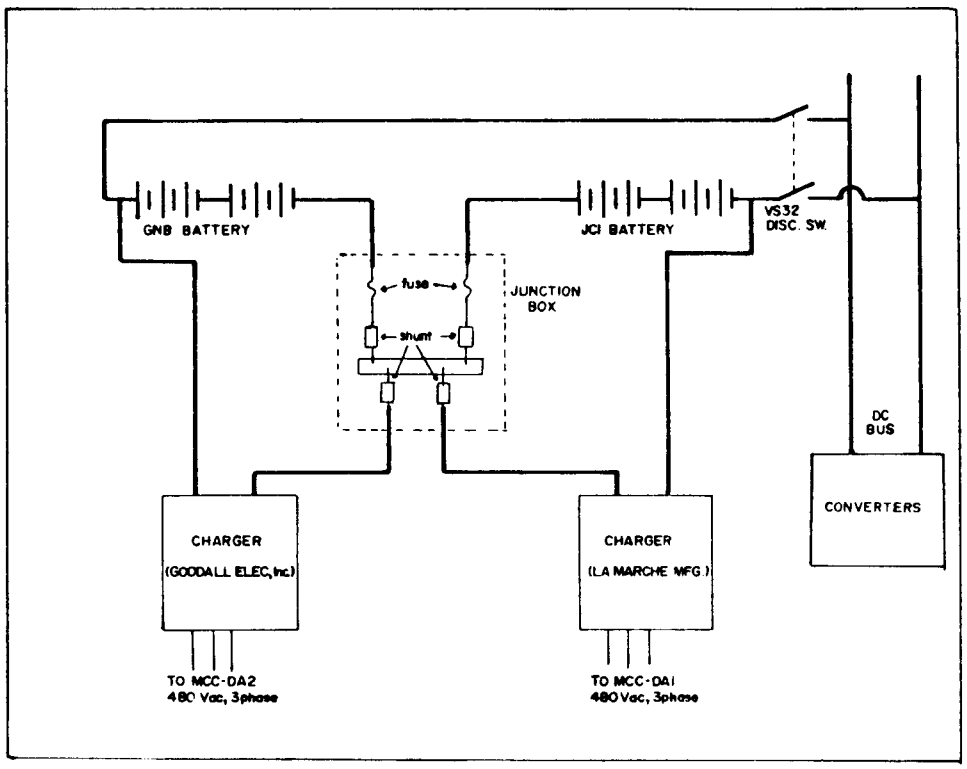

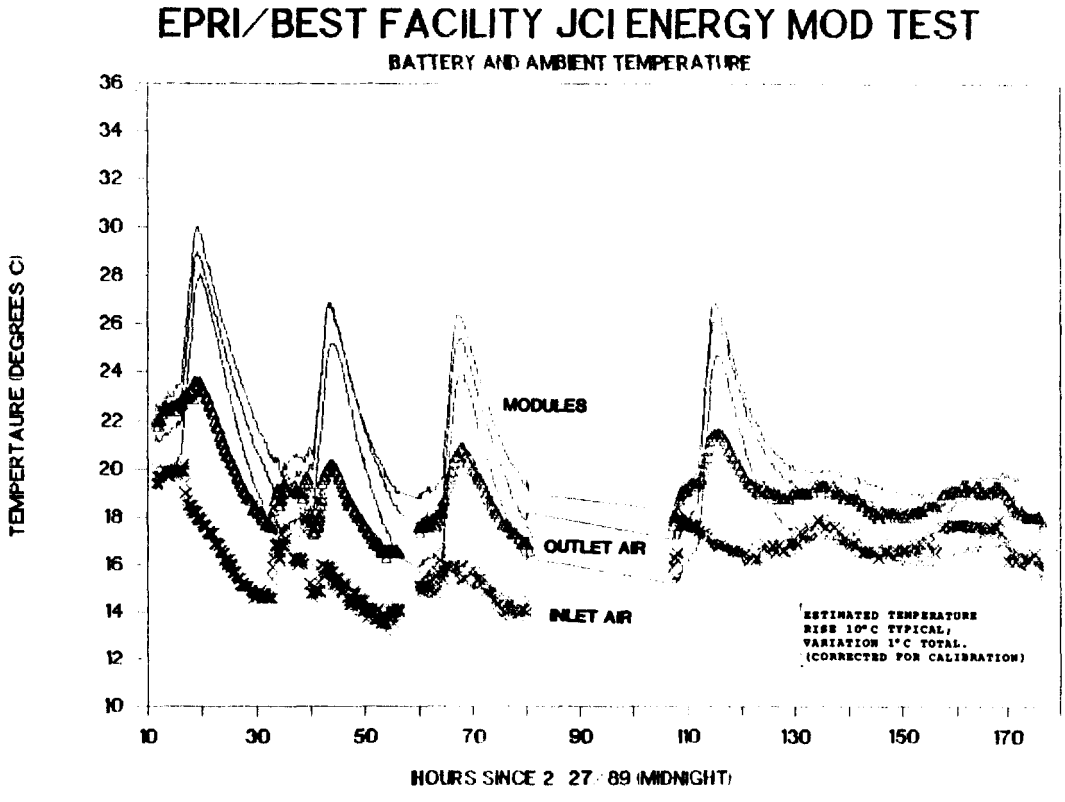

FIGURE 9: THREE JCI MODULE, INLET AND OUTLET AIR TEMPERATURES

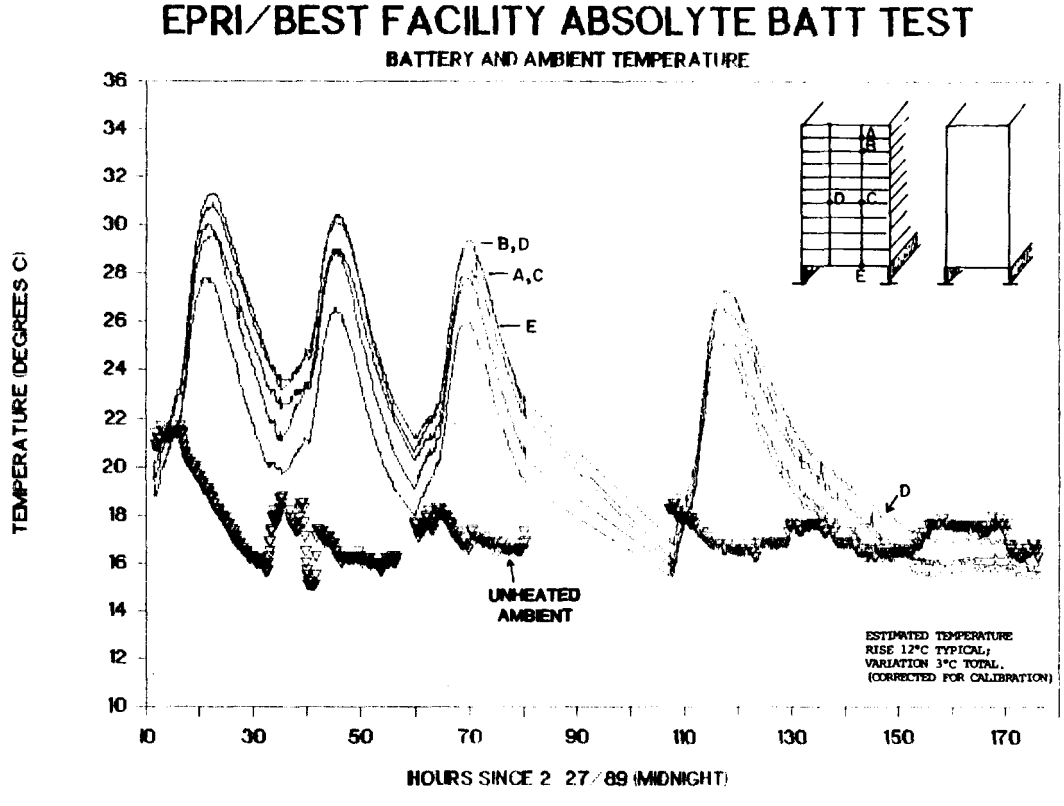

FIGURE 10: SURFACE TEMPERATURE OF FIVE GNB CELLS AND AMBIENT AIR TEMPERATURE

MONITORING STATE OF CONDITION OF LEAD-ACID BATTERIES USED IN UTILITY APPLICATIONS

A. J. Salkind, J. J. Kelley, J. B. Ockerman
Rutgers University and UMDNJ-Robert Wood Johnson Medical School
Piscataway, NJ 08854

B. M. Radimer, E. A. Hyman
Public Service Electric and Gas Company
Somerville, NJ 08876

G. M. Cook
EPRI
Palo Alto, CA 94303

Lead-acid battery systems are used by utilities for a variety of applications. They include uninterruptible power supply (UPS) units for computer and control systems, emergency dc power for plant critical equipment, and for utility energy storage.

In the case of emergency dc power and similar applications, state of condition of the battery is extremely important and, in many cases, the battery cannot be removed from the system for testing. The state of condition is the ability to meet some necessary prescribed load profile and is different from the state of charge.

A literature study of various non-invasive on-line monitoring methods was carried out to determine which might prove suitable for use in this utility application. These are quite different from the old traditional methods of discharge cycling, pilot cells, coulometry, and measurement of specific gravity.

The new techniques mainly use ac or dc perturbation methods and/or measurements of impedance and capacitance.

In emergency dc power applications the station battery is a critical component. When loss of ac power to the station occurs, the battery must function in an emergency capacity to operate critical equipment. Chief among these is operation of the dc emergency oil pump; which lubricates seals on the hydrogen cooling system and turbine generator bearings. Loss of the oil seals could lead to leakage of hydrogen and possible fire or explosion.

In the case of nuclear plants, batteries are also part of a redundant plant emergency shut down system. The nuclear industry is interested in providing monitoring capability which will give assurance that the battery systems will function when called upon.

The three typical duty cycles of utility batteries are:

1. Nuclear Class 1E and Generating Station Control - typically the battery is 125V at 400 to 1000 ampere hours. The battery is used to clear the breakers - 1/4 second high rate pulse twice a day (300 ampere load initially followed by station maintenance loads of 200 amperes over two hours or more followed by recharging). Back up is a diesel generator system.

2. Generating Station 250V Battery - the battery must start and operate oil pumps lubricating bearings and seals of the hydrogen cooling system.

3. A T&D Station Battery - the battery is typically small, 100 A hours or less. An initial high rate pulse is required to clear the breakers and up to 12 hours discharge to maintain power to the station. Following this the battery must be capable of clearing the breakers - a high rate pulse.

In order to meet these somewhat diverse service conditions both high rate pulse capability and overall capacity are important battery parameters.

Acknowledgement:

This research is supported by the Electric Power Research Institute.

EXAMPLE OF BATTERY SYSTEMS AND SIZES IN A SINGLE NUCLEAR PLANT

BATTERY ID NO.			BATTERY CELL RATING - TYPE MFGR. ID NO.	AH/8HR RATE	NO. CELLS
1AD411	125VDC	(1E)	LC-25	1800	60
1BD411	|	|	|	|	|
1CD411	|	|	|	|	|
1DD411	|	|	|	|	|
1CD447	|	|	KC-15	577	|
1DD447	|	|	|	|	|
1A1D471	125VDC		LC-23	1650	60
1A2D471	|		|	|	|
1B1D471	|		|	|	|
1B2D471	|		|	|	|
1A1D477	|		|	|	|
1A2D477	|		|	|	|
1B1D477	|		|	|	|
1B2D477	|		|	|	|
1OD511	|		LC-21	1500	|
1AD301	24VDC		DCU-9	100	24
1BD301	|		|	|	|
1OD421	250VDC	(1E)	KC-21	825	120
1OD431	|	|	KC- 9	330	|
1OD141	250VDC		KC-21	825	120

STATE OF CHARGE (%)	CELL VOLTAGE (VOLTS)	SPECIFIC GRAVITY (g/cm^3)
100	2.11	1.260
87	2.09	1.240
75	2.07	1.220
62	2.05	1.200
50	2.03	1.180
37	2.01	1.160
25	1.99	1.140
12	1.97	1.120
0	1.95	1.110

A difference of 60 millivolts in the open circuit voltage corresponds to a change in the battery from 100% charged to discharged. Over the same capacity range, electrolyte specific gravity changes by 0.160 g/cm^3.

ALKALINE-CARBONATE ELECTROLYTES FOR ZINC/NICKEL OXIDE BATTERIES

Frank R. McLarnon, Thomas C. Adler and Elton J. Cairns
Applied Science Division
Lawrence Berkeley Laboratory
Berkeley, California 94720

Zinc/nickel oxide batteries can be designed to deliver good specific energy (>70 ı/kg) and excellent specific power (>150 W/kg), so they may provide a viable power ɔurce for electric vehicles. Major efforts to develop Zn/NiOOH batteries were ɔcluded in the DOE Near-Term Battery Program, but they were discontinued in FY 1982 1). A major problem with the Zn/NiOOH battery is its limited cycle life, which has een correlated to the redistribution of active material (shape change) in the zinc lectrode. A number of approaches have been shown to extend the cycle life of the n/NiOOH battery: (*i*) modifications to the electrode composition, (*ii*) modifications o the electrolyte composition, (*iii*) novel electrode structures, (*iv*) specially esigned separators, (*v*) non-standard electrical charging waveforms, and (*vi*) gitation of one or more cell components during charge. There is evidence that each f these approaches can extend Zn/NiOOH cell lifetimes. However, there is often an ɔnwelcome concomitant effect, such as significant degradation in cell specific energy ɔr specific power, increased cost, mechanical complexity, poor low-temperature ɔerformance, or inability to perform under deep-discharge regimens.

It is well known that the rate of shape change can be decreased by reducing the ɔincate-ion concentration in the electrolyte. Because the solubility of zinc depends ɔtrongly on the hydroxyl-ion concentration, substitution of various anions for ɔydroxyl ions in the electrolyte can significantly lower the zincate-ion solubility ɯhile maintaining acceptable conductivity. Nichols *et al.* successfully applied this ɔtrategy using fluoride and borate anions (2). Jost patented an alkaline-carbonate ɔlectrolyte for Zn/NiOOH cells in 1969 (3). Here we report the results of an ɔvaluation of alkaline-carbonate electrolytes in small test cells.

Zinc electrodes of 1.3-1.5 Ah capacity were fabricated as cakes pressed to each side of a lead-plated copper mesh current collector. The dry electrode composition (in wt %) was 93% ZnO, 2% PbO, 4% Teflon and 1% newsprint, and three layers of Celgard 3401 microporous polypropylene surrounded each zinc electrode. Two sintered NiOOH electrodes (capacity one-third that of the zinc electrode) were surrounded by single layers of Pellon 2524 wick, and the zinc electrode was sandwiched between them. Teflon spacers maintained a uniform pressure of 27.6 kN/m^2, and the cells were vented to the atmosphere through CO_2 scrubber tubes.

Zn/NiOOH cells were cycled on a computer-controlled battery test system developed by Katz *et al.* (4). A test cycle began with a constant-current charge which continued until the cell reached 1.93 V; charge was completed at this plateau voltage using a reduced current. After a 15-minute open-circuit interval the cell was discharged at constant current to a 1.1-V limit, followed by another 15-minute open-circuit interval to complete the cycle. Charge and discharge times typically ranged from 7 to 12 hours and 2 to 3 hours, respectively. Testing was terminated when the cell failed to sustain a capacity greater than 60% of its initial value, at 100% depth of discharge.

Two different electrolytes were evaluated for cycle-life performance: standard high-alkalinity electrolyte (6.8 M KOH - 0.6 M LiOH) and alkaline-carbonate electrolyte (2.5 M KOH - 2.5 M K_2CO_3 - 0.5 M LiOH.) The alkaline-carbonate cell reached the test-termination criterion at 334 cycles, which is more than three times

the 106 cycles obtained for the standard cell (Fig. 1). Shape change was monitored throughout the cycle-life tests of these cells using *in situ* X-ray photographs. Greatly reduced zinc-electrode shape change was evident in the cell containing alkaline-carbonate electrolyte, compared to the standard-electrolyte cell. After 100 cycles, the zinc electrode in the alkaline-carbonate electrolyte showed a mottled but generally uniform appearance, whereas the standard-electrolyte cell showed severe zinc material redistribution, *i.e.* most of the material migrated to the edge regions of the electrode.

When the cells began to lose their ZnO reserve (an imbalance caused by operating the cells in the vented mode), they were fully discharged. The fraction of original capacity that was recovered during such an excursion is a good measure of the quantity of active zinc remaining on the zinc electrode. After 100 cycles, the cell containing alkaline-carbonate electrolyte retained a quantity of zinc equivalent to more than 90% of its original capacity, whereas the standard-electrolyte cell retained only 60% of its original capacity. Previous investigations have shown that significant amounts of zinc deposit in the NiOOH electrode, and the alkaline-carbonate electrolyte may have inhibited this deleterious process.

A number of cells were employed to evaluate a range of alkaline-carbonate electrolyte compositions. All combinations behaved well, except for a 0.6 M KOH - 4.5 M K_2CO_3 - 0.2 M LiOH electrolyte. This electrolyte produced low nickel-electrode efficiencies and very long constant-voltage charging periods (10-20 h). These deficits were probably caused by a hydroxyl-ion concentration that was too low to support the electrochemical reactions, and perhaps by poisoning of the nickel-electrode reaction due to excessive carbonate content. These tests provided the data shown in Fig. 2, which illustrate the functional limits of alkaline-carbonate electrolytes on a ternary diagram. Other tests have demonstrated that alkaline-carbonate electrolytes perform well in starved-electrolyte and sealed-cell configurations.

Acknowledgement

This work was supported by the Assistant Secretary for Conservation and Renewable Energy, Office of Energy Storage and Distribution, Energy Storage Division of the U.S. Department of Energy under Contract No. DE-AC03-76SF00098.

References

1. R. Roberts, "Status of the DOE Battery and Electrochemical Technology Program IV," Mitre Corporation Report No. MTR-82W232 (1983).
2. J.T. Nichols, F.R. McLarnon and E.J. Cairns, *Chem. Eng. Commun.* **37**, 355 (1985).
3. E.M. Jost, U.S. Patent No. 3,485,673 (1969)
4. M.H. Katz, F.R. McLarnon and E.J. Cairns, *J. Power Sources* **10**, 149 (1983).

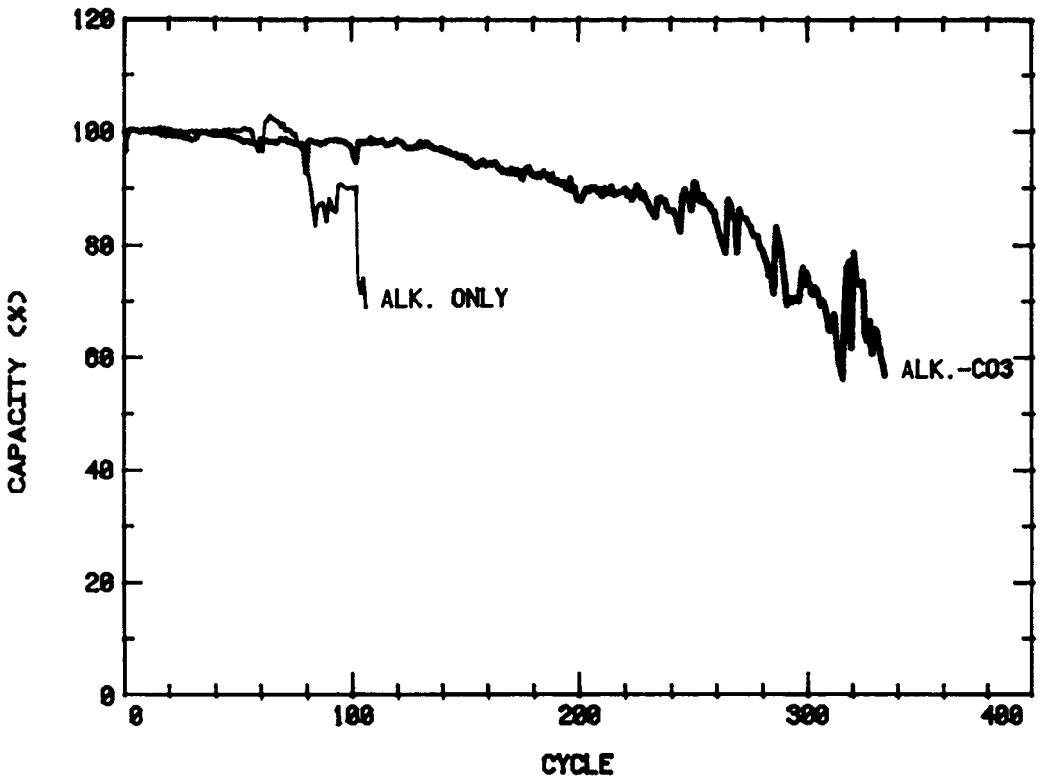

Figure 1. Capacity *vs* Cycle Number for Standard-Electrolyte and Alkaline-Carbonate-Electrolyte Zn/NiOOH Cells.

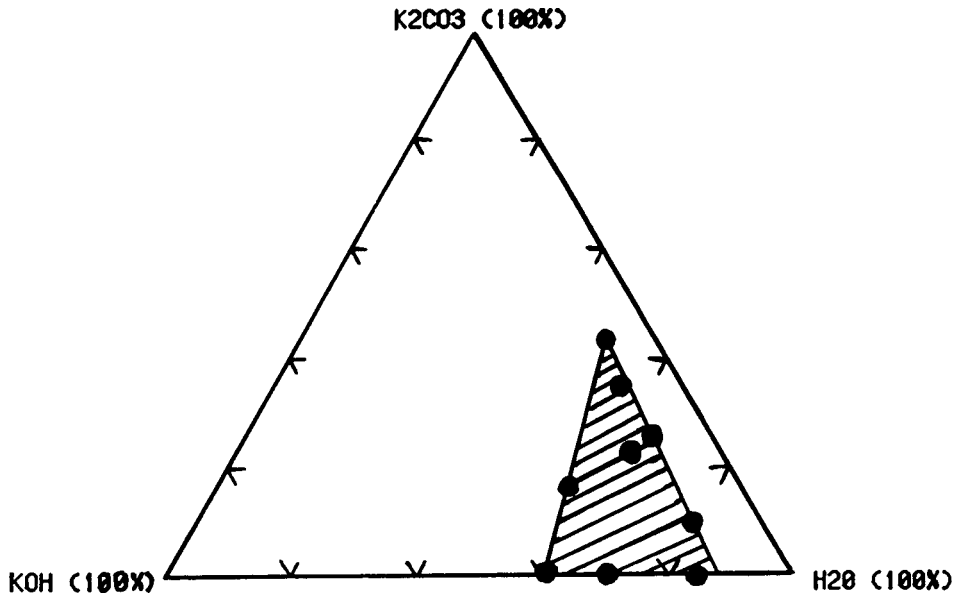

Figure 2. Ternary Diagram of Alkaline-Carbonate Electrolytes. The Cross-Hatched Area Shows the Zn/NiOOH Cell Functional Region.

TUBULAR LEAD-ACID BATTERIES

J. Hampton Barnett, ELECTROTEK Concepts, Inc. and
Brian Phillips, Chloride EV Systems

INTRODUCTION

ELECTROTEK Concepts, Inc. (ELECTROTEK), in cooperation with the Electric Power Research Institute (EPRI) is continuing the test and evaluation of electric vehicles (EVs), EV batteries, and component systems that was performed previously by the Tennessee Valley Authority (TVA). The tests are being conducted at the Electric Vehicle Test Facility (EVTF) in Chattanooga, Tennessee. The facility serves as the national EV test center for EPRI and the utility industry. The 9600 square-foot structure contains a battery laboratory, an electronics laboratory for charger testing, an engineering test center (chassis dynamometer), a critical maintenance and service bay, charging facilities, and staff offices. Real-world testing is performed on an adjoining one-mile oval test track and on designated urban routes in downtown Chattanooga. The purpose of this effort is to identify an EV technology for utility and commercial fleet applications.

It is widely recognized that the battery is the key to the EV's success. The more energy that can be stored in a battery, the farther the vehicle can be driven before refueling or recharging is required. Research by EPRI, the Department of Energy, and battery manufacturers is providing promising batteries for testing in EVs at the EVTF.

IN-VEHICLE BATTERY TESTING

The principle effort of the EPRI/ELECTROTEK EV projects is the in-vehicle testing of battery systems. It is important to the user that information concerning operating and life-cycle performance of traction batteries under field-test conditions is available. Batteries are put into similar test-bed vehicles (GM Griffons) and driven daily on the track or roads. Range tests (SAE J227a C Cycle and 35 mi/h constant speed) are conducted every month on the track. Laboratory discharge load tests under controlled conditions are carried out every other month to determine each battery's capacity and degradation. Twelve battery systems have been tested at the EVTF. These include 6 lead acid, 1 zinc chloride, 2 nickel cadmium, 2 nickel zinc, and 2 nickel iron. The EVTF has been supportive of advance battery development. A 36-volt lithium aluminum-iron sulfide subpack test program was conducted at Argonne National Laboratory. ELECTROTEK received a sodium-sulfur battery in September from Chloride Silent Power Limited of England to test in a Griffon.

Tubular Plate Lead-Acid Battery

Early in the evaluation program at the EVTF, it became obvious that the near-term lead-acid grid or flat plate batteries had life problems. The emphasis was then directed toward the tubular positive-plate battery manufactured abroad. The test results indicate that this is one of the leading batteries for near-term EV operation.

Three different type tubular plate systems have and are being tested at ELECTROTEK's EVTF. This is part of EPRI's EV Battery Test Program. All were installed in test-bed EVs and tested to the end of practical life.

Three Hoppecke 2x5PE193 battery packs were tested in Volkswagen electric transporters. One of the systems utilized an EVTF-designed thermal management system with a variable flow of ambient air to maintain uniform temperature across the pack. Each pack was made up of 24 six-volt modules connected in series to provide a nominal pack voltage of 144 volts. Aquagen recombiner caps were installed in all 3 cells of each module. Watering requirements were reduced due to the caps' palladium catalyst which combined the hydrogen and oxygen gases generated at the end of charge into water; the water then dripped back into the electrolyte. These batteries did not have a central-point watering system and therefore had to be watered manually. In each life test an on-board Hoppecke charger provided the charge.

Two of the tests began in the spring of 1982 and the thermally controlled one in the fall of 1984. All were unacceptable for EV applications because of relatively short lives. The first two achieved 10,500 miles while the one that was thermally controlled ran for 12,500 with 320 charge cycles.

The laboratory-type test with a constant current discharge of 75 amperes (2-hour rate) was used for all static load tests. The capacity varied among packs from 127 to 130.6 Ah. The specific energy was approximately 22 Wh/kg.

The second type of tubular plate lead-acid battery evaluated at the EVTF was the EV5T. It is manufactured by Chloride EV Systems (CEVS) of Redditch, England, for deep-cycle mobile applications. Six packs were tested to end of life; two in VW vans and four in Griffon vans. All six batteries were very similar in operating performance and life. For that reason, the data of only one battery is reported in this abstract.

A Chloride Spegel off-board, 30-ampere charger provides the battery charge current and periodic refresh charging. The pack also has central-point watering to reduce the battery maintenance. The pack is divided in quarters through the use of spark suppression in the water fill lines.

The third type of tubular plate battery evaluated at the EVTF is an improved version of the EV5T designated 3ET205 by CEVS. There are presently two of these batteries under life test in GM Griffons; a third pack is being shipped from England to the EVTF. These batteries used a 35-ampere Chloride Spegel off-board charger and central-point watering and gas management systems.

The 3ET205 is the battery used in the new GM G Vans to be field tested soon. In fact, CEVS is the component supplier of the total powertrains.

Overall Results and Conclusions

The EV5T pack accumulated 29,100 miles in a Griffon with 748 charge cycles. The battery test was terminated when the pack reached 60% of rated capacity with 25% of the modules replacted. The two 3ET205 batteries have accumulated 13,000 miles each to date. They appear to have similar life characteristics to the EV5T. These comparisons can be seen in Figure 1.

The typical real-world driving range of a Griffon with an EV5T and 3ET205 battery on a 75 degree F day is 75 and 82 miles respectively. This would decrease to approximately 45 to 50 miles, respectively, at an ambient temperature of 20 degrees F.

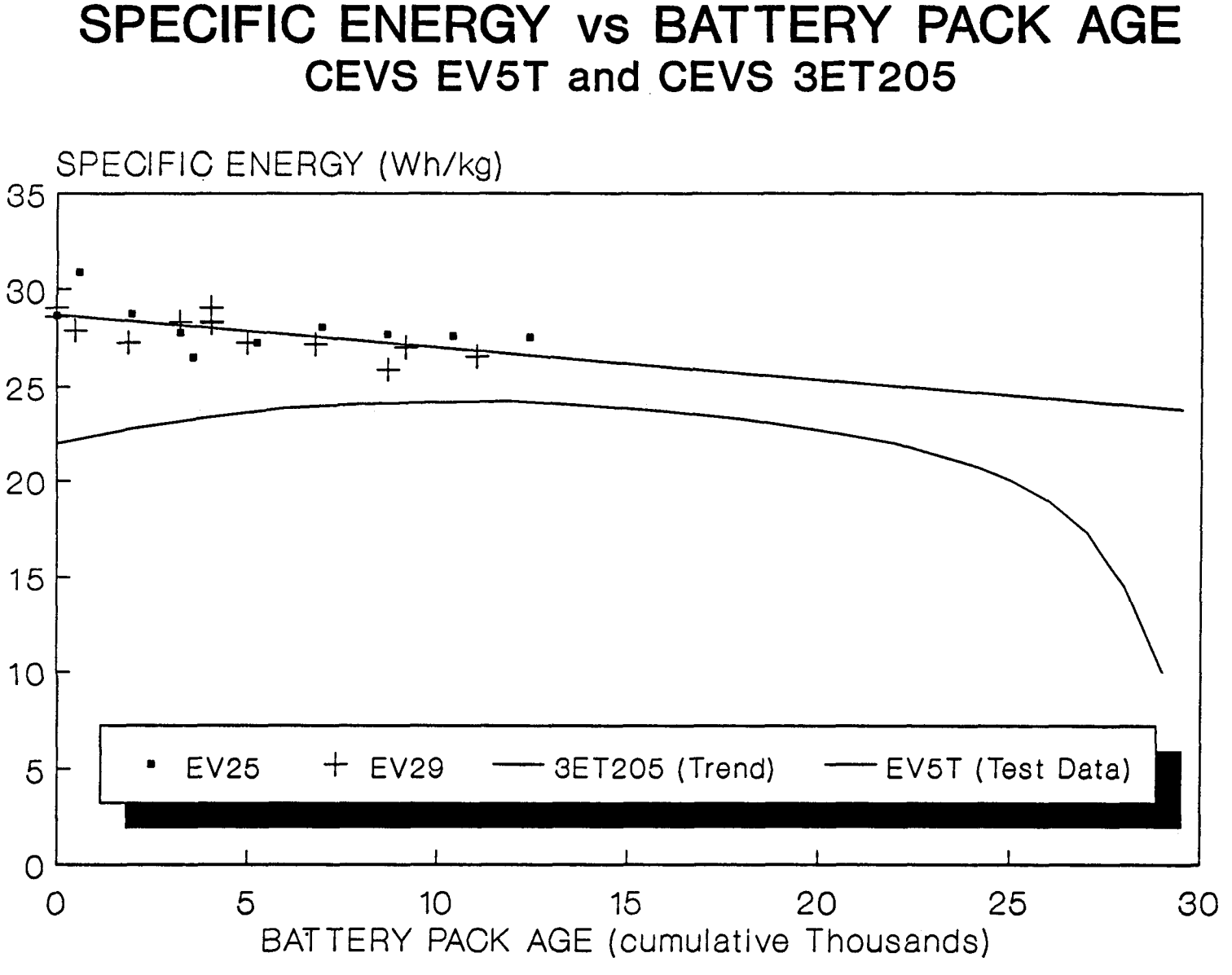
SPECIFIC ENERGY vs BATTERY PACK AGE
CEVS EV5T and CEVS 3ET205
SPECIFIC ENERGY (Wh/kg)
35
30
25
20
15
10
5
0
0
5
10
15
20
25
30
BATTERY PACK AGE (cumulative Thousands)
EV25
EV29
3ET205 (Trend)
EV5T (Test Data)

Figure 1.

NICKEL-IRON BATTERY TEST AND EVALUATION

J. Hampton Barnett, ELECTROTEK Concepts, Inc. and
Gary Paul, Eagle-Picher Industries

INTRODUCTION

The nickel-iron battery for electric vehicle (EV) applications has been under development for many years by Eagle-Picher Industries (EPI) of Joplin, Missouri, and others. The EPI positive electrodes are made from thick-, porous-, sintered-nickel plaque in which the pores have been electrochemically impregnated with active material. The early negative electrodes were acquired from the Swedish National Development Company while the later ones were acquired from SAB NIFE. They consist of an expanded-iron substrate on which iron powder has been sintered.

NICKEL-IRON IN-VEHICLE TESTS

Two nickel-iron battery systems are presently under test at ELECTROTEK's Electric Vehicle Test Facility (EVTF) in Chattanooga, Tennessee. Part of the EPRI EV Battery Test Program, both batteries are installed in test-bed EVs and are tested to the end of practical life.

The EPI NIF270 battery pack in a Volkswagen electric van consisted of 22 modules, each of which was made by heat sealing together 5 individual cells. The 110 cells in series gave a nominal pack voltage of 144 volts. The cells were rated at 270 Ah and designed with a forced-air system to dilute gases evolved during charge and to control pack temperature during charge and discharge. The pack also was equipped with a dual-section central-point watering system. Each half of the pack, consisting of 11 modules, was watered separately.

An off-board charger was provided to charge the battery. The charger was built by Lester Electrical of Nebraska to EPI charge profile specifications. The charge begins at about 75 Amperes and tapers off to a finishing current of 40 Amperes. The rate of change of pack voltage with time (dV/dt) is the criteria used to determine the charge cutoff point. The gas dilution fans continue to run for two hours after the charge current is stopped.

The test was initiated in October 1983. Data is recorded on battery static load tests, vehicle range tests, battery thermal management tests, and battery watering. In addition, a daily log is maintained on vehicle operation which includes odometer readings and kWh (ac) meter readings at the charge station.

A laboratory-type test with a constant-current discharge of 90 Amperes (3-hour rate) was used for all static load tests performed on this pack instead of the 75 Amperes (approximately 2-hour rate) used on other vehicle battery packs. The ampere-hour capacity has varied from a low of 194.9 to a high of 289.3 (72.2% to 107.1% of rated capacity). The last load test (November 1987) as a full pack showed the capacity at 98% of rated capacity. The specific energy in Whrs/kg has shown a high of 50.4 This is the maximum energy output determined by the load test divided by the weight of the battery pack. The life history is shown in Figure 1 plotted against accumulated mileage on the pack.

A spare module, placed in the pack in mid-1984 following a hydrogen detonation, limited the pack capacity for approximately a year. This module had been stored in a dead-short condition at the manufacturer's recommendation and was reactivated with difficulty. However, with continued pack cycling, the module recovered to its rated capacity.

Vehicle range tests starting with a fully charged battery are performed every month. One test is run at 35 mi/h constant speed until the battery voltage reaches a cutoff point. A second range test is performed using the SAE J227a "C" Cycle. Recorded along with the range data is the cumulative pack miles, vehicle weight, wind velocity, ambient temperature, and mean battery temperature. A multiple linear regression analysis is performed on this data to determine which factors have a significant effect (.95 level) on the test range. With this nickel-iron pack, the significant factors have been ambient temperature and cumulative pack miles (life).

The test was interrupted in January 1988 with a gas ignition that ruined half the pack. The vehicle had accumulated over 46,000 miles at this point. A decision was made by EPRI to evaluate the remaining half pack to determine the full life of the pack. These tests started again this last May after the electrolyte was changed.

The second battery pack (NIF220-5) was installed in a General Motors Griffon electric van and delivered to ELECTROTEK on December 30, 1988. It consists of 34 (5 cell) monoblocks connected in series to provide a 216 volt power supply. The modules were rated at 220 Ah (C/2 discharge rate). The pack is cooled during charge by an off-board fan system and has an automatic or manual central-point watering system with an on-board reservoir.

An off-board battery charger designed by Lester Electronics uses an optimized profile to minimize overcharging and gassing. The control has the flexibility to provide numerous charge profiles and cut-off strategies.

Part of this system also experienced a hydrogen ignition during acceptance testing. Six modules were damaged in one watering string. No origin of ignition was found but there is a suspicion that a spark was generated during simultaneous charging and watering. The six modules were recased and the vehicle is back in service after a leak was fixed in the sump tank.

OVERALL RESULTS AND CONCLUSIONS

The NIF270 reconfigured pack has accumulated over 50,000 miles and 721 charge cycles as of August 1989. It is presently at near the same capacity as when the system was new; however, there is a noticeable growth in the nickel electrode. This is the most miles and life ($\approx$ 6 years) ELECTROTEK's EVTF staff has accumulated on any electric vehicle battery pack. If the cycle life exceeds 1,000 (and we think it will), this mileage could nearly double. Also, this battery provides a daily range twice that of the best lead-acid battery. The higher capacity allows the nickel-iron battery to be practical for EV applications.

The overall energy efficiency of this system is somewhat lower than other battery systems tested at ELECTROTEK. The average ac energy consumption over the total life has been 0.86 kWh/mi. This is 10 to 20 percent higher than most lead-acid batteries tested in the same type vehicle. This is attributed primarily to the higher charge factor used with the nickel-iron battery.

Because of numerous initial system problems associated with the NIF220 battery, the pack has only accumulated 1,160 miles and 25 charge cycles. This is the battery selected for the Chrysler TEVan in the final stages of completion on four prototypes. The vehicle is designed for a 120-mile range in urban driving. Performance tests on the TEVan will begin at the EVTF this September. A pilot production facility for the NIF220 is planned to solve the economic problems of this technology.

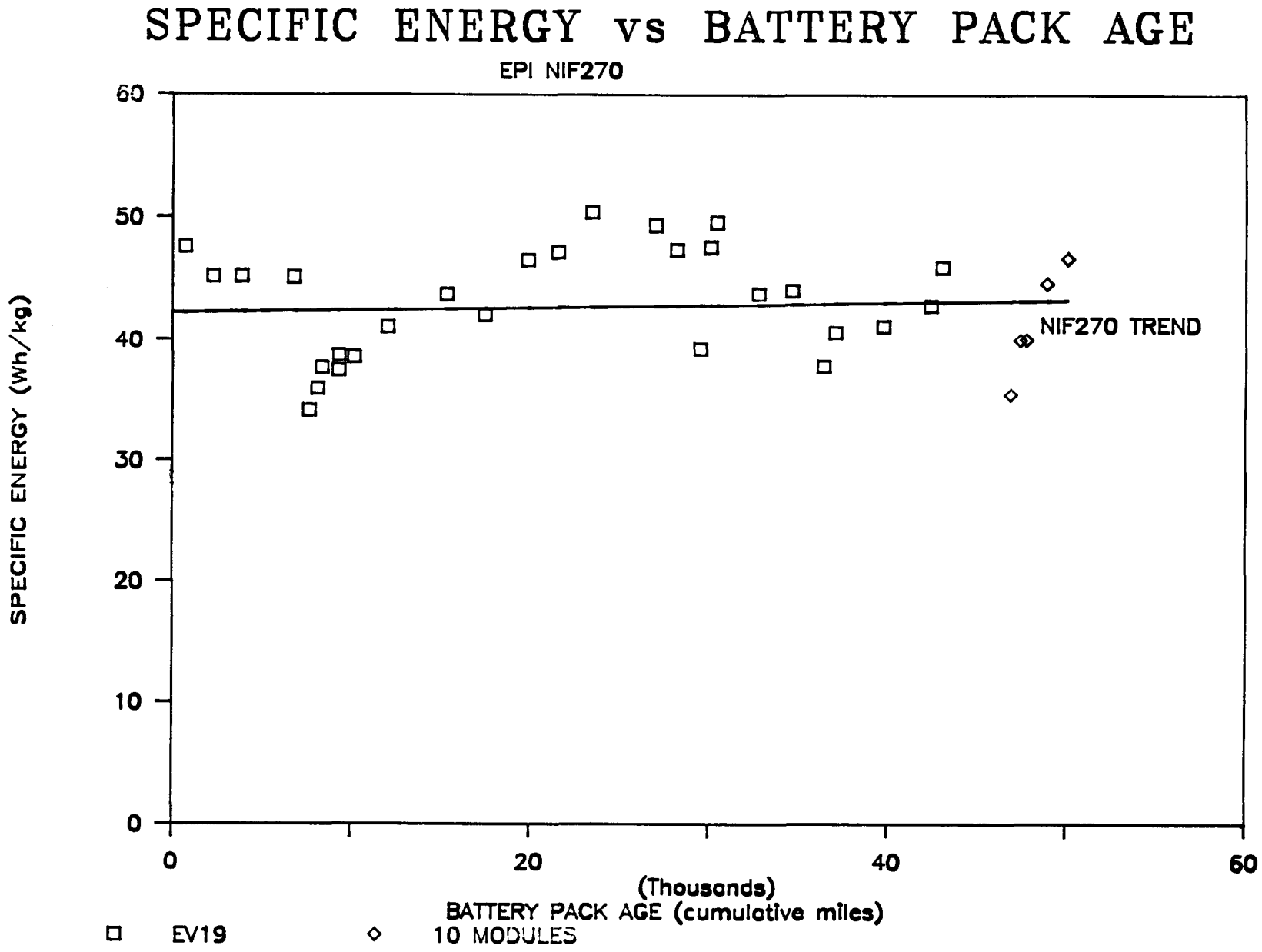
SPECIFIC ENERGY vs BATTERY PACK AGE
EPI NIF270
SPECIFIC ENERGY (Wh/kg)
60
50
40
30
20
10
0
NIF270 TREND
0
20
40
60
(Thousands)
BATTERY PACK AGE (cumulative miles)
EV19
10 MODULES

Figure 1

TEST AND EVALUATION OF AQUEOUS ELECTRIC VEHICLE BATTERIES AT ARGONNE NATIONAL LABORATORY

W. H. DeLuca, C. E. Webster, R. L. Hogrefe, A. F. Tummillo and J. A. Smaga
Argonne National Laboratory
Chemical Technology Division
Argonne, Illinois

During FY1989, Argonne evaluated five aqueous electric-vehicle (EV) battery technologies for the Department of Energy (DOE) and the Electric Power Research Institute (EPRI). Four single cells and nine 2- to 5-cell modules fabricated by four industrial firms were tested to determine their performance and life characteristics. The maturity of the technologies varied from research cells (flow-through lead-acid and electrolyte-flow iron/air) to production-type modules (advanced nickel/iron and tubular lead-acid). Standardized performance and life tests were applied to the more mature technologies, while variations of these tests were used with research cells because a shorter life and/or limited performance was anticipated. The results provide an interim measure of the progress being made in battery R&D programs, a comparison of battery technologies, and a source of basic data for modeling and continuing R&D.

Composite plots of available energy vs. discharge power rate and peak power vs. depth-of-discharge (DOD) for the evaluated technologies are given in Figs. 1 and 2, respectively. For comparison, the test results from a 1/3-size Na/S battery are also included. The values of specific peak power were derived from driving profile discharge data and are plotted in Fig. 2 as a function of the DOD during that discharge. The ranges projected for vehicles powered by the evaluated battery technologies under different driving profile discharges are listed in Table 1. The results of the aqueous battery tests at ANL are discussed below.

Iron/Air Technology - Westinghouse Electric Corp. is developing the iron/air electrolyte-flow technology for the DOE Office of Transportation Systems, Electric and Hybrid Propulsion Division (DOE/OTS/EHP). Two prototype 80-Ah (60-Wh) cells from this program were tested at ANL. The cells had to be operated at 40°C, and new electrolyte installed about every 20 cycles. One cell still retained ~80% of its initial capacity after 113 cycles but had virtually no power capability. This cell achieved a maximum specific energy of ~43 Wh/kg at the 4-h rate (assuming a specified dry cell weight of 760 g). The second cell was operated for 133 cycles, most of which were with driving profile discharges (SFUDS/IDSEP) to 100% DOD. This cell had a slightly higher voltage and capacity than those of the first and achieved an initial specific energy of 47.6 Wh/kg. For the SFUDS79 discharges, a cell weight of 490 g was used to limit the peak power demand (79 W/kg) to the cell power limit specified by the manufacturer (38 W).

Flow-Through Lead-Acid Technology - Johnson Controls, Inc. (JCI) is developing an improved lead-acid EV battery for DOE/OTS/EHP based on the forced flow of electrolyte by the active material. As part of this program, two prototype flow-through 75-Ah lead-acid cells and a 3-cell flow-by 75-Ah module were delivered to ANL for testing. The cells and module underwent an abbreviated performance characterization followed by life evaluations with SFUDS discharges. All achieved good performance but had a very limited life (<30 cycles). Because of their rapidly decreasing capacity (~1 %/cycle rate), the acquired performance data was not reproducible and its interpretation was difficult.

Tubular Lead-Acid Technology - Two advanced tubular lead-acid modules (3ET205) manufactured by Chloride EV Systems Ltd. are being evaluated under the EPRI Battery Test and Evaluation Program. These three-cell modules have tubular positive electrodes and are intended to have higher power and capacity than earlier designs (EV5T). Both modules completed performance characterization tests in FY1988 and are undergoing life tests using driving profile discharges (J227aC/G-Van) to 100% DOD. Deep discharges were selected to evaluate a worst-case condition. One module has attained more than 500 cycles with no degradation in performance. The second module completed 435 cycles with no loss of capacity, but life testing was suspended at the request of EPRI to conserve funds. Both modules achieved their 205-Ah rated capacity at a 5-h rate (41 A).

Advanced Nickel/Iron Technology - Four advanced Ni/Fe modules (NIF220) fabricated by Eagle-Picher Industries (EPI) are being evaluated under the EPRI Battery Test and Evaluation Program. Two of these modules are spares for the battery pack delivered to Electrotek Concepts, Inc. for in-vehicle testing, and two are spares for the pack delivered to Chrysler. All of these modules are rated at 220 Ah and utilize nickel sintered-plate technology. They are designed to have 30% greater capacity in the same package as the 170-Ah DSEP module. The Chrysler modules are presently undergoing characterization tests. Performance characterization tests and life testing with driving profile discharges (J227aC/G-Van) to 100% DOD have been completed on the Electrotek modules. These modules were only operated for ~240 cycles before their capacity declined to less than 75% of the initial level. Reference electrode measurements showed that the nickel was the discharge limiting electrode in all five cells. A teardown analyses was initiated on the lowest capacity cell. Visual inspection showed that the nickel electrode was in good condition while there was severe degradation of the iron electrode. Active material losses from the outermost iron plates left sections of the grids exposed, and the interior plates had blisters that covered 25 to 40% of the surface. Significant amounts of iron were found in the sludge at the bottom of the cell, in the microporous separator, and on the exposed surface of the nickel electrode. The high level of iron contamination on the nickel plate appeared to be restricted to a depth of 25 μm. Additional electrode analyses are planned.

Charging tests are included in the performance characterization of Ni/Fe technologies to evaluate proposed charge methods and overcharge requirements. The test results from the EPRI evaluations showed that with a fixed overcharge, charge current profile had no measurable impact on discharge capacity. However, module capacity was directly related to applied overcharge and inversely related to open-circuit standtime after charge (OCAC). Module charge acceptance was only ~20% with charge returns of 135⇒160%. A capacity loss of ~2% resulted with a 1-h OCAC (fixed overcharge of about 140%). From these data, a charge method and overcharge level were selected for use in the remainder of the EPRI test program.

Base Technology Nickel/Iron Studies - Eagle-Picher Industries (EPI) is developing an improved nickel/iron EV battery technology for DOE/OTS/EHP. This technology is based on low-cost fiber nickel electrodes that are up to twice as thick as previous designs in order to achieve improved performance with reduced battery cost. As a part of this program, tests were performed on five modules at ANL. A summary of the test results is given in Table 2. Life tests were continued on four Ni/Fe modules (three 2-cell and one 5-cell) with fiber-type Ni electrodes, and performance characterization and life tests were initiated on a 5-cell module with powdered nickel electrodes. The life tests use constant-current discharges of 120 A (~1.8 h rate). Only one of the 2-cell modules (#36) remains under test. It

still has 86% of its initial capacity (187 Ah; 440 Wh) after accumulating over 630 cycles. Testing of the 5-cell, fiber-electrode module (#39) was suspended in January 1989 because it retained only 76% of its initial capacity after eight months and 206 cycles of operation. Reference electrodes were installed in this module, and it was determined that the nickel was the discharge-limiting electrode.

Two of the 2-cell modules were voluntarily removed from testing to conserve funding. One module (#34) still retained 84% of its initial capacity after completing twenty-five months and 807 cycles of operation. The second module (#32) had 74% of its initial capacity after twenty months and 600 cycles of operation.

A fifth module (#40) having 5 cells with Ni powder electrodes was received at ANL in March 1989. This module (NIF220 design) represents the state-of-the-art for the powdered electrode technology and is to be evaluated for a performance baseline. The module is undergoing performance characterization and life testing. A maximum capacity of 231 Ah (1.42 kWh) was achieved with a 330-Ah charge (143% return), and 228 Ah (1.40 kWh) was obtained with a 305-Ah charge (134% return). The module was first operated with forced ambient air cooling, and the temperature rise during discharge was ~23°C (30⇒53°C). It has since been placed in a 22.5°C water bath and achieved a capacity of 225 Ah with a 305-Ah charge. Resistance and peak-power data were derived using the module current and voltage measurements during driving profile discharges. The data show that the module has a peak power of ~94 W/kg at 50% DOD and a resistance that is constant (~4 mΩ) for the first 50% DOD and then increases to 5.4 mΩ at 100% DOD.

COMPOSITE RAGONE PLOT

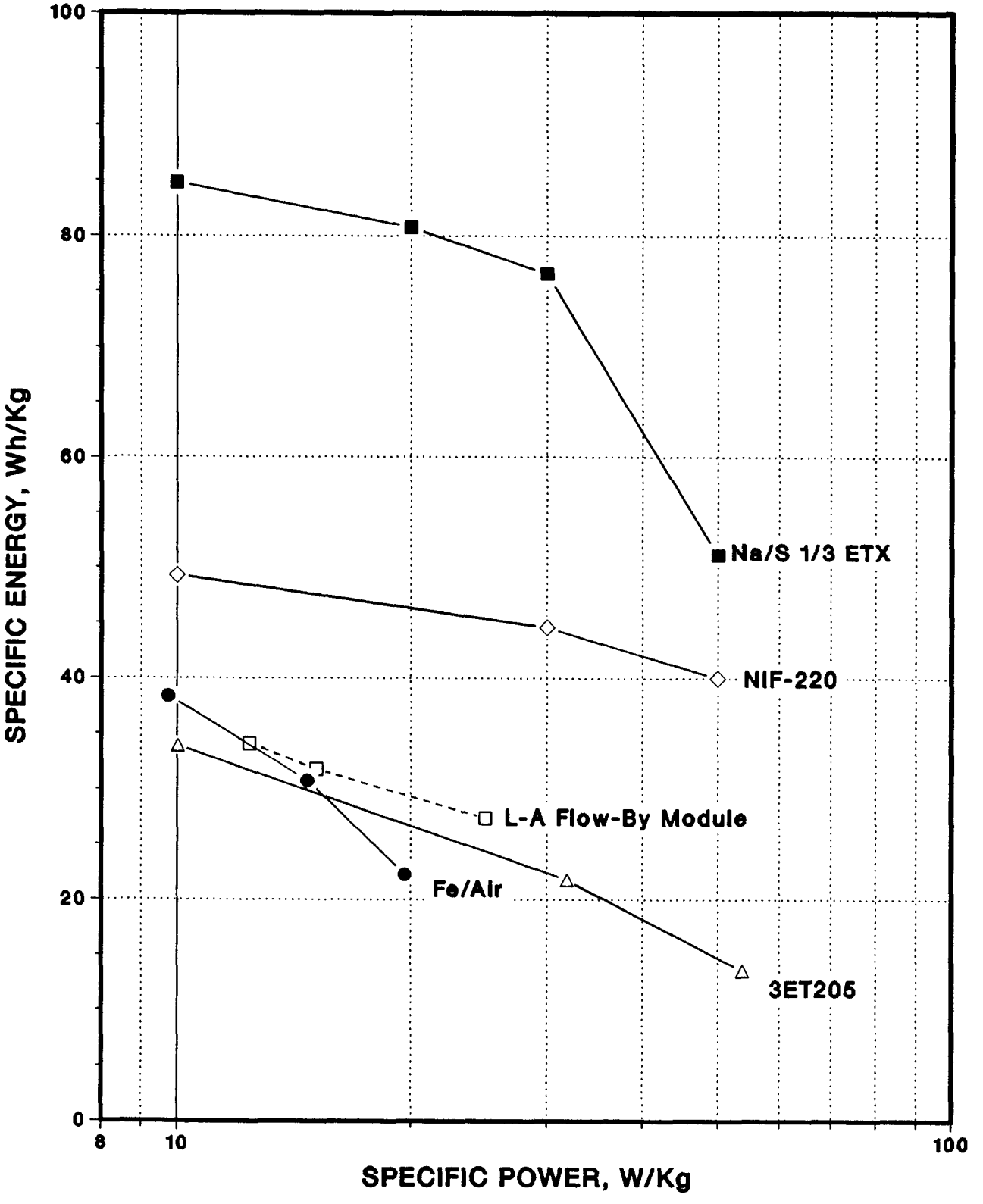

COMPOSITE PEAK POWER PLOT

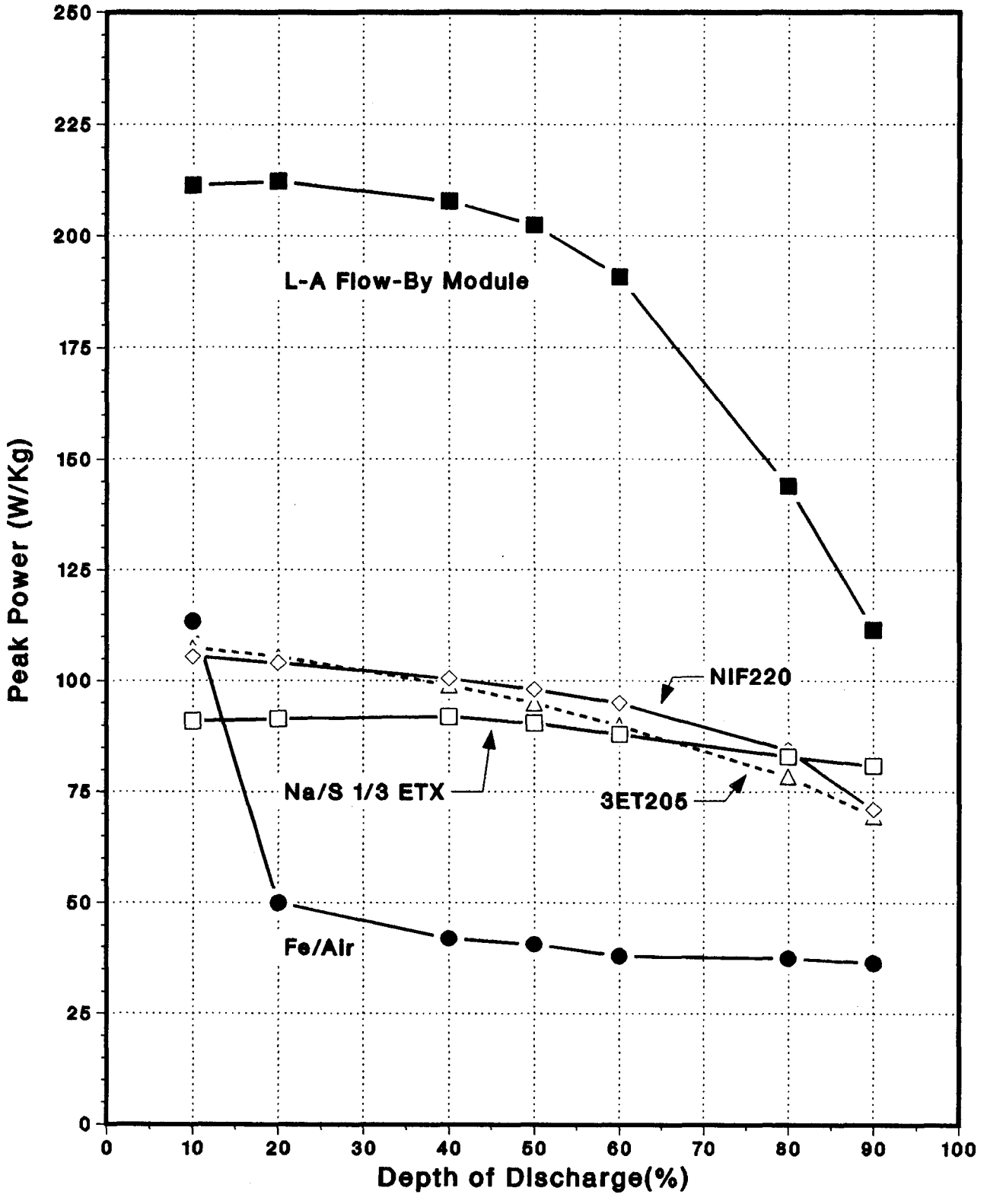

Table 1. Projected Ranges For Simulated Driving Profiles

Driving Profile			
- Driving Schedule	SFUDS79	J227aD	J227aC
- Vehicle Type	IDSEP	IETV-1	G-Van
- Battery Weight, kg	695	488	1180
- Avg. Speed, mph	19.0	28.3	15.1
- Peak Power, W/kg	79	48	36
- Avg. Power, W/kg	9.9	12.0	7.3
Battery	**Projected Range in Miles [Discharge Ah/kWh]**		
- Na/S 1/3 Battery	148 [306/17.6]	182 [308/17.8]	135 [262/15.9]
- Ni/Fe NIF220	75 [166/0.95]	98 [194/1.10]	93 [185/1.11]
- Lead-Acid 3ET205	47 [143/0.76]	54 [146/0.77]	65 [181/1.02]
- Lead-Acid Flow-By	56 [55/0.32]	65 [53/0.31]	74 [67/0.40]
- Iron/Air Cells	72 [28/0.02]	99 [37/0.02]	--

Table 2. Ni/Fe Base Technology Modules Tested at ANL in FY1989

Module No.	No. of Cells	Module Type	Initial 120 A Capacity Ah	Initial 120 A Capacity Wh	Present 120 A Capacity Ah	Present 120 A Capacity Wh	% of Initial Capacity	Cycles to 8-1-89
32*	2	Fiber	168	391	125	293	74.4	600
34*	2	Fiber	154	360	130	317	84.4	807
36	2	Fiber	187	440	161	374	86	632
39**	5	Fiber	202	1153	153	884	76	206
40	5	Powder	226	1343	224	1333	99	92

* Testing suspended to conserve program funds.
** Testing halted due to capacity decline.

NICKEL/HYDROGEN BATTERY EVALUATION

Donald M. Bush
Sandia National Laboratories

The nickel/hydrogen battery was developed in the early nineteen-seventies as an energy storage subsystem for commercial communication satellites in geosynchronous orbits. It has since qualified for low earth orbit applications and is an option for electrochemical storage on the Space Station. The advantages offered by nickel/hydrogen batteries include long calender life, high cycle life, low maintenance, and high reliability. These battery attributes would make it very useful for applications on earth, such as stand-alone photovoltaic systems. The major drawback to the wider use of the nickel/hydrogen battery is its high initial cost.

Under the sponsorship of the United States Department of Energy, Sandia National Laboratories (SNL) established and has directed cost-shared programs to address developmental and cost-reduction issues concerned with implementing a terrestrial version of the nickel/hydrogen battery. The primary objective of these programs is to reduce the cost of the battery to the point where it would be cost competitive with the lead-acid battery on a life-cycle cost basis, without unduly compromising its performance.

Development effort during the past several years has been conducted by Johnson Controls, Inc. (JCI). The principal activity during this period has been to continue the effort to reduce component costs, and to incorporate these new components into a 7-kWh battery that was delivered to SNL for evaluation. The 7-kWh battery incorporates a number of design changes from aerospace technology that enhance performance of the nickel/hydrogen system for terrestrial service. Individual prismatic cells are housed in a common pressure vessel. Thicker positives are used which result in lower cost by reducing the number of components, and higher specific energy. A new electrolyte management system was developed for this prismatic configuration; and the peripheral seal, used as an aid in assembly, enhances oxygen recombination. Also, the use of additives, along with a change in electrolyte concentration, improves high-temperature performance.

The 7-kWh battery consists of four, 12-volt battery modules, each containing ten, 150-Ah cells in a reusable pressure vessel. With the modules wired in a series/ parallel configuration, the nominal rating of the battery is 300 Ah at 24 volts. This was the configuration used during the initial evaluation at SNL, which began in January 1988. Both cycling and solar tests have been conducted.

The 7-kWh battery was recently cycled by charging with a constant 340-Ah at 30 A, and discharging to 1.0 V/cell at 27 A. A complete cycle took about 24 hours. Figure 1a is a plot of voltage vs. time for the first module in each of the two strings; the curves are virtually identical until the very end of discharge, indicating a well-balanced system. Figure 1b is a plot of string current using the same time base; here too, the load is shared equally with a slight divergence at the end of discharge. Output for this cycle was 328.9 Ah and 8.623 kWh, resulting in a coulombic efficiency of 96.7% and an energy efficiency of 85.6%.

Solar tests have been conducted with the 7-kWh battery using a photovoltaic array and an electrical load. Since the gases generated on overcharge are recombined internally, it was not necessary to use a controller between the three elements; however, the array was disconnected when the battery reached a temperature of 35°C, and reconnected when the temperature dropped to 30°C.

The 7-kWh battery was recently reconfigured from a nominal 24-volt, 300-Ah unit to a 12-volt, 600-Ah unit; this was accomplished by wiring the four battery modules in parallel.

A portion of an existing fixed, flat plate photovoltaic array in the Photovoltaic Advanced Systems Test Facility (PASTF) at SNL was used to charge the battery. Each of the photovoltaic modules has a nominal rating of 60 watts at 5 volts, and they were arranged in a 4x4 array. The loads consisted of a 12-volt refrigerator and three, 12-volt fluorescent lights. The refrigerator was attached continuously, while three lights were shed when the state-of-charge (SOC) dropped to 60% and reconnected at 65%; the SOC was determined from the hydrogen pressure.

Load current and state-of-charge vs. time for a 24-day period are plotted in Figure 2a and 2b, respectively. The SOC averaged 68%, and ranged from 58% to 81%. This relatively small range reflects the large battery capacity compared to the continuous load, and the shedding of the heavier load which was disconnected 16% of the time. Capacity flows in amp-hours are summarized below:

	ARRAY	LIGHTS	REFRIG	BAT CHRG	BAT DISCH
DAILY AVG	176	134	30	115	104
MAX	212	160	37	155	121
MIN	28	50	24	20	69
24 DAY TOTAL	4213	3208	719	2764	2494

Operating away from the battery overcharge region resulted in good efficiencies. The total load consumption was 3927 Ah, which is 93% of the total array output.

This work is supported by DOE Contract #DE-AC04-76-DP00789.

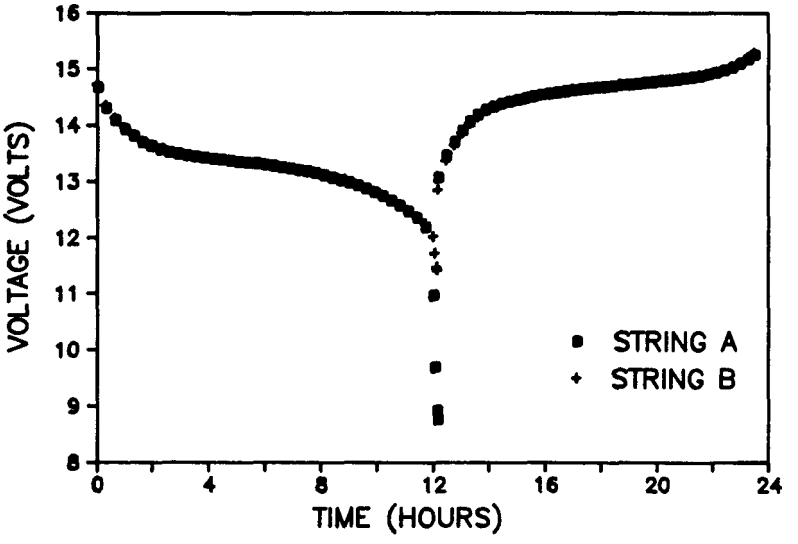

Fig. 1a – Battery Voltage vs. Time

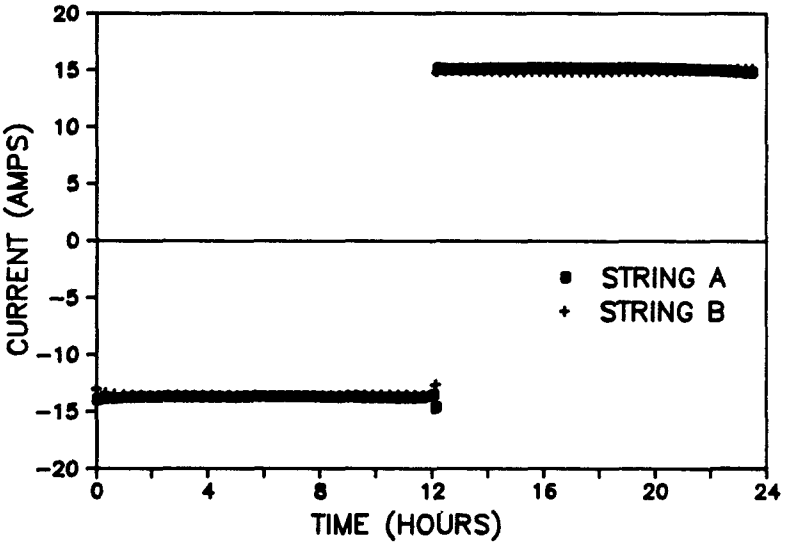

Fig. 1b – Battery Current vs. Time

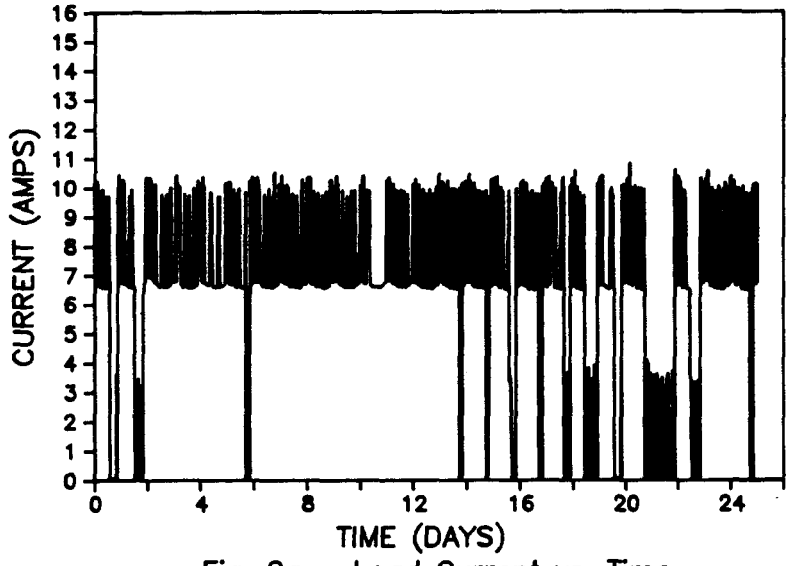

Fig. 2a – Load Current vs. Time

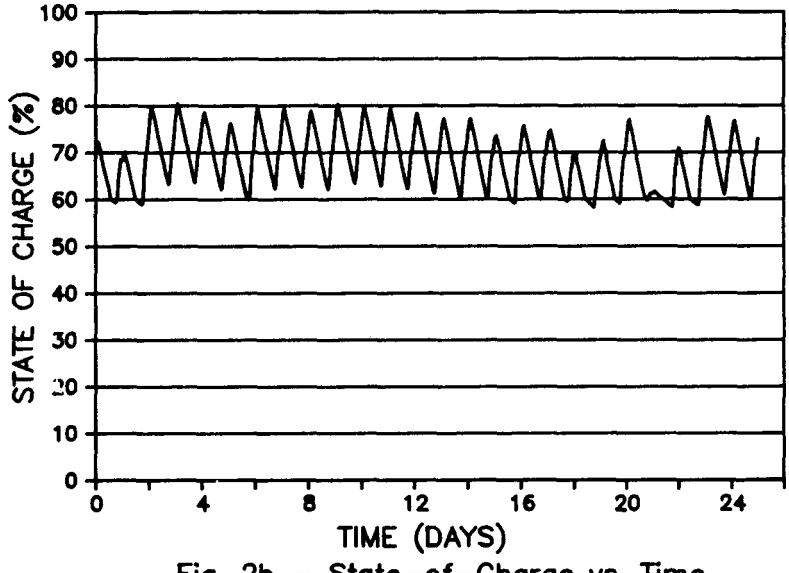

Fig. 2b – State–of–Charge vs. Time

METAL/AIR BATTERIES

CHAIRPERSON:

Kim Kinoshita
Lawrence Berkeley Laboratory

AIR SYSTEMS OVERVIEW

Philip N. Ross
Materials and Chemical Sciences Div.
Lawrence Berkeley Laboratory
Berkeley, CA 94720

Fuel Cells

The technological barriers to the development of practical fuel cell powerplants for vehicular propulsion are formidable. Using the phosphoric acid fuel cell (PAFC) technology as a reference point [1], with a nominal ambient pressure performance of 120 WSF at 40 % efficiency on natural gas, and an estimated capital cost of $2500 per kW, it is evident that the technology is too voluminous, too heavy and too expensive for widespread practical use in vehicles. The problem, of course, is how to make it better! Reduced to the most simplistic terms, research to improve the technology can be placed in two categories: 1.) new catalysts for both the anode and cathode, which ideally are both more active than Pt and less expensive (per unit activity); 2.) new electrolytes.

The search for more active catalysts is virtually never-ending, since the most direct way to improve the technology is through the catalysts. While not a new class of materials, new types of macrocyclic catalysts have been developed recently with some promising results as air cathodes, particularly in alkaline electrolytes. These will be described in the paper from Case Western University. There has been comparatively little effort on new catalysts for direct electro-oxidation of methanol. At LBL, we are trying to understand how adatoms like Sn, Bi and Ge act to increase the activity of Pt surfaces. This understanding could point us in the direction of what kinds of new materials might be promising catalysts. There is renewed interest in macrocyclic compounds as catalysts for methanol, but this is such a large class of materials that there needs to be a better understanding of what properties one is looking for in order to make an effective selection of a subgroup to examine. In summary, for acid fuel cells, there are no new catalytic materials that appear to provide an immediate or near-term improvement. Long term research, however, is clearly warranted and essential to move the technology forward. For alkaline fuel cells, there are a number new developments in air cathodes which are promising for near-term application.

Studies of new electrolytes has been the most area of research in fuel cell technology in the last decade. There is significant disagreement in the community as to the direction this research should take, particularly in the area of polymer electrolytes. NAFION® is not a new electrolyte, and it is easy to see that it is a polymeric form of perfluoro-n-methylsulfonic acid [-$(CF_2)_nSO_3H$], and that its

fundamental electrochemical properties should be identical to those of perfluoro-n-methylsulfonic acid. The properties of a number of alternative acid electrolytes, including NAFION-like sulfonic acids, is given in Table I. Intensive study of the electrochemistry of a number of perfluoro-n-methylsulfonic acids has shown that these electrolytes are too hydrophobic to be used in very concentrated form, thus limiting the cell temperature to less than 100°C [2]. At these temperatures, the cells suffer from short life due to poisoning of the anode catalysts when using any type of hydrocarbon-based fuel. Bicarbonate electrolytes are not new, but there are new catalysts that work extremely well in bicarbonate electrolyte, so well that re-examination of bicarbonate electrolyte cell concepts is warranted. However, in neither acidic nor basic medium do there appear to be any near-term improvements to the baseline PAFC tchnology on the basis of new electrolytes.

Metal-Air Batteries

There have been significant improvements in both the activity and endurance of air electrodes for alkaline metal-air batteries. New catalysts and new support materials are approaching near-term application. However, the limitations of the iron-air and aluminum-air battery systems are becoming clearer, and one has to question the continued development of these systems. The mechanical recharging of aluminum appears to be more problematic than anticipated. The iron-air battery can probably be made to work, but with a cell voltage, power density, energy density and efficiency that is unattractive. The recent improvements in the zinc electrode, presented at this conference by MATSI, together with the recent improvements in air electrodes make this battery system the leading contender of all air systems for electric power propulsion.

Acknowledgments

This work was supported by the Assistant Secretary for Conservation and Renewable Energy, Office of Energy Storage and Distribution, Electrochemical Energy Systems Division of the US Department of Energy under contact DE-AC03-76SF00098.

References

1.) S. Penner, Energy 11(1986)1
2.) H. Saffarian and P. Ross, Annual Report to the Gas Research Institute, Report GRI-89/0060, January 1989.

TABLE I

Alternative Acid Electrolytes for Fuel Cells

	Fluorosulfonic Acids	Nafion-like Sulfonic Acids	Fluorinated Sulfonimides
	CF_3SO_3H	$HO_3S(CF_2)_nO(CF_2)_nSO_3H$	$CF_3(CF_2)_nSO_2NHSO_2CF_3$
	$CF_3(CF_2)_nSO_3H$	n = 2, 4, 6, etc.	n = 1, 3
	n = 1, 5, 7		
	$HO_3SCF_2(CF_2)_nCF_2SO_3H$		
	n = 0, 2, 4		
Advantages:	High O_2 solubility	High O_2 solubility	High O_2 solubility
	No adsorption on Pt	Small adsorption on Pt	High solubility in H_2O
Disadvantages:	Volatility for small n	Decomposes at high T	Thermal stability?
	Low conductivity at high n		Volatility?
	Low solubility in H_2O at high n		

AIR ELECTRODES

E. Yeager, S. Gupta and D. Tryk
Case Center for Electrochemical Sciences and
the Department of Chemistry
Case Western Reserve University
Cleveland, Ohio 44106-2699

The overall objective of this research is an in-depth understanding of the factors controlling O_2 reduction and generation on various electrocatalysts and the use of this understanding to identify much higher activity, stable catalysts.

The specific catalyst systems investigated have included a) transition metal macrocycles including sheet-type polymeric phthalocyanines b) heat-treated macrocycles and nitrogen-containing polymers and c) transition metal oxides including pyrochlores as dual function O_2 reduction and generation catalysts (including self-supported).

New features of the recent work include: 1) the comparison of sheet-type polymeric and monomeric phthalocyanines; 2) in-situ and ex-situ FTIR studies of macrocycle catalysts adsorbed at monolayer levels on smooth substrates; 3) controlled poisoning of macrocycles by CN^-; 4) EXAFS studies of non-heat-treated and heat-treated macrocycles on carbon; 5) pyrochlore catalysts both for O_2 reduction and generation supported on carbon and self-supported; 6) use of polymer coatings to stabilize catalysts for O_2 reduction and generation; and 7) improved catalyst supports.

1. Comparison of Sheet-Type Polymeric and Monomeric Phthalocyanines

These studies are undertaken with a view to checking our models for the interaction of the transition metal with the substrate and the O_2, and particularly the role of structural factors in the O_2 reduction. Voltammetric studies indicate that the redox properties of the adsorbed polymeric phthalocaynines (Pc's) are similar to those of the corrseponding monomers under similar conditions. However, there are some differences in the peak potentials. The heights of the voltammetric peaks for polymers are much less than for the corresponding monomers. These differences are probably due to differences in the nature of the adsorbed layers. This is confirmed by Raman (SERS) studies of the sheet-polymeric and the monomeric Pc's on silver. The sheet-polymeric FePc supports the 4-electron reduction of O_2 to OH^- in alkaline solution at low polarization similar to monomeric FePc's but is expected to be more stable.

UV-visible absorption spectroscopic studies for monomeric and polymers FePc's have been carried out in DMF, DMA and DMSO solutions. The effect of the peripheral substituents in the phthalocyanine ring as well as environmental conditions such as solvent, air and light on the spectral properties have been investigated. This provides essential information for the electronic properties of iron complexes in the solution phase.

2. In-situ and Ex-situ FTIR Studies of Macrocycles Adsorbed on Smooth Substrates

In order to examine the interaction of macrocycle electrocatalysts with substrate surfaces, both ex-situ and in-situ FTIR reflectance-absorption spectra (FTIRRAS) have been examined for monolayers of adsorbed Fe and Co tetrasulfonated phthalocyanine (TsPc) on silver, highly ordered pyrolytic graphite (HOPG) and ordinary pyrolytic graphite (OPG). In preliminary studies, only vibrational modes

for the sulfonic acid groups are evident in the IR spectra of the FeTsPc adsorbed on Ag and not the remainder of the macrocycle ligand. Possible explanations will be discussed.

In-situ uv-visible reflectance spectra indicate no major differences between bulk solution and monolayer adsorbed FeTsPc on Ag. This supports the perpendicular ligand surface orientation proposed by the CWRU group.

The adsorption layer of cobalt tetramethoxyphenyl porphyrin (CoTMPP) has been formed on HOPG from its acetone solution by injecting an acetone solution of the complex into an aqueous 0.05 M H_2SO_4 solution (O_2 free) (corresponding to a stoichiometry of 1 x 10^{-5} M CoTMPP in 0.05 M H_2SO_4, 1:100 acetone-water). A similar procedure was used to form CoTMPP layers on Pt under aerobic and nonaerobic conditions. The mechanism of O_2 penetration into such hydrophobic CoTMPP layers and its reduction are discussed. The dry cave effect and an intercalation model are considered. Conditions for maximum adsorption of TsPc's corresponding to a compact monolayer on OPG have also been established.

3. Controlled Poisoning of Macrocycles by CN^-

The effects of CN^- on Fe and CoTsPc and TMPP have been examined. The major focus has been on the competitive interaction of the CN^- and O_2 with the transition metal in the axial position. The results confirm that a strong axial interaction of O_2 with the transition metal is an important factor for O_2 electrocatalysis. This study has also helped in confirming the redox processes associated with the voltammetric peaks obtained with the transition metal macrocycles.

4. EXAFS Studies of Macrocycles

EXAFS studies of CoTMPP adsorbed at monolayer levels on steam-activated Shawinigan black (SASB) carbon with and without heat-treatment at 800°C have been carried out at the Stanford Synchrotron light source by Prof. D. Scherson and I. Bae, a graduate student working with Prof. Yeager. The data indicate that a significant amount of the cobalt is retained in N_4 centers. These results are similar to those of McBreen and O'Grady. In experiments without heat treatment, the EXAFS measurements provide further evidence that the CoTMPP complex does not undergo chemical change when adsorbed on carbon and is physically bound to the surface, as reported earlier by this laboratory.

5. Pyrochlore Catalysts for O_2 Reduction and Generation

The lead ruthenate pyrochlores are very active as catalysts for both O_2 reduction and generation. Therefore it is important to understand the kinetics and mechanism for O_2 reduction and generation on these catalysts. The redox properties and O_2 reduction kinetics of $Pb_2Ru_2O_{6.5}$ pyrochlore have been investigated in alkaline solutions using cyclic voltammetry and the rotating ring-disk electrode technique. Reaction mechanisms for O_2 reduction and generation consistent with the observed Tafel slope and the reaction order are proposed respectively.

Rate constants for peroxide decomposition were obtained by monitoring its concentration changes using a rotating Au disk electrode. The effect of OH^- concentration on H_2O_2 decomposition by the pyrochlore $Pb_2Ru_2O_{6.5}$ have also been studied using 0.1 M to 4.0 M KOH solutions.

The pyrochlore $Pb_2Ru_2O_{6.5}$, prepared by the alkaline solution method at ~80°C, was further heat-treated between 300°C and 500°C in flowing air and characterized by X-ray diffraction and XPS. The material is converted from a rather amorphous to

crystalline form. The TGA for $Pb_2Ru_2O_{6.5}$ shows a weight loss of 3 to 3.5% over the temperature range 100-900°C due to the loss of chemically bound water.

The measurements with the pyrochlore $Pb_2Ru_2O_{6.5}$ in self-supported form (i.e., without high area carbon in the active layer) have shown that the electrode structure and performance can be improved greatly with the use of a pore-former. The O_2 reduction performance with such electrodes is now significantly better than previously achieved with carbon supports. With further optimization of the electrode structure, improvements are expected.

6. Use of Polymer Coatings to Stabilize Catalysts

A particularly fluorinated anion exchange membrane (RAI 4035) pressed onto the electrolyte side of an electrode made from $Pb_2[Ru_{1.67}Pb_{0.33}]O_{6.5}$ and SB carbon gives O_2 reduction behavior similar to that obtained without the membrane, but the O_2 generation behavior was considerably improved. A similar but smaller effect was observed for an electrode painted with a hydrogel suspension. This electrode performed very well at high cathodic current density, giving the lowest polarization yet seen from a metal oxide catalyst at -800 mA cm^{-2}. The polymer layers help to retain the solution-phase component of the pyrochlore in the cathode structure and thus minimize surface chemical changes.

7. Improved Catalyst Supports

Preliminary experiments were conducted with mildly fluorinated SB carbon obtained from Electrosynthesis Co., Inc., NY, as the support material. No improvements for the O_2 reduction behavior were observed for the mildly fluorinated SB carbon alone or the CoTMPP-catalyzed SB carbon respectively. However, work is in progress to ascertain the effect of mild fluorination of high area carbons on the activity and stability of such carbons for O_2 reduction and generation with and without catalysts present on such supports.

Future Work

1. Further examination of the structure and orientation of the adsorbed macrocycle films on HOPG and OPG including EXAFS studies for the non-heat-treated and heat-treated macrocycles on carbon.

2. Controlled poisoning of macrocycles by CO.

3. Adsorbed layers of mixtures of macrocycles on graphite and carbon surfaces and their role in promoting the 4-electron reduction of O_2.

4. O_2 reduction and generation on pyrochlores and other oxide catalysts.

5. Solid ionomer polymeric coatings for O_2 reduction.

6. Alternative and modified catalyst supports.

Acknowledgement

This research is supported by the U.S. Department of Energy through a contract with the Lawrence Berkeley Laboratory.

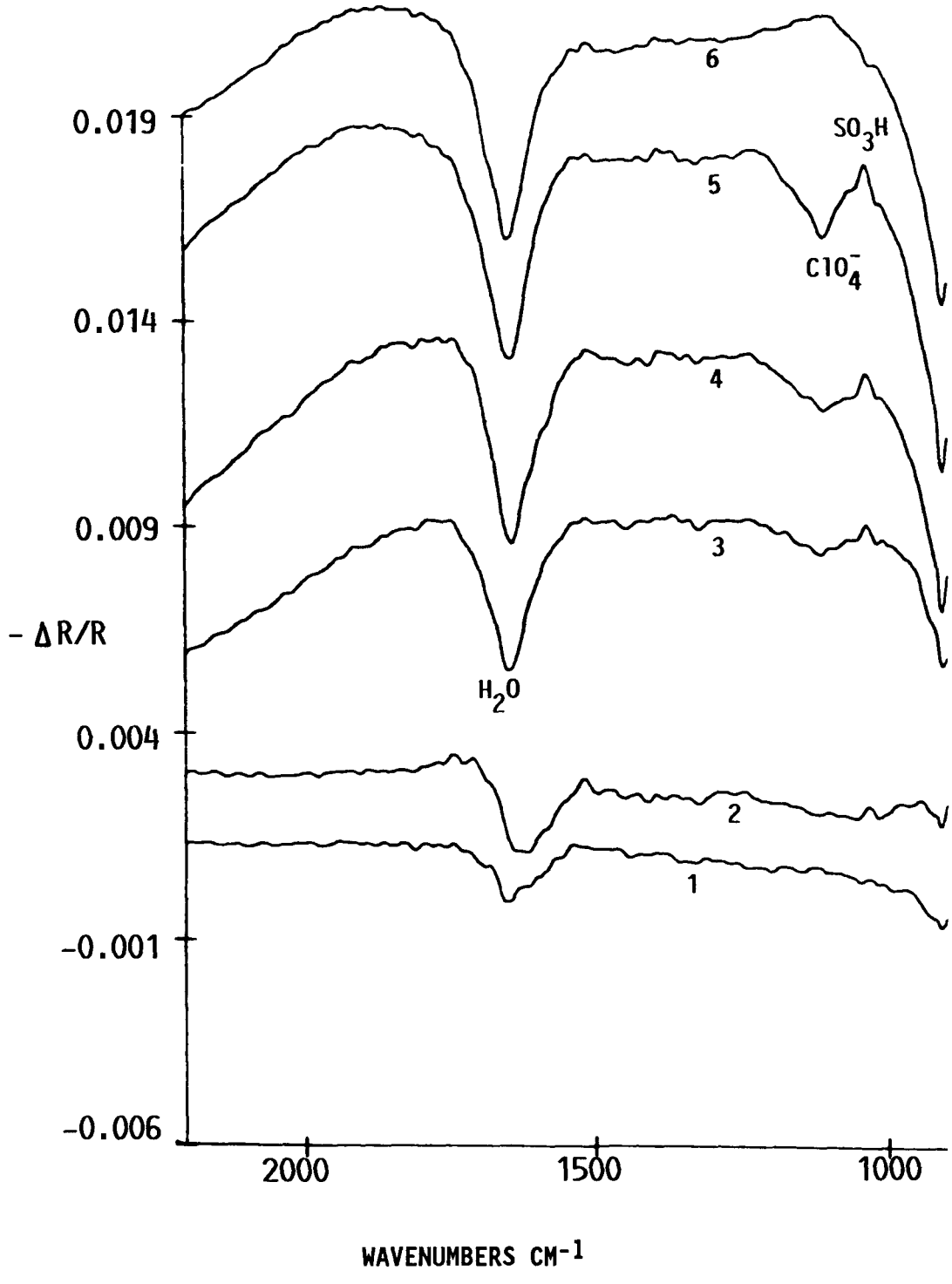

Fig. 1. In-situ Fourier transform infrared reflection absorption (FTIRRA) spectra of monolayer adsorbed FeTsPc on Ag in 0.1 M $HClO_4$ at fixed potentials. P-polarized light. Angle of incidence = 70°. E (V) vs. SCE.

1. -0.1 V	4. -0.4 V
2. -0.2 V	5. -0.5 V
3. -0.3 V	6. +0.15 V

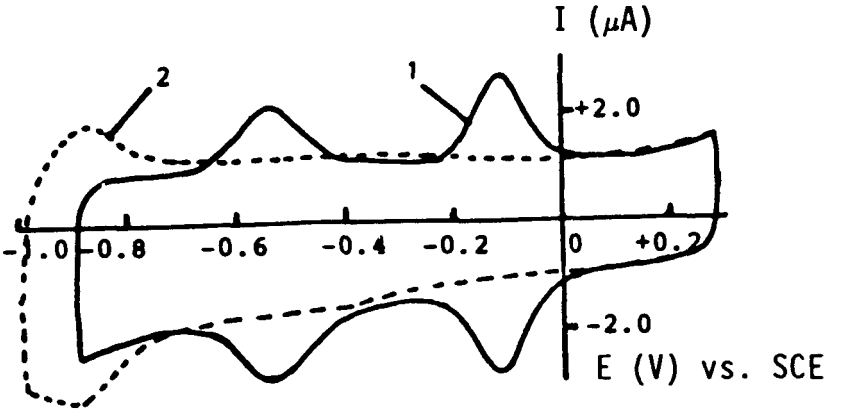

Fig. 2. Cyclic voltammograms (Peaks 2, 3) of FeTsPc adsorbed on OPG in 0.1 M NaOH (Ar satd.) without and with 1 x 10^{-3} M CN^- in solution. Disk area = 0.2 cm^2. Scan rate = 150 mV/s.

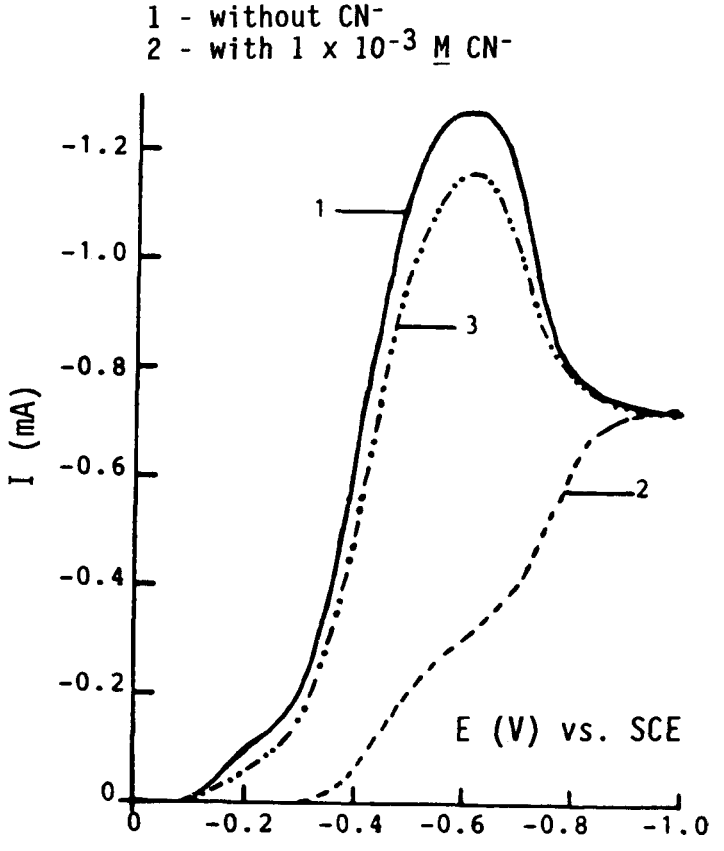

Fig. 3. Polarization curves for O_2 reduction (1 atm) on FeTsPc adsorbed on OPG in 0.1 M NaOH without and with 1 x 10^{-3} CN^- in solution. Disk area = 0.2 cm^2. Scan rate = 10 mV/s; 2500 rpm.

1 - without CN^-
2 - with 1 x 10^{-3} M CN^-
3 - electrode after 2, washed and dipped in fresh 0.1 M NaOH (O_2 satd.) without CN^-

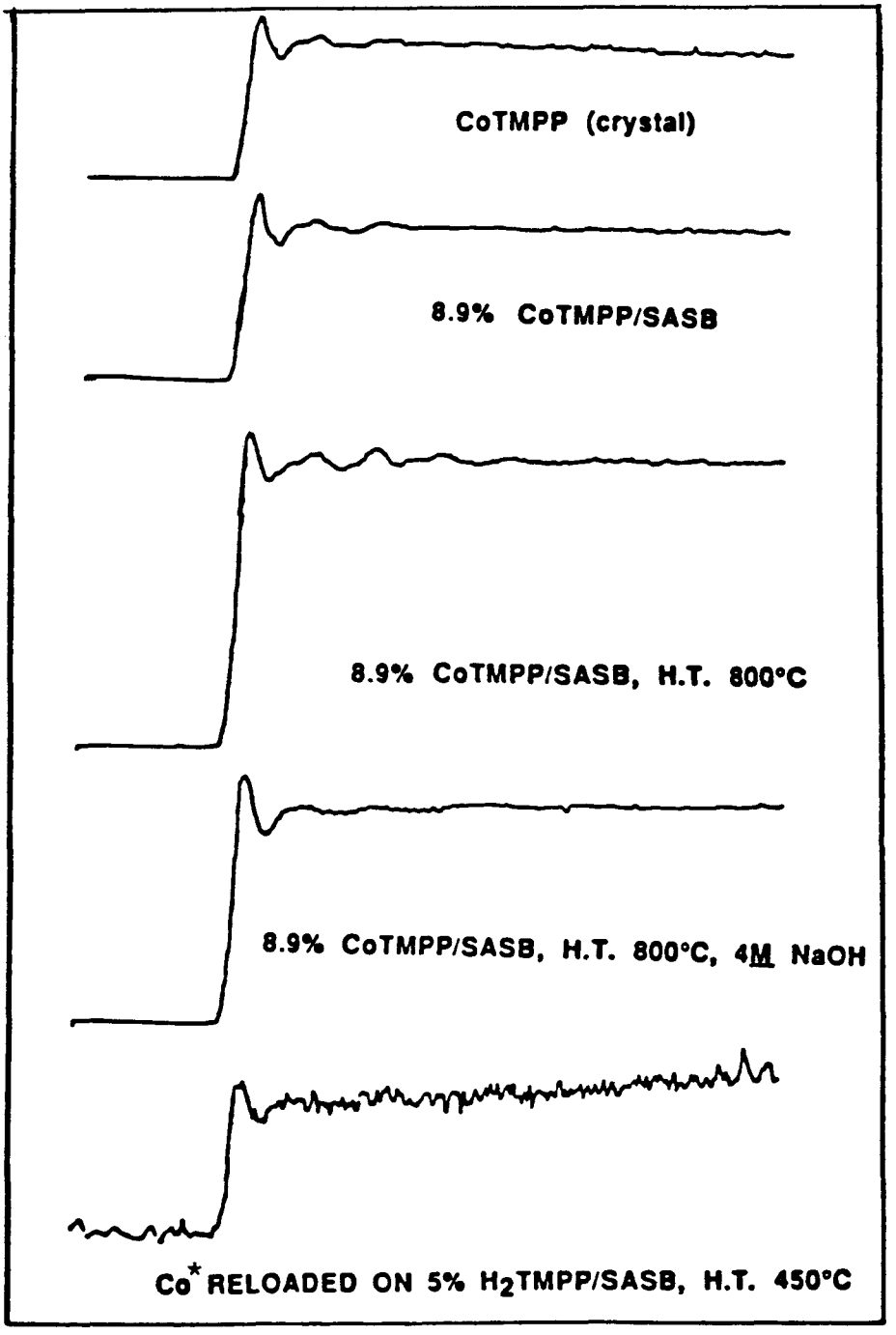

Fig. 4. EXAFS SPECTRA OF CoTMPP IN BULK FORM AND ADSORBED ON STEAM ACTIVATED SHAWINIGAN BLACK

*The source of cobalt was a solution of $Co(CH_3CO_2)_2$

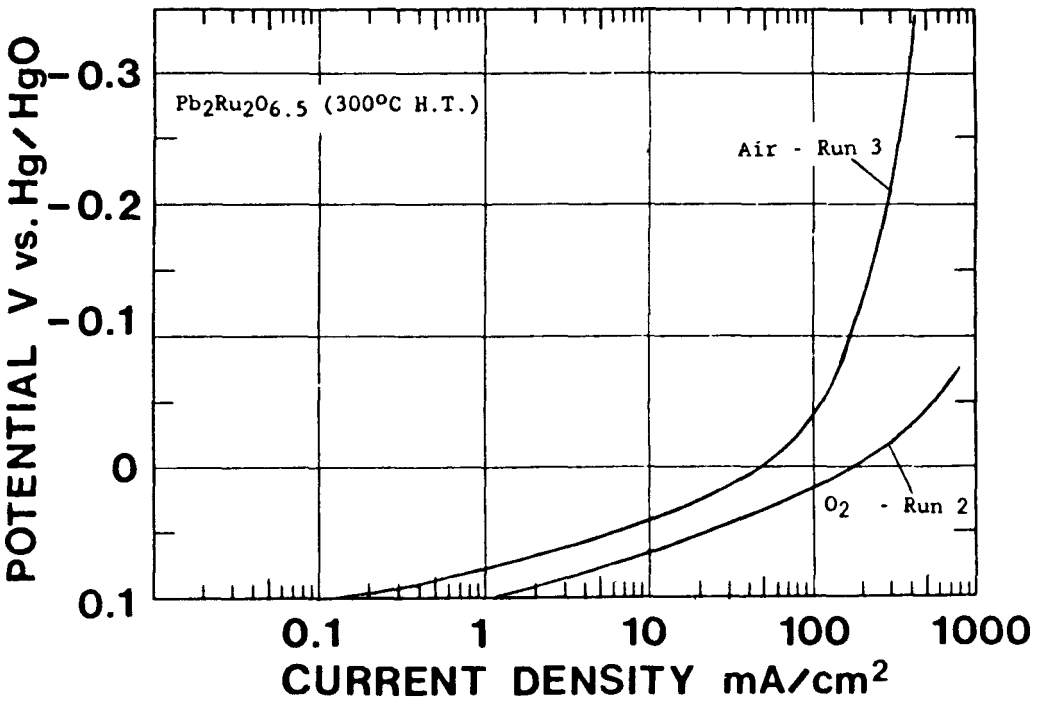

Fig. 5. Polarization curves for O_2 reduction with a $Pb_2Ru_2O_{6.5}$ gas-fed electrode using O_2 and air at 1 atm in 5.5 M KOH at 25°C. The electrode contained 83.3 mg/cm² pyrochlore and 27.8 mg/cm² (25 wt.%) Teflon T30B and was heat-treated at 330°C for 2 h in flowing helium. Ammonium bicarbonate (18.8 mg/cm²) was used as pore-former. Data were recorded point-by-point in the cathodic direction.

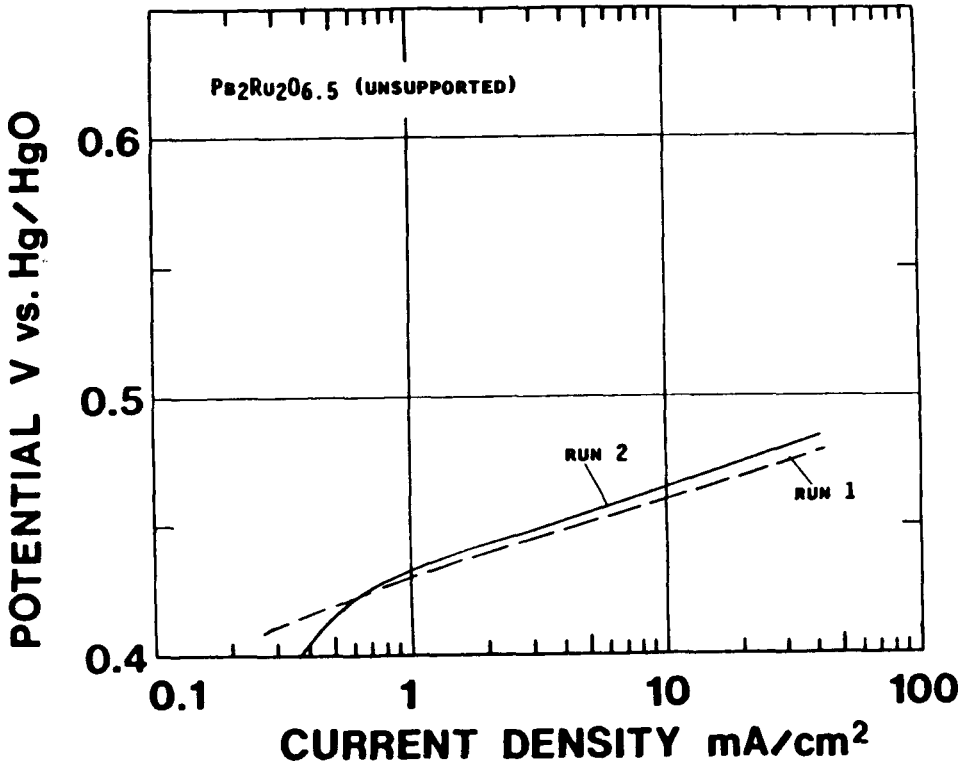

Fig. 6. Polarization curves for O_2 generation with a gas-fed (1 atm) electrode in 5.5 M KOH at 22°C. The electrode contained 54.2 mg/cm² pyrochlore and 4.1 mg/cm² Teflon T30B and was heat-treated at 270°C for 2 h in flowing helium.

THE DEVELOPMENT OF ALUMINUM-AIR BATTERIES FOR ELECTRIC VEHICLES

E. J. Rudd
ELTECH Research Corporation

An alternative to the secondary battery as the power source in an electric vehicle is a fuel cell. Metals such as aluminum, zinc, lithium and iron when coupled with oxygen from the air, yield such a fuel cell and aluminum is a particularly attractive candidate. Aluminum metal has high energy and power densities, it is environmentally acceptable (as are the products of the cell reaction), it is easy to handle and has a large industrial base for its production and distribution.

The battery is a multi-component system, represented schematically as Figure 1, and any development program must focus upon the several challenges, e.g.:

(a) the need for high performance electrodes
(b) the separation of aluminum hydroxide crystals from the electrolyte, and
(c) a cell design that allows rapid replacement of the anode

THE ELECTRODES

The aluminum anode. A variety of alloys have been evaluated in terms of the corrosion and polarization behavior in aqueous alkaline electrolytes [1]. Target levels of performance were established to facilitate the identification of suitable alloys and it was found that alloys containing low levels of indium, manganese, magnesium, gallium, thallium, tin or bismuth, (usually in combinations as ternary or quaternary alloys) provided performance levels approaching the targets.

The air cathode. The present cathode is a two layer structure combining a relatively hydrophilic catalyzed layer (the active layer), in which the electro-reduction reaction occurs, and a hydrophobic gas supply layer. Several transition metal macrocycles have been shown to be effective catalysts for the reaction, in particular, the cobalt tetramethoxy phenylporphyrin. In an alkaline environment, carbon dioxide in the air feed to the gas diffusion electrode forms an alkali metal carbonate, which precipitates within the microporous structure of the electrode. The results of a recent experimentally designed study [2] indicated that levels of carbon dioxide greater than 100 ppm would cause an unacceptable degree of deterioration in cathode performance.

ELECTROLYTE MANAGEMENT

The Helipump impeller fluidizer (Figure 2) is a device for separating, contacting and pumping solid-liquid slurries and appeared capable of efficiently separating fine particles. The characterization of the fluidizer has been completed and it was shown that the separation efficiency was dependent upon the weight% solids in the slurry, the particle size and the ratio of the length to the diameter of the vessel. A mathematical model has also been developed to describe the behavior of the fluidizer.

CELL DESIGN

The wedge cell addressed the need for a "rapidly rechargeable battery" but a sealed, lighter and more compact battery was clearly required. The B-300 cell was developed at ELTECH (Figure 3) and stable operation of both single cells and a multi-cell stack has been demonstrated. The design of the B-300 cell allowed relatively rapid replacement of the anode plates when necessary. The dependence of the performance of the cell upon fluid flowrates has been determined using a statistically designed experimental study. A mathematical model has been developed that adequately describes the mass transfer, ohmic and kinetic phenomena in the B-300 cell.

REFERENCES

1. "Aluminum-Air Battery Development", Final Report, ELTECH Research Corporation, Report No. UCRL-21018, Volume 4, Section X (1987).

2. "Aluminum-Air Battery development", Final Report, ELTECH Research Corporation, Report No. UCRL-21018, Volume 4, Section IX (1987).

Al/AIR BATTERY

PROCESS DIAGRAM

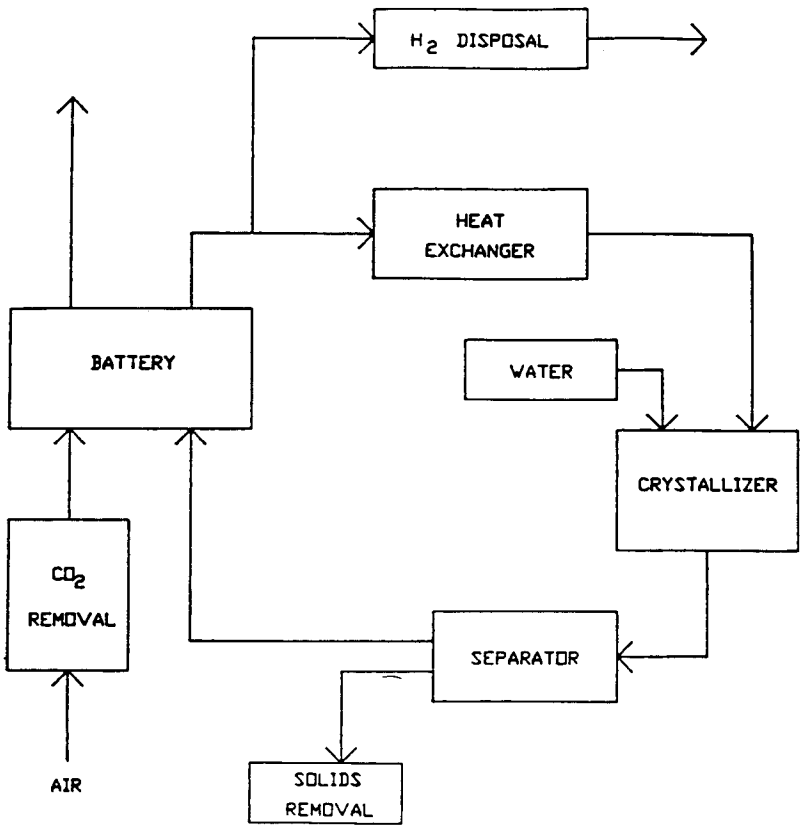

FIGURE 1

Mechanism of Fluidization

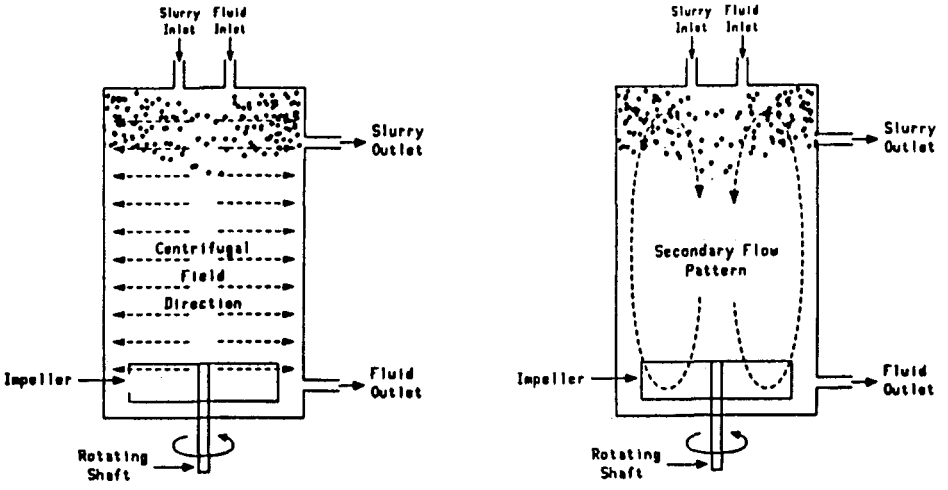

FIGURE 2

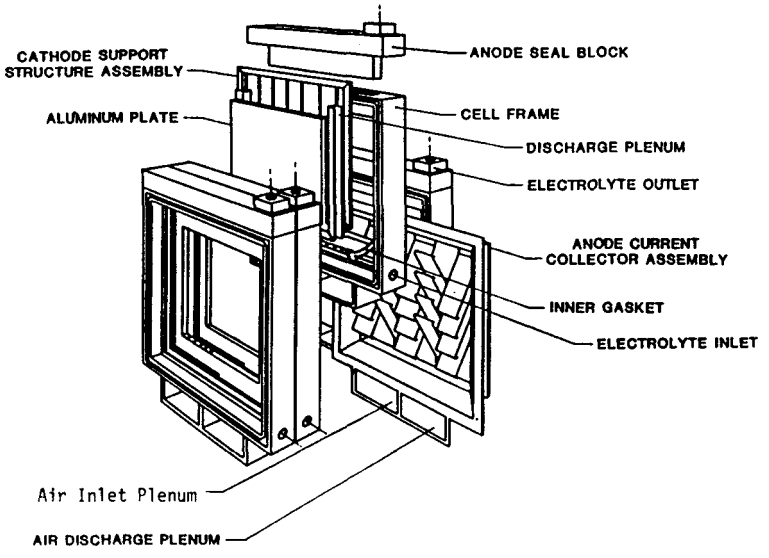

ALUMINUM AIR BIPOLAR BATTERY

FIGURE 3

AN ALUMINUM-AIR BATTERY IS A PROMISING CANDIDATE FOR A POWER SOURCE IN AN ELECTRIC VEHICLE

- **RANGE** — ESTIMATED 400-500 KM NON-STOP 800 KM WITH WATER ADDITIONS

- **REFUELABILITY** — ANODE REPLACEMENT IS A FUNCTION OF CELL DESIGN, CAN BE SHORT

- **ENVIRONMENTALLY ACCEPTABLE**

- **LARGE INDUSTRIAL BASE FOR PRODUCTION AND DISTRIBUTION OF THE ALUMINUM (FUEL)**

ANY DEVELOPMENT PROGRAM MUST FOCUS UPON

- THE NEED FOR HIGH PERFORMANCE ELECTRODES

- SEPARATION OF SOLIDS FROM THE ELECTROLYTE

- CELL DESIGN TO ALLOW RAPID REPLACEMENT OF THE ANODE

- A VARIETY OF ALLOYS HAVE BEEN EVALUATED IN TERMS OF CORROSION AND POLARIZATION BEHAVIOR IN ALKALINE ELECTROLYTE

- ALLOYS CONTAINING LOW LEVELS OF INDIUM, MANGANESE, MAGNESIUM, GALLIUM, THALLIUM, TIN OR BISMUTH PROVIDED PERFORMANCE LEVELS APPROACHING THE ESTABLISHED TARGETS

- THE FABRICATION "PRACTICE" CAN MARKEDLY AFFECT ELECTROCHEMICAL PERFORMANCE

- THE HELIPUMP IMPELLER FLUIDIZER IS A DEVICE THAT APPEARED CAPABLE OF EFFICIENTLY SEPARATING FINE PARTICLE AND COMPATIBLE WITH THE BATTERY SYSTEM

- CHARACTERIZATION OF THE FLUIDIZER SHOWED SEPARATION EFFICIENCY TO BE DEPENDENT UPON

  (a) WEIGHT % SOLIDS IN ELECTROLYTE

  (b) PARTICLE SIZE

  (c) VESSEL GEOMETRY

IRON-AIR BATTERY DEVELOPMENT FOR EV APPLICATIONS

J. F. Jackovitz, C. T. Liu, J. S. Lauer, N. Pessall
Westinghouse Science and Technology Center

The major accomplishment in the past year has been in bifunctional air electrode development to achieve 300 stable cycles of at least 8 hours duration at 25 mA/cm^2 and with discharge voltage of -0.150 V and charge voltage of +0.520 V versus an Hg/HgO reference. Empirical modeling of the air and iron electrodes is progressing concurrently with the evolution of experimental data on electrodes and cells. Work has also concentrated on scaleup and demonstration of full size iron-air cells and parallel stacks to achieve 50 W/kg, 50 Wh/kg and 300 stable cycles at 50% Wh efficiency.

New expert system knowledge refinement tools have been applied to the refinement of our current models and processing knowledge of iron and air electrodes. The expert system techniques allowed identification of conflicts between knowledge rules obtained from the human expert and new knowledge extracted by inductions from raw data. Subsequent resolution of the conflicts has produced an expert system that represents "refined" knowledge pertinent to our current model of air electrode preparation and performance. The system, while still under continuous refinement, is now being used to evaluate new experimental air electrodes. The basic processes involved in scientific modeling and discovery are shown in Figure 1.

Construction of a bifunctional air electrode in accordance with our presently developed model requires three or four basic material mixtures, blending of various size grades and amounts of these mixtures (to conform to structures indicated by the model), and then final hot pressing of the faces to complete the electrode. Each basic material mixture in turn consists of several selected components blended using narrowly confined conditions. Preparation and blending of the various materials and mixtures have not always been reproducible and the differences eventually are shown in the life of the electrode. Based on our current model and subsequent refinements, the material mixtures and blending procedures now fall within well defined limits. Reproducibility in life and performance ultimately depends on the creation of a uniform pattern of wet and non-wet regions within an electrode by the electrolyte. During the past year, we have accomplished our goals of life and performance by making air electrodes with three current collection layers, new blending techniques and temperature gradient hot-pressing. Cell 2-8, shown in Figure 2, is representative of our latest bifunctional air electrode at 300 cycles of performance.

Two full size (400 cm^2) cells were constructed early in the year at the Westinghouse Science and Technology Center and were eventually evaluated at the National Battery Test Facility at ANL. These cells achieved greater than 100 cycles and delivered near 50 Wh/kg energy density and 50 W/kg power density for a good portion of the test period. New generation air electrodes are expected to increase this performance and life considerably.

Also, the first prototype-size iron-air parallel stack was assembled and tested during the past year. The air electrodes for this stack were constructed using technology developed prior to the onset of modeling studies. The stack consisted of 5 parallel full-size electrically connected cells with a common electrolyte, air supply and case. This stack was cycled under both constant current and S-FUDS drive cycling regimes. The constant current cycling regime calls for discharging the stack at 50 to 80 A for a given number of amp-hours (Ah) or to a specified cut-off (0.65 V) followed by a constant current recharge to 225 Ah or a limit of 1.8 V. The

performance summary for the stack is given in Figure 3. Constant current conditions of 50 A discharge and 80 A charge were followed for the first eleven cycles. The stack typically delivered 180 to 200 Ah. Drive cycle evaluation at cycle 12 produced 50 to 53 peak watts through 94 modified FUDS cycles as shown in Figure 4. The upper limit current was 100 A for this discharge and the cut-off was 0.40 V. The stack operated for 60 cycles before some air electrode malfunctions and subsequent removal of one of the cells terminated the testing. Performance of the stack was similar to single prototype cells in voltage and polarization behavior.

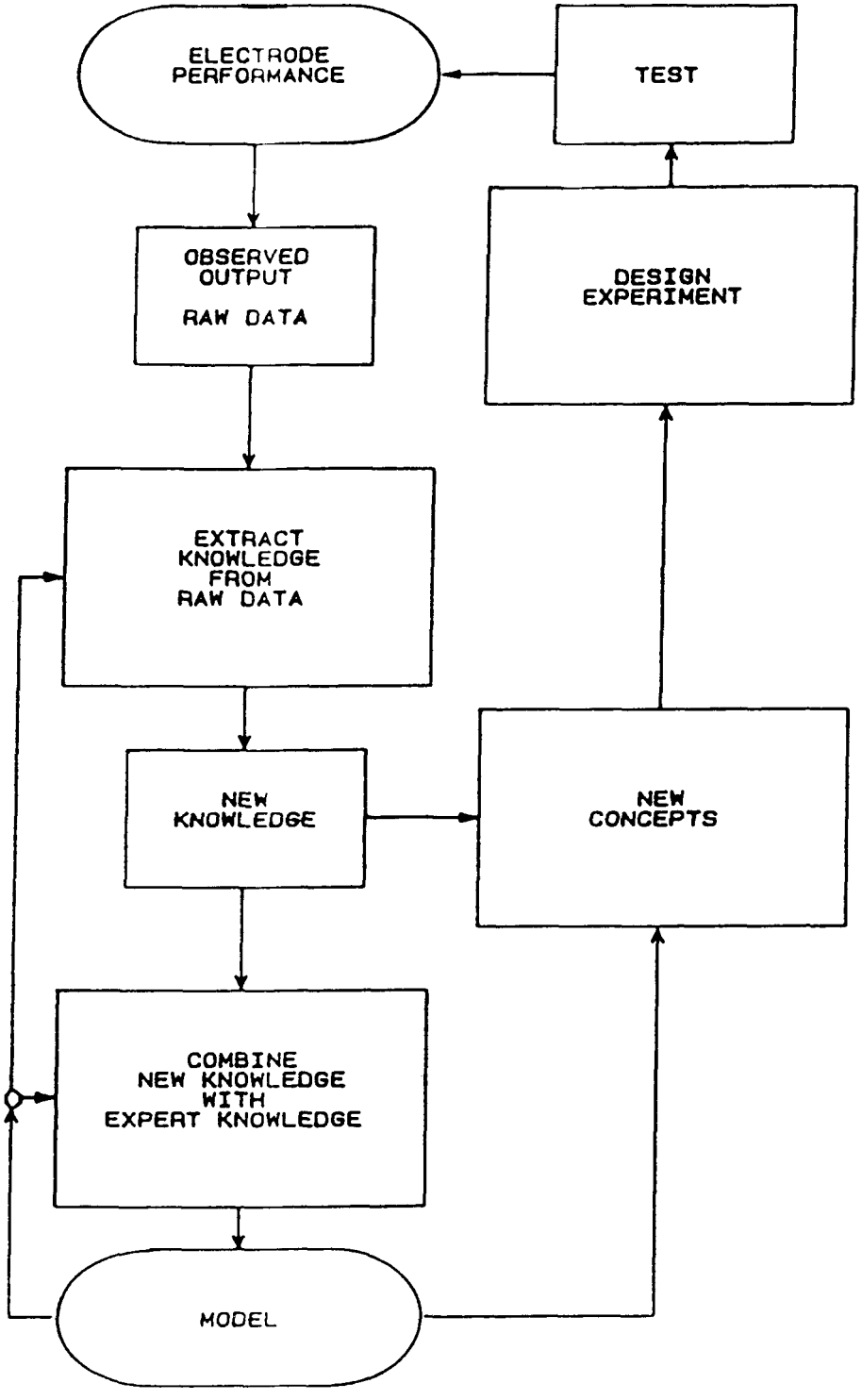

Figure 1 - Basic Processes Involved in Scientific Modeling and Discovery

Curve 757483-A

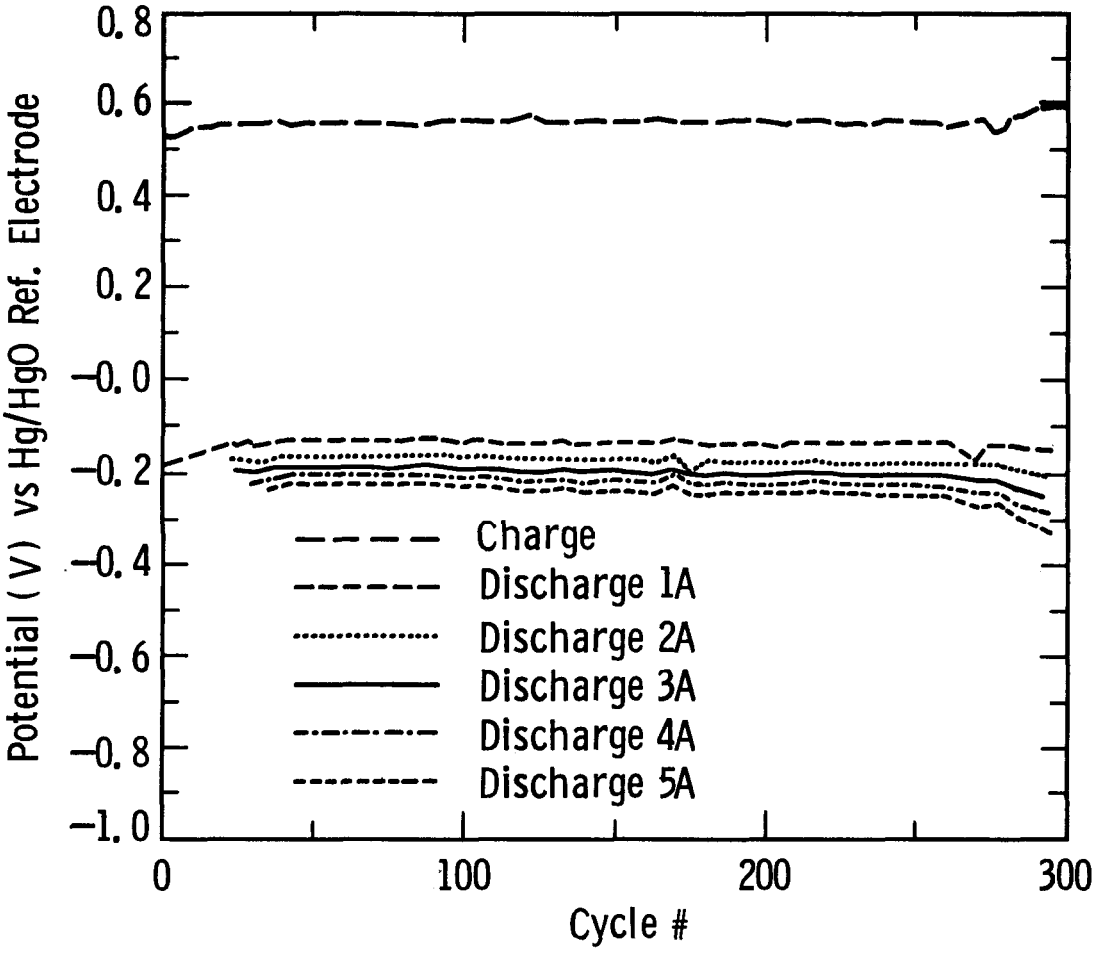

Fig. 2—Performance of air electrode 2-8. Each cycle was 8 hours

Curve 757482-A

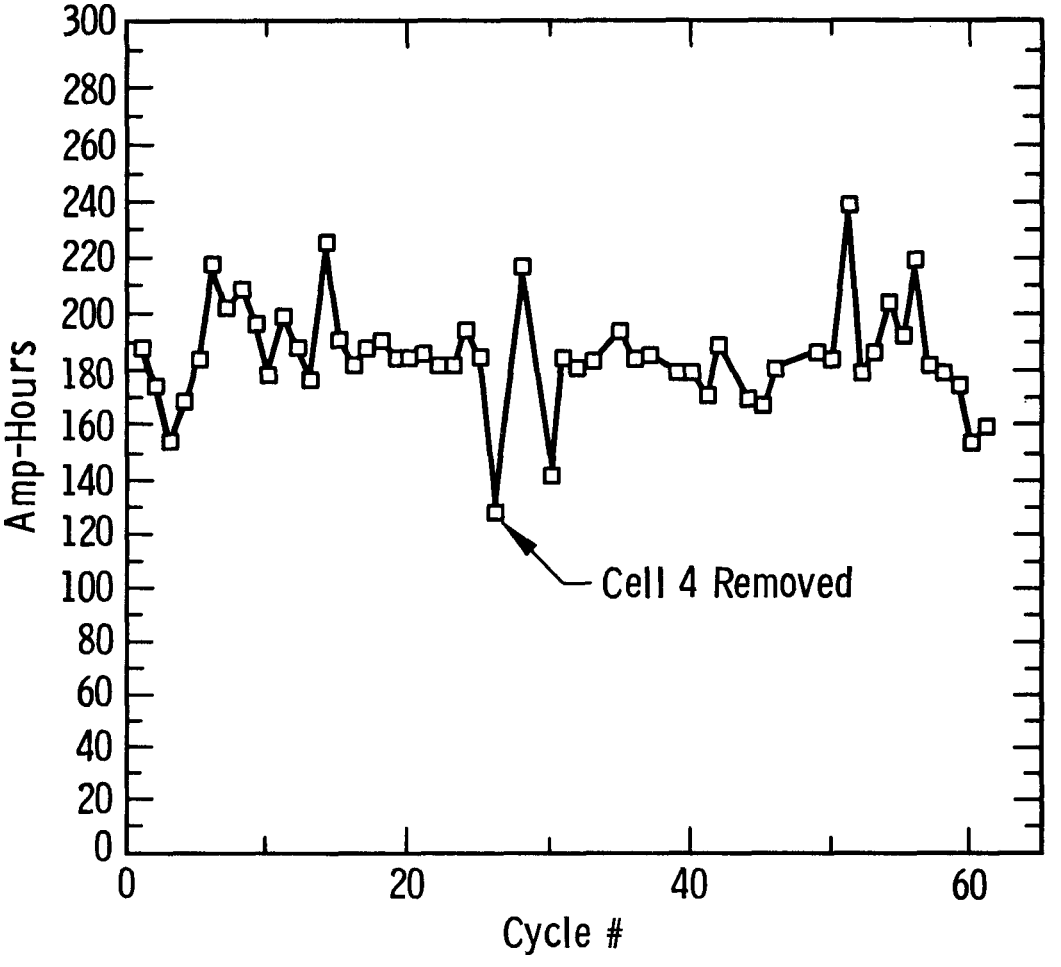

Fig. 3—Performance of five-cell parallel stack

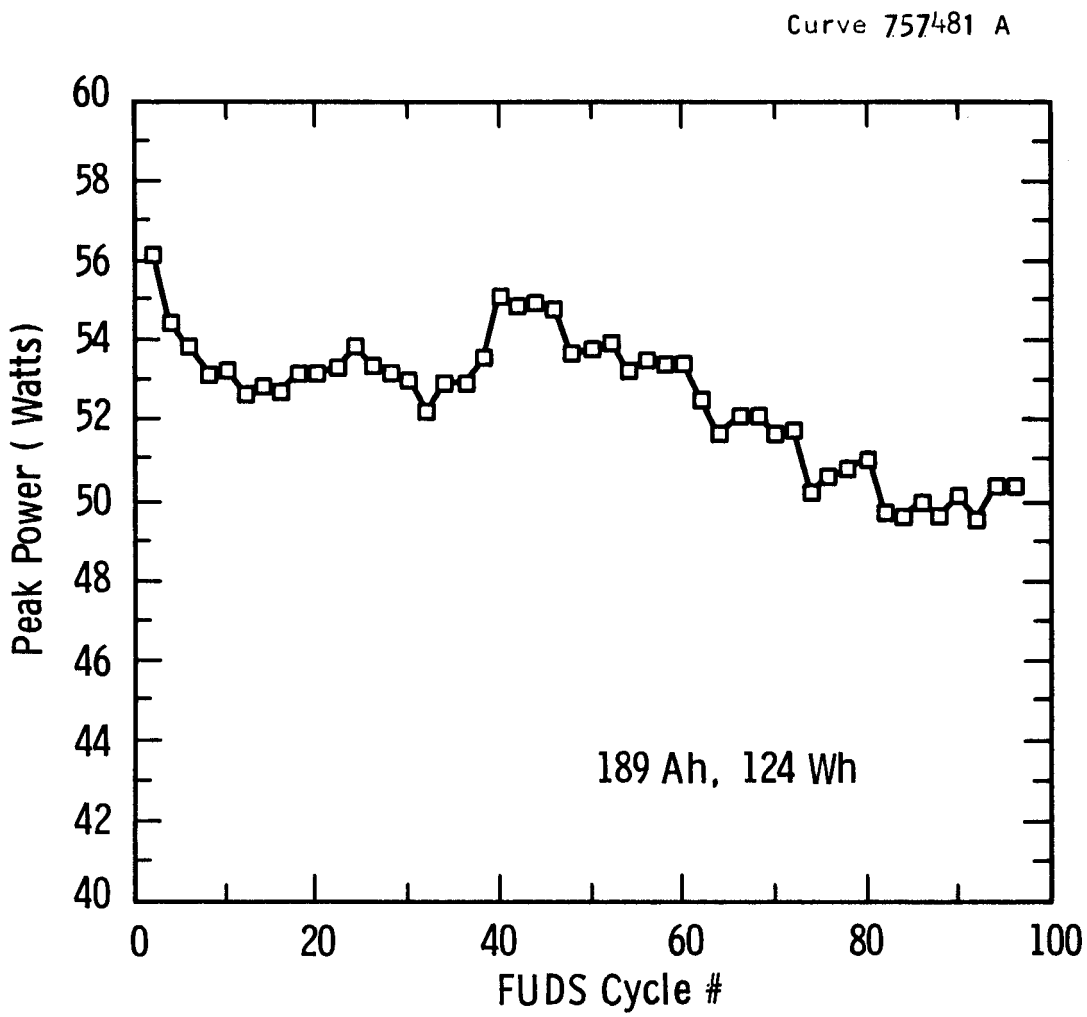

Fig. 4—Peak power versus FUDS cycle # for discharge of the five cell parallel stack at cycle 12

RESEARCH ON ZINC-AIR CELLS

J. W. Evans and G. Savaskan
Lawrance Berkeley Laboratory
and
Dept. of Materials Science and Mineral Engineering
University of California
Berkeley

The zinc-air cell has been the subject of several investigations because zinc is a readily available, innocous metal that holds both the promise of satisfactory cell energy density and the opportunity for either electrical recharging or mechanical "recharging" with simple recovery of the zinc. Two difficulties encountered in the past with zinc-air cells have been shape change of the zinc electrode and limited capacity of alkaline electrolytes for the products of zinc oxidation. One approach to avoiding the first difficulty has been to use particulate electrodes and fluidized or slurry electrodes have been investigated in the past. An alternative has been suggested by Ross (LBL report 21437) who demonstrated that a copper foam could form a substrate and current distributor for the electrodeposition/ electrodissolution of zinc and succesfully passed a laboratory zinc-air cell based on this concept through 150 cycles. Table I shows the calculated performance of full scale batteries based on this concept.

The difficulty of accomodating the zinc electrodissolution products in the elecetrolyte has been addressed by other investigators. As shown in Table II it has been found possible to increase the amount of zinc in the electrolyte (expressed in AmpHours/liter of electrolyte) by using various additives.

The present paper describes a zinc-air cell that offers promise for use in electric vehicles. The cell performance, in laboratory scale experiments, is comparable to the Ross cell. Table I compares the predicted performance of batteries based on the two designs, furthermore, high values of Amp hours/liter have been achieved in this cell without the use of additives (see Table II). Two laboratory scale cells have been constructed, using the new concept, with cross sections of 80 and 400 cm^2. Figure 1 shows the discharge of the smaller cell at an average current density of 18.8 mA/cm^2. After 7.5 Ah the current density was stepped as shown yielding the voltage/ current characteristics of Figure 2. The rapid return of the cell voltage following these excusions should be noted in Figure 2. Figure 3 shows the discharge curve for the larger cell at a constant 32 mA/cm^2.

The paper presents additional information on cell performance, on design features and on other issues (such as the long time behaviour of air electrodes in the presence of zinc).

Acknowledgement:

This research supported by DOE through LBL.

References:

1. P. N. Ross, Lawrance Berkeley Laboratory Report, LBL 21437, 1986

2. P. C. Foller, "Effect of additives on the suspension of products of discharge of zinc in alkaline solutions", J. Applied Electrochem., 17, 1296-1303, (1987)

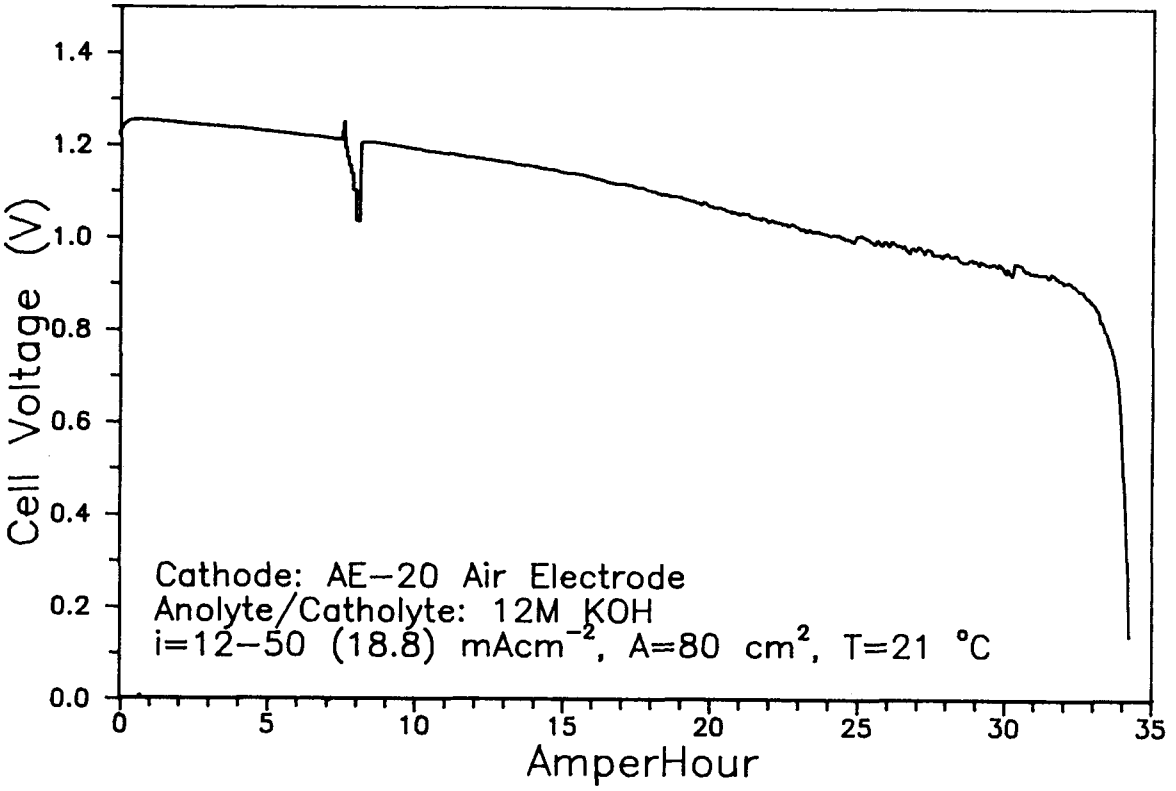

Figure 1. Cell Voltage vs. Ah for Exp.# D1889

Table I

Characteristics of a 32 kWh Zinc-Air Alkaline Battery Advanced Technology

	Ross[1]	Present Work
Design Parameters		
Voltage (V)	1.25	1.15
Current Density($mA.cm^2$)	20.00[a]	20.00
Electrolyte Capacity (Ah/l)	220.00[b]	536.00[c]
Electrolyte weight (Kg)	200.00	90.00
Zinc weight (Kg)	31.20	33.90
Auxilliary weights (Kg) (pumps, manifold, substrate, frame, air electrode, air scrubbers)	64.00	64.10
Total weight (Kg)	295.20	188.00
Energy density (Wh/Kg)	108.40	170.00
Power density (W/Kg)	132.00[d]	250.00[e]

(a) Assumed
(b) Taken from literature
(c) Achieved in 400 cm^2 cell
(d) Peak power density
(e) Calculated using 120 $mWcm^{-2}$ peak power

Table II

Capacity Comparison of Zinc-Air Alkaline Batteries

Source	Conditions	Capacity (Ah/l)
Present Work	12M KOH without any additives at 32.2 $mAcm^{-2}$ discharge rate	536
Foller[2]	12M KOH + additives (SiO_2+LiOH) at 200 $mAcm^{-2}$ discharge rate	220
Marshall[2]	14M KOH + .15M SiO_2 at 33 $mAcm^{-2}$ discharge rate	263
	14M KOH without any additives at 33 $mAcm^{-2}$ discharge rate	48

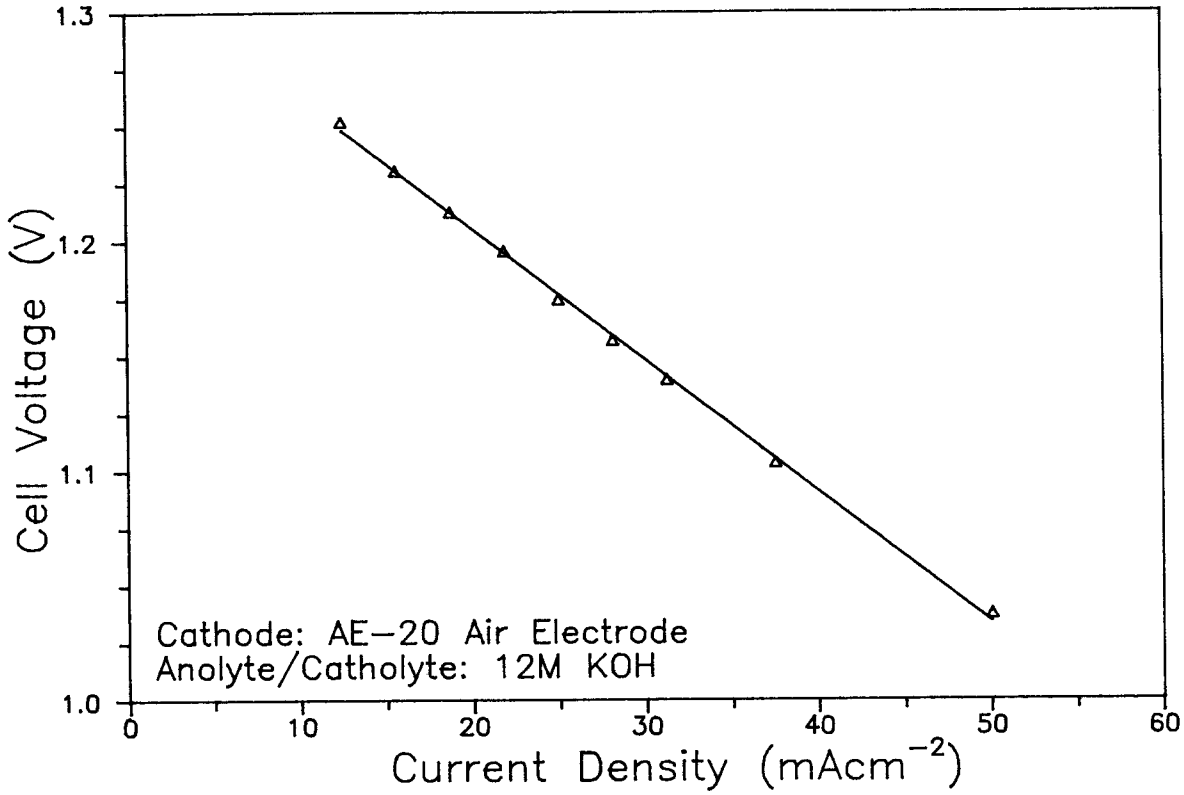

Figure 2. Current Density vs. Cell Voltage After 7.5 Ah discharge at 18.8 mAcm

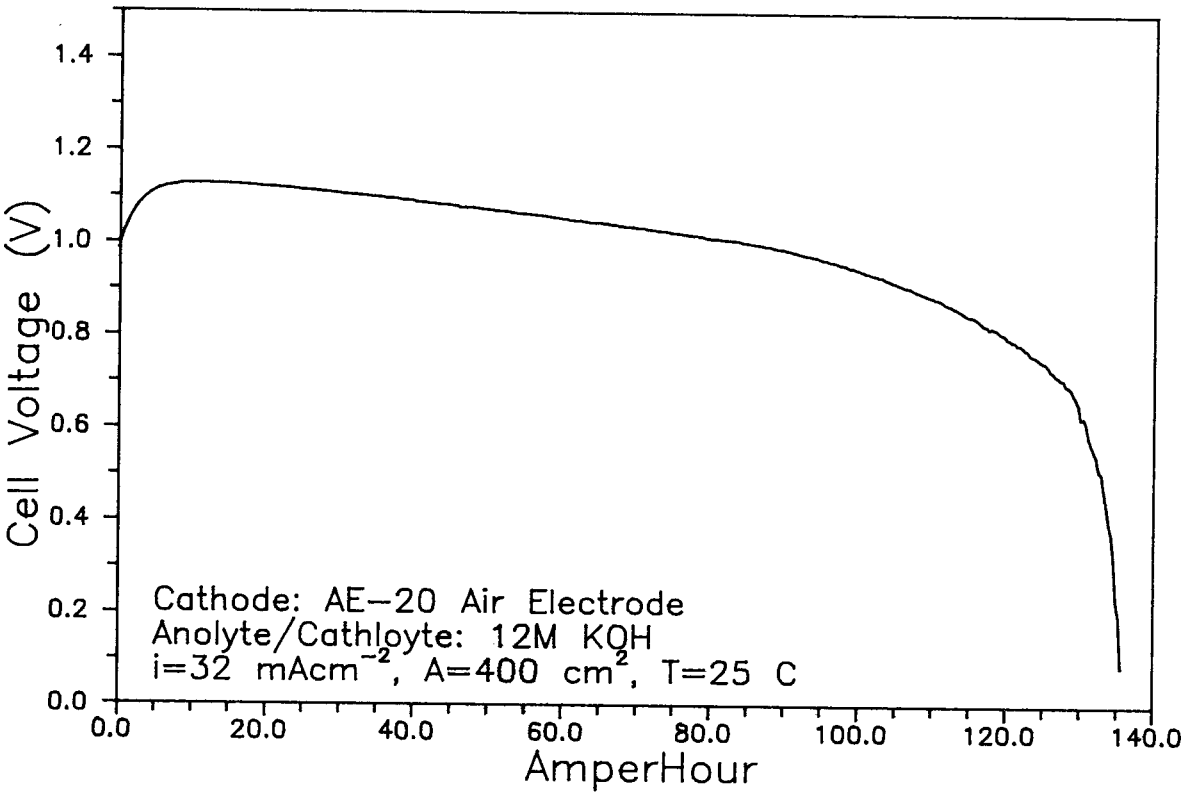

Figure 3. Voltage vs. Ah for Exp. # DN189

NOVEL ZINC-AIR CELLS

Ron Putt and Glenn Merry
MATSI, Inc.

The purpose of this project is to further the development of the Lawrence Berkeley Laboratories negative electrode concept for a zinc-air, electric vehicle battery.

The LBL concept (Figure 1) employs a copper foam negative electrode substrate onto which zinc is plated from an alkaline zincate electrolyte. This substrate has a very open pore structure (10-20 pores per inch), through which the electrolyte is pumped in the direction parallel to the electrode, for the supply and removal of zincate ions during charge and discharge, respectively. A bifunctional air electrode presses a microporous separator against the negative to constrain flow within its pores. And a gas space behind the positive provides air access for supply and removal of oxygen.

The premise of the negative electrode design is that the zinc will plate throughout the foam structure, reducing the actual current density by more than an order of magnitude from the superficial current density. This would reduce the potential for dendrite formation, thus improving cycle life.

The present work has focused on the negative electrode and separator, with two goals, namely increasing the capacity density (loading) of the negative electrode and identifying the factors limiting cycle life.

Most of the experimental work at LBL, which preceded this work, employed Ni/NiOOH counter electrodes, since the bifunctional air electrode is still under development. We saw the need for a less problematic counter electrode in our program, which would allow automatic, hands-off, and trouble-free cycle testing. This led us to develop a zinc-zinc cell concept, in which both the working and counter electrodes are zinc (Figure 2). In this design, a constant current power supply drives the cell for both charge and discharge.

The zinc-zinc cell concept has proven very practical for continuous cycle testing. Since one electrode is in charge (zinc deposition) while the other is in discharge (zinc stripping) there is no net change in zincate concentration, thereby eliminating one variable in an experiment, and the electrolyte can be circulated in series from working to counter electrode, which simplifies the flow system. Further, since the steady state open circuit voltage of the cell is zero, voltage recording can be on a much lower scale (eg 0-250 mV), thereby making it more precise. For half-cycle zinc deposition studies, in which the test is halted at the end of charge on the working electrode, we employ a planar, nickel-plated steel counter electrode which evolves oxygen.

The experimental portion of this project has two objectives, namely increasing the negative electrode loading from 50 mAh/cm2 (the initial value specified by LBL) to 100 mAh/cm2 and demonstrating cycle capability of the system. Findings to date are as follows:

1. Zinc deposit morphology, in the range 5-10 mA/cm2, is generally mossy. It is heaviest at the face adjacent the separator, with a

penetration depth less than 3 mm at loadings of 150 mAh/cm2. The pore structure becomes completely filled in by mossy zinc at loadings greater than 100 mAh/cm2, the target loading for this project. Nonetheless, through proper separator selection (see below), loadings of over 360 mAh/cm2 have been achieved.

2. Substrate preparation is critical for satisfactory zinc deposition on the metal foam. Zinc deposition on bare copper is frequently non-uniform, with regions which do not plate at all. In this instance, a copper/hydrogen-zinc corrosion couple is set up which results in low current efficiency. We have therefore developed a process for pre-plating the copper substrate. This process yields a dense, uniform, continuous zinc plate on all filaments of the substrate, which provides a good base for subsequent deposition of mossy zinc.

3. The choice of separator has a strong effect on deposit morphology. A microporous polyvinyl alcohol synthetic paper (as used in primary alkaline zinc batteries) is penetrated by dendrites in one cycle. Celgard (Celanese) resists dendrite penetration initially, but is penetrated by dendrites usually within 50 cycles. We are currently experimenting with a novel separator which appears to be much more resistant to dendrites. Two cells have each exceeded 80 cycles to date with no incidence of dendrite shorting.

4. Repeated discharge to 100% depth of discharge causes a gradual but substantial polarization increase (greater than 100 mV at 10 mA/cm2) to a non-preplated electrode. This may be related to the formation of a rust-colored layer on the surface of the substrate.

5. We have not experienced any cycle life limitations thus far which are inherent to the electrode itself. If the substrate is preplated it can be fully discharged to eliminate any deposit non-uniformities which may develop with cycling.

6. Pulse plating tests have been inconclusive to date. In some trials we have observed deposits which were heavier at the back side of the electrode than the front, the opposite of what is usually observed. However, there is a lack of reproducibility in these trials, which indicates that there is at least one other variable which is not being controlled. In general, current efficiencies have been lower for pulse plating than they have been for steady current plating.

7. Commercially available zinc plating additives yield dense, metallic deposits, as contrasted with mossy, soft deposits obtained in their absence. The plating additives cause extensive dendrite penetration of the separator, however, militating against their use in this system.

The current-voltage behavior of the zinc-zinc cell is ohmic (Figure 3), with nearly all of the resistance attributed to the separator. Typical charge-discharge curves, once again for the zinc-zinc cell, are shown in Figure 4. The voltage profile is flat in both charge and discharge for a cell with preplated substrates and

depths of discharge less than 100%, reflecting the ohmic nature of the cell. However, when bare copper substrates were employed, and the cells were taken to 100% depth of discharge, a polarization excursion (kneeover) occurred at end of discharge. This polarization would carry over to start of charge, then subside during charge. We consider this to be evidence of a resistive layer on the substrate, whose formation is partially reversible, but which is the cause for the gradual increase in cell polarization with cycling, discussed in item 4 above.

Preliminary costing has been carried out on the elements of the cell stack. For large volume production, the foam metal substrate is projected to cost approximately $9.50/kWh, and the preferred separator material is projected to cost $6.50/kWh. Costing of the bifunctional air electrode is unavailable at present, since it is still under development elsewhere.

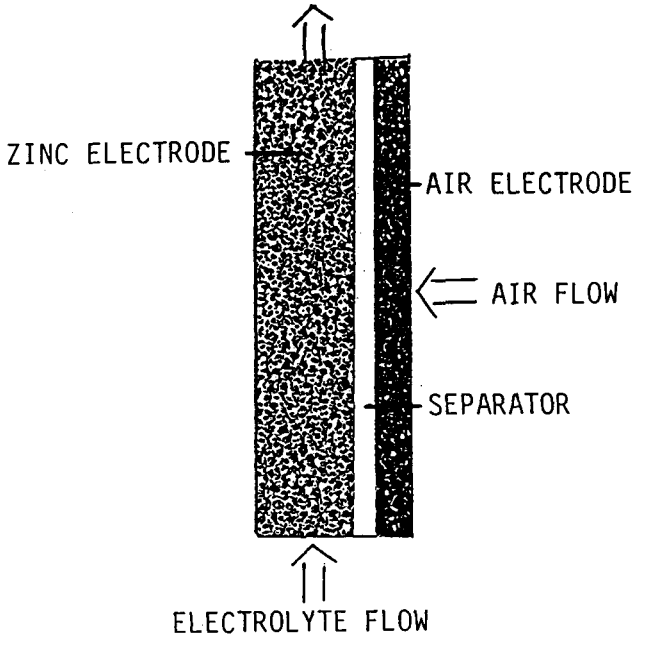

FIGURE 1: CELL DESIGN CONCEPT

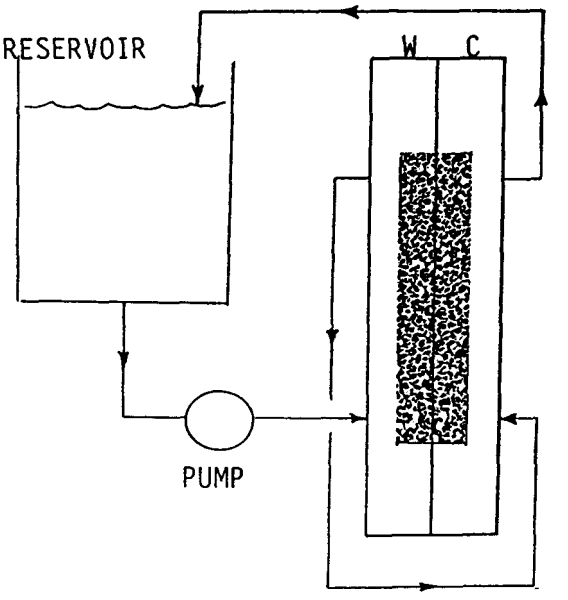

FIGURE 2: ZINC-ZINC CYCLE TEST SYSTEM

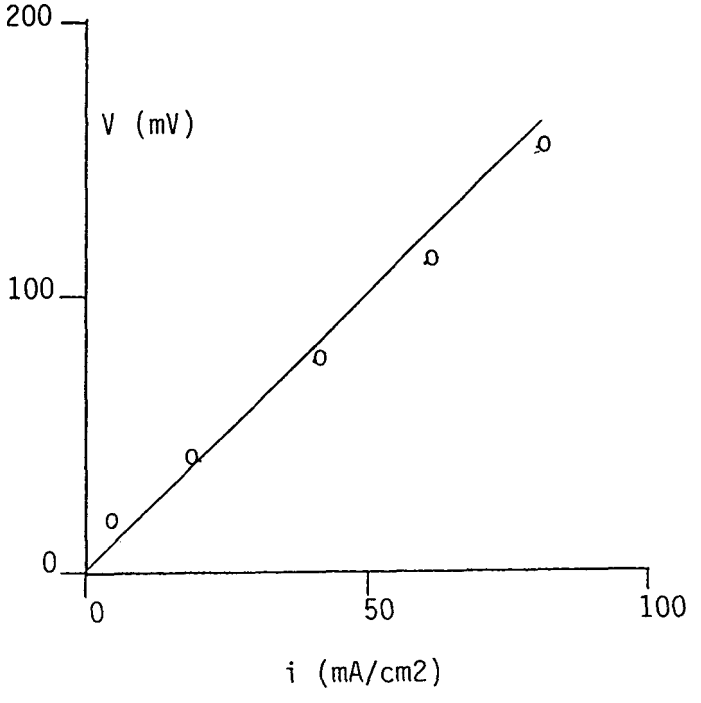

FIGURE 3: VOLTAGE-CURRENT CURVE;
ZINC-ZINC CELL

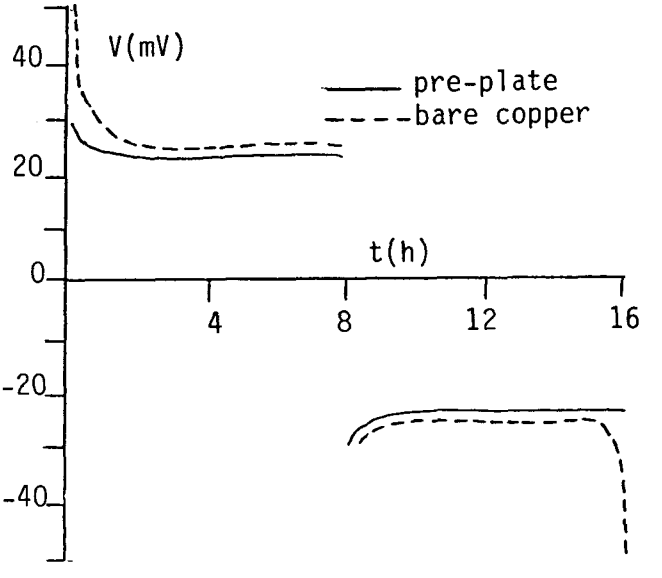

FIGURE 4: CHARGE-DISCHARGE CURVE;
ZINC-ZINC CELL,
10 mA/cm2